Doctorat en Biomedicina i Farmàcia

Advances in antioxidant phytochemical for inflammatory skin diseases: mangiferin and naringin nanocarriers based lipids

Tesis Doctoral presentada por:

María Pleguezuelos Villa

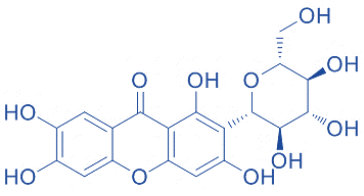

Directores:

Amparo Nácher Alonso

Octavio Diez Sales

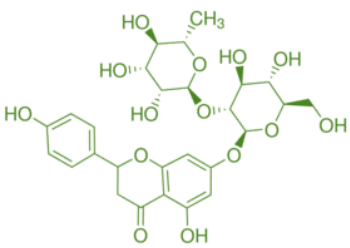

Valencia, mayo 2020

Doctorat en Biomedicina i Farmàcia

Advances in antioxidant phytochemical for inflammatory skin diseases: mangiferin and naringin nanocarriers based lipids

Tesis Doctoral presentada por:

María Pleguezuelos Villa

Directores:

Amparo Nácher Alonso y Octavio Diez Sales
Departament de Farmàcia i Tecnologia Farmacèutica i Parasitologia

Valencia, mayo 2020

Departament de Farmàcia i Tecnologia Farmacèutica i Parasitologia

Doctorat en Biomedicina i Farmàcia

Octavio Diez Sales, Profesor Titular de la Universitat de Valencia

Amparo Nácher Alonso, Profesora Titular de la Universitat de Valencia

CERTIFIES:

The work submitted by the Graduate María Pleguezuelos Villa, entitled "Advances in antioxidant phytochemical for inflammatory skin diseases: mangiferin and naringin nanocarriers based lipids", to obtain a PhD, has been carried out in *the Department of pharmacy and pharmaceutical technology and parasitology of the University of Valencia*, under our direction and advice.

Completed the experimental and bibliographic research, I authorize the presentation of the Thesis to be judged by the assessment panel appointed.

Valencia, 10th May 2020

Octavio Diez Sales

Amparo Nácher Alonso

Se una persona è perseverante, anche se è difficile per lui capire, diventerà intelligente e anche se è debole diventerà forte (Leonardo da Vinci)

A mi familia: a los que están conmigo y

a los que el recuerdo mantiene vivo

AGRADECIMIENTOS

Parece que fue ayer cuando empecé hacer el trabajo final de máster en el laboratorio y, sin embargo, han pasado casi cinco años. Recuerdo mis primeros días intentando aprender a usar el HPLC, en una ciudad que solo conocía por las fallas y por ser la cuna de la naranja. Durante este camino he conocido a mucha gente, y hoy quiero dedicarles unas palabras a aquellas personas de las que he recibido apoyo y generosidad.

Quisiera agradecer a mis directores de tesis, Octavio y Amparo por la oportunidad de realizar este trabajo. Gracias por tantos momentos compartidos y consejos, por transmitirme vuestros conocimientos y guiarme durante todos estos años. A Octavio por conseguir que me supere a mí misma. A Amparo por nuestras confidencias, su mediación, cariño y confianza.

A María Jesús, por descubrirme el maravilloso mundo de la reología y dejar en mis manos su bien más preciado, el reómetro. Por recordarme a mi tierra y por sus ánimos. A Virginia, por comprender la importancia de conseguir este sueño. Colaborar contigo es uno de los mejores recuerdos que me llevo de mi paso por Valencia.

A Carmina, Inma, José, por ser el alma de la secretaria del departamento. A Mamen, la esencia de la secretaria de Farmacología, por orientarme siempre con una sonrisa.

A mi compañera de tesis, Silvia por ayudarme a emprender este camino. A Salva, Lourdes, Miguel e Iván gracias por poner ritmo a mis días de formulación. Por compartir conmigo pasarela y dejarme robaros hielo.

A Inma, Raquel y Eli, por convertir las semanas de experimentos con ratones en una experiencia única, sin vuestra ayuda no hubiese sido lo mismo.

A mis amigos del departamento de Farmacología, por acogerme como una más y amenizar la hora de la comida con relatos y colores. Gracias por alegrarme los días en Valencia, María Tecno nunca olvidara las historias vividas. A Carmen por tener siempre una palabra de ánimo. A Laura C por sus clases magistrales de valenciano, su ayuda, comprensión y su locura, nunca he corrido más en mi vida ni he tenido más agujetas. A Laura V por transmitirme su alegría y su visión positiva de la vida. A Emilio por dar cordura a nuestras

ocurrencias. A Lola y Andrea, por su amistad y apoyo incondicional en los peores momentos, por tantas horas de risas y lamentos, nunca olvidaré los últimos meses en que estuvimos juntas las tres. A Vicente, aunque nos conocimos tarde, has compartido conmigo el final de esta tesis y el comienzo de mis días en Cerdeña.

Gracias a todos por ser los mejores amigos que uno puede desear.

A Manconi, Carla y Mari por su cariño, apoyo y colaboración en esta tesis. Mari, tu ayuda y confianza son incalculables, gracias por estar siempre de forma incondicional. Carla, tus cumplidos son únicos y originales, me has alegrado muchas mañanas y ayudado siempre. Manconi, por acogerme en el laboratorio y hacerlo sencillo. Francesca, no podría imaginar empezar las mañanas sin el momento café, gracias por tu cariño. Cris nos conocimos con el UV y fue una suerte compartir contigo esos momentos. A los doctorandos, por alegrarme las horas del laboratorio y hacerme sentir como en casa. En especial a Ele por desentrañarme secretos arqueológicos y descubrirme la poesía italiana, a Mo por enseñarme italiano entre placas de células y el sur de Cerdeña, a Matteo P," la radio andante", por alegrar el laboratorio con sus canciones y contagiar su alegría. Giulia y Luca compartimos poco tiempo, pero sois geniales. Matteo A por tantas risas y bromas, eres la "tartaruga" más rápida del mundo, a Fede la última incorporación, nadie me" prende in giro" con tanto arte y gentileza como tú, somos un gran equipo. Por supuesto, a Javi por su amistad, las aventuras vividas y ser una pequeña Andalucía en Italia.

A mi familia, tan lejos y tan cerca a la vez, que puedo decirles, me harían falta hojas en blanco para expresar todo lo que siento. El tiempo durante estos años ha pasado lento y rápido a la vez, pero siempre habéis estado en mi mente y corazón, sois el pilar de mi vida y la razón por la que, al fin, puedo escribir esta tesis. Hoy siento que todo lo que no hemos podido vivir juntos, se recompensa un poco y estoy convencida que los kilómetros que nos separan se volverán metros. Gracias por apoyarme en esta aventura, por comprender mis sueños y vivirlos como si fueran los vuestros. Esta tesis es tanto mía como vuestra. Se que os lo digo poco, pero os quiero.

DOCTORAND'S SCIENTIFIC PRODUCTION

The scientific publications generated by María Pleguezuelos Villa during her doctorate and directly associated with this Doctoral Thesis Report of the University of Valencia are the following:

Pleguezuelos-Villa M, Mir-Palomo S, Díez-Sales O, Buso MAOV, Sauri AR, Nácher A. *A novel ultradeformable liposomes of Naringin for anti-inflammatory therapy.* Colloids Surf B Biointerfaces. 2018,162:265–70.

Pleguezuelos-Villa M, Nácher A, Hernández MJ, Ofelia Vila Buso MA, Ruiz Sauri A, Díez-Sales O. *Mangiferin nanoemulsions in treatment of inflammatory disorders and skin regeneration*. Int J Pharm. 2019,564:299–307.

Pleguezuelos-Villa M, Diez-Sales O, Manca ML, Manconi M, Sauri AR, Escribano-Ferrer E, et al. *Mangiferin glycethosomes as a new potential adjuvant for the treatment of psoriasis*. Int J Pharm. 2020, 573;118844.

Pleguezuelos-Villa M, Octavio Diez-Sales, Maria Letizia Manca, Carla Caddeo, Maria Manconi, Amparo Ruiz Sauri, Amparo Nácher. *Mangiferin-naringin vesicles: Improvements in the treatment of chronic inflammatory and oxidative skin diseases*. Draft to be submitted.

INDEX

ABBREVIATIONS

AA	Antioxidant activity
AD	Atopic dermatitis
AMP	Antimicrobial peptides
CD	Donor compartment
CR	Receptor compartment
Cryo-TEM	Cryo-transmission electron microscopy
DE	Dermis
DLS	Dynamic light scattering
DMEM	Medium Eagle de Dulbecco
DMSO	Dimetylsulfoxide
DXM	Dexamethasone
EE	Entrapment efficiency
EP	Epidermis
FF-TEM	Freeze-fracture TEM
FTIR	Fourier Transform Infrared Spectroscopy
HA	Hyaluronic acid
HPLC	High-performance liquid chromatograph
LOD	Limit of detection
LOQ	Limit of quantification
LUV	Large unilamellar vesicles
LVR	Linear viscoelastic region
M3-PALS	Mixed Mode Measurement-Phase Analysis Light Scattering
MLV	Multilamellar vesicles
MPO	Myeloperoxidase
MTT	[3 (4,5-dimethylthiazolyl-2)-2,5-diphenyltetrazolium bromide]
NA	Naringin
NE	Nanoemulsion
PCS	Photon Correlation Spectroscopy

PI	Polydispersity index
PS	Psoriasis
PUVA	Ultraviolet A exposure
SC	Stratum corneum
SUV	Small unilamellar vesicles
TEM	Transmission electron microscope
TSLP	Thymic stromal lymphopoietin
TNF	Tumor-necrosis factor
TPA	Phorbol 1, 2-myristate 1, 3-acetate

ABSTRACT

Chronic inflammatory skin diseases are the most common topical disorders and the fourth cause of global disability. Among all, psoriasis (PS) and atopic dermatitis (AD) are the most frequent chronic and recurrent inflammatory diseases of the skin. Atopic dermatitis has a strong Th2 factor while psoriasis is a disease driven by Th17. The actual treatment, which involve the combination of topical, systemic and biological therapy, is characterized by numerous adverse effects, which reduce patient compliance, lead to the limitation of long-term use and limit the therapeutic efficacy. Therefore, there is a great need for the continuous development of novel, effective and safe coadjuvant treatments. In recent years, preclinical studies have demonstrated the role of oxidative stress in the pathogenesis of both psoriasis and atopic dermatitis and natural antioxidant compounds seem to be ideal molecules for the treatment of these diseases. For this reason, mangiferin and naringin, natural polyphenols with potent antioxidant properties were selected to be used as coadjuvant in the treatment of these diseases. However, the effectiveness of mangiferin and naringin is limited by their low solubility and low bioavailability in vivo. Thus, their incorporation into innovative and effective nanocarrier as seems to be the most suitable solution aimed at obtaining the therapeutic effect. Among the different nanocarriers, phospholipid vesicles and nanoemulsion are considered the most promising systems for the incorporation of these polyphenols and for their application on the skin.

In the light of this, the aim of this work was the formulation of specific nanoemulsions and phospholipid vesicles. In particular, naringin was successfully incorporated into transfersomes, while mangiferin into nanoemulsions dispersed in hyaluronate gels and into innovative phospholipid vesicles called glycethosomes. To evaluate the possible synergistic effect, mangiferin and naringin were co-loaded into different vesicular systems: transfersomes, glycethosomes, glycerosomes, glycethohyalurosomes and glycerohyalurosomes. All the developed nanocarriers were deeply characterized by using different techniques (TEM, Cryo-TEM, Photon Correlation Spectroscopy, Rheological studies, FTIR). In vitro permeation studies were performed to evaluate the accumulation and distribution of mangiferin and naringin into and through the skin. Moreover, the protective effect of the formulations against oxidative stress damages was evaluated in mouse fibroblast cells, whereas the wound healing effect was evaluated in vivo by means

of a TPA mouse model. The composition of the hydrating medium used to prepare the vesicular systems significantly affected the permeation and the capacity to restore the wound of both polyphenols.

Overall results underlined that both vesicular systems and nanoemulsions can be promising systems for the treatment of psoriasis and atopic dermatitis by means of coadjuvant therapies.

Keywords. Inflammation; skin diseases; psoriasis; atopic dermatitis; phospholipid vesicles; nanoemulsions; hyaluronic acid; in vitro studies; fibroblasts; TPA model; mangiferin; naringin.

INTRODUCTION

Inflammation is a mechanism of defense against external changes or cellular lesions that induces the release of mediators from the immune system at the site of inflammation (Pireddu et al. 2016). However, an excess of inflammatory response can damage normal tissues and cause chronic inflammation, that is the base of inflammatory skin diseases, (Zeng et al. 2018). These diseases are the most common disorders in dermatology and the fourth cause of global disability. They sometimes represent the primary manifestation of a systemic disease and have a substantial impact on the quality of life of patients and on the healthcare system (Maniadakis et al. 2018).

Among all, psoriasis (PS) and atopic dermatitis (AD) are chronic, pruritic inflammatory skin diseases of unknown etiology, due to a complex interplay between environmental, immune factors and genetic (Parisi et al. 2013).

Atopic dermatitis usually starts in early infancy, affecting 11-30% of children (Griffiths, van de Kerkhof, and Czarnecka-Operacz 2017), but also affects a great number of adults.

Psoriasis affects 2-3% of person among children and adults. The incidence is most common between 15 and 25 years/ages, but it can affect individuals of any age (Sampogna et al. 2019).

The skin lesions associated with psoriasis differ from that of atopic dermatitis as they tend to be more visibly defined and chronic plaques, generally with coarse scale. However, when viewed as pathogenic disease processes in the skin, there are many similarities and overlaps especially in immune activation.

Atopic dermatitis has a strong Th2 T-cells factor related with the over-production of interleukins (IL) such as IL-4 and IL-13, while psoriasis is a disease driven by Th17 T-cells and associated with IL-17 activation, both diseases have Th 22 T-cells activation and Th1 T-cells with an increased release of IL-22 (Klonowska et al. 2018). The acute phase of atopic dermatitis is characterized by an abnormal production by Th2 of cytokines such as IL-5, IL-4, IL-13 and IL-31, whereas the chronic phase is characterized by the recruitment of Th1, Th22 and Th17 subsets (Figure 1), which inducing keratinocyte responses, attract additional circulating immune cells to the epidermis, induce epidermal thickening, with excessive release of IL-1, TNF-α, IL-6, IL-12 and IL-18 by recruited monocytes and alter keratinocyte differentiation (Werfel et al. 2016).

Moreover, atopic dermatitis lesions are characterized by dendritic cells and Langerhans cells activated by the release of IL-25, IL-33 and cytokine TSLP (Thymic stromal lymphopoietin) from keratinocytes, which in turn play an important role in skin barrier dysfunction, chemokine production, suppression of antimicrobial peptides (AMP), and allergic inflammation (IgE) (Brandt and Sivaprasad 2011). Clinical studies have suggested that IL-5 and IgE, are less important for AD pathogenesis and that IL-22 has a pathogenic role only in severe cases of AD (Guttman-Yassky et al. 2018), associated with abnormal epidermal markers, such as keratin 16 and keratin 6.

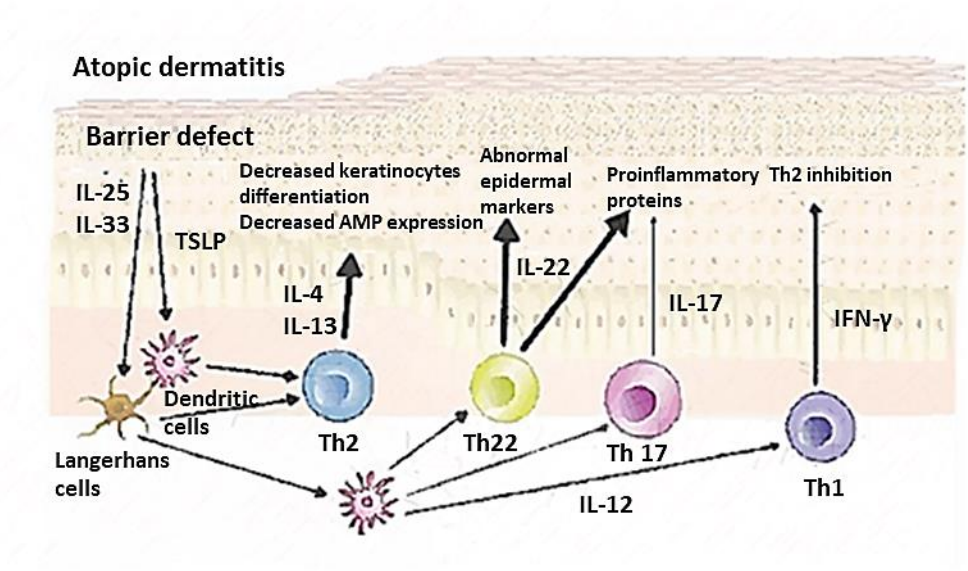

Figure 1. Atopic dermatitis immune mechanisms. Modified from (Guttman-Yassky, Krueger, and Lebwohl, 2018)

The inflammatory events liable of psoriasis are characterized by the activation of TNF (tumor necrosis factor) and induction of nitric oxide synthase–producing DCs (Tip-DCs), which produce TNF and IL-23 and subsequently induce activation of Th17 cells (Hawkes, Chan, and Krueger 2017). Cytokines IL-17, TNF and IL-23 have a pivotal role in the pathogenesis of psoriasis (Figure 2). TNF might also contribute to the development of psoriatic dermatitis through the activation of keratinocytes: TNF and IL-17 synergistically stimulate keratinocytes to fully produce key inflammatory molecules in psoriasis, such as IL-8 and CCL20. Besides, IL-17 ligands activate IL-17 receptors on keratinocytes and immune

cells and work in synergy with IL-22 leading to an increased expression of the proinflammatory proteins S100A7, S100A8, S100A9 and S100A12 and antimicrobial proteins (AMPs) (Niyonsaba 2016).

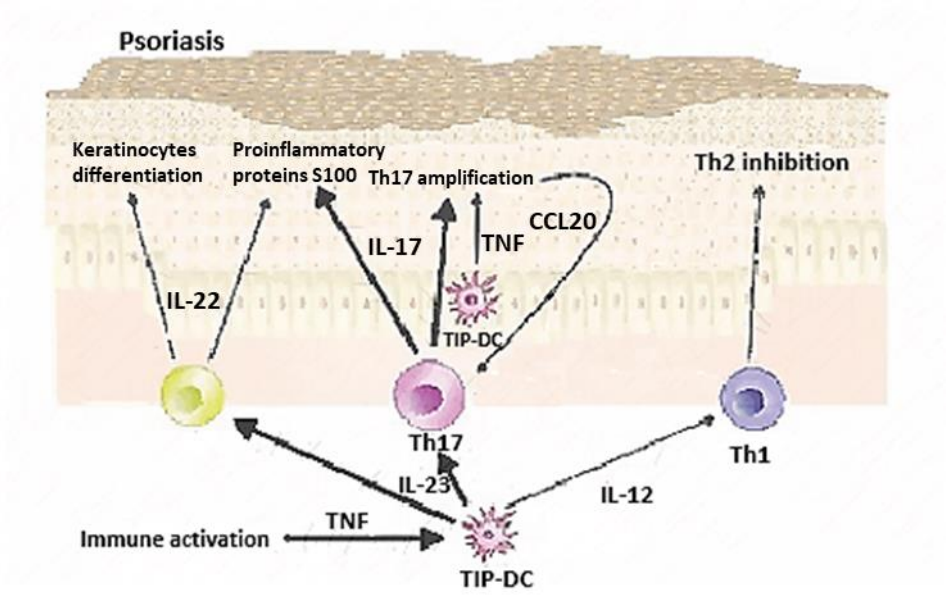

Figure 2. Psoriasis immune mechanisms. Modified from (Guttman-Yassky, Krueger, and Lebwohl, 2018)

Atopic dermatitis and psoriasis are becoming increasingly recognized as systemic rather than localized cutaneous diseases because skin inflammation is often associated to metabolic, cardiovascular and other co-morbidities (Boehncke 2018)**.** The pathogenesis of co-morbid disease in patients affected by both psoriasis and atopic dermatitis remains unknown and the magnitude of the risks has not been well defined (Ayala-Fontánez, Soler, and McCormick 2016).

Some studies have reported that patients affected by atopic dermatitis are more susceptible of developing other types of dermatitis such as allergic contact dermatitis and irritant contact dermatitis. It has been also suggested that the risk of epilepsy is increased by the number of allergic disorders, as well as by the AD severity (Silverberg 2018). However, less attention has been given to the risk of non-allergic comorbidities of AD, which include cutaneous and extra-cutaneous infections, cardiovascular disease and some cancers. In addition, different studies underlined the possible connection between atopic dermatitis and type 2 diabetes (Drucker and Harvey 2019), lymphoma (Ruff et al. 2017) or

autoimmune diseases (Crohn's disease, ulcerative colitis, celiac disease) (Andersen et al. 2017; Oliveira and Torres 2019).

On the other hand, several studies have underlined the possible connection between metabolic syndrome (insulin resistance, obesity, hypertension) and psoriasis. Hu and Lan (2017) found an increased risk of myocardial infarction in patients affected by severe psoriasis. Besides, psoriasis has been associated with developing dyslipidemias, indicating that there is a genetic component in this disease. Several studies suggested that chronic inflammation, especially vascular, may be more frequent in patients with psoriasis and may contribute to atherogenesis (Puig 2017).

Both diseases are associated with several psychiatric disorders, including depression, anxiety, and suicide tendency (Farzanfar et al. 2018), mainly related to the negative effect of this disease on the quality of the life of patients. For this reason, an early recognition of the disease and an adequate treatment to decrease the risk of physical and psychologic morbidity is needed. The treatment generally involves different approaches, which include education of patients and their families, identification of triggers and pharmacological and non-pharmacological measures aimed at relieving pruritus and reducing inflammation.

Regarding pharmacological treatment the conventional therapies can be divided into topical administration, systemic therapy and biologics.

Among the topical drugs, calcineurin inhibitors, steroids, vitamin D3 derivatives, retinoids, dithranol, keratolytic agents, and coal tar are the most effective. The choice of a topical treatment depends on different factors such as the type of psoriasis, the site of the lesion and the patient's needs (Torsekar and Gautam 2017). Calcineurin inhibitors (tacrolimus and pimecrolimus), which inhibit an intracellular enzyme involved in the regulation of gene transcription in T lymphocytes, are used especially in the most difficult to treat cases. Corticosteroids are used to treat acute disease exacerbation mainly because of its ability to produce vasoconstriction. Vitamin D3 analogs (calcipotriol, calcitriol, and tacalcitol), act inhibiting keratinocyte proliferation and differentiation along with the inflammatory response (Mahajan 2016). Recent studies reported that the combination of topical corticosteroids and vitamin D3 analogs may be more effective thanks to the synergistic effect of the different drugs.

Keratolytic agents including salicylic acid, lactic acid, and urea are also widely used for the treatment of these skin disorders as they promote physiological shedding by disrupting intra-keratinocyte adhesion in the uppermost layer of the epidermis (Jacobi, Mayer, and Augustin 2015).

Phototherapy, such as ultraviolet B irradiation or the combination of psoralens and ultraviolet A irradiation (PUVA), represent one of the oldest topical therapy for psoriasis, based on the induction of apoptosis in T lymphocytes and Langerhans cells (J. Thomas and Parimalam 2016).

Generally, conventional topical treatment is not able to effectively counteract the diseases mainly because of their low rate of absorption. For this reason, to keep the disease under control, multiple periods of treatment are required which are often associated with an increased risk of adverse effects (Pinson, Sotoodian, and Fiorillo 2016), especially in those patients with moderate to severe generalized psoriasis.

Table 1 Summarizes the adverse effects associated with conventional topical treatment.

Table 1. Adverse effects connected with conventional topical treatments

Topical agent	**Effects Adverse**
Calcineurin inhibitors	Itching and stinging
Glucocorticosteroids	Skin atrophy after long term use
Vitamin D3 derivatives	Stinging, burning, and peeling skin
Retinoids	Redness, peeling, itching, burning sensation
Keratolytics	Redness, swelling, tenderness, and pustules
Dithranol	Redness and irritation
Coal tar	Redness, burning, itching, and skin staining
Ultraviolet B irradiation (UVB)	Burning and itching
Psoralens plus ultraviolet A exposure (PUVA)	A risk for skin cancer

Patients with moderate/severe psoriasis and atopic dermatitis who do not adequately respond to topical therapy, need to be treated with systemic drugs and biological therapy. Cyclosporine, an immunomodulatory drug that inhibits IL-2 production, is the first option for systemic treatment of AD. Mycophenolic acid (MPA) is used in adult patients when cyclosporine therapy is not effective (Giavina-Bianchi and Giavina-Bianchi 2019). Moreover, a randomized trial demonstrated that the effect of both azathioprine (a purine synthesis inhibitor) and methotrexate (antimetabolite) was similar in patients with severe AD and PS (Johnson et al. 2019).

Increasing knowledge regarding the molecular pathogenesis of psoriasis has hastened the development of targeted therapy by using monoclonal antibodies that target specific mediators of inflammation, avoiding the release of cytokines or other mediators that play an essential role in the pathogenesis of this disease (H. J. Kim and Lebwohl 2019). Dupilumab is an interleukin (IL)-4 receptor α-antagonist that inhibits the release of IL-4 and IL-13 when administered subcutaneously resulting in a significant clinical and symptomatic improvement in adult patient with moderate to severe AD (de Bruin-Weller et al. 2018). Tralokinumab and lebrikizumab are specific inhibitors of IL-13, while nemolizumab is a specific inhibitor of IL-31, which have demonstrated good potential in clinical trials (Mihara et al. 2019; Wollenberg et al. 2019). Fezakinumab, a monoclonal antibody against IL-22, was also effective in the treatment of patients with severe AD in phase 2 trial (Guttman-Yassky et al. 2018). Recently, Janus kinase (JAK) inhibitors as barcitinib have been used for the treatment of a wide range of inflammatory diseases, demonstrating their efficacy in AD and psoriasis (Fragoulis, McInnes, and Siebert 2019).

However, even with the availability of various options of systemic and biologic treatment, most of the efficient treatment modalities are costly.

Although treatment can afford patients greater degrees of disease improvement, there is no cure for theses inflammatory skin diseases and the most effective are often associated with different adverse effects, which lead to the limitation of long-term use and dramatically reduce the compliance of the patients.

Table 2 summarize the side effects connected with the use of systemic drug or biologic therapy.

Table 2. Adverse effects connected with systemic administration of drugs and biologic therapy. Modified from (Alexander et al. 2019)

Systemic agent	**Effects Adverse**
Ciclosporin	Hypertension, thrombocytopenia, liver enzyme increase, dyslipidemia, leukopenia
Methotrexate	Infections, liver enzyme increase, anaemia, leukopenia, pancytopenia, fatigue, renal impairment, fever, malaise
Azathioprine	Lymphopenia, neutropenia, liver enzyme increase, skin infection
Mycophenolate mofetil	Nausea, headache, fatigue, muscle ache, infections, serum creatinine increase, leukopenia
Dupilumab	Nasopharyngitis, headache, conjunctivitis, skin infections, herpes viral infections
Nemolizumab	Nasopharyngitis, peripheral oedema, headache, impetigo
Ustekinumab	Nasopharyngitis
Fezakinumab	Viral upper respiratory tract infection
Baricitinib	Headache, nasopharyngitis, cellulitis, infections
Tralokinumab	Nasopharyngitis, arthralgia, syncope

The combination of biologics with complementary and alternative medicines may guaranty the reduction of the dosage, the maintenance of the initial response of biologics and the reduction of the side effects. In the light of this, different studies revealed that the use of natural products for the treatment of atopic skin diseases and psoriasis can represent a

valid alternative as they are safe, systemically non-toxic, cost-effective, efficacious in combination with conventional therapeutic strategies and improve the compliance of the patiences.

In the last years, a large range of crude natural extracts and herbal oils have been applied, alone or in combination, to relieve the symptoms and reduce severity of these skin diseases. Natural herbal oils such as *grape seed oil*, *olive oil* and *virgin coconut oil* have demonstrated to be able to reduce the exacerbation and alleviate the disease progression. Many studies have shown that the phytochemicals as phenolic acid and polyphenols contained in *virgin coconut oil* exhibited a strong effect decreasing inflammation in both psoriasis and atopic dermatitis (Chew 2019). It has also been observed that the application of a cream containing *olive oil* on skin lesions, strongly reduced psoriatic signs. Luteolin-7-glucoside, a flavonoid present in olives, seemed to have a promising role in modifying cell cycle regulation (Santangelo et al. 2018). However, further studies seem to be necessary to evaluate the real contribution of this herbal oils on T cells imbalance, that is a trait of this immune diseases.

Among several therapeutically viable crude extracts, *malva sylvestris* leaves have shown promising anti-inflammatory activity in acute models of skin inflammation as it was able to counteract the proliferation and migration of leukocytes and the oedema. Prudente et al. (2017) demonstrated that these effects were mainly related to the main active compounds (malvidin 3-glucoside and other anti-inflammatory compounds) contained in the hydroalcoholic extract.

Artemisia capillaris and *mahonia aquifolium* extracts showed potential therapeutic effects as well. It was reported that the application of the alcoholic extract of *artemisia capillaris*, reduced the atopic dermatitis-like skin lesions in Nc/Nga mice (S. Y. Lee et al. 2018).

The extract of *mahonia aquifolium* contains berberine, an isoquinoline alkaloid that was able to reduce immune markers, hyperproliferation and inflammation in psoriatic and atopic dermatitis lesions (Janeczek et al. 2018).

In spite of these good properties, the components contained in crude extracts are usually complex and their content is often uncontrollable. Therefore, there is a great need for the

continuous development of novel, effective and safe treatment for psoriasis and atopic dermatitis.

In recent years, preclinical and clinical studies have demonstrated the role of oxidative stress in the pathogenesis of inflammatory diseases (Xu et al. 2017; Kizilyel et al. 2019). Hence, pure natural antioxidant compounds as curcumin, resveratrol, baicalin, rottlerin, delphinidin have gained much attention as possible candidates for novel therapies (Nardo et al. 2018; M. J. Kim et al. 2019). For this reason, *naringin* and *mangiferin*, polyphenols with antioxidant properties were tested in this work as a possible bioactives to be used as coadjuvant in the treatment of both PS and AD.

Naringin (Figure 3), 4 ', 5,7-trihydroxy flavonone-7-ramnoglycoside, is a glycosylated flavanone that is formed from naringenin and neohesperidosa and is the main active component of Chinese medicinal herbs, such as Drynaria fortunei, Citrus aurantium L. and Citrus medica L. (J. Zhang et al. 2014; Yin et al. 2015; Chtourou et al. 2015). There are several in vivo and in vitro studies describing their pharmacological effects: anti-inflammatory (El-Desoky et al. 2018) anti-cancer (Ming et al. 2018), anti-oxidant (Zhou et al. 2019) and anti-microbial (AlMatar et al. 2019). Several studies confirmed that *naringin* plays an important role in increasing and regulating the gene expression of superoxide dismutase and catalase (Jeon et al. 2001).

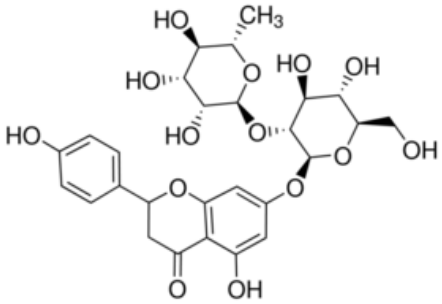

Figure 3. *Naringin*: chemical structure

(https://www.sigmaaldrich.com/catalog/product/sigma/71162?lang=it&region=IT)

Mangiferin (Figure 4), 1,3,6,7-tetrahydroxyxanthone-C2-β-D-glucoside, is a C-glucosyl xanthone, and it is the main active component of the Anacardiaceae and Gentianaceae

families. It can be isolated from several parts of Mangifera indica L. (mango), including leaves, bark, stem, fruit peels and root.

It has been proven that *mangiferin* exhibits many pharmacological and biological activities such as anti-oxidant (Peng et al. 2019), anti-tumoral (G. Yang et al. 2019), anti-microbial (Biswas et al. 2015), anti-inflammatory (Rocha et al. 2018). Further, it is well known that *mangiferin* can modulate the genes related to nuclear factor-kappa B (NF-kB), reduce the protein expression of cyclooxygenase-2 (COX-2), and enhance the glyoxalase 1 function, which are all involved in its anti-inflammatory effects (Bhatia et al. 2008).

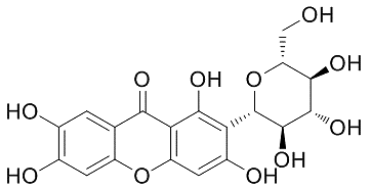

Figure 4. *Mangiferin:* chemical structure
(https://focusbio.com.au/products/mangiferin/)

However, the effectiveness of these natural products is limited by their low solubility, high molecular weight and bioavailability in vivo. As a consequence, they do not reach the site of action in an adequate concentration to exert an effective pharmacological effect, thus, their potential health benefits are significantly limited. Topical administration of these natural compounds could be a promising approach to increase their bioavailability and enhance their therapeutic efficacy, but it requires an efficient penetration of these compounds through the skin barrier by a passive diffusion process. Unfortunately, the skin, which represent the most important natural barrier of our body, comprises a series of layers that are a big obstacle for most of the drugs topically applied. The main layers of the skin, from the deepest to the outermost strata are hypodermis, dermis and epidermis. The dermis is composed of fibrous proteins, salts and water. Blood and lymphatic vessels, nerve endings and sweat glands are embedded within the dermis. The epidermis does not contain

blood vessels and consists of five layers, basal layer, spiny stratum, granular stratum, lucid stratum and stratum corneum. The stratum corneum is considered as the speed-limiting barrier in transdermal permeation of most molecules, it comprises 15-20 layers of corneocytes (Zsikó et al. 2019).

Basically, molecules applied on the skin surface can follow two diffusive pathways: trans-appendageal and trans-epidermal routes. The trans-appendageal route includes the transport of active molecules through hair follicles and sweat glands. These routes have a relatively small area and has been considered of minor importance. However, recent research indicated that sebaceous glands and hair follicles are associated with dermatological disorders such as alopecia, skin tumors and acne (Villablanca et al. 2017). Further, the pilosebaceous glands may be the most important route for large polar molecules and ions that hardly permeate through the stratum corneum. The trans-epidermal routes involves crossing the skin layers through two different pathways: intracellular (across the lipid matrix and the corneocytes) and intercellular (across the continuous lipid matrix between corneocytes) (Chaulagain et al. 2018). Despite its high tortuosity, intercellular route is widely accepted as the main route for a few natural compounds and for those slightly lipophilic (Jankowski, Dyja, and Sarecka-Hujar 2017).

To overcome these limitations, during the last decades, numerous studies have been focused on the development of innovative nanocarriers able of both incorporate adequate amounts of hydrophilic bioactive compounds and promote the accumulation and passage of them into and through the skin. A successful drug delivery system designed to be applied topically must be able to overcome/cross the main barrier of the skin (stratum corneum), taking into account its properties such as gap of tight junction, anatomical locations and thickness of the skin (Nauman R. Khan et al. 2015). Among various novel vehicles, the nanosized carrier has attained a distinctive position among transdermal/dermal delivery systems, especially for the treatment of dermatological disorders such as atopic dermatitis and psoriasis (Pradhan et al. 2018).

The choice of the most appropriate carrier is very important, since it may influence the release mechanism of the incorporated molecules (altering the skin barrier properties or promoting compound solubilities in the stratum corneum). During the last decades,

numerous versatile lipid-based nanocarriers have been developed for dermatological applications, as they are capable of fluidizing the stratum corneum as a function of size, shape, surface charges, and hydrophilic-hydrophobic balance, as well as facilitating molecules penetration/permeation through/across the external layers of the stratum corneum (M. Yang et al. 2019). Among the different lipid-based nanocarriers, nanoemulsions and phospholipid vesicles have obtained an increased attention especially for the topical delivery of flavonoids designed to treat skin inflammatory diseases such as psoriasis and atopic dermatitis (Mishra, Shandilya, and Mishra 2018). In table 3 some examples are reported.

Table 3. Flavonoids incorporated in nanocarrier for the treatment of skin inflammatory diseases

	Nanocarrier effect	**Ref**
Nanoemulsions	Enhance curcumin permeation to deeper skin layers and improve their anti-inflammatory effects in wound healing	(Yousef et al. 2019) (Ahmad et al. 2019)
Gellan-transfersomes	Improved baicalin activity for restoring the structural and functional conditions on damaged skin by TPA	(Manconi et al. 2018)
Hyaluronan ethosomes	Increase curcumin anti-inflammatory activity on inflamed ear skin induced by imiquimod	(Y. Zhang et al. 2019)

Nanoemulsions and liposomes could enhance the chemical stability of unstable molecules by protecting them from oxidative and light degradation. These carriers have been used to incorporate a great variety of hydrophobic phytochemicals as nobiletin, luteolin, quercetin (Liao et al. 2018; Shin et al. 2018; Hatahet et al. 2018). The similarity of these transdermal systems with the skin membrane especially for lipid composition, as well as their small size, improve/promote the permeation of different active biomolecules into deeper skin layers, ensure their controlled release and decrease their clearance from the epidermis. Therefore, using nanocarriers side effects reduction and greater effectiveness along with

an increased patient's compliance can be reached. Further, nanocarriers are often the first choice for the topical delivery of bioactives thanks to their biodegradability and increased agent active load.

Nanoemulsions are biphasic dispersion consisting of droplets dispersed in an external phase, completely immiscible with the internal one, and stabilized by an appropriate surfactant mixture. These systems, even having similar size distribution, differ significantly from microemulsion in terms of thermodynamic stability (microemulsions are thermodynamically stables). Indeed, nanoemulsions have superior kinetic properties, improved drug incorporation and stability in comparison with conventional emulsions, mainly because of the nanometer range of the droplets. The small size of the particles and the low surface tension among oil and aqueous phase avoid the agglomeration or precipitation of the particles along with creaming or sedimentation phenomena (Sutradhar and Amin 2013). Some research indicates that the droplet size of the nanoemulsions should be <100 nm (Marzuki, Wahab, and Hamid 2019), but recently many authors confirmed that droplets can have size in the range between 20 and 400 nm and are generally characterized by a homogeneous distribution (Shaker et al. 2019). Nanoemulsions can be classified in three main classes: oil in water (o/w), in which the oil phase is dispersed in the continuous/external aqueous phases; water in oil (w/o) in which the internal water phase is dispersed in the continuous/external oil phases; and bi-continuous/multiple emulsion where micro domains of oil and water phases are inter-dispersed within the system (Gupta et al. 2019). In the w/o nanoemulsions the active agents are mainly solubilized in the aqueous phase, while in those o/w the active molecules are dissolved in the oil phase. The o/w nanoemulsions are preferred whe lipophilic or poorly aqueous soluble bioactives are used.

The appropriate selection of both preparation method and stirring speed/shear stress is considered the key points for the preparation of an ideal formulation for topical application (Raval et al. 2018). Among the different preparation methods, high or low energy methods are the most used. High-energy method is based on the generation of intense forces able of breaking the oil and water phases, forming nanometer-sized droplets (microfluidizers, high pressure homogenizers or ultrasonic methods). Low-energy methods use internal

physical properties of the system (Jasmina et al. 2017), thus the emulsification is ensured by changing some parameters such as composition or temperature, which may affect the hydrophilic/lipophilic balance of the nanoemulsions, giving spontaneous emulsification, phase inversion methods, and solvent displacement.

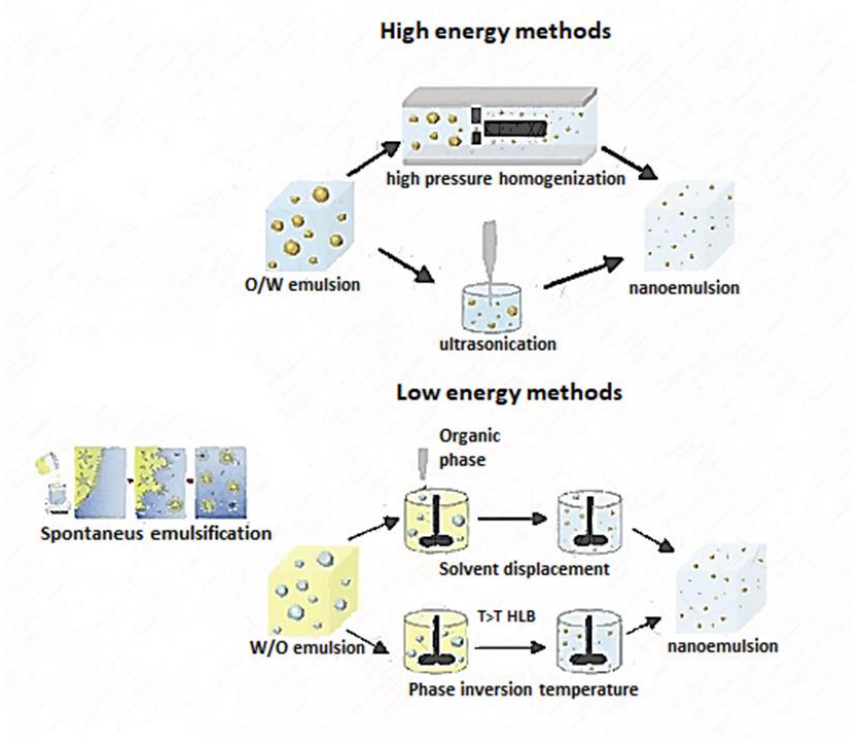

Figure 5. Nanoemulsions: preparation methods. Modified from (Gupta et al. 2016)

The High-Pressure Homogenization is the most efficient and used method for the preparation of nanoemulsion. It is based on the combination of different forces such as turbulence and cavitation. During the preparation all the components (oil, water and surfactants) are forced to pass through a small orifice under high pressure, which, depending on the number of homogenization cycles, led the production of nanoemulsion with very small droplets (up to 1 nm). The microfluidization is the most used method for the preparation of high amount of nanoemulsions. Sonication and ultrasonic homogenization methods are widely used to produce, in a small/laboratory scale, small and homogeneous nanoemulsions. Ultrasonication is based on the production of cavitation and mechanical vibration, which provide the energy requested for the formation of small droplets. The size of droplets is significantly affected by the ultrasonic homogenization

duration, the power of ultrasonication and the concentration of surfactant. Nanoemulsions prepared by using high energy emulsification techniques are thermo-kinetically stable, whereas nanoemulsions prepared by using low energy emulsification methods produce thermo-dynamically stable nanoemulsion. Low-energy methods are more attractive for large-scale production. Phase inversion temperature method is based on transition of phases during the emulsification process. Depending on the progressive temperature change, the affinity of emulsifiers varies toward water and oil. The solvent displacement method consists in pouring the organic phase (containing oil dissolved) into aqueous phase (containing surfactants). The diffusion of organic solvent produced the nanoemulsions. The principal limitation of this method is that organic solvent may be removed later by vacuum and needs a high ratio of solvent to oil to produce small droplets. Spontaneous emulsification methods are obtained by adding water to an oil solution and surfactant stepwise maintaining the dispersion under constant stirring to obtain a homogeneous nanoemulsion. The emulsification process depends on surfactant structure, interfacial tension and concentration, among others (Jasmina et al. 2017; Gurpreet and Singh 2018; Kumar et al. 2019).

Liposomes are vesicular systems consisting of one or more concentric lipid bilayers that enclose an equal number of aqueous compartments. They are mainly composed of phospholipids, which in water are able to form bilayers because of their amphipathic nature. These system are highly versatile as they are able to incorporate both hydrophilic and lipophilic drugs (Nisini et al. 2018). Indeed, drug molecules can either be encapsulated in the aqueous space (hydrophilic compounds) or intercalated into the lipid bilayer (lipophilic compounds) depending on their physicochemical properties. Liposomes can be classified according to the preparation method (thin film hydration, extrusion techniques or reverse-phase evaporation) and lamellarity (multi-, oligo- and uni-lamellar vesicles). A single bilayer enclosing an aqueous compartment is referred to uni-lamellar lipid vesicle, which in turn can be divided into large uni-lamellar vesicles (LUV) or small uni-lamellar vesicles (SUV) depending on their size. Multilamellar vesicles (MLV) are instead composed of numerous bilayers. Properties of liposomes are significantly affected by the preparation method chosen, by the types and amounts of phospholipid used, by the charge properties

of the components, and by the time of hydration. There are multiple techniques for preparing liposomes, from which several types of vesicles can be formed (Powers and Nosoudi 2019).

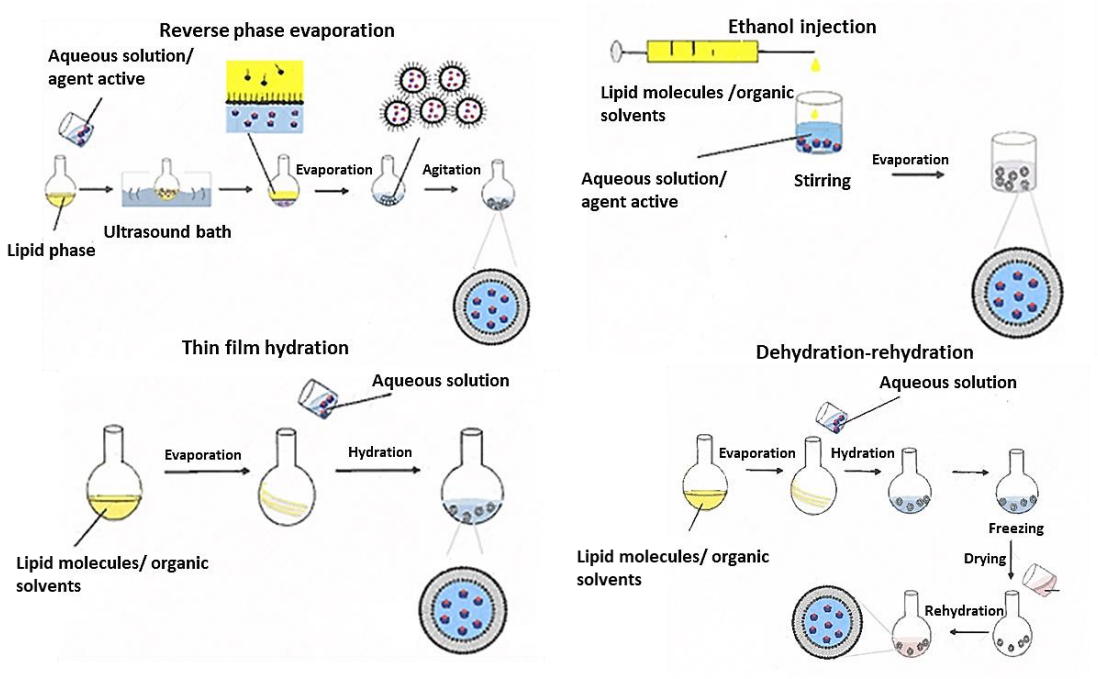

Figure 6. Liposomes: preparation methods. Modified from (Gharib et al. 2015)

One of the most widely used techniques for the preparation of liposome is the thin-film hydration method, which involves the dissolution of the phospholipids and all the other lipophilic components in an organic solvent, the solvent is then evaporated to allow the formation of a thin lipid film that is finally hydrated by using aqueous media. This method generally produce multilamellar vesicles, so other methods like extrusion or sonication are required to obtain smaller and uni-lamellar vesicles (H. Zhang 2017).

The solvent-injection and reverse-phase evaporation methods afford lipids hydration by means of organic solvent. These methods ensure high encapsulation efficiency but are conditionate by the lipid solubility in organic solvent and the removal of the solvent (Shi and Xianrong 2018).

The detergent-depletion methods imply the lipid film hydration with a detergent solution producing liposomes large MLV. The dehydration-rehydration method allows the

formation of vesicles by means of controlled cycles of dehydration and rehydration process.

To reach the desired liposomes properties (lamellarity, size and homogeneity properties) different additional methods can be chosen to ameliorate these parameters post-formation. Among all, extrusion and sonication are the most common and efficient methods. Extrusion consists in forcing the passage of liposomes through a membrane filter with a defined pore size, while by sonication high energy is given to liposomal suspension. Both methods reduce the vesicles size and produce more homogeneous systems (Nkanga et al. 2019).

Over the past three decades, lipid-based nanocarriers as transdermal delivery systems have been successfully developed by using the preparation methods described above.

North American guidelines, the International European guidelines, and the German S3 guidelines confirm that the treatment of skin diseases with innovative topical therapies plays a crucial role to reach the desired therapeutic effect. Nevertheless, not all lipid-based nanocarriers are equally capable of modifying the permeability of the skin barrier. It has been suggested that the hydrating properties of the lipid bilayer promote the intercellular perturbation of the stratum corneum, forming lipid domains channels, which reduce the diffusional resistance through the skin layers and consequently increase agent active penetration (Hua 2015)**.** In this sense, the components of the nanocarriers may change the water gradient in the skin layers, avoiding transepidermal water loss, exhibiting an occlusive effect and modifying their viscoelasticity, which could affect the skin permeation. Thus, vesicles and nanoemulsions composition play a significant role in promoting the performances of skin delivery systems, confirming the theory of many authors according which specifically designed vesicular and nanoemulsions carriers can be obtained by using specific additives, capable of promoting penetration and permeation of different drugs into and through the stratum corneum.

The selection of a suitable oil considering the psychochemical properties of bioactives and a good combination with surfactant and/or co-surfactant should improve the topical performances of nanoemulsions (Shaker et al. 2019). Oil phase like almond oil, olive oil, isopropyl myristate among others have an intrinsic penetration enhancing ability, as they

affect the stratum corneum moisturize and improve penetration through this limiting and protective barrier. Musa et al. (2017) reported that a higher oil content may promote the hydration and perturbation of the ordered structure of the skin thus improving cyclosporine loading in the stratum corneum.

The incorporation of surfactants enhances stability and improves skin permeation and drug release. Non-ionic surfactants as Tween 80 are able to fluidify the lipid components of stratum corneum at the intercellular level and then interact with filaments of keratin due to the diffusion of surfactant in the intercellular matrix. Su et al. (2017) confirmed that the effect of Tween 80 is temperature dependent as its solubility increase as the temperature also increases. Therefore, the surfactant ability to reduce interfacial tension is determine by their dehydrated head groups, promoting o/w nanoemulsions formation. Sometimes co-surfactants are also needed with a potential dermal enhancer property as Transcutol-P. Hussain et al. (2016) suggested that the combination of Tween 80 as surfactant and Transcutol-P as co-surfactant in nanoemulsions improved amphotericin B penetration and permeation.

Conventional liposomes applied in the skin are generally accumulated in the stratum corneum or in the upper layers of epidermis. To overcome these limitations transfersomes, ethosomes and glycerosomes, among others have been formulated and tested.

Transfersomes consist of phospholipids and a biocompatible surfactant as Span or Tween, that acts as edge activators to improve vesicle deformability. Transfersomes have the ability to retain water and penetrate intact in the skin, thanks to their property to reversibly deform the lipid bilayer without compromise vesicle integrity. Several studies with elastic liposomes were carried out (Rai, Pandey, and Rai 2017; Hasanpouri et al. 2018). Amnuaikit et al. (2018) compared liposomes with invasomes and transfersomes as topical delivery systems for phenylethyl resorcinol. Results showed that this type of vesicles presented higher elasticity and improved the retention of phenylethyl resorcinol in the skin compared to liposomes and invasomes.

In addition, the use of small-chain biocompatible alcohols such as glycerol or ethanol in vesicles formulation as a tool to improve drug penetration has been investigated by

different authors. Among others, glycerosomes and ethosomes seem to be the most promising carriers for the delivery of different drugs to the skin.

Glycerosomes are mainly composed of phospholipids, glycerol and water. It has been shown that glycerol have important properties as it retains water in the skin; plasticizes and hydrates the skin to avoid dehydration and the consequential physical hurt; is highly biocompatible; stabilizes the formulation; promote the performance of the topical delivery systems (Suzuki et al. 2018). Manca et al. (2016) confirmed that the addition of glycerol to liposomal formulations in high amount (20-30%) favoured diclofenac accumulation and permeation into the skin, due to its moisturizing properties and to the improved flexibility of the liposomal bilayer, thus increasing the ability to target drug over the skin. A similar phenomenon was observed by Zhang et al. (2017) that underlined the effectiveness of glycerosomes as topical carriers for paeoniflorin. The in vitro skin permeation studies shown that glycerol increase the paeoniflorin affinity with the water dermis layers, thus enhancing the nanocarrier ability to cross the stratum corneum.

Ethosomes contain high amount of ethanol (20-45%), they can interact with amphipatic intercellular polar head of the lipids reducing lipids melting point and modifying stratum corneum permeability. Various reports underlined the ability of ethosomes in enhancing skin permeability and facilitating the drug diffusion into deeper skin layers (Natsheh, Vettorato, and Touitou 2019; Nauman Rahim Khan and Wong 2018; Marto et al. 2016).

Zhang et al. (2014) demonstrated that psoralen loaded ethosomes was able to penetrate deeply into the skin.These liposomal formulations exhibit superior skin penetration ability and are able to transport the active substances more effectively through stratum corneum and the deeper layers of the skin. Besides, some authors use a combination of different cosolvents to improve the properties of nanocarriers (Manconi et al. 2019).

Moreover, the efficacy of the formulations could be improved by using polymers biodegradables and biocompatibles as alginate or pullulan. Alginate, an anionic polysaccharide is able to form hydrogel networks with divalent cations or cross-linking agents. This has been widely used in the field of controlled release, ion exchange, and in the vapor-permeation membrane-separation technique (Llorens-Gámez and Serrano-Aroca 2018).

Pullulan, a highly water-soluble biodegradable homopolysaccharide consisting of maltotriose units has been widely used as coating agent and as an additive in drug delivery systems (Y. Wang et al. 2019).

Among the biopolymer for biomedical applications chitosan, gelatin and hyaluronic acid are the most widely used in the last years as key components in liposomal and nanoemulsion formulations.

Chitosan, poly β (1, 4) 2-amino-2-deoxy-D-glucose is a hydrophilic polymer obtained industrially by hydrolysis of the aminoacetyl groups of chitins by alkaline treatment. His mucoadhesive and biocompatible properties have been used in biomedical fields for tissue engineering, drug delivery and wound therapy (Mengoni et al. 2017). In addition, chitosan is able to open the tight junctions modifying keratin structure, fluidifying the lipid bilayer and enhancing the permeation of the drug through the skin. Thomas L. et al. (2017) investigated the influence of chitosan in wound healing in combination with curcumin loaded in nanoemulsions. Results showed that chitosan accelerate polymononuclear cells infiltration, improve collagen production and fibroblast proliferation.

Recently, Lee et al. (2019) demonstrated the potential effect of chitosan coated liposomes in enhancing the permeation of indocyanine green through the skin for photodynamic therapy of melanoma, besides the polymer on liposome surface conferred a great stability to the system.

Gelatin, biodegradable and thermally denatured protein derived from collagen, has been widely used for the formulation of controlled release systems. Modifying its isoelectric point at physiological pH, gelatin positively charged (gelatin A) can be obtained by acidic treatment, while gelatin negatively charged (gelatin B) is obtained by alkaline treatment (X. Wang et al. 2017). Hathout el al. (2017) confirms that vesicles with gelatin are efficient systems to control the release of hydrophilic molecules such as sodium salicylate**.**

Hyaluronic acid (HA) is widely use for the treatment of skin diseases and seems to be an attractive candidate for the delivery of natural compounds into and through the skin (Fallacara et al. 2018a). It is a linear polysaccharide composed of D-glucuronic acid units linked by β (1—> 4) bonds and by 2-acetamido-2-deoxy-β-residues D glucose bound according to a β (1—> 3) pattern. Hyaluronic acid exhibits biomedical implications in tissue

regeneration (Bukhari et al. 2018), specific tumor-targeting affinity for CD44 cancer cells (J. H. Kim et al. 2018) and anti-inflammatory diseases (Chen et al. 2018). In aqueous solutions HA forms viscoelastic gels that in the skin provide beneficial effects such as skin hydration and regeneration. However, the mechanisms of HA mediated skin penetration are still poorly understood. There are differents hypothesis: some authors suggest that the general effect of skin hydration may facilitate the absorption and retention of natural compounds within the more hydrated epidermal layers involving an active transport via HA receptors. Others propose that the HA skin penetration can facilitate flavonoid delivery via a cotransport (Witting et al. 2015).

Advances in nanotechnology have underlined the beneficial effect connected with the use of HA and its derivates as biomaterial for the formulation of drug delivery systems able to promote the healing of dermal and subcutaneous wound of various etiologies**.**

Most studies have reported that hyaluronic acid and its salt are able to improve transdermal drug delivery and stabilize the formulations (M. L. Manca et al. 2015; Castangia et al. 2016; Son et al. 2017)**.**

Berlitz et al. (2019) developed azelaic acid loaded nanoemulsion with hyaluronic acid. The use of hyaluronic acid in combination with nanocarriers provided a controlled delivery of the drug and increase its retention in the deeper layers of the skin. Besides, it states that hyaluronic acid has receptors in dermal fibroblasts and epidermal keratinocytes, which increases affinity for these cells, maintaining the drug at the site of action for a longer time. Kawar et al. (2019) prepared and tested hyaluronic acid gel-core liposomes containing ketoprofen. The presence of hyaluronic acid in liposomal formulations increase by 3-fold the transdermal permeation in comparison with ethosomes, liposomes and propylene glycol (PG)-liposomes. In this work the authors hypothesize that long chains of hyaluronic acid can jut out of vesicles and producing system steric stabilization.

Considering all these aspects, the aim of this research was the incorporation of mangiferin and naringin into innovative nanocarriers and the evaluation of their therapeutic potential for the treatment of inflammatory skin diseases such as psoriasis and atopic dermatitis. Mangiferin was formulated into nanoemulsions stabilized with hyaluronate gels and into new phospholipid vesicles called glycethosomes. Naringin was incorporated into

transfersomes aiming at improving its stability and delivery into and through the skin. In addition, to evaluate the possible synergistic effect connected with the combination of mangiferin and naringin, innovative vesicles were formulated as well by using different hydrating medium to obtain transfersomes, glycethosomes, glycerosomes, glycethohyalurosomes and glycerohyalurosomes.

In view of the importance of using biocompatible materials for a better stabilization of the formulation and aiming at promoting the performance of the delivery systems, a natural biopolymer as hyaluronic acid and specific penetration enhancers such as glycerol, ethanol, tween 80 and Transcutol-P were selected and included in the vesicular and nanoemulsion formulations.

It is well known that interactions between the skin and these nanocarriers mainly depend on the physicochemical properties of the different components. For these reasons, the most important physico-chemical properties of liposomes and nanoemulsions (particle size and their distribution, zeta potential, visual outward, encapsulation efficiency) are evaluated by using different techniques.

The size and size distribution of particles, has been evaluated by size-exclusion chromatography, dynamic light scattering (DLS) and field-flow fractionation. DLS is based on the Brownian motion of the dispersed particles. The particles movement occurs thanks to the energy transferred when the particles collide with the molecules of the solvent. The light scattered by the particle is detected at a certain angle over time and the resulting signal determine the particle size by means of the Stokes-Einstein equation. The distribution of size populations within a sample is determined by the PDI (polydispersity index). The numerical PDI value represents the homogeneity (PDI < 0.3) or heterogeneity (PDI ~0.8 - 1) of particles sizes (Malm and Corbett 2019). Microscopic techniques are also been used to study the particle size and the morphology of the nanocarriers. Among others, transmission electron microscope (TEM) is the most commonly used. However, this method can cause structural change of the samples. To avoid this problem and to achieve a better differentiation, cryo-transmission electron microscopy (cryo-TEM) and freeze-fracture TEM (FF-TEM) techniques have been commonly used for liposome and nanoemulsions analysis (Franken, Boekema, and Stuart 2017). Zeta potential

determination provides important information about the surface charge of nanocarriers. The electrophoretic light scattering has been used to determine particle velocity under an electric field which allows zeta potential calculation. Zeta potential is altered by pH, ionic strength and ions present in the dispersant liquid (Jain and Thareja 2019).

The amount of natural compound loaded into nanocarriers represents a critical parameter of the formulations, especially when the delivery of the active agent to a specific target tissue is requested. The encapsulation efficiency can be measured by using different procedures such as filtration, filtration–centrifugation, ultracentrifugation, or dialysis membrane (Sánchez-López et al. 2019).

The characterizations of these nanocarriers represent a critical step which enable the researchers to predict their behavior both in vitro and in vivo. To evaluate the potential of these systems as future commercial products for the treatment of skin disease, is important to determine their ability to penetrate and permeate the skin by using Franz diffusion cells and by choosing the appropriate skin model. There are clear variations in dermal absorption between different animals and human skin due to physiological differences. However, anatomical investigations show comparable characteristics between porcine ear skin and human skin with respect to epidermal thickness and the stratum corneum (Todo 2017). Excised human skin obtained from plastic surgery and reconstructed human epidermis has been also employed to investigate the mechanism of action of lipid-based nanocarriers for the delivery of flavonoid into and through the skin. The use of reconstructed human epidermis has been recently reviewed and it was concluded that some models (SkinEthic®, EpiSkin®, and EpiDerm®) are closed to human skin in some aspects as their structure, composition and biochemical features are similar. Unfortunately, their major limitation is their relatively weak barrier nature, which makes them more permeable (Pedrosa et al. 2017). Besides, the optimal receptor solutions that do not damage skin membranes and provide sink conditions need to be evaluated considering the properties of the natural products.

Other important aspects are the control of the release of the payload and the rheological properties of the systems. The release kinetics of the natural compounds is described by using different kinetic models (Higuchi model, zero order and first order). The possible

supramolecular interactions between the different components of both vesicles and nanoemulsions can be evaluated by rheological assays by means of flow tests (to evaluate the flow properties of the different systems and determine the viscosity and values shear thinning behavior) and oscillatory test (to obtain information about the internal structure of the systems) (Walicka, Falicki, and Iwanowska-Chomiak 2019). FTIR spectroscopy is another important technique that can be used to provide information regarding the possible structural interactions and conformational rearrangements taking place between molecules. It is complementary to rheological measurements and it can provide the qualitative and quantitative chemical composition of the studied system (Mohamed et al. 2017).

Further in vitro experiments with cells are necessary to evaluate the biocompatibility and antioxidant activity of nanocarriers especially when an inflammatory disorder should be treated. Indeed, reactive oxygen species as hydrogen peroxide, are important factor relationed with the wound healing process since mediate angiogenesis, fibroblast proliferation and enhance re-epithelialization. Some authors confirmed that higher cellular uptake of lipid-based nanocarriers containing antioxidant substances led to a faster wound healing (Hajialyani et al. 2018).

To analyze the complex biochemical processes of wound repair and to evaluate the effective role of different polyphenols containig nanocarriers on reducing/counteracting the inflammatory response associated with psoriasis and atopic dermatitis pathogenesis, animals' models have been studied. Animal models of cutaneous inflammation as carrageenan-Induced Paw Edema (widely used to assess the anti-inflammatory activity, is associated with cyclooxygenase pathway), TPA-Induced skin edema (12-O-tetradecanoylphorbol-13-acetate is used in mouse skin to induce oxidative stress, oedema and infiltration of inflammatory cells), Oxazolone-Induced Ear Edema (increases CD8+ T-lymphocytes and produces skin sensitization, repeated application of oxazolone induces chronic contact dermatitis) and Arachidonic Acid-Induced Ear Edema (ear edema is due to produce leukotrienes and prostaglandins), among others, are employed to identify the effectiveness of the selected compounds on the treatment of inflammatory skin diseases (Patil et al. 2019).

The new mangiferin and naringin nanocarriers formulated during this research, were deeply characterized by using most of the above-mentioned techniques (Cryo-TEM, TEM, Photon Correlation Spectroscopy, Rheological studies, FTIR). In vitro permeation studies were performed to evaluate the accumulation and distribution of mangiferin and naringin into and through the skin. Moreover, an extensive in vitro study was carried out to assess the biocompatibility and the protective effect of the formulations against oxidative stress damages in mouse fibroblast cells, along with an in vivo study to evaluate the wound healing effectiveness in a mouse model (TPA murine model).

OBJECTIVES

1. Design of innovative formulations based on nanosystems for the topical administration of natural anti-inflammatory and antioxidant products such as naringin and mangiferin, for the treatment of chronic inflammatory skin diseases;

2. Evaluation of the physico-chemical properties of the developed formulations by using different techniques (TEM, Cryo-TEM, Photon Correlation Spectroscopy, Rheological studies, FTIR);

3. In vitro evaluation of the permeation/retention capacity of the formulations tested, by using Franz diffusion cells;

4. Evaluation of the biocompatibility and the protective effect of the formulations against oxidative stress damages by using fibroblast cells;

5. Determination of the anti-inflammatory effectiveness of these formulations in CD-1 mice by using TPA model and evaluation of their possible therapeutic application as coadjuvant treatment;

6. Comparison between the results obtained aiming at defining the most suitable nanovehicle composition for mangiferin and naringin.

EXPERIMENTAL SECTION

1. Nanoformulations preparation

Preformulation studies were carried out to evaluate the best composition able to incorporate naringin in transferosomes and mangiferin in both nanoemulsions and glycethosomes. The preparation of naringin ultradeformables liposomes and mangiferin glycethosomes was similar. The buffer phosphate solution (pH 7.4) and the glycerol: ethanol: water blend (50:25:25) were used to hydrate lipoid S75 and tween 80 in naringin and mangiferin vesicles, respectively. Different amounts of flavonoids were added in these systems: 3, 6 and 9 mg/mL for naringin ultradeformable vesicles and 2, 4, 6 and 8 mg/mL for mangiferin glycethosomes. The obtained dispersions were sonicated for 4 min with an ultrasonic disintegrator and then extruded through a 0.20 µm membrane to improve the homogeneity of the systems.

Mangiferin nanoemulsions containing hyaluronate gels were formulated by using a two steps procedure: firstly the aqueous phase containing mangiferin, glycerin and hyaluronic acid at different molecular weight, and the oil phase containing lipoid S75, tween 80, tocopherol, almond oil and Transcutol-P (if present) were mixed together by homogenizing them with an Ultraturrax at 10.000 rpm. In the second step, an ultrasonic disintegrator equipped with a continuous Flow Vessel surrounded by a cooling jacket were used (3 cycles of 10 min).

Mangiferin-naringin were co-loaded in different types of vesicles: transfersomes, glycerosomes, glycethosomes, glycethohyalurosomes and glycerohyalurosomes. Different dispersion medium have been used to hydrate the lipid phase: a) 33.33% ethanol, 33.33% glycerol, 33.33% water; b) 20% ethanol, 40% glycerol, 40% water; c) 33.33% ethanol, 33.33% glycerol, 33.33% sodium hyaluronate solution d) 20% ethanol, 40% glycerol, 40% sodium hyaluronate solution, to obtain glycethosomes A, glycethosomes B, glycethohyalurosomes A and glycethohyalurosomes B, respectively. The dispersions were sonicated during 4 min with an ultrasonic disintegrator to reduce vesicle size and improve the homogeneity of the systems.

All nanocarriers (1mL), irrespective of their composition, were purified from the non-incorporated bioactives by dialysis by using Spectra/Por® membranes (12–14 kDa MW cut-

off, 3 nm pore size; Spectrum Laboratories Inc., DG Breda, the Netherlands) at room temperature. Empty nanoformulations were prepared as well, and used as references.

2. Nanoformulations characterization

Morphology and formation of nanoformulations were confirmed by cryogenic Transmission Electron Microscopy (cryo-TEM) and Transmission electron microscopy (TEM). For cryo-TEM analyses, a thin aqueous film was formed by placing a sample drop on a glow-discharged holey carbon grid and then blotting the grid against filter paper. The film was vitrified by plunging the grid into ethane using a Vitrobot. The vitreous films were transferred to a Tecnai F20 TEM and the samples were observed in a low-dose mode at 200 Kv and at a temperature ~173°C.

TEM analyses were performed by using a JEM-1010 microscope, equipped with a digital camera MegaView III. Samples were spread on the coated copper grids and stained with phosphotungstic acid (2%, w/w) before observation. Images were acquired at an accelerating voltage of 80 KV.

Mangiferin glycethosomes were examined by cryo-TEM, while mangiferin nanoemulsions and naringin ultradeformables liposomes by TEM.

The average diameter, polydispersity index (PDI) and zeta potential of nanoformulations were measured by Dynamic and Electrophoretic Light Scattering using a Zetasizer nano-ZS (Malvern Instruments, Worcestershire, UK).

The entrapment efficiency (EE) of transferosomes and glycethosomes was measured as the percentage of the amount of flavonoid recovered after dialysis versus the amount initially used. The flavonoids content was measured by HPLC after disruption of non-dialysed and dialysed vesicles with Triton X-100 (10%) or methanol (1:100), by using a Perkin Elmer® Series 200 equipped with a photodiode array UV detector. The detection of naringin was performed at 280 nm by using a mixture of methanol and ultrapure water adjusted at pH 4 (50:50, v/v) as mobile phase. Mangiferin was detected at 254 nm and an isocratic mobile phase composed of a mixture of hydrochloric acid (pH 4.0) and methanol (60:40, v/v) was used. For mangiferin-naringin vesicles the entrapment efficiency was expressed as the percentage of antioxidant activity of dialyzed samples versus non-dialyzed samples. The antioxidant activity of both flavonoids was assessed by means of the DPPH test, in other

words by measuring the ability of both drugs to scavenge the DPPH radical. An extensive rheological analysis and Fourier transform infrared studies (FTIR) were carried out to investigate the possible supramolecular interactions between the different components of the nanoformulations. FTIR assays were performed at room temperature by using ATR Agilent Cary 630 in a spectral region between 500 and 4000 cm^{-1}. Rheological measurements were carried out by using a rheometer equipped with a Haake K10 thermostatic bath for temperature control. Before rheological analyses, samples were allowed to rest for at least 300s for stress relaxation and temperature equilibrium. Two types of rheological measurements were performed: flow curves and amplitude oscillation sweep tests. Step flow curves were performed in controlled stress mode and the viscosities results were fitted to the simplified Carreau model. Oscillatory measurements were performed in the linear viscoelastic region (LVR) at a constant stress, only the frequency was modified from 0.01 to 10 Hz (9 points per decade).

3. In vitro skin delivery

Experiments were carried out by using Franz diffusion cells. The full-thickness epidermis obtained by heat separation (Chilcott et al. 2001), was placed between the donor and receptor compartments of Franz diffusion vertical cells. In the case of mangiferin-naringin vesicles full thickness skin was used. The receptor compartment was filled with tween 80 (1%) aqueous solution or buffer phosphate solution (pH 7.4), continuously stirred and thermostated at 37°C. Nanoformulations were applied onto the skin surface and at regular intervals of time, the receiving solution was withdrawn and replaced with the same volume of pre-thermostated fresh aqueous solution up to 24 h. To verify the integrity of the epidermis, 1 mL of phenol red solution was applied on the skin surface. After 24 h the epidermis was removed and putted in glass vials with methanol and maintained under constant stirring to allow the complete extraction of flavonoids, then the extractive solution was analyzed by HPLC. In the case of mangiferin-naringin vesicles, at the end of the experiment (24 h), the skin was removed from the Franz diffusion cells, the stratum corneum was separated by stripping with adhesive tape, while epidermis and dermis were separated with a surgical scalpel. The tape strips and the skin strata were cut, placed each in in glass vials with methanol and sonicated for 2 min (Vitonyte et al. 2017) to ensure the

complete extraction of the bioactives from the skin. All the extractive dispersions were filtered and assayed for mangiferin and naringin content by HPLC (isocratic mobile phase was composed of a mixture of hydrochloric acid (pH 4.0) and methanol (50:50, v/v).

4. In vitro biocompatibility and antioxidant activity of nanoformulations

Cell viability was evaluated by means of MTT [3 (4,5-dimethylthiazolyl-2)-2,5-diphenyltetrazolium bromide] colorimetric assay. Fibroblasts (3T3 cells) were seeded into 96-well plates, cultured for 24 h, and exposed to the samples properly diluted with medium to achieve the desired concentration of flavonoids. Afterwards, MTT was added to each well, and then, after 3 h the formazan crystals formed were dissolved in DMSO and the number of alive cells was determined by measuring the absorbance of the final solution at 570 nm. The results are presented as a percentage of untreated cells (100% viability).

To evaluate the protective effect of the nanoformulations against oxidative damages induced in fibroblast with hydrogen peroxide, cells were seeded into 96-well plates, incubated for 24 h, and exposed simultaneously to hydrogen peroxide (appropriately diluted) and nanoformulations. After 4 h, cells were washed with PBS, and the MTT assay was performed to evaluate the protective effect of the samples against death caused by oxidative stress. Untreated cells (100% viability) were used as a negative control, and cells exposed to hydrogen peroxide only were used as a positive control.

5. Evaluation of the effectiveness of nanoformulations: TPA model of mice

Inflammation and ulceration were induced by topically applying TPA dissolved in acetone (3 µg/20 µL) to the shaved dorsal area of female CD-1 mice. All nanoformulations were applied as well, in the same site 3 h after TPA application. The protocol was repeated for 3 days. Mice were sacrificed on day fourth by cervical dislocation and the treated dorsal skin was excised and weighed to evaluate oedema and MPO inhibition. For histological assays, skin samples were fixed in 0.4% formaldehyde and analyzed using a light microscope, after having stained the skin with hematoxylin and eosin.

Myeloperoxidase activity was evaluated by homogenizing skin biopsies in 750 µL of phosphate buffer (pH 5.4) with an Ultra-Turrax T25, the dispersion was then centrifuged at 10.000 g for 15 min at 4 °C and the obtained supernatant was incubated with a mixture of

sodium phosphate buffer (pH 5.4), phosphate buffer (pH 7.4), hydrogen peroxide and 3,30,5,50-tetramethylbenzidine dihydrochloride. The reaction was stopped by using H_2SO_4 2 N and the absorbance of the final solution was measured at 450 nm.

RESEARCH ARTICLES

CHAPTER I.

A novel ultradeformable liposomes of Naringin for anti-inflammatory therapy

Pleguezuelos-Villa M, Mir-Palomo S, Díez-Sales O, Buso MAOV, Sauri AR, Nácher A.

Colloids Surf B Biointerfaces (2018) 162:265–270

A novel ultradeformable liposomes of Naringin for anti-inflammatory therapy

María Pleguezuelos-Villa[1, *], Silvia Mir-Palomo[1], Octavio Díez-Sales [1,2], M.A. Ofelia Vila Buso[3], Amparo Ruiz Sauri [4], Amparo Nácher[1, 2].

[1]Department of Pharmacy, Pharmaceutical Technology and Parasitology, Faculty of Pharmacy, University of Valencia, Av. Vicent Andrés Estellés s/n, 46100, Burjassot, Valencia, Spain.

[2]Instituto Interuniversitario de Investigación de Reconocimiento Molecular y Desarrollo Tecnológico (IDM), Universitat Politècnica de València, Universitat de València, Av. Vicent Andrés Estellés s/n, 46100, Burjassot, Valencia, Spain.

[3]Department of Physical Chemistry, Faculty of Pharmacy, University of Valencia, Av. Vicent Andrés Estellés s/n, 46100, Burjassot, Valencia, Spain.

[4] Department of Pathology, University of Valencia, Av. Blasco Ibañez 17, 46010 Valencia, Spain.

***Corresponding author**: M. Pleguezuelos-Villa; e-mail address: maplevi@alumni.uv.es

Abstract

Ultradeformable liposomes were formulated using naringin (NA), a flavanone glycoside, at different concentrations (3, 6 and 9 mg/mL). Nanovesicles were small size (~100 nm), regardless of the NA concentration used, and monodisperse (PI < 0.30). All formulations showed a high entrapment efficiency (~88%) and a highly negative zeta potential (around -30 mV). The selected formulations were highly biocompatible as confirmed by *in vitro* studies using 3T3 fibroblasts. *In vitro* assay showed that the amounts (%) of NA accumulated in the epidermis (~ 10%) could explain the anti-inflammatory properties of ultradeformable liposomes. *In vivo* studies confirmed the higher effectiveness of ultradeformable liposomes respect to betamethasone cream and NA dispersion in reducing skin inflammation in mice. Overall, it can conclude that NA ultradeformable liposomes can be considered as a promising formulation for the treatment of skin inflammatory diseases.

Keywords: naringin, ultradeformable liposomes, anti-inflammatory, transdermal penetration, fibroblasts, *in vivo* studies

1. Introduction

The incidence of skin inflammatory diseases (dermatitis, psoriasis, rash) has increased significantly in the last decades and bioflavonoids such as quercetin, curcumin and baicalin have been widely used for treatment of this injures [1-4]. Citrus fruits peels represent an important source of phenolic acids and flavonoids, mainly polymethoxyflavones (PMFs), flavanones and glycosylated flavanones [5,6]. Naringin (NA), a bioactive component of citrus species, is a glycosylated flavanone formed by naringenin (flavanone) and the disaccharide neohesperidose (Fig.1).

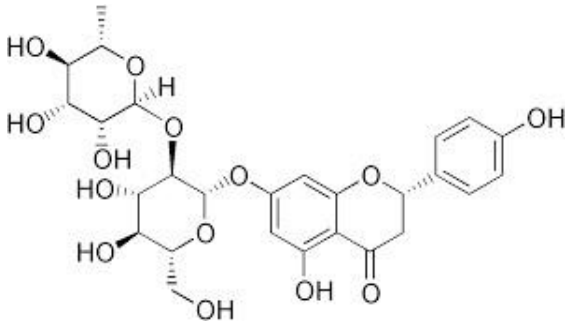

Fig 1. Chemical structure of Naringin (NA).

This compound shows a wide variety of pharmacological effects such as antioxidant, blood lipid–lowering and anticarcinogenic activity. Moreover, several studies have highlighted its potential to suppress the production of proinflammatory cytokines and attenuate the inflammatory response [7-12] and it has been proposed in combination with corticoids to treat skin diseases such as dermatitis [13].

On the other hand, most of conventional therapies failed because of their low capacity to deliver therapeutic drug concentrations to the target tissue. Different approaches have been attempted to overcome this problem by providing “selective” delivery of drugs to the affected area, using various pharmaceutical carriers. In the last years, among the different types of particulate carriers, liposomes have received a great attention [14] and have been used as delivery systems of different bioactive agents. The list of actives incorporated in nanoliposomes is huge, ranging from pharmaceutical to cosmetics and nutraceuticals substances (opiods, curcumin, resveratrol, quercetin, silibinin, glycyrrhizic acid, vitamin C, and others) [15-21]. In general, these systems are able to enhance the performance of the incorporated bioactive agents by improving their solubility and bioavailability, their *in vitro*

and *in vivo* stability, as well as preventing their unwanted interactions with other molecules [22, 23]. Another advantage of nanoliposomes is cell-specific targeting, which is a prerequisite to ensure the adequate drug concentrations required for optimum therapeutic effects in the target site while minimizing adverse effects on healthy cells and tissues. Among them, ultradeformable liposomes have been found to be promising for herbal extracts delivery [6,24]. Since, this type of phospholipid vehicles increases the accumulation on the skin as well as reduces adverse effects. Recent reports showed that ultradeformable nanosized liposomes may be postulated as a novel dermal delivery carrier due to their biocompatibility and high elasticity [25, 26], which is attributed to of the combination of phospholipids and surfactant (such as sodium cholate, deoxycholate, Span, Tween and dipotasium glycyrrhizinate). The surfactant acts as an ´edge activator´ that modify the organization of the lipid bilayers increasing its deformability [27].

The purpose of this study is to develop ultradeformable liposomes. To do this, the vesicles were formulated using different concentrations of naringin (NA) and characterized in terms of zeta potential, mean size, size distribution and vesicles encapsulation efficiency. *In vitro* transdermal penetration was also quantified. Cytotoxicity test was carried out as well to evaluate the biocompatibility of the formulations on 3T3 mouse dermal fibroblast cells. In addition, NA ultradeformable liposomes ability to attenuate skin inflammation induced by phorbol 1, 2-myristate 1, 3-acetate (TPA) in mice was studied.

2. Materials and methods

2.1. Materials

Monosodium phosphate was purchased from Panreac quimica S.A. (Barcelona, Spain). Lipoid® S75, a mixture of soybean lecithin containing lysophosphatidylcholine (3% maximum), phosphatidylcholine (70%), phosphatidylethanolamine (10%), fatty acids (0.5% maximum), triglycerides (3% maximum), and tocopherol (0.1–0.2%) were a gift from Lipoid GmbH (Ludwigshafen, Germany). Polysorbate 80 was purchased from Scharlab S.L. (Barcelona, Spain). Glycerin and ethanol were purchased from Guinama S.L.U. (Valencia, Spain), N-octanol (special grade for measurement of partition coefficients) was purchased from VWR chemicals S.A. S (France), Disodium phosphate were purchased from Scharlab

S.L. (Barcelona, Spain). Betamethasone was from IFC Acofarma S.A. (Santander, Spain). Phorbol 1,2-myristate 1,3-acetate and naringin with a molecular formula ($C_{27}H_{32}O_{14}$) and weight (580.54 g/mol) were purchased from Sigma-Aldrich.

2.2. Analytical method

A high-performance liquid chromatograph (HPLC) PerkinElmer® Series 200 equipped with an auto-injector and a photodiode array UV detector was used for NA quantification in experimental samples [28]. The column used was a Teknokroma® Brisa "LC2" C18, 5.0 µm (150 cm x 4.6 mm). The mobile phase consisted of a mixture 50:50 (V/V) of methanol and ultrapure water adjusted at pH 4. The detection wavelength was 280 nm, the injection volume was 20 µL and the flow rate was 1.0 mL/min. Linearity, limit of quantification (LOQ), detection (LOD), precision and accuracy of the analytic method were carried out.

2.3. Physicochemical properties

2.3.1. Crystalline structure

NA structure was analyzed with the X-ray diffractometer KAPPA CCD. The system has a goniometer of four circles and a two-dimensional KAPPA CCD detector with beryllium window of 90 mm diameter maintained at - 60°C.

2.3.2. Solubility

The solubility of the flavonoid at 25°C was determined in different vehicles: water, pH 7.4 buffered solution and polysorbate 80 (1%, w/w) in aqueous medium. Flavonoid was added to saturation in each system during 24 hours under constant agitation (500 rpm). Finally, an aliquot of each sample was filtered (0.22 µm) and quantified.

2.3.3. Partition coefficient determination

Octanol-water partition coefficient (P_{oct}) value was obtained by equilibrating the NA aqueous solution with 1-octanol in a shaker bath at 25ºC overnight [29]. Distribution of NA between the aqueous and the organic phase was estimated by the differences between the NA concentration at the beginning and at the equilibrium step, according to the following equation (Eq. (1)):

$$P_{oct} = \frac{(Co - Ce)/Vo}{Co/Va} \quad (1)$$

where C_o, is the initial NA aqueous solution concentration, C_e, the solution concentration at equilibrium, V_o, volume of the organic phase (50 mL) and V_a, the volume of aqueous solution (50 mL).

2.4. Ultradeformable liposomes

A preformulation studies was carried out in order to select the best formulations able to load increasing amount of NA (from 1 to 24 mg/mL). According to stability data (average particle size <150 nm, polydispersity values < 0.5 and zeta potential value < -25 mV), one formulation was selected with different amount of NA: liposomes I (3 mg/mL), liposomes II (6 mg/mL) and liposomes III (9 mg/mL). NA (3 or 6 or 9 mg/mL), polysorbate 80 (2.5 mg/mL) and Lipoid® S75 (120 mg/mL) were added in a glass vial. These mixtures were hydrated overnight at room temperature (25°C) with a buffer phosphate solution (pH 7.4). The obtained dispersions were sonicated for 4 min using an ultrasonic disintegrator (CY-500, Optic Ivymen system, Barcelona, Spain). Then liposome suspensions were extruded through a 0.20 µm membrane with an Avanti® Mini-Extruder (Avanti Polar Lipids, Alabaster, Alabama) to obtain homogeneous dispersions. NA dispersion (9 mg/mL) in phosphate buffer solution containing polysorbate 80 (1%, w/w) and empty liposomes (without NA) were prepared as control.

2.5. Characterization of liposomes

2.5.1. Transmission electron microscopy

Ultradeformable liposomes morphology was examined through a negative staining technique using a JEM-1010 microscope (Jeol Europe, Croissy-sur-Seine, France), equipped with a digital camera MegaView III at an accelerating voltage of 80 Kv.

2.5.2. Determination of entrapment efficiency (EE %)

1 mL of each sample and dialyzed against buffer (100 mL) for 24 hours, at room temperature using a membrane Spectra/Por, (12–14 kDa MW cut-off; Spectrum Laboratories Inc., DG Breda, The Netherlands). Dialyzed and non-dialyzed ultradeformable liposomes were disrupted with methanol (1:100). The samples were assayed by HPLC as described in Section 2.2.

EE (%) of liposomes I, II and III was calculated as follows (Eq. (2)):

$$\text{EE } \% = \left(\frac{\text{actual NA}}{\text{initial NA}}\right) \text{X } 100 \qquad (2)$$

where actual NA is the amount of the active in ultradeformable liposomes after dialysis, and initial NA is the amount before dialysis.

2.5.3. Determination of vesicle size, zeta potential and polydispersity index

Average diameter and polydispersity index (PI) of the samples were performed in triplicate by means of Photon Correlation Spectroscopy using a Zetasizer Nano-S® (Malvern Instruments, Worcester-shire, United Kingdom) at 25ºC. Moreover, zeta potential was estimated by electrophoretic light scattering in a thermostated cell in a Zetasizer Nano-S®. The ultradeformable liposomes stability was evaluated over 30 days at ~ 4°C.

2.6. Cell viability studies

3T3 mouse fibroblasts (ATCC, Manassas, VA, USA) were cultured in Dulbecco's modified Eagle's medium (DMEM, Sigma Aldrich, Spain), supplemented with penicillin (100 U/mL), 10% (V/V) fetal bovine serum, and streptomycin (100 mg/mL) (Sigma Aldrich, Spain) in 5% CO_2 incubator at 37 °C to maintain cell growth.

3T3 cells ($2x10^5$ cells/well) were seeded in 96-well plates at passage 14-15. After one day of incubation, 3T3 cells were treated with NA dispersion (9 mg/mL) or empty or NA loaded liposomes I, II and III for 24 hours. In each well 25 µL of formulation were added and filled with 225 µL of cultured medium.

Cell viability was evaluated by MTT [3 (4,5-dimethylthiazolyl-2)-2,5-diphenyltetrazolium bromide] colorimetric assay [30]. After 24 h experiment, 100 µL of MTT was added to each well, and then, after 3 h the formazan crystals formed were dissolved in DMSO (50 µL). The

reaction was measured at 570 nm with a spectrophotometer. All experiments were repeated three-fold (n=3).

2.7. *In vitro* diffusion

A diffusion study was performed using Franz diffusion cells (with an effective diffusion area of 0.784 cm^2) and new born pig skin from a local slaughterhouse. The receptor compartment (CR) was filled with buffer phosphate solution (pH 7.4), continuously stirred and thermostated at 32ºC. Epidermal membranes were obtained from heat separation through immersing in water (at 60ºC) for 75 s [31]. On the epidermis surface 800 µL of different formulations assayed were applied. At different time intervals up to 24 hours, receptor solutions were withdrawn and assayed for drug content by HPLC, (Section 2.2). At the end of the experiment, 1 mL of phenol red solution (0.05%, w/w) was applied in the donor compartment for checking the integrity of the epidermis [32].

2.8. *In vivo* assay

Female CD-1 mice (5–6 weeks old, 25–35 g) were obtained from Harlan laboratories (Barcelona, Spain) and acclimatized for one week before use. All studies were performed in accordance with European Union regulations for the handling and use of laboratory animals and the protocols were approved by the Institutional Animal Care and Use Committee of the University of Valencia (code 2016/VSC/PEA/00112 type 2).

One day before the experiment the back skin of mice (n=4 per group) was shaved. The first day, TPA dissolved in acetone (3 µg/20 µL) was applied to the shaved dorsal area to induce cutaneous inflammation and ulceration. Negative control mice only received acetone (20 µL). After 3 h, 200 µL of empty or NA loaded ultradeformable liposomes (I, II and III), NA dispersion or betamethasone cream (20 mg) were topically applied in the dorsal area. The procedure was repeated on the second and third day. The fourth day, mice were sacrificed by cervical dislocation.

Two biomarkers: oedema formation and myeloperoxidase (MPO) activity were used to evaluate the effect of the formulations [33]. First, dorsal skin area was excised, weighed to assess oedema formation and stored at -80°C. Second, biopsies were dispersed in 750 µL of phosphate buffer (pH 5.4) and, with an Ultra-Turrax T25 homogenizer (IKA1 Werke

GmbH & Co. KG, Staufen, Germany), were homogenized in a ice bath. The supernatant obtained after centrifugation was diluted with PBS 5.4 (1:10) in order to assay MPO activity. Briefly, in a 96-well plate, 10 µL of diluted sample, 20 µL of sodium phosphate buffer (pH 5.4), 200 µL of phosphate buffer (pH 7.4), 40 µL of 0.052% hydrogen peroxide and 20 µL of 18 mM 3,30,5,50-tetramethylbenzidine dihydrochloride were added to each well. At the end of experiment, 50 µL of SO_4H_2 2N was added to stop the reaction. The absorbance was measured at 450 nm. The MPO activity was calculated from the linear portion of a standard curve.

2.9. Histological examination

Mice skin was excised, fixed and stored in formaldehyde (0.4%, V/V). Longitudinal sections (5 mm) were marked with hematoxylin and eosin and observed using a light microscope (DMD 108 Digital Micro-Imaging Device, Leica, Wetzlar, Germany).

2.10. Statistical analysis of data

Statistical differences were determined by one-way ANOVA test and Tukey's test for multiple comparisons with a significance level of $p < 0.05$. All statistical analyses were performed using IBM SPSS statistics 22 for Windows (Valencia, Spain). Data are shown as mean ± standard deviation.

3. Results and discussions

3.1. Analytical method

The analytical method (HPLC) for NA quantification was firstly validated. Calibration curves covering the whole range of NA concentrations were prepared. Excellent plots correlating the peak areas and NA concentrations were obtained ($r > 0.999$), demonstrating good linearity. Precision was evaluated by calculating the relative error (RE, %) and accuracy by coefficient of variation (CV, %); both values were less than 9 %. The limits of detection (LOD) and quantification (LOQ) were 0.11 µg/mL and 0.34 µg/mL, respectively. These data satisfy the standard validation.

3.2. Physicochemical properties

The flavanone glycoside (NA) was characterized with the RX technique. The spectrum shows that it is a flavonoid with crystalline structure. Molecules are spatially distributed in a regular and symmetrical form, so they require more energy for their separation. All this property may be responsible of their low solubility and bioavailability. Indeed, the solubility of NA in water and phosphate buffer at pH 7.4 is 2.69±0.01 mg/mL and 1.94 ± 0.01 mg/mL, respectively. As it was expected, NA is more soluble (14.4±0.4 mg/mL) in presence of polysorbate 80 (1%, w/w), probably because of the formation of micelles, which allows the solubilization of a greater amount of flavonoid. In addition, NA is a hydrophilic compound (log P_{oct}= – 0.66 ± 0.03) with a molecular weight superior to 580 g/mol, which could lead to a low percutaneous absorption.

3.3. Characterization of ultradeformable liposomes

In Fig.2 the formation of spherical nanometric vesicles can be observed.

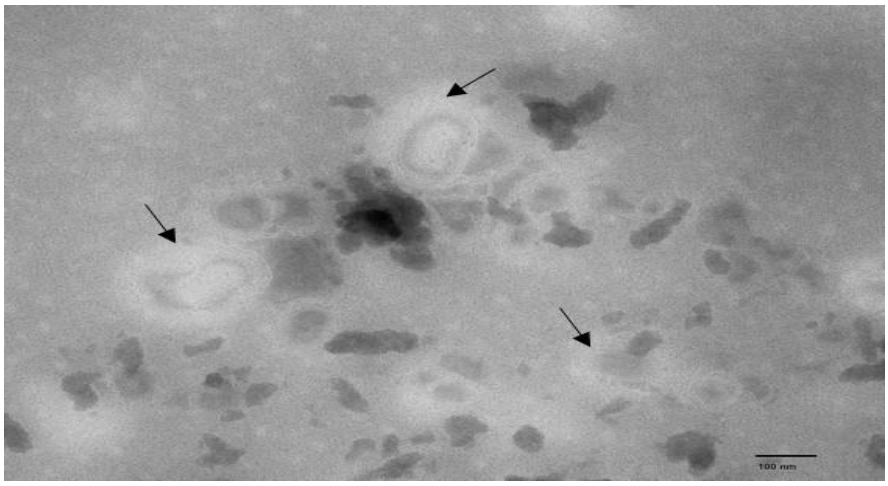

Fig 2. TEM (Transmission electron microscopy) images of ultradeformable liposomes. The arrows indicate the lamellae of vesicles.

All ultradeformable liposomes (I, II and III) showed a monodisperse distribution (PI < 0.30) (Table 1).

Table 1

Average size, polydispersity index (PI), zeta potential and NA (naringin) entrapment efficiency of liposome I (3 mg/mL), liposome II (6 mg/mL) and liposome III (9 mg/mL). All values are mean ± standard deviations (n=3).

Formulations	Size (nm)		PI		Potential Z (mV)		EE (%)
	0 days	30 days	0 days	30 days	0 days	30 days	
Empty liposome	88.3 ± 1.7	100.1 ± 0.8	0.25	0.16	-32.5 ± 0.4	-31.9 ± 1.7	---
Liposome I	90.2 ± 1.6	90.9 ± 2.3	0.23	0.22	-33.9 ± 1.4	-30.1 ± 1.1	91.03 ± 0.04
Liposome II	86 ± 1.0	84.1 ± 2.5	0.25	0.20	-32.6 ± 1.1	-26.9 ± 0.8	88.70 ± 0.25
Liposome III	86.3 ± 1.1	84.6 ±0.9	0.22	0.22	-27.7 ± 1.1	-28.0 ± 1.5	92.72 ± 0.10

In all cases, the mean size was very similar (approximately 100 nm), and no statistical differences were observed from batch to batch. The zeta potential was highly negative (-30 mV), for the different NA concentrations. Liposomes were able to incorporate NA in high amount (entrapment efficiency approximately 90%), no significant differences were detected among the groups (p > 0.05), confirming that the flavonoid was effectively/efficiently incorporated into vesicle. Ultradeformable liposomes were stable during 30 days of storage, according to zeta potential and mean size values (Table 1). Such data ensure good stability of ultradeformable liposomes, due to the great electrostatic repulsion between the vesicles.

3.4. Cell viability studies

The biocompatibility of each formulation was evaluated *in vitro* on cells, which represents a good and reliable method to select formulations that will be used for further *in vivo* studies. 3T3 mouse dermal fibroblasts were incubated with different formulations: empty or NA ultradeformable liposomes (I, II and III). Cells viability after 24 hours of incubation with the formulation is approximately 100% and similar to that of the control group (p > 0.05). These results are in accordance with Cao et al [34], confirming the low toxicity of flavonoid and liposomes.

3.5. *In vitro* diffusion

Permeation study was performed for 24 h using ultradeformable liposomes (I, II and III). Fig.3 shows the cumulative amounts (Q, %) of NA in the donor compartment (CD), epidermis (EP) and receptor compartment (CR) for all formulations tested at 24 hours.

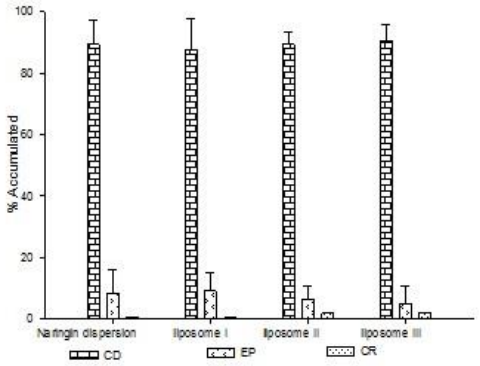

Fig 3. Transdermal permeation of NA (naringin) dispersion and loading liposomes I (3 mg/mL), II (6 mg/mL), III (9 mg/mL). Amount accumulated in CR (receptor compartment), CD (donor compartment) and EP (epidermis) after 24 h at 32°C. The results were expressed as the mean and standard deviation (error bars). No significate differences have been found among the groups ($p > 0.05$).

The cumulative amount of NA (%) in the CR was negligible (less than 0.5 %) regardless the formulation tested. The amounts (%) of NA accumulated in the EP (~ 10%) could explain the anti-inflammatory properties of ultradeformable liposomes detected during the *in vivo* assay. Finally, the amount of NA present in the CD (> 90 %), confirmed the low flavonoid bioavailability. The NA low permeability could be mainly attributed to its difficulty to permeate through the stratum corneum, which serves as a lipophilic barrier against the penetration of hydrophilic molecules (NA has log P oct = - 0.66). In addition, the high molecular weight (~580 g/mol) of NA could have limited its transdermal delivery by the high resistance of skin towards diffusion [35, 36].

3.6. *In vivo* assay

TPA application in mice has been used for the evaluation of anti-inflammatory activity of drugs. This compound induces a variety of histological and biochemical changes in the skin

[37]. In this work, TPA was daily applied on mice dorsal skin for 3 days, inducing skin ulceration, loss of epidermis integrity with scale and crust formation. Besides, it stimulates the oedema formation, due to an increase in vascular permeability. Table 2 summarizes the results obtained. The phorbol ester (TPA) caused a 3-fold increase in skin weight, compared to healthy mice. The administration of liposomes I, II and III was more active than NA dispersion and betamethasone cream in reducing skin oedema (~20%). Statistical differences were observed between samples (p < 0.01), probably because the ultradeformable liposomes promoted the internalization of NA in epithelial cells, avoiding vascular congestion and oedema formation. The MPO activity was quantified as a marker of the inflammatory process, since it is proportional to the neutrophil concentration in the inflamed tissue. The efficacy of NA loaded ultradeformable liposomes was assayed and compared with betamethasone cream, as commercial reference, and NA dispersion. The ultradeformable liposomes displayed a superior ability to reduce MPO activity in the injured tissue respect to the betamethasone cream (Table 2).

Table 2

Oedema inhibition and MPO (myeloperoxidase test) activity in skin mice inflamed with TPA (control +). Skin mice inflamed were treated to 200 µL of NA dispersion, empty liposomes or loading liposomes I (3 mg/mL), II (6 mg/mL), III (9 mg/mL) and betamethasone cream (20 mg). The results were expressed as the mean and standard deviation (error bars). * p < 0.01 liposomes (I, II and III) vs betamethasone cream and NA dispersion. ANOVA-Tukey. # p < 0.01 liposome III vs NA dispersion. ANOVA-Tukey**.**

Formulations	% Oedema inhibition	% MPO inhibition
Control +	0.5 ± 1.15	0.5 ±1.01
Cream	13.06 ± 2.81	12.70 ± 1.81
NA dispersion	27.48 ± 3.37	65.82 ± 2.94
Empty liposome	23.67 ± 2.29	60.25 ± 3.05
Liposome I	36.01* ± 3.03	74.61 ± 4.03
Liposome II	37.29* ± 3.19	78.72 ± 4.59
Liposome III	43.18* ± 3.36	86.75# ± 4.93

No significant differences were observed (p > 0.05) between the three vesicular formulations containing different amounts of NA, which indicates that, in our experimental conditions, ultradeformable liposomes can promote the NA beneficial activity independent of the concentration used. Liposomes (III) have a greater activity respect to NA dispersion (p < 0.01), despite having the same concentration of flavonoid, as shown in Table 2. Thus, this phospholipidic system could be considered as promising tools for treatment of skin inflammation. The macroscopic observations are in agreement with the MPO and oedema values. The macroscopic images of mice clearly showed the positive effect of NA ultradeformable liposomes on injured skin (Fig. 4).

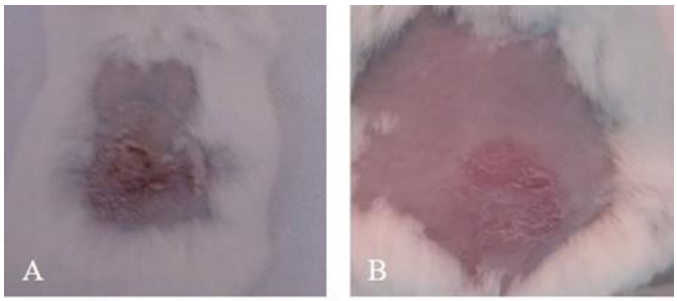

Fig 4. Macroscopic appearance of mice skin lesions inducted with TPA (A) and treated with liposome III: 9 mg/mL (B).

With regard to the histological study, morphological alterations of mice skin exposed to TPA were evaluated by hematoxylin and eosin staining, and compared with untreated skin (Fig. 5).

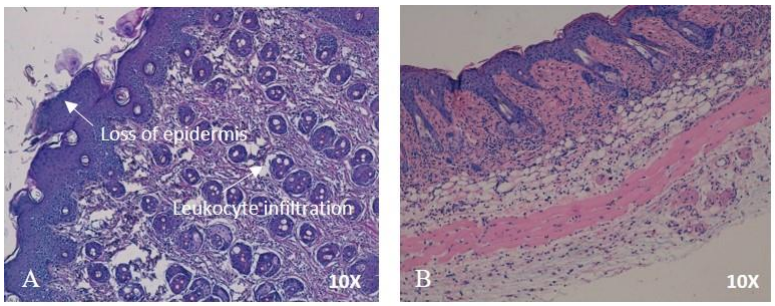

Fig 5. Representative histological sections of mouse skin: treated with TPA-inflamed skin (A) and treated with liposome III: 9 mg/mL (B).

The skin treated with acetone only (control-) showed a regular structure and normal appearance of both epidermis and dermis, as well as the tissues directly underneath (i.e.,

subcutaneous cellular tissue, skeletal muscle and adipose tissue), with only some mononuclear and polymorphonuclear cells in the muscular region. Otherwise, mice skin treated with TPA displayed severe dermal and subcutaneous alteration, with a large number of leukocytes infiltrating, and showing pathological features of inflammatory damage, such as vascular congestion (control +). Similar results of injured skin were obtained using betamethasone cream, but the application of the NA ultradeformable liposomes reduced TPA-induced lesions, along with mild to moderate inflammatory infiltrates of mononuclear cells, eosinophils and neutrophils. Therefore, the results obtained *in vivo* seem to indicate a remarkable therapeutic potential of NA ultradeformable liposomes.

4. Conclusions

The loading of NA into ultradeformable liposomes represents an innovative approach to prevent and treat skin lesion and restore skin integrity. Results demonstrated that NA liposomes were highly biocompatible and more effective than betamethasone cream and NA dispersion as demonstrate *in vivo* model (TPA test). In conclusion NA ultradeformable liposomes can be considered as a promising formulation for the treatment of inflammatory diseases.

Acknowledgment

We wish to express our gratitude to Lipoid GmbH (Ludwigshafen, Germany) for providing the phospholipid used in this work for free.

References

[1] H Chen, Lu C, Liu H, Wang M, Zhao H, Yan Y et al, 2017. Quercetin ameliorates imiquimod-induced psoriasis-like skin inflammation in mice via the NF-κB pathway. International Immunopharmacology. 48, 110-117.

[2] KM Parmar, Itankar PR, Joshi A, Prasad SK, 2017.Anti-psoriatic potential of Solanum xanthocarpum stem in Imiquimod-induced psoriatic mice model. Journal of etnopharmacology.23(198),158-16

[3] M. L Manca., Castangia I, Zaru M, Nácher A, Valenti D, Fernàndez-Busquets et al, 2015. Development of curcumin loaded sodium hyaluronate immobilized vesicles (hyalurosomes) and their potential on skin inflammation and wound restoring. Biomaterials. 71, 100-109.

[4] C Caddeo, Nacher A, Vassallo A, Armentano M. F., Pons R, Fernàndez-Busquets et al,2016. Effect of quercetin and resveratrol co-incorporated in liposomes against inflammatory/oxidative response associated with skin cancer. International journal of pharmaceutics. 513(1), 153-163.

[5] L Castro-Vazquez, Alañon M, Rodriguez-Robledo V, Pérez-Coello M S, Hermosín-Gutierrez, Díaz-Maroto M C, 2016. Bioactive Flavonoids, Antioxidant Behaviour, and Cytoprotective Effects of Dried Grapefruit Peels (Citrus paradisi Macf.). Oxidative Medicine and Cellular Longevity. 2016, 2016:8915729.

[6] M Manconi, Manca M. L, Marongiu F, Caddeo C, Castangia I, Petretto et al, 2016. Chemical characterization of Citrus limon var. pompia and incorporation in phospholipid vesicles for skin delivery. International journal of pharmaceutics.506 (1), 449-457.

[7] R Chen, Qi Q L, Wang M T, Li Q Y, 2016. Therapeutic potential of naringin: an overview. Pharmaceutical Biology.54 (12), 3203-3210.

[8] A Ramakrishnan, Vijayakumar N, Renuka M, 2016. Naringin regulates glutamate-nitric oxide cGMP pathway in ammonium chloride induced neurotoxicity. Biomedecine and pharmacotherapie.84:1717-1726.

[9] S. F Ahmad, Attia S. M, Bakheet S. A, Zoheir K. M, Ansari M. A, Korashy H. M, et al, 2015. Naringin attenuates the development of carrageenan-induced acute lung inflammation through inhibition of NF-κb, STAT3 and pro-inflammatory mediators and enhancement of IκBα and anti-inflammatory cytokines. Inflammation.38 (2), 846-857.

[10] K Gopinath, Sudhandiran G, 2012. Naringin modulates oxidative stress and inflammation in 3-nitropropionic acid-induced neurodegeneration through the activation of nuclear factor-erythroid 2-related factor-2 signalling pathway. Neuroscience. 227, 134-143.

[11] Y. L Luo, Zhang C. C, Li P. B, Nie Y. C, Wu H, Shen J. G. et al, 2012. Naringin attenuates enhanced cough, airway hyperresponsiveness and airway inflammation in a guinea pig model of chronic bronchitis induced by cigarette smoke. International immunopharmacology.13 (3), 301-307.

[12] X Guihua, Shuyin L, Jinliang G, Wang S, 2016. Naringin protects ovalbumin-induced airway inflammation in a mouse model of asthma. Inflammation. 39(2), 891-899.

[13] K Itoh., Masuda M., Naruto S., Murata K., Matsuda H ,2009. Antiallergic activity of unripe Citrus hassaku fruits extract and its flavanone glycosides on chemical substance-induced dermatitis in mice. Journal of natural medicines.63 (4), 443-450.

[14] A Tamer. ElBayoumi and Vladimir P. Torchilin. 2010. Current trends in liposomes research in Liposomes Methods and Protocols, Volkmar Weissig (eds.) volume 1, cap. 1, pp.1-27.

[15] S. Vahabi, A. Eatemadi, 2017.Nanoliposomes encapsulated anesthetics for local anesthesia application. Biomedicine Phaemacotherapy.86,1-7.

[16] N. Kianvash, A. Bahador, M Pourhajibagher, H Ghafari, V Nikoui, SM Rezayat. et al, 2017.Evaluation of propylene glicol nanoliposomes containing curcumin on burn wound model in rat: biocompatibility, wound healing, and anti-bacterial effects. Drug Delivery and Translational Research.

[17] J Rokka, A Snellman, M Kaasalainen, J Salonen, C Zona, B La Ferla et al,2016. (18) F-labeling syntheses and preclinical evaluation of functionalized nanoliposomes for Alzheimer`s disease. European Journal of Pharmaceutical Sciences.10 (88),257-266.

[18] P Ganesan, HM Ko, IS Kim, DK Choi, 2015.Recent trends in the development of nanophytobioactive compounds and delivery systems for their posible role in reducing oxidative stress in Parkinson`s disease models. International Journal Nanomedicine.10,6757-6772.

[19] MM Ochi, G Amoabediny, SM Rezayat, A Akbarzadeh, B Ebrahimi, 2016.In vitro Co-Delivery of Novel Pegylated Nanoliposomal Herbal Drugs of Silibinin and Glycyrrhizic Acid (Nano-Phytosome) to Hepatocellular Carcinoma Cells.Cell.18(2),135-148.

[20] HJ Park, N Liu, 2010.Factors effects on the loading efficiency of Vitamin C loaded chitosan-coated nanoliposomes. Colloids and Surfaces B: Biointerfaces.76 (1),16-19.

[21] S Yang, C Liu, W Liu, H Yu, H Zheng, W Zhou et al, 2013.Preparation and characterization of nanoliposomes entrapping medium-chain fatty acids and vitamin C by lyophilization. International Journal of Molecular Sciences.14(10),19763-19773.

[22] M.R. Mozafari, 2010.Nanoliposomes: Preparation and Analysis in Liposomes Methods and Protocols, Volkmar Weissig (eds.) volume 1, cap. 2, pp.29-50.

[23] PG Kakadia, Conway BR, 2015.Lipid nanoparticles for dermal drug delivery. Current pharmaceutical design. 21(20), 2823-2829.

[24] S Mir-Palomo, Nácher A, Díez-Sales O, Ofelia Vila Busó MA, Caddeo C, Manca ML et al, 2016. Inhibition of skin inflammation by baicalin ultradeformable vesicles. International Journal of Pharmaceutics. 511(1):23-29.

[25] J Vitonyte, Manca M. L., Caddeo C, Valenti D, Peris J. E., Usach I et al, 2017. Bifunctional viscous nanovesicles co-loaded with resveratrol and gallic acid for skin protection against microbial and oxidative injuries. European Journal of Pharmaceutics and Biopharmaceutics. 114, 278-287.

[26] N Kianvash, Bahador A, Pourhajibagher M, Ghafari H, Nikoui V, Rezayat S. M. et al,2017. Evaluation of propylene glycol nanoliposomes containing curcumin on burn wound model in rat: biocompatibility, wound healing, and anti-bacterial effects. Drug Delivery and Translational Research.1-10.

[27] J Chen, Lu W. L, Gu W, Lu S. S, Chen Z. P, Cai B. C ,2013. Skin permeation behavior of elastic liposomes: role of formulation ingredients. Expert opinion on drug delivery.10 (6), 845-856.

[28] LM Cordenonsi, Bromberger NG, Raffin RP, Scherman EE, 2016.Simultaneous separation and sensitive detection of naringin and naringenin in nanoparticles by chromatographic method indicating stability and photodegradation kinetics. Biomedical chromatography. 30(2), 155-162.

[29] G Morikawa, Suzuka C, Shoji A, Shibusawa Y, Yanagida A,2016. High-throughput determination of octanol/water partition coefficients using a shake-flask method and novel two-phase solvent system. Journal of Pharmaceutical and Biomedical Analysis. 117,338-344.

[30] WM Harris, Zhang P, Plastini M, Ortiz T, Kappy N, Benites J, et al, 2017.Evaluation of function and recovery of adipose-derived stem cells after exposure to paclitaxel. Cytotherapy.19 (2), 211-221.

[31] RP Chilcott, Jenner J, Hotchkiss S. A. M, Rice P, 2001. In vitro skin absorption and decontamination of sulphur mustard: comparison of human and pig-ear skin. Journal of applied toxicology. 21(4), 279-283.

[32] V Merino., Micó-Albiñana T., Nácher A., Díez-Sales O., Herráez M., Merino-Sanjuán, M. 2008. Enhancement of nortriptyline penetration through human epidermis: influence of chemical enhancers and iontophoresis. Journal of Pharmacy and Pharmacology, 60(4), 415-420.

[33] H Sato, Nakayama Y, Yamashita C, Uno H, 2004. Anti-inflammatory effects of tacalcitol (1, 24(R) (OH) 2D3, TV-02) in the skin of TPA-treated hairless mice. The Journal of Dermatology.31 (3), 200-217.

[34] X Cao, Lin W, Liang C, Zhang D, Yang F, Zhang Y, et al,2015. Naringin rescued the TNF-α-induced inhibition of osteogenesis of bone marrow-derived mesenchymal stem cells by depressing the activation of NF-κB signaling pathway. Immunologic Research.62 (3):357-367.

[35] T Han., Das, D. B., 2013. Permeability Enhancement for Transdermal Delivery of Large Molecule Using Low-Frequency Sonophoresis Combined with Microneedles. Journal of pharmaceutical sciences.102 (10), 3614-3622.

[36] Y Gao., Ni J., Yin X., Shen, X, 2010. Study on transdermal absorption of piperine in Erxiekang plaster. Journal of Chinese materia médicaper. 35(24), 3294-3296.

[37] C Caddeo, Sales O.D, Valenti D, Saurí A.R, Fadda A.M, Manconi M, 2013. Inhibition of skin inflammation in mice by diclofenac in vesicular carriers: liposomes, ethosomes and PEVs. International journal of pharmaceutics. 443(1), 128–136.

CHAPTER II.

Mangiferin Nanoemulsions in treatment of Inflammatory Disorders and Skin Regeneration

María Pleguezuelos-Villa, Amparo Nácher, M.J. Hernández, M.A. Ofelia Vila Buso, Amparo Ruiz Sauri, Octavio Díez-Sales

International Journal of Pharmaceutics 564 (2019) 299–307

Mangiferin Nanoemulsions in treatment of Inflammatory Disorders and Skin Regeneration

María Pleguezuelos-Villa[1], Amparo Nácher[1, 2*], M.J. Hernández[3], M.A. Ofelia Vila Buso[4], Amparo Ruiz Sauri[5], Octavio Díez-Sales [1,2]

[1]Department of Pharmacy, Pharmaceutical Technology and Parasitology, Faculty of Pharmacy, University of Valencia, Av. Vicent Andrés Estellés s/n, 46100, Burjassot, Valencia, Spain.

[2]Instituto Interuniversitario de Investigación de Reconocimiento Molecular y Desarrollo Tecnológico (IDM), Universitat Politècnica de València, Universitat de València, Av. Vicent Andrés Estellés s/n, 46100, Burjassot, Valencia, Spain.

[3]Department of Earth Physics and Thermodynamics, Faculty of Physics, University of Valencia, Av. Vicent Andrés Estellés s/n, 46100, Burjassot, Valencia, Spain.

[4]Department of Physical Chemistry, Faculty of Pharmacy, University of Valencia, Av. Vicent Andrés Estellés s/n, 46100, Burjassot, Valencia, Spain.

[5]Department of Pathology, University of Valencia, Av. Blasco Ibañez 17, 46010 Valencia, Spain.

*****Corresponding author at: Department of Pharmacy, Pharmaceutical Technology and Parasitology, Faculty of Pharmacy, University of Valencia, Av. Vicent Andrés Estellés s/n, 46100 Burjassot, Valencia, Spain.

E-mail address: amparo.nacher@uv.es (A. Nácher).

Abstract

In this paper mangiferin nanoemulsions were developed using hyaluronic acid of different molecular weight, in absence or presence of Transcutol-P. An extensive study was carried out on the physico-chemical properties of nanoemulsions. Nanosizer and transmission electron microscopy showed oil droplets average size 296 nm with monodisperses distribution (PI ≤ 0.30). The zeta potential was highly negative (-30 mV). FTIR analysis confirms the existence of physical interactions among compounds. Rheological measurements allowed to conclude that all formulations present a pseudoplastic behavior (s~0.4) in presence of the biopolymer. Moreover, mangiferin release depends on the molecular weight of the polymer. Permeability assays on pig epidermis showed that nanoemulsions with low molecular weight hyaluronic acid improve the permeation, being this effect more pronounced in nanoemulsions with Transcutol-P. Administration of mangiferin nanoemulsions on TPA-inflamed skin mice model provided an attenuation of oedema and leucocyte infiltration. Macroscopic appearance of mice skin lesions has a good correlation with the histological study. The topical application of these formulations shows an appropriate anti-inflammatory effect.

Keywords: Nanoemulsions, mangiferin, Transcutol-P, hyaluronic acid, skin regeneration

1. Introduction

The interest in natural pharmacologically active compounds has widely increased in the recent years (Riccardo et al. 2017; Agrawal et al. 2017; Shal et al. 2018). Experimental studies reported that herbs and/or their constituents have anti-inflammatory, anti-proliferative, anti-angiogenic, anti-cancerous properties, among others, together with anti-oxidative stress role and tissue repair action (Rady et al. 2018; Fujii et al. 2017; Khazdair et al. 2018). These activities may explain the apparent benefits of the topical multi-herbal formulations on skin disease treatments. Moreover, no serious adverse events have been associated with their use (Deng et al. 2017, Deng et al. 2014; Liu et al. 2016; Sheng et al. 2018; Zhao et al. 2017). Natural products as baicalin or naringin could represent a potential adjuvant treatment (Mir-Palomo et al. 2016; Pleguezuelos-Villa et al. 2018) as conventional therapies in topical disorders.

In this sense, other natural products as mangiferin (Imran et al. 2017; Y. Zhao et al. 2017; Ochocka et al. 2017) used in several autoimmune inflammatory diseases, such as rheumatoid arthritis, dermatitis and psoriasis have been analyzed (Jeong et al. 2014; Garrido-Suárez et al. 2014). Mangiferin is a natural xanthone glycoside, isolated from various plants such as Gentianaceae, Zingiberaceae and Mangiferaceae (Morais et al. 2012). Due to its low hydrosolubility (0.111 mg/mL) (Acosta et al. 2016; Van der Merwe et al. 2012), the mangiferin has a poor bioavailability, which restricts its clinical application. Therefore, new formulation strategies should be developed to improve this topical efficacy.

Special attention has lately been focused on different nanosystems, such as nanoemulsions, solid lipid nanoparticles and nanovesicles, as potential vehicles for active agent delivery. These nanosystems enhance skin permeation, pharmacological activity and stability of different active substances (Roberts et al. 2017; Dong et al. 2017).

Nanoemulsions are metastable colloidal systems consisting on droplets of one liquid dispersed within another immiscible liquid (Rosen and Kunjappu 2012). They represent versatile carriers for local delivery of hydrophilic, liphophilic and amphiphilic molecules. In fact, these systems have arisen as a novel carrier system for improving the bioavailability of poorly absorbed herbs actives/extracts (Yoo et al. 2010; Wais et al. 2017).

Several studies have concluded that incorporation of surfactants, as phospholipids or polysorbate, enhances nanoemulsions stability, and improves drug release and skin permeation (El-Leithy et al., 2018; Sedaghat Doost et al., 2018; Zhang et al., 2014). These surfactants are biocompatible with the skin and have non-toxic properties (Manconi et al., 2011). In addition, the incorporation of cosurfactants, such as Transcutol-P, which may improve the retention/permeation of compounds into and through the skin has been also investigated**.**

Hyaluronic acid (HA) is a biopolymer that promotes the stabilization of the formulation and plays a role for the controlled release drug delivery (Gao et al., 2014; Rodríguez-Belenguer et al., 2015). It exhibits biomedical implications in tissue regeneration (Badawi et al. 2013), specific tumor-targeting affinity for CD 44 cancer cells (Kim and Park 2017) and anti-inflammatory diseases (Chen et al. 2018; Xiao et al. 2017). To extend the residence time of a topical formulation and improve mangiferin bioavailability, hyaluronate muco-adhesive nanoemulsions could be formulated.

The aim of this paper was to develop mangiferin nanoemulsion hyaluronate gels for inflammatory disorders in absence or presence of transcutol-P. Nanoemulsions were elaborated and characterized by analyzing their droplet size, polydispersity index (PDI), zeta potential and performing electronic microscopy, FTIR and rheological measurements. Ex vivo permeation assays and release studies were also carried out. The efficacy of the formulations was evaluated by means of an *in vivo* mice model of acute inflammation.

2. Material and methods

2.1. Materials

Lipoid® S75 a mixture of soybean lecithin containing lysophosphatidylcholine (3% maximum), phosphatidylcholine (70%), phosphatidylethanolamine (10%), fatty acids (0.5% maximum), triglycerides (3% maximum), and tocopherol (0.1–0.2%) were a gift from Lipoid GmbH (Ludwigshafen, Germany). Polysorbate 80 and tocopherol were purchased from Scharlab S.L. (Barcelona, Spain). HA of different molecular weights: low (40.000-50.000 Da), high (1.000.000-1.200.000 Da) were purchased from Carbosynth Limited (UK) and biophil Iberia S.L. (Barcelona, Spain), respectively. Mangiferin was purchased to Carbosynth Limited (UK). Glycerin were purchased from Guinama S.L.U.

(Valencia, Spain), N-octanol (special grade for measurement of partition coefficients) was purchased from VWR chemicals S.A. (France). Diethylene glycol monoethyl ether (Transcutol-P) was obtained from Alfa Aesar (Kandel, Germany). Almond oil and dexamethasone (DXM) were from Acofarma S.A. (Barcelona, Spain). Phorbol 1, 2-myristate 1, 3-acetate was purchased from Sigma-Aldrich.

2.2. Content and physico- chemical mangiferin properties

Mangiferin content was analyzed by a high-performance liquid chromatography (HPLC) Perkin Elmer® Series 200 equipped with a photodiode array UV detector. Samples were injected in a C18 reverse-phase column (Teknokroma®Brisa "LC2" 5.0 µm, 150 mm × 4.6 mm). The isocratic mobile phase was a mixture of hydrochloric acid (pH 4.0) and methanol (60:40, v/v) and the flow rate 1.2 mL/min (Bartoszewski et al. 2014). The detection wavelength was set at 254 nm. Standard calibration curves covering the whole mangiferin range concentrations in experimental samples were obtained. The limit of detection (LOD) and quantification (LOQ) were estimated using the calibration curve procedure. Three calibration curves were prepared (0.7 mg/mL-0.005 mg/mL) to determine the sensitivity of the method.

The limit of quantification may be expressed as follows:

$$LOD = \frac{3.3 * SD}{S} \quad (1)$$

The detection limit may be expressed as follows:

$$LOQ = \frac{10 * SD}{S} \quad (2)$$

The LOD and LOQ were determined based on the standard deviation (SD) of the y-intercept and the slope of the linear calibration curve (S).

Solubility determinations of mangiferin, mangiferin-phospholipid (1:10) and mangiferin-phospholipids-polysorbate 80 (1:10:5) were carried out by adding an excess of the different mixtures in water (2 mL). Samples were maintained under constant stirring for 24 hours at 25°C, then an aliquot of each dispersion was filtered through 0.22 µm membranes and injected into HPLC system to measure the mangiferin content.

In addition, an octanol-water partition coefficient values were obtained by equilibrating mangiferin, mangiferin-phospholipid or mangiferin-phospholipid-polysorbate 80 in aqueous solution with 1-octanol for 24 h at 25 °C in a shaker bath (Morikawa et al. 2016). Distribution of mangiferin between the aqueous and the organic phase was determined by HPLC method. Each sample was carried out in triplicate (n=3).

2.3. Mangiferin nanoemulsion gel formulation

A preformulation design was carried out in order to select the final nanoemulsion gel composition. Different amounts of HA (between 0.25% and 1%), polysorbate 80 (1 and 5%), almond oil (5 and 10%) and phospholipid (5 and 10 %) were formulated. According to the stability data (average particle size <500 nm, polydispersity index < 0.5 and zeta potential value < -30 mV), the best nanoemulsion gel composition was selected. Moreover, HA of different molecular weight (low and high) in presence or absence of Transcutol-P were also evaluated.

In this study, mangiferin (1%) and glycerin (3%) were added to distilled water in a glass tube in absence or presence of HA (1%) to obtain aqueous phases. Lipoid ® S75 (5%), polysorbate 80 (1%), tocopherol (0.1%) and almond oil (10%) were also mixed inside a glass tube with or without Transcutol-P (4%) to obtain the oil phases. Both receptacles were placed in a thermostat bath at 55 ± 0.5 °C. Then, aqueous phase was poured over to oil phase and subsequently homogenized with an Ultraturrax (DI25-basic, IKA-Germany) at 10.000 rpm for 5 min. After this, nanoemulsions were sonicated (3 cycles of 10 min) with an ultrasonic disintegrator (CY-500, Optic Ivymen system, Barcelona, Spain) equipped with a continuous Flow Vessel. This vessel was surrounded by a cooling jacket with a suitable cooling liquid. This method allows the preparation of a stable nanoemulsion O/W with variable consistence according to HA the molecular weight of used.

Several formulations to evaluate the in vivo efficacy of mangiferin in a mice model were tested: NE 0 (control without HA), NE I (HA, high molecular weight), NE II (HA, high molecular weight with Transcutol-P), NE III (HA, low molecular weight) and NE IV (HA, low molecular weight with Transcutol-P). In order to know the vehicle influence, empty

nanoemulsions (empty NE I, empty NE II, empty NE III and empty NE IV) were also prepared.

2.4. Characterization of formulations

Shape and surface morphology of nanoemulsions were examined using a JEM-1010 microscope (Jeol Europe, Croissy-sur-Seine, France) equipped with a digital camera MegaView III. A drop of the samples was spread on the coated copper grids and stained with phosphotungstic acid (2%, w/w) before observation. The TEM graphs were taken at an accelerating voltage of 80 KV.

Measurement of average diameter and polydispersity index (PI) of nanoemulsions were carried out by Photon Correlation Spectroscopy at 25 °C. The zeta potential was estimated by electrophoretic light scattering in a thermostatic cell. All determinations were performed using a Zetasizer Nano-S ® (Malvern Instruments, Worcester-shire, United Kingdom). Nanoemulsions stabilities were assessed by monitoring the droplets average size of the internal phase and zeta potential over 30 days at 4°C. In order to evaluate nanoemulsion-flavonoid interactions Fourier transform infrared studies (FTIR) were taken using ATR Agilent Cary 630 (Germany) at room temperature in a spectral region between 500 and 4000 cm^{-1}.

2.5. Rheological measurements

A controlled stress rheometer (RheoStress 1, Thermo Haake, Germany) equipped with control and data logging software (RheoWin 4.0.1) and a Haake K10 thermostatic bath for temperature control was used. After loading, samples were allowed to rest for at least 300 s for stress relaxation and temperature equilibrium. Cone-plate sensor (2°, 35 mm and 60 mm diameters) were used. Two types of rheological measurements were performed: flow curves and small amplitude oscillation sweeps tests. All measurements were performed in triplicate, at 25°C.

Step flow curves were performed in controlled stress mode (30 s each step-in logarithmic distribution), so shear stress range was chosen in order to obtain viscosities corresponding to very low shear rates until approx. 100 s^{-1}. The viscosities results can be fitted to the simplified Carreau model.

$$\eta = \frac{\eta_0}{\left(1+\left(\frac{\dot{\gamma}}{\dot{\gamma}_c}\right)^2\right)^s} \qquad (3)$$

where η_0 is the zero-shear viscosity, $\dot{\gamma}_c$ is critical shear rate, and s the shear thinning index. Oscillatory measurements at a constant stress in the linear viscoelastic region (LVR) were performed, varying the frequency from 0.01 to 10Hz (9 points per decade). In order to establish LVR, stress sweeps at a frequency of 1 Hz were performed for all systems.

2.6. Flavonoid release studies

The release of mangiferin from nanoemulsions was determined with Franz diffusion cells. An artificial membrane (0.45 µm cellulose acetate membrane, Teknocroma, Barcelona, Spain) was placed between the donor and receptor compartments of the Franz cells (effective diffusion area of 0.784 cm^2). The Franz cells were immersed in a bath system at 37.0 ± 0.5°C and kept under agitation. The receptor compartment (6 mL) was filled with an aqueous solution of polysorbate 80 (1%) to maintain sink conditions. A weighted amount of each nanoemulsion (500 mg) was loaded onto the surface of the membrane. At regular intervals, up to 24 h, the receptor solution was removed (200 µL), replaced with the same volume of a fresh aqueous solution and analysed by HPLC to determine the content of mangiferin.

In order to describe the flavonoid release mechanism, the mean percentages of cumulative amounts of mangiferin were fitted according to Power law model (Table 2).

2.7. *In vitro* permeation assays

The experiments were performed using Franz diffusion cells according to the procedure described previously in epigraph 2.6. In this case, cellulose-acetate membrane was replaced by new born pig epidermal skin from a local slaughterhouse. The epidermis was mounted between the donor and receptor compartments of the Franz cells with the stratum corneum side facing upward the donor compartment. Epidermal membranes were obtained from heat separation through immersing in water (at 60°C) for 75 s (Chilcott et al. 2001).

The cumulative amounts of mangiferin *(*Q) permeated through the epidermis were fitted to the equation derived of the Fick's Second Law to the diffusion process (Eq. (4)):

$$Q_{(t)}=A\cdot P\cdot L\cdot C\left[D\cdot\frac{t}{L^2}-\frac{1}{6}-\frac{2}{x^2}\cdot\sum_{n=1}^{\infty}\cdot Exp\left(\frac{-D\cdot n^2\cdot x^2\cdot t}{L^2}\right)\right] \qquad (4)$$

where Q (t) is the amount of mangiferin through the skin and reaches the receptor solution at a given time t; A is the diffusion surface area (0.784 cm^2); P is the partition coefficient of mangiferin between the skin and the donor solution; L is the diffusion pathway; D is the diffusion coefficient of mangiferin in the skin; and C is the concentration of mangiferin in the donor vehicle. By fitting the equation 4, lag time (t_L=1/6D, h), permeability coefficient (K_p = P·D, cm/h) and flux (J=k_p·C, µg/cm^2/h) were calculated.

At the end of the permeation experiments, the epidermis integrity was verified. Briefly, 1 mL of phenol red solution (0.5 mg/mL) was applied onto the skin surface in the donor compartment. When the phenol red amount in receptor compartment was <1%, the epidermis was considered intact. The concentration of mangiferin retained in the epidermis (R_{24}) was also quantified. The epidermis sheet was removed from the Franz diffusion cell and extracted with 10 mL of methanol. Subsequently, it was maintained for 24 hours at 2-8 °C. The suspension was homogenized with an Ultratturrax and sonicated for 30 min. Finally, the supernatant was filtered through a 0.45 µm filter and analysed by HPLC. To evaluate the affinity of mangiferin for the epidermal layers and the influence of the formulation R_{24} / Q_{24} ratios were calculated.

2.8. Acute inflammation assays

For the inflammation study, female CD-1 mice (5–6 weeks old, 25–35 g) were supplied by Harlan laboratories (Barcelona, Spain). Mice were acclimated for one week before use. All studies were performed in accordance with European Union regulations for the handling and use of laboratory animals. The protocols were approved by the Institutional Animal Care and Use Committee of the University of Valencia (code 2016/VSC/PEA/00112 type 2). Briefly, dorsal skin of mice (n=4 per group) was shaved and 24 h later the topical formulations were applied. The first day, TPA dissolved in acetone (3 µg/20 µL) was topically administered to the shaved dorsal area (1 cm^2) to induce cutaneous inflammation and ulceration. After 3 h, 200 µL of five formulations selected were topically

applied in the same areas. This procedure was repeated for two consecutive days. Mice were sacrificed on day fourth by cervical dislocation and biopsies from the treated dorsal skin were excised and weighed to evaluated oedema and histological study, previously stored at -80°C.

For histological assays, tissue samples were stored in formaldehyde (0.4%, V/V). Longitudinal sections (5mm) on a rotary microtome were mounted on slides and marked with hematoxylin and eosin according to standard protocols. The tissues were analyzed and observed using a light microscope (DMD 108 Digital Micro-Imaging Device, Leica, Wetzlar, Germany).

Myeloperoxidase (MPO) activity was determined using a minor modification of the method of Grisham et al. (1990). The tissue was thawed and homogenized in 750 µL of phosphate buffer (pH 5.4) with an Ultra-Turrax T25 homogenizer (IKA1 Werke GmbH & Co. KG, Staufen, Germany). The homogenate was centrifuged at 10.000 g for 15 min at 4°C.The supernatant obtained was diluted with PBS 5.4 (1:10). A sample of supernatant (10 µL) was added to a 96-well plate and incubated at 37 °C for 5 min with a mixture of 20 µL of sodium phosphate buffer (pH 5.4), 200 µL of phosphate buffer (pH 7.4), 40 µL of 0.052% hydrogen peroxide and 20 µL of 18 mM 3,30,5,50-tetramethylbenzidine dihydrochloride. The reaction is finalized by 50 µL of SO_4H_2 2N. The absorbance was determined at 450 nm. The MPO activity was calculated from the linear portion of a standard curve. The oedema was expressed as the percentage of inhibition versus the positive control (TPA) value and MPO was expressed as percentage of activity.

2.9 Statistical analysis

Statistical differences were determined by one-way ANOVA test and Tukey's test for multiple comparisons with a significance level of $p < 0.05$. All statistical analyses were performed using IBM SPSS statistics 22 for Windows (Valencia, Spain). Data are shown as mean ± standard deviation.

3. Results and discussion

In the present study, the effect of biopolymer (HA) on the properties of nanoemulsions was evaluated, in order to optimize the formulation for the transdermal mangiferin administration.

3.1 Content and physico-chemical mangiferin properties

Excellent plots correlating the peak areas and mangiferin concentrations were obtained. Calibration graphs presented a correlation coefficient value r >0.999, demonstrating good linearity. The limits of detection and quantification were 0.21 µg/mL and 0.54 µg/mL, respectively.

Mangiferin solubility values from different mixtures were determined. The mangiferin-phospholipid-polysorbate 80 solubility (0.71 ± 0.03 mg/mL) was higher than mangiferin and mangiferin-phospholipid solubilities: 0.10 ± 0.01 mg/mL and 0.25 ± 0.02 mg/mL, respectively.

Octanol-water partition coefficient value was obtained in different mixtures. Mangiferin-phospholipid-polysorbate 80 partition coefficient (5.23 ± 0.17) was also higher than mangiferin and mangiferin-phospholipid partition coefficients: 0.12 ± 0.01 and 2.10 ± 0.12, respectively.

3.2 Characterization of formulations

Nanoemulsions present oil droplets size range from 194.5 to 397.9 nm (Table 1). These results are in accordance with Callender Shannon et al. (2017). All nanoemulsions showed monodisperses distribution (PI ≤ 0.30) and spherical shape (Fig. 1).

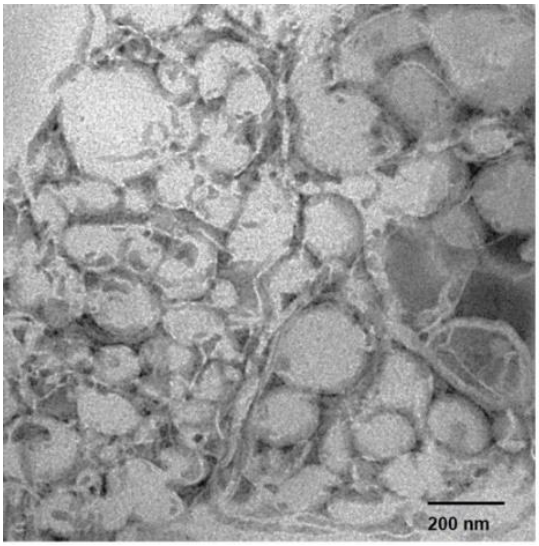

Fig. 1. TEM graphs of nanoemulsions

The zeta potential was always highly negative (<-30 mV). The physical stability of nanoemulsions (NE 0 to NE IV) was monitored over 30 days of storage at 4 °C. As can be seen in Table 1 nanoemulsions were stable. The average size and zeta potential of the oil core depend on HA molecular weight. Short-chain HA nanoemulsions have smaller particle sizes and zeta potentials more negative, being similar to the nanoemulsion without polymer.

Table 1

Average size, polydispersity index (PI) and zeta potential of nanoemulsions during 30 days of storage at 4 °C (Mean Value ± SD; n=4).

Sample	Size (nm)		PI		Potential Z (mV)	
	0 days	30 days	0 days	30 days	0 days	30 days
NE 0 without polymer	319.4 ± 5.7	289.4 ± 5.7	0.26	0.24	-40.4 ± 1.3	-39.1 ± 1.3
HA High molecular weight						
NE I	393.0 ± 4.1	372.3 ± 6.3	0.30	0.30	-37.2± 1.6	-35.4 ± 1.3
NE II	397.9 ± 6.1	320.5 ± 2.7	0.25	0.25	-32.7± 0.4	-33.5 ± 0.3
HA Low molecula weight						
NE III	221.5 ± 7.0	194.5 ± 3.4	0.19	0.21	-38.2 ± 0.1	-38.2 ± 0.2
NE IV	323.2± 8.0	281.5 ± 7.2	0.23	0.20	-40.2 ± 2.0	-38.3 ± 0.4

FTIR analyses provided information about the interactions of the different components of nanoemulsions (Ferreira et al. 2013). Fourier transform infrared (FTIR) studies are indicated in Fig. 2.

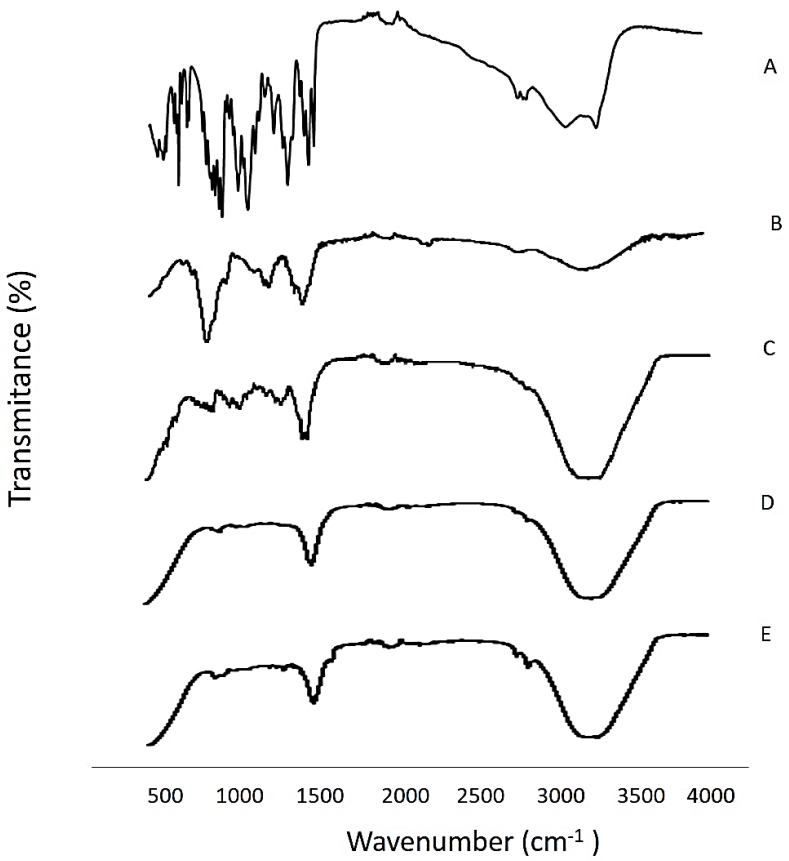

Fig.2. FT-IR spectra of A) Mangiferin B) Mangiferin and hyaluronic acid (HA) C) Mangiferin and lipoid® S 75 D) Mangiferin, lipoid S® 75 and polysorbate 80 E) Nanoemulsion loaded with Mangiferin.

In these spectra, profiles the mangiferin (A), mangiferin and HA (B), mangiferin and lipoid ®S 75 (C), mangiferin with lipoid S ®75 and polysorbate 80 (D) and nanoemulsion loaded with mangiferin (E) were shown. The FT-IR spectrum of mangiferin showed absorption bands at 3373 cm^{-1} (hydroxyl group) and 2933 cm^{-1} (C-H asymmetric stretching). Bands at 1255cm $^{-1}$(-C-O -) and 1093 cm^{-1}(-C-O-C). An aromatic conjugated carbonyl group can be observed at 1651 cm^{-1} together with signals of aromatic nucleus. By comparison of the spectra, the major changes observed occurred in the region from 1800 to 500 cm^{-1}. Some IR bands of mangiferin had disappeared completely or had their intensities altered. In nanoemulsion, bands at 1651, 1622 cm^{-1} were observed, confirming the presence of mangiferin. In addition, at 3373 cm^{-1} the band intensifies verifying the integration of the hydroxyl groups of mangiferin in the system. Mangiferin interactions with HA of different molecular weight showed satisfactory physico-chemical properties related with the formulation stability.

3.3 Rheological measurements

The low viscosity of the NE 0 nanoemulsion (data not shown) is not the most suitable for topical administration. For this reason, new formulations were developed in presence of HA different molecular weight (high and low). A rheological test was performed in order to understand the nanoemulsions gel properties. The experimental data fits to the simplified Carreau model showed that nanoemulsions with HA high molecular weight had a higher viscosity (NE I, 863.5 ± 16.8 Pa s and NE II, 508.5 ± 11.2 Pa s) than the HA low molecular weight nanoemulsions (NE III, 68.8 ±2.9 Pa s and NE IV,64.8 ± 8.9 Pa s). Flow curves obtained for nanoemulsions NE I, NE II, NE III and NE IV are presented in Fig. 3A.

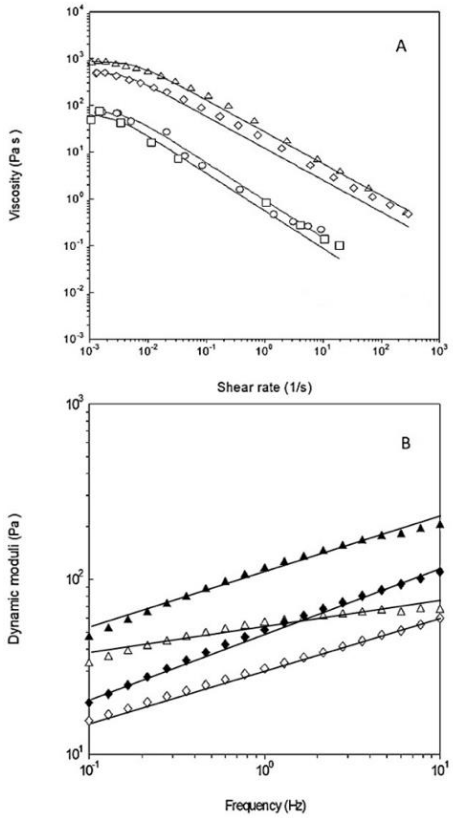

Fig. 3. Rheological measurements. A) Flow curves fitted to Carreau model for nanoemulsions: NE I (△), NE II (◊), NE III (○) and NE IV (□). B) Viscoelastic moduli as a function of oscillation frequency for nanoemulsions: NE I (△), NE II (◊). Closed symbols: elastic modulus, G'; open symbols: viscous modulus, G".

Also, all nanoemulsions had a pseudoplastic behavior (s ~ 0.40). The presence of Transcutol-P did not modify the pseudoplastic behavior. To investigate the nanoemulsions gel structure, oscillatory measurements at a constant stress, in the linear viscoelastic region (LVR), were performed. Nanoemulsions with HA low molecular weight

(NE III and NE IV) were out of the LVR, for this reason it was not possible to measure dynamic curves. Fig. 3B shows results obtained on dynamic tests. As can be seen, NE I and NE II, in the presence and absence of Transcutol-P, exhibited an elastic behavior (G`> G``) and low frequency dependence, which promoted the formation of controlled release systems (Díez-Sales et al. 2005). This behavior was confirmed with loss tangent (tan δ, 1 Hz) values, 0.59 and 0.49 for NE I and NE II, respectively.

3.4 Flavonoid release studies

The amount of mangiferin released at 24 h was greater than 20% in nanoemulsions without polymer (NE 0). The mangiferin release can be significantly modified depending on the molecular weight of the biopolymer (Agubata et al. 2014; Morsi et al. 2017). In fact, the presence of HA reduces the percentage released (Fig. 4A), being more evident in high molecular weight nanoemulsions (NE I, NE II). Nanoemulsions with Transcutol-P (NE II and NE IV) showed a slight ability to enhance mangiferin release in comparison with the other nanoemulsions.

Mangiferin release data were analyzed according to power law equation (epigraphs 2.6). The fitting results are summarized in Table 2. In accordance with the power model, the release mechanism is zero order (n ~1) (Siepmann and Peppas 2001). These results could be attributed to polymer obstructive mechanism, which depends on the molecular weight of the polymer.

In accordance with the following equation, (Barry, 1983).

$$Kp = \frac{Ko}{1 + 2\emptyset/3} \qquad (5)$$

where K_0 and Kp are the diffusion constants of the mangiferin in water in absence and presence of polymer, respectively. Ø is the proportion of water inmobilized by the polymer.

The water retention values (Ø) have been determined (Eq. (5)): $\emptyset_{NE\ I}$ = 17.3 and $\emptyset_{NE\ III}$ = 2.5. In fact, the greater amount of water retained by the polymer, the less amount of mangiferin released.

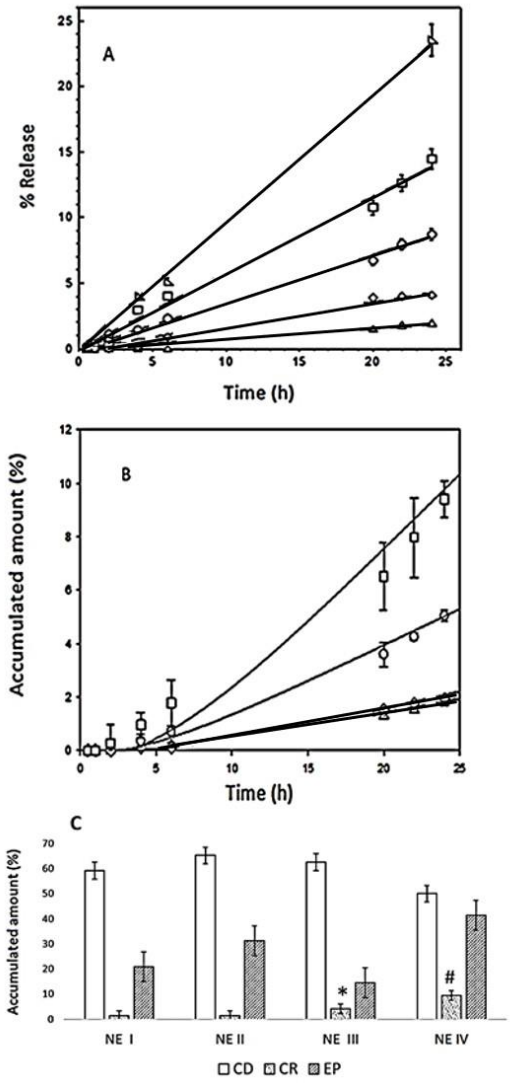

Fig. 4. A) Graphical representation of percentage of mangiferin released in function of time for the differents nanoemulsions: NE 0 (◺) NE I (△), NE II (◊), NE III (○) and NE IV (□). B) Profiles of cumulative amount of mangiferin accumulated in receptor compartment after 24 h treatment with nanoemulsions (NE I-NE IV). C) Cumulative amount of mangiferin accumulated in receptor compartment (CR), epidermis (EP) and donor compartment (CD) after 24 h of treatment with nanoemulsions (NE I-NE IV). Bars represent the mean ± standard deviation of at least four independent experimental determinations. * $p < 0.05$ values statistically different compared permeation of NE III vs NE I. # $p < 0.05$ values statistically different compared permeation of NE II vs NE IV.

Table 2

Results of release mangiferin fitting different models at 24 hours (Mean Value ± SD; n=4).

Nanoemulsions					
Models	Without polymer	HA High molecular weight		HA Low molecular weight	
	NE 0	NE I	NE II	NE III	NE IV
Power law					
$M_t=K \cdot t$					
K (h^{-1})	0.69 ± 0.12	0.010± 0.006	0.08 ± 0.04	0.36 ± 0.07	0.57 ± 0.16
N	1.09 ± 0.05	1.58 ± 0.13	1.26 ± 0.18	0.99 ± 0.06	1.01± 0.07
R>	0.997	0.998	0.992	0.997	0.990

M_t is the fraction of flavonoid release at each time t; K is a constant reflecting structural and geometric characteristic of the devic; n is the release exponent characterizing the diffusion mechanism.

3.5 *In vitro* permeation assays

The results of in vitro permeation studies are showed in Table 3. As can be observed, the molecular weight of HA affects a percutaneous absorption. For the lag time, no significant differences were shown between formulations ($p>0.05$). Nanoemulsions with HA of high molecular weight presented a lower penetration at 24 hours (Q_{24}). In the case NE I (1.81 ± 0.01µg/cm^2) and NE II (1.93 ± 0.01µg/cm^2) the presence of Transcutol-P does not significantly enhance ($p>0.05$) the skin permeation. The highest penetration occurs in low molecular weight HA nanoemulsions. NE III increase 2.5-fold the mangiferin amount in the receptor compartment (Q_{24}=5.04 ± 0.01µg/cm^2), and the incorporation of Transcutol-P (NE IV) increase 5-fold the amount permeated (Q_{24}=9.41 ± 0.01µg/cm^2). As expected, the last nanoemulsion has the highest flux value (J=0.55 ± 0.09 µg/cm^2/h). These results were confirmed by R_{24} / Q_{24} ratio.

Table 3

Results of in vitro permeation studies on nanoemulsions (Mean Value ± SD; n=4).

Nanoemulsions	Q_{24} (μg, cm^2)	P	$D*10^2$(cm/h)	Lag time(h)	Flux (μg/cm^2/h)	R_{24} (μg/cm^2)	R_{24}/Q_{24}
HA High molecular weight							
NE I	1.81 ± 0.01	4.79 ± 1.10	2.1±0.4	8 ± 1	0.10 ± 0.01	2.03 ± 0.08	1.12
NE II	1.93 ± 0.01	7.33 ± 2.14	1.9±0.3	9 ± 2	0.13 ± 0.01	2.02 ± 0.04	1.04
HA Low molecular weight							
NE III	5.04 ± 0.01	9.09 ± 2.65	2.9±0.7	6 ± 1	0.26 ± 0.02	10.52 ± 0.02	2.08
NE IV	9.41 ± 0.01	23.19 ± 10.60	2.4±0.8	7± 2	0.55 ± 0.09	28.94 ± 0.07	3.07

Q_{24} is the amount of mangiferin through the skin and reaches the receptor solution; P is the partition coefficient of mangiferin between the skin and the donor solution; D is the diffusion coefficient of mangiferin in the skin; R_{24} is the concentration of mangiferin retained in epidermis.

Fig. 4B showed the profiles of cumulative amount of mangiferin and Fig. 4C the cumulative amount of mangiferin (%) in donor compartment (CD), epidermis (EP) and receptor compartment (CR). As can be seen in this figure, nanoemulsions with Transcutol-P showed the highest accumulation in the epidermis (NE II, 35 % and NE IV,45%). Probably, the oil core could penetrate into the epidermis, due to a synergistic mechanism between surfactants and the intercellular lipids of pig skin (Manconi et al. 2011; Blume et al. 1993).

3.6 Acute inflammation assays

Topical application of TPA was used in skin to induce oxidative stress, oedema and infiltration of inflammatory cells and inflammation. By repeating TPA application scaly, peeling and crusted mice skin with desquamation was observed (Fig. 5A).

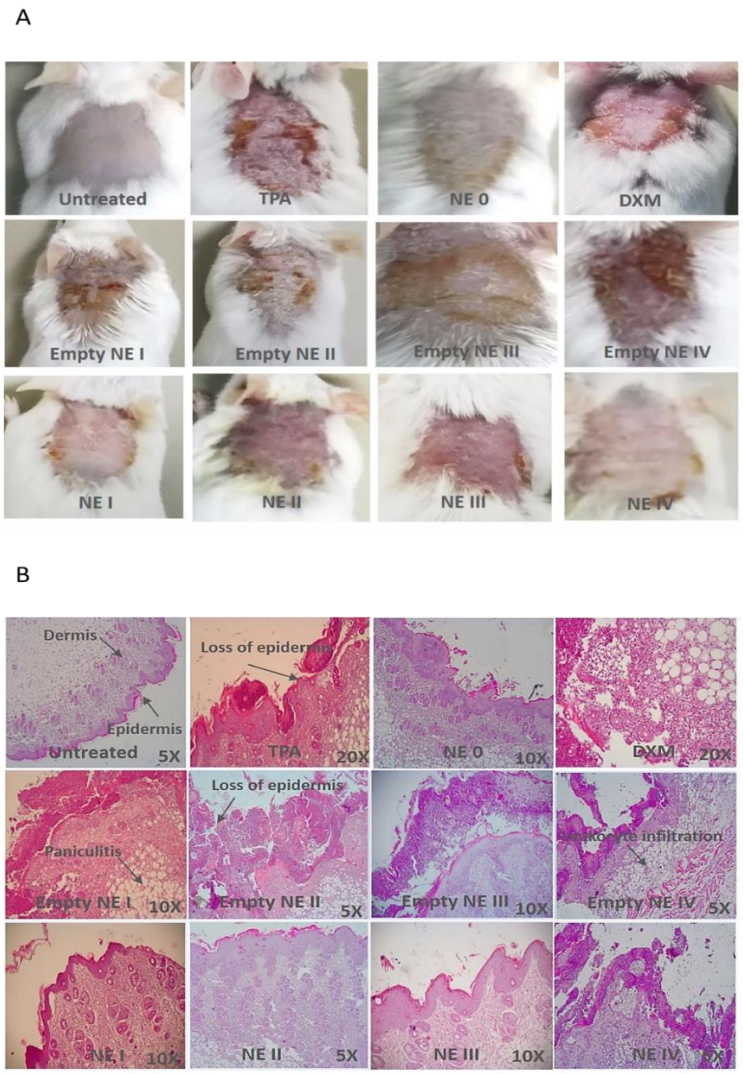

Fig 5. A) Macroscopic appearance of skin lesions of mice treated with dexametasone (DXM), nanoemulsions (NE 0, NE I, NE II, NE III and NE IV) in comparison with untreated skin and empty nanoemulsions. B) Histological appearance of mice skin treated with dexametasone (DXM),nanoemulsions (NE 0, NE I, NE II, NE III and NE IV) in comparison with untreated skin and empty nanoemulsions

All animals treated with mangiferin formulations presented a significant amelioration of the skin. The ability of mangiferin nanoemulsion to wound healing in comparison with empty nanoemulsions was evidenced (Fig. 5A). Histological study showed that mice skin treated with TPA displayed severe dermal and subcutaneous alteration, with a large number of leukocytes infiltrating, and showing pathological features of inflammatory damage, such as vascular congestion. Untreated skin with TPA showed a regular structure and normal appearance of epidermis. As can be observed in Fig. 5B, nanoemulsions with

mangiferin reduced TPA-induced lesions. Nanoemulsions loaded with mangiferin (NE I, NE II, NE III, NE IV) induced both strong inhibition of oedema and reduction of MPO activity. Statistic differences ($p<0.01$) have been found with respect to empty nanoemulsions and TPA treatment results (Fig. 6A).

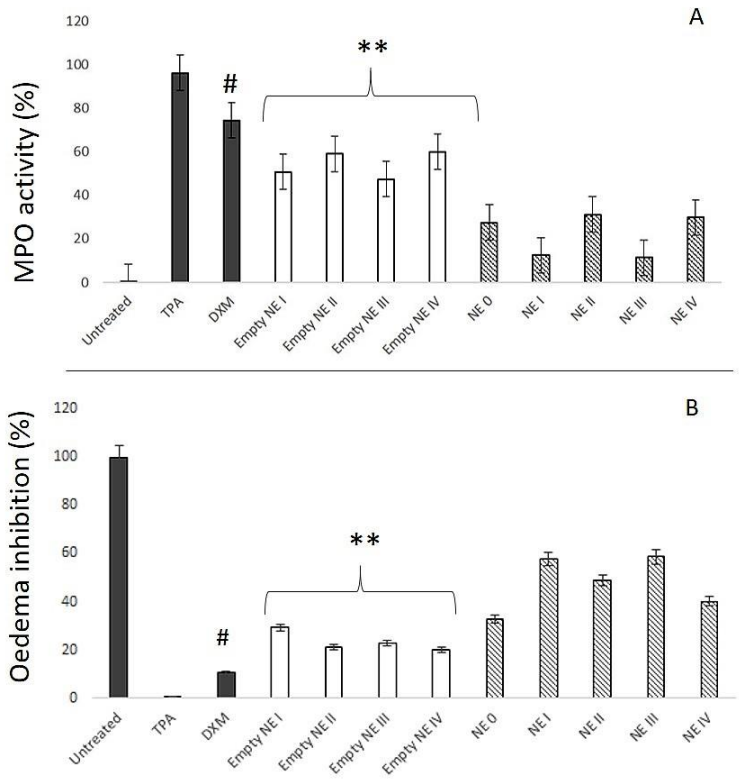

Fig 6. A) Myeloperoxidase activity (%) (MPO) and B) oedema inhibition (%) values, obtained after TPA treatment and application of nanoemulsions (NE 0 - NE IV), dexametasone (DXM) and empty nanoemulsions (n=4). Mean values ± standard deviation were reported. ** $p< 0.01$ values statistically different from those of skin treated with empty nanoemulsions. # $p< 0.05$ values statistically different compared DXM with mangiferin nanoemulsions.

Nanoemulsions with mangiferin showed a significant decrease in oedema inhibition: ~20-fold higher than empty nanoemulsions (Fig. 6B). MPO levels dramatically increased with repeated TPA and DXM exposure, it was ~80-fold higher than those found in untreated skin. Therefore, the results obtained in vivo seem to indicate a remarkable therapeutic potential of mangiferin nanoemulsions.

4. Conclusion

This investigation reveals that the design and development of nanoemulsions could be a promising device to restore inflammatory skin disorders. The topical application of these formulations shows an appropriate anti-inflammatory effect.

Funding

This research did not receive any specific grant from funding agencies in the public, commercial, or not-for-profit sectors.

Disclosure of conflicts of interest

None

References

Jhoany, Acosta, Sevilla, Iliana, Salomón, Suslebys, Nuevas, Lauro, Romero, Aylema, Amaro, Daniel, 2016. Determination of mangiferin solubility in solvents used in the biopharmaceutical industry. J. Pharmacy Pharmacognosy Res. 4 (2), 49–53.

Shivankar, Agrawal, Acharya, Debabrata, Adholeya, Alok, Barrow, Colin J., Deshmukh, Sunil K., 2017. Nonribosomal peptides from marine microbes and their antimicrobial and anticancer potential. Front. Pharmacol. 8, 828.

Agubata, Chukwuma O., Nzekwe, Ifeanyi T., Obitte, Nicholas C., Ugwu, Calister E., Onunkwo, Godswill C., 2014. Effect of oil, surfactant and co-surfactant concentra- tions on the phase behavior, physicochemical properties and drug release from self-emulsifying drug delivery systems. J. Drug Discov. Development 1, 1–7.

Badawi, Alia A., El-Laithy, Hanan M., Nesseem, Demiana I., El-Husseney, Shereen S., 2013. Pharmaceutical and medical aspects of hyaluronic acid-ketorolac combination therapy in osteoarthritis treatment: radiographic imaging and bone mineral density. J. Drug Target. 21 (6), 551–563.

Rafal, Bartoszewski, Hering, Anna, Marszałł, Marcin, Hajduk, Justyna Stefanowicz, Bartoszewska, Sylwia, Kapoor, Niren, Kochan, Kinga, Ochocka, Renata, 2014. Mangiferin

has an additive effect on the apoptotic properties of hesperidin in cyclopia sp. tea extracts. PloS One 9 (3).

Alfred, Blume, Jansen, Michael, Ghyczy, Miklos, Gareiss, J., 1993. Interaction of phospholipid liposomes with lipid model mixtures for stratum corneum lipid. Int. J. Pharmaceutics 99 (2), 219–228.

Barry, Brian W., 1983. Dermatological Formulations: Percutaneous Absorption. Marcel Dekker, New York. Callender Shannon, P., Mathews, Jessica A., Kobernyk, Katherine, Wettig, Shawn D., 2017. Microemulsion utility in pharmaceuticals: implications for multi-drug delivery. Int. J. Pharm. 526 (1–2), 425–442.

Hui, Chen Li, Xue, Jian Feng, Zheng, Zhi Yong, Shuhaidi, Muhammad, Thu, Hnin Ei, Hussain, Zahid, 2018. Hyaluronic acid, an efficient biomacromolecule for treatment of inflammatory skin and joint diseases: a review of recent developments and critical appraisal of preclinical and clinical investigations. Int. J. Biol. Macromol. 116,572–584.

Chilcott, R.P., Jenner, J., Hotchkiss, S.A., Rice, P., 2001. In vitro skin absorption and decontamination of sulphur mustard: comparison of human and pig-ear skin. J. Appl. Toxicol. 21 (4), 279–283.

Shiqiang, Deng, Cheng, Jianwen, Zhao, Jinmin, Yao, Felix, Jiake, Xu, 2017. Natural compounds for the treatment of psoriatic arthritis: a proposal based on multi-targeted osteoclastic regulation and on a preclinical study. Res. Protocols 6 (7), e132.

Shiqiang, Deng, May, Brian H., Zhang, Anthony L., Chuanjian, Lu, Xue, Charlie C.L., 2014. Topical herbal formulae in the management of psoriasis: systematic review with meta-analysis of clinical studies and investigation of the pharmacological ac- tions of the main herbs. Phytotherapy Res. 28 (4), 480–497.

Díez-Sales, O., Garrigues, T.M., Herráez, J.V., Belda, R., Martín-Villodre, A., Herráez, M., 2005. In vitro percutaneous penetration of acyclovir from solvent systems and car- bopol 971-P hydrogels: influence of propylene glycol. J. Pharm. Sci. 94 (5), 1039–1047.

Zhaoqiang, Dong, Guo, Jing, Xing, Xiaowei, Zhang, Xuguang, Yimeng, Du, Qinghua, Lu, 2017. RGD modified and PEGylated lipid nanoparticles loaded with puerarin: for- mulation, characterization and protective effects on acute myocardial ischemia model. Biomed. Pharmacother. 89, 297–304.

El-Leithy, Eman S., Makky, Amna M., Khattab, Abeer M., Hussein, Doaa G., 2018. Optimization of nutraceutical coenzyme Q10 nanoemulsion with improved skin permeability and anti-wrinkle efficiency. Drug Dev. Ind. Pharm. 44 (2), 316–328.

Ferreira, Fabricia da Rocha, Valentim, Iara Barros, Ramones, Edgar Luís Catarí, Trevisan, Maria Teresa Salles, Olea-Azar, Claudio, Perez-Cruz, Fernanda, de Abreu, Fabiane Caxico, Goulart, Marília Oliveira Fonseca, 2013. Antioxidant activity of the mangi- ferin inclusion complex with β-cyclodextri. Food Sci. Technol. 51 (1), 129–134.

Airi, Fujii, Okuyama, Tetsuya, Wakame, Koji, Okumura, Tadayoshi, Ikeya, Yukinobu, Nishizawa, Mikio, 2017. Identification of anti-inflammatory constituents in Phellodendri cortex and Coptidis rhizoma by monitoring the suppression of nitric oxide production. J. Nat. Med. 71 (4), 745–756.

Yuanyuan, Gao, Cheng, Xiaojie, Wang, Zhiguo, Wang, Juan, Gao, Tingting, Li, Peng, Kong, Ming, Chen, Xiguang, 2014. Transdermal delivery of 10,11-methylenediox- ycamptothecin by hyaluronic acid based nanoemulsion for inhibition of keloid fi- broblast. Carbohydr. Polym. 112, 376–386.

Garrido-Suárez, Bárbara B., Garrido, Gabino, Castro-Labrada, Marian, Merino, Nelson, Valdés, Odalys, Rodeiro, Idania, Hernández, Ivonnes, Godoy-Figueiredo, Jozi, Ferreira, Sergio H., Delgado-Hernández, René, 2014. Anti-hypernociceptive effect of mangiferin in persistent and neuropathic pain models in rats. Pharmacol. Biochem. Behav. 124, 311–319.

Grisham, M.B., Benoit, J.N., Granger, D.N., 1990. Assessment of leukocyte involvement during ischemia and reperfusion of intestine. Methods Enzymol. 186, 729–742.

Muhammad, Imran, Arshad, Muhammad Sajid, Butt, Masood Sadiq, Kwon, Joong-Ho, Arshad, Muhammad Umair, Sultan, Muhammad Tauseef, 2017. Mangiferin: a natural

miracle bioactive compound against lifestyle related disorders. Lipids Health Dis. 16 (1), 84.

Jeong, Jin-Ju, Jang, Se-Eun, Hyam, Supriya R., Han, Myung Joo, Kim, Dong-Hyun, 2014. Mangiferin ameliorates colitis by inhibiting IRAK1 phosphorylation in NF-KB and MAPK pathways. Eur. J. Pharmacol. 652–661.

Khazdair, Mohammad Reza, Ghorani, Vahideh, Alavinezhad, Azam, Boskabady, Mohammad Hossein, 2018. Pharmacological effects of zataria Multiflora Boiss L. and its constituents focus on their anti-inflammatory, antioxidant, and im- munomodulatory effects. Fundam. Clin. Pharmacol. 32 (1), 26–50.

Kim, Joo-Eun, Park, Young-Joon, 2017. Improved antitumor efficacy of hyaluronic acid-complexed paclitaxel nanoemulsions in treating non-small cell lung cancer. Biomolecules and Therapeutics 25 (4), 411–416.

Kang, Liu, Wu, Lianguo, Shi, Xiaolin, Wu, Fengqing, 2016. Protective effect of naringin against ankylosing spondylitis via ossification, inflammation and oxidative stress in mice. Exp. Therapeutic Medicine 12 (2), 1153–1158.

Maria, Manconi, Caddeo, Carla, Sinico, Chiara, Valenti, Donatella, Mostallino, Maria Cristina, Biggio, Giovanni, Fadda, Anna Maria, 2011a. Ex vivo skin delivery of diclofenac by transcutol containing liposomes and suggested mechanism of vesicle- skin interaction. Eur. J. Pharm. Biopharm. 78 (1), 27–35.

Maria, Manconi, Sinico, Chiara, Caddeo, Carla, Vila, Amparo Ofelia, Valenti, Donatella, Fadda, Anna Maria, 2011b. Penetration enhancer containing vesicles as carriers for dermal delivery of tretinoin. Int. J. Pharm. 412 (1–2), 37–46.

Riccardo, Martini, Esposito, Francesca, Corona, Angela, Ferrarese, Roberto, Ceresola, Elisa Rita, Visconti, Laura, Tintori, Cristina, 2017. Natural product kuwanon-L in- hibits HIV-1 replication through multiple target binding. Chembiochem: Eur. J. Chem. Biol. 18 (4), 374–377.

Debora van der, Merwe J., Joubert, Elizabeth, Manley, Marena, de Beer, Dalene, Malherbe, Christiaan J., Gelderbloom, Wentzel C.A., 2012. Mangiferin glucuronida- tion: important hepatic modulation of antioxidant activity. Food Chem. Toxicol. 50 (3–4), 808–815.

Silvia, Mir-Palomo, Nácher, Amparo, Octavio Díez-Sales, M.A., Busó, Ofelia Vila, Caddeo, Carla, Manca, Maria Letizia, Manconi, Maria, Fadda, Anna Maria, Saurí, Amparo Ruiz, 2016. Inhibition of skin inflammation by baicalin ultradeformable vesicles. Int. J. Pharm. 511 (1), 23–29.

Cavalcante, MoraisTalita, Lopes, Synara Cavalcante, Carvalho, Karine Maria Martins Bezerra, Arruda, Bruno Rodrigues, Correia, Francisco Thiago, de Souza, Maria, Trevisan, Teresa Salles, Rao, Vietla Satyanarayana, Santos, Flávia Almeida, 2012. Mangiferin, a natural xanthone, accelerates gastrointestinal transit in mice involving cholinergic mechanism. World J. Gastroenterol. 18 (25), 3207–3214.

Go, Morikawa, Suzuka, Chihiro, Shoji, Atsushi, Shibusawa, Yoichi, Yanagida, Akio, 2016.High-throughput determination of octanol/water partition coefficients using a shake- flask method and novel two-phase solvent system. J. Pharm. Biomed. Anal. 338–344. Nadia, Morsi, Ibrahim, Magdy, Refai, Hanan, El Sorogy, Heba, 2017. Nanoemulsion-based electrolyte triggered in situ gel for ocular delivery of acetazolamide. Eur. J. Pharm.Sci. 302–314.

Ochocka, Renata, Hering, Anna, Stefanowicz-Hajduk, Justyna, Cal, Krzysztof, Barańska, Helena, 2017. The effect of mangiferin on skin: penetration, permeation and in- hibition of ECM enzymes. PLoS ONE 12, (7).

Pleguezuelos-Villa, María, Mir-Palomo, Silvia, Octavio Díez-Sales, M.A., Buso, Ofelia Vila, Sauri, Amparo Ruiz, Nácher, Amparo, 2018. A novel ultradeformable liposomes of naringin for anti-inflammatory therapy. Colloids and Surfaces. B, Biointerfaces 265–270.

Rady Islam, Melissa B. Bloch, Roxane-Cherille N. Chamcheu, Sergette Banang Mbeumi, Md Rafi Anwar, Hadir Mohamed, Abiola S. Babatunde, 2018. Anticancer properties of

graviola (Annona Muricata): a comprehensive mechanistic review. Oxidative Medicine and Cellular Longevity 2018, 1826170.

Roberts, M.S., Mohammed, Y., Pastore, M.N., Namjoshi, S., Yousef, S., Alinaghi, A., Haridass, I.N., 2017. Topical and cutaneous delivery using nanosystems. J. Control. Release 247, 86–105.

Rodríguez-Belenguer, P., Nácher, A., Hernández, M.J., Díez-Sales, O., 2015. Characterization of novel hyaluronic acid matrix systems for vaginal administration of metronidazole. J. Appl. Polym. Sci. 132 (3).

Rosen, Milton J., Kunjappu, Joy T., 2012. Surfactants and Interfacial Phenomena, 4th ed. Wiley.

Sedaghat Doost, Ali, Koen Dewettinck, Frank Devlieghere, Paul Van der Meeren, 2018. Influence of non-ionic emulsifier type on the stability of cinnamaldehyde nanoemulsions: a comparison of polysorbate 80 and hydrophobically modified inulin. Food Chemistry, 237–244.

Bushra, Shal, Ding, Wei, Ali, Hussain, Kim, Yeong S., Khan, Salman, 2018. Anti-neuroinflammatory potential of natural products in attenuation of Alzheimer's disease. Front. Pharmacol. 9, 548.

Xuan, Sheng, Wang, Jiayue, Guo, Jingjing, Yurong, Xu, Jiang, Huaide, Zheng, Chaoran, Xu, Zixi, 2018. Effects of baicalin on diabetic cardiac autonomic neuropathy medi- ated by the P2Y12 receptor in rat stellate ganglia. Cell. Physiol. Biochem. 46 (3), 986–998.

Siepmann, J., Peppas, N.A., 2001. Modeling of drug release from delivery systems based on hydroxypropyl methylcellulose (HPMC). Adv. Drug Deliv. Rev. 48 (2–3), 139–157.

Mohammad, Wais, Aqil, Mohammad, Goswami, Priyanka, Agnihotri, Jaya, Nadeem, Sayyed, 2017. Nanoemulsion-based transdermal drug delivery system for the treat- ment of tuberculosis. Recent Pat. Anti-Infect. Drug Discovery 12 (2), 107–119.

Bo, Xiao, Zhigang, Xu, Viennois, Emilie, Zhang, Yuchen, Zhang, Zhan, Zhang, Mingzhen, Han, Moon Kwon, Kang, Yuejun, Merlin, Didier, 2017. Orally targeted delivery of

tripeptide KPV via hyaluronic acid-functionalized nanoparticles efficiently alleviates ulcerative colitis. Mol. Ther. 25 (7), 1628–1640.

Hee, Yoo Jeoung, Shanmugam, Srinivasan, Thapa, Pritam, Lee, Eung-Seok, Balakrishnan, Prabagar, Baskaran, Rengarajan, Yoon, Sang-Kwon, 2010. Novel self-nanoemulsi- fying drug delivery system for enhanced solubility and dissolution of lutein. Pharmacal Res. 33 (3), 417–426.

Yue, Zhang, Shang, Zhenhua, Gao, Chunhui, Man, Du., Shixia, Xu., Song, Haiwen, Liu, Tingting, 2014. Nanoemulsion for solubilization, stabilization, and in vitro release of pterostilbene for oral delivery. AAPS PharmSciTech 15 (4), 1000–1008.

Le, Zhao, Cen, Fang, Tian, Feng, Li, Min-Jie, Zhang, Qi, Shen, Hong-Yi, Shen, Xiang-Chun, Zhou, Ming-Mei, Du, Jun, 2017. Combination treatment with quercetin and resver- atrol attenuates high fat diet-induced obesity and associated inflammation in rats via the AMPKα1/SIRT1 signaling pathway. Exp. Therapeutic Med. 14 (6), 5942–5948.

Yunpeng, Zhao, Wang, Wenhan, Wu, Xihai, Ma, Xiaoqian, Qu, Ruize, Chen, Xiaomin, Liu, Chenghao, 2017. Mangiferin antagonizes TNF-α-mediated inflammatory reaction and protects against dermatitis in a mice model. Int. Immunopharmacol. 174–179.

CHAPTER III.

Mangiferin glycethosomes as a new potential adjuvant for the treatment of psoriasis

Pleguezuelos-Villa M, Octavio Diez-Sales, Maria Letizia Manca, Maria Manconi, Amparo Ruiz Sauri, Elvira Escribano-Ferrer , Amparo Nácher

International Journal of Pharmaceutics 573 (2020);118844

Mangiferin glycethosomes as a new potential adjuvant for the treatment of psoriasis

Pleguezuelos-Villa M[1*], Octavio Diez-Sales[1,2], Maria Letizia Manca[3], Maria Manconi[3], Amparo Ruiz Sauri[4], Elvira Escribano-Ferrer[5], Amparo Nácher[1,2]

[1] Department of Pharmacy, Pharmaceutical Technology and Parasitology, Faculty of Pharmacy, University of Valencia, Av. Vicent Andrés Estellés s/n, 46100, Burjassot, Valencia, Spain.

[2] Instituto Interuniversitario de Investigación de Reconocimiento Molecular y Desarrollo Tecnológico (IDM), Universitat Politècnica de València, Universitat de València, Av. Vicent Andrés Estellés s/n, 46100, Burjassot, Valencia, Spain.

[3] Dept. of Scienze della Vita e dell'Ambiente, University of Cagliari, via Ospedale 72, 09124, Cagliari, Italy

[4] Department of Pathology, University of Valencia, Av. Blasco Ibañez 17, 46010 Valencia, Spain.

[5] Biopharmaceutics and Pharmacokinetics Unit, Institute for Nanoscience and Nanotechnology, University of Barcelona, Barcelona, Spain

---

*Corresponding author: Pleguezuelos-Villa M; e-mail address: maplevi@alumni.uv.es

telephone number: +34963544912

Fax number: +34963544911

Abstract

Mangiferin, a natural compound isolated from Mangifera indica L, was incorporated in glycerosomes, ethosomes and alternatively in glycerol-ethanol phospholipid vesicles (glycethosomes). Actually, only glycethosomes were able to stably incorporate the mangiferin that was loaded at increasing concentrations (2, 4, 6, 8 mg/mL). The morphology, size distribution, rheological properties, surface charge and entrapment efficiency of prepared vesicles were deeply measured. All vesicles were mainly spherical, oligolamellar, small in size (~145 nm) and negatively charged (~-40 mV), as confirmed by cryo-TEM observation and dynamic laser light scattering measurements. The higher concentration of mangiferin (8 mg/mL) allowed an increase of vesicle mean diameter up to ~288 nm. The entrapment efficiency was inversely proportional to the amount of loaded mangiferin.

In vitro studies performed by using human abdominal skin, underlined that, the dose-dependent ability of vesicles to promote mangiferin retention in epidermis. In addition, glycethosomes were highly biocompatible and showed a strong ability to protect *in vitro* the fibroblasts against damages induced by hydrogen peroxide. *In vivo* results underlined the superior ability of mangiferin loaded glycethosomes respect to the mangiferin dispersion to promote the heal of the wound induced by TPA, confirming their potential application for the treatment of psoriasis or other skin disorders.

Keywords. Mangiferin, phospholipid vesicles, glycethosomes, antioxidant, skin permeation, psoriasis.

1.Introduction

Inflammatory skin diseases are cause of important adverse events and disability for a large number of patients, thus negatively affecting their quality of life. The incidence of these skin diseases, which include atopic dermatitis and psoriasis acute, recurrent or chronic, is increasing in recent years, especially in developed countries (Owczarek and Jaworski 2016).

Currently, the treatment of both atopic dermatitis and psoriasis includes the use of different drugs such as corticoids, calcineurin inhibitors, antihistamines, for topical application and immunosuppressants and biological drugs for systemic treatments (Rodríguez-Luna et al. 2017). However, many patients, especially those with generalized psoriasis, are not adequately treated and long-term therapies are often combined with various side effects of different degrees.

The role of oxidative stress in these diseases has been previously demonstrated in preclinical and clinical studies (Body-Malapel et al. 2018; Tanaka et al. 2018) and the use of antioxidants may represent an ideal strategy to reduce and control the damages caused by psoriasis and atopic dermatitis.

During the last decades, the use of phytodrugs for the treatment of different skin disorders has haroused a great scientific interest (Martinez et al. 2016; Furue et al. 2017; Janeczek et al. 2018). Among the different natural antioxidant molecules, curcumin and quercetin have generated great attention since their large number of important biological and beneficial activities (Abrahams et al. 2019; Rauf et al. 2018).

Considering the promising properties of these, new alternative natural antioxidant molecules such as baicalin, berberin and mangiferin have been isolated and their beneficial properties evaluated (Mir-Palomo et al. 2019; Manca et al. 2019). Mangiferin or 1,3,6,7-tetrahydroxyxanthone-C2-β-D-glucoside (C-glucosyl xanthone) is an antioxidant molecule isolated from Mangifera indica L, a member of the anacardiaceae family. It possesses strong free radical-scavenging (Saha et al. 2016) and anti-inflammatory activities (Szandruk et al. 2018) and it is effective in a variety of diseases, including tumorigenesis (Zou et al. 2017), hypersensitivity (Guo et al. 2014) and tissue repair (Imran et al. 2017). Like other natural antioxidants, it is in vivo biological effectiveness is limited by low bioavailability (1.71%) (Gu et al. 2018; Du et al. 2018) especially when applied on the skin. To overcome these limitations, the loading of natural

antioxidants into nanocarriers has been proposed aiming at increasing their bioavailability and reducing possible side effects (Pimentel-Moral et al. 2018). Many studies have demonstrated an improvement of the effectiveness of these molecules when topically applied. In particular, liposomes or modified phospholipid vesicles disclosed optimal performances in the skin delivery providing an accumulation up to the lower tissues (Manconi et al. 2018b; Fang et al. 2018; Doppalapudi et al. 2017). The analysis of research studies demonstrated that each molecule requires a specific ad hoc tailored phospholipid vesicle formulation to maximizes the efficacy.

Taking into account these results, in this work, specific phospholipid vesicles were tailored to stably deliver mangiferin in the skin. After a pre-formulation study, a special kind of phospholipid vesicles loading mangiferin were prepared hydrating phospholipid with a mixture of water, glycerol and ethanol and so called glycethosomes. Mangiferin was loaded at increasing concentrations (2, 4, 6, 8 mg/mL). The choice of glycerol was mainly related to its moisturizing and cosolvent properties (Angelova-Fischer et al. 2018), which are requested for the treatment of atopic dermatitis, as reported by the therapeutic guidelines (Ring et al. 2012; Eichenfield et al. 2014). While the addition of ethanol was linked to their penetration ability.

Glycethosomes loaded with mangiferin were fully characterized measuring size, size distribution, surface charge, stability on storage and rheological properties. Their ability to promote the accumulation and distribution of mangiferin into and through the skin was evaluated using human abdominal skin. In addition, their potential therapeutic application for the treatment of psoriasis was evaluated in vivo using a 12-O-tetradecanoylphorbol-13-acetate (TPA)-treated mice model.

2. Material and methods

2.1 Materials

Lipoid® S75 a mixture of soybean lecithin containing lysophosphatidylcholine (3% maximum), phosphatidylcholine (70%), phosphatidylethanolamine (10%), fatty acids (0.5% maximum), triglycerides (3% maximum) was purchased from Lipoid GmbH (Ludwigshafen, Germany). Tween 80 were purchased from Scharlab S.L. (Barcelona, Spain). Mangiferin was purchased to Carbosynth Limited (UK). Glycerol was purchased from Guinama S.L.U. (Valencia, Spain), Ethanol was purchased from VWR chemicals S.A.

(France). Phorbol 1, 2-myristate 1, 3-acetate was purchased from Sigma-Aldrich (Madrid, Spain). Cell medium, foetal bovine serum, penicillin and streptomycin and all the other reagents for cells studies, were purchased from Thermo Fisher Scientific Inc. (Waltham, MA, US).

2.2 Analytical method

Mangiferin content was determined by high-performance liquid chromatography (HPLC) using a Perkin Elmer® Series 200 equipped with a photodiode array UV detector and a C18 reverse-phase column (Teknokroma®Brisa "LC2" 5.0 µm, 150 mm × 4.6 mm). The isocratic mobile phase consisted of a mixture of hydrochloric acid (pH 4.0) and methanol (60:40, v/v), the flow rate was 1.2 mL/min. The detection wavelength was set at 254 nm.

2.3 Preparation of vesicles

A preformulation study was performed to evaluate the best composition able to incorporate and retain high amount of mangiferin and promote its efficacy for the topical treatment of psoriasis and atopic dermatitis. Various amounts of different phospholipids were tested, tween 80 was added as excipient aiming at ameliorating the physico-chemical properties of vesicles, Table 1.

Table1

Composition of hydrating medium, mean diameter (MD), polydispersity index (PI) and zeta potential (ZP) of liposomes, glycerosomes, ethosomes and glycethosomes loading mangiferin (2 mg/mL). Each value represents the mean ± standard deviation of at least three determinations.

Formulation	Hydrating medium	MD (nm)	PI	ZP (mV)
Liposomes	Water	452±3	0.40	-37±2
Glycerosomes	Glycerol:water	391±2	0.50	-31±1
Ethosomes	Ethanol: water	643±3	0.40	-39±1
Glycethosomes	Glycerol:ethanol:water	140±1	0.32	-42±1

Among all formulation tested, those obtained using S75 as phospholipid and a mixture of glycerol, ethanol and water (50:25:25) seemed to be the ideal vesicle as it was the smaller and homogeneous system. The glycerol: ethanol: water blend was used to hydrate S75

(100 mg/mL) and tween 80 (5 mg/mL). The mixture was slightly heated (40°C) in a water bath and then different amounts of mangiferin (2, 4, 6 and 8 mg/mL) were added to evaluate the higher quantity of mangiferin which could be stably incorporated and retained in these systems. The dispersions were sonicated for 4 min with a CY-500 ultrasonic disintegrator (Optic Ivymen system, Barcelona, Spain) and then extruded through a 0.20 µm membrane (Whatman, GE Healthcare, Fairfield, Connecticut, US) by using Avanti® Mini Extruder (Avanti Polar Lipids, Alabaster, Alabama). Mangiferin dispersion (8 mg/mL) and empty glycethosomes were also prepared as control. The composition of vesicles is given in Table 2.

2.4 Characterization of vesicles

Vesicle formation and morphology were checked by cryogenic Transmission Electron Microscopy (cryo-TEM). A thin aqueous film was formed by placing a sample drop on a glow-discharged holey carbon grid and then blotting the grid against filter paper. The film was vitrified by plunging the grid in ethane maintained at its melting point with liquid nitrogen, using a Vitrobot (FEI Company, Eindhoven, The Netherlands). The vitreous films were transferred to a Tecnai F20 TEM (FEI Company) and the samples were observed in a low-dose mode. Images were acquired at 200 kV at a temperature between -170 -175 °C, using low-dose imaging conditions not exceeding 20 e-/Å2, with a CCD Eagle camera (FEI Company). The average diameter and polydispersity index (PI) of glycethosomes were measured by Photon Correlation Spectroscopy (PCS) using a Zetasizer nano-ZS® (Malvern Instruments, Worcestershire, UK). Zeta potential was estimated using the Zetasizer nano-ZS by means of the M3-PALS (Mixed Mode Measurement-Phase Analysis Light Scattering) technique, which measures the particle electrophoretic mobility.

The stability on storage was evaluated for 90 days at 4 °C, by measuring the particle size, PI and Zeta potential of glycethosomes every 30 days, which provided useful information about changes in size distribution and surface charge.

The entrapment efficiency (EE) of the glycethosomes was determined as the percentage of the amount of mangiferin recovered after dialysis versus the amount initially used. Each sample (1 mL) was loaded into Spectra/Por®tubing (12–14 kDa MW cut-off; Spectrum Laboratories Inc., DG Breda, The Netherlands) and dialyzed against 1L of water

at room temperature for 8 hours. The mangiferin content was measured by HPLC after disruption of non-dialysed and dialysed vesicles with Triton X-100 (10 %).

2.5 Rheological measurements of mangiferin loaded vesicles

Rheological measurements were carried out at 25±1 °C, using a controlled stress rheometer (RheoStress 1, Thermo Haake, Germany) equipped with a Haake K10 thermostatic bath control and data logging software (RheoWin 4.0.1). Samples were allowed to rest for at least 300 s for temperature equilibrium and stress relaxation. Cone-plate sensor (2°, 35 mm diameter) were used for the analyses.

Step flow curves were obtained in a controlled stress mode (30 s each step in logarithmic distribution). The shear stress range was chosen to evaluate viscosities corresponding to very low shear rates (up to ~100 s^{-1}). All measurements were performed in triplicate, at 25°C. The viscosities results can be calculated by using the simplified Carreau model.

$$\eta = \frac{\eta_0}{\left(1+\left(\frac{\dot{\gamma}}{\dot{\gamma}_c}\right)^2\right)^s} \qquad (1)$$

where η_0 is the zero-shear viscosity, $\dot{\gamma}_c$ is the critical shear rate, and s the shear thinning index.

2.6 Evaluation of in vitro skin delivery of mangiferin loaded vesicles

Experiments were performed using human abdominal skin obtained from donors aged 40-50 years who undergone cosmetic surgical procedures. The skin was given by Hospital Clinic Universitario (Valencia, Spain) after informed consent obtained from patients. The skin was prepared within the first 3 h after excision, removing all subcutaneous fatty tissue, and was stored at -80 °C until use (Alves et al. 2007). The full-thickness human epidermis was placed between the donor and receptor compartments of Franz diffusion vertical cells (effective diffusion area of 0.784 cm^2). The receptor compartment (6 mL) was filled with an aqueous solution containing 1% of tween 80, thermostated at 37±1 °C, and continuously stirred. The different formulations (200 µL) were applied onto the surface of epidermis. At regular time intervals, the receiving solution was withdrawn, replaced with the same volume of pre-thermostated fresh aqueous solution up to 24 hours and analysed by HPLC for mangiferin content. At the end of the permeation

experiments, to verify the integrity of the epidermis, 1 mL of phenol red solution (0.5 mg/mL) was applied on the skin surface, which was considered intact when the amount of phenol red in the receptor compartment was lower than 1%.

After 24 hours the skin surface was removed and gently washed and dried with filter paper, then it was putted in glass vials and methanol (5 mL) was added to allow the extraction of mangiferin accumulated in the epidermis. The extraction procedure was performed for 24 hours under constant stirring (350 rpm) at room temperature (25±1 °C), then the extractive solution was analysed by HPLC for mangiferin content.

2.7 Evaluation of in vitro biocompatibility of mangiferin loaded vesicles

3T3 mouse fibroblasts (ATCC, Manassas, VA, USA) were grown as monolayers in 75-cm^2 flasks, incubated at 37°C in 5% CO_2 and 100% humidity. Dulbecco's modified Eagle's medium (DMEM), supplemented with 10% (V/V) fetal bovine serum, penicillin/streptomicin (100 U/mL), and 0.1% fungizone was used as culture medium. For biocompatibility experiments, 3T3 cells were seeded in 96-well plates at density of $1x10^4$ cell/well. After 24 hours of incubation, 3T3 cells were exposed for 48 h to mangiferin in dispersion (8mg/mL) or loaded in vesicles (2,4,6,8 mg/mL) at different dilutions (1:1000, 1:10000; 1:100000 and 1:1000000). Cell viability was evaluated by means of MTT [3 (4,5-dimethylthiazolyl-2)-2,5-diphenyltetrazolium bromide] colorimetric assay. MTT (100 µL, 0.5 mg/mL final concentration) was added to each well, and then, after 3 h the formazan crystals formed were dissolved in DMSO (100 µL). The reaction was spectrophotometrically measured at 570 nm using a microplate reader (Multiskan EX, Thermo Fisher Scientific, Inc., Waltham, MA, US). The experiments were repeated at least three times. The results are presented as a percentage of untreated cells (100% viability).

2.8 Protection of cells against oxidative stress by using mangiferin loaded vesicles

3T3 cells were seeded into 96-well plates and exposed to hydrogen peroxide (1:40000 dilution) and simultaneously treated with mangiferin in dispersion or loaded in vesicles (8 mg/mL and 2, 4, 6 and 8 mg/mL for dispersion and vesicles, respectively). After 4 h, the cells were washed with PBS and cell viability was evaluated by MTT assay. Untreated cells were used as negative control, while cells treated with hydrogen peroxide only were used

as positive control. Final results are reported as the percentage of untreated cells (100% viability).

2.9 Study of effectiveness of mangiferin loaded vesicles in Inflammatory mice models

Mice were supplied by Envigo laboratories (Barcelona, Spain), and were acclimated for one week before their use. All studies were performed in accordance with the European Union regulations for the handling and use of laboratory animals. The protocols were approved by the Institutional Animal Care and Use Committee of the University of Valencia (code 2018/VSC/PEA/0032 type 2).

Inflammation and ulceration were induced by applying topically TPA, dissolved in acetone (3 µg/20 µL), to the shaved dorsal area (1 cm^2) of female CD-1 mice (5–6 weeks old, 25–35 g). All glycethosomes (200 µL) were topically applied in the same dorsal site 3 h after TPA application. The protocol/experimental plan was repeated for 3 days. Mice (n=5, per group) were sacrificed on day fourth by cervical dislocation. Visual inspection of the skin after the treatment, along with myeloperoxidase activity (MPO) and oedema formation were measured. Inhibition of MPO activity was evaluated as previously reported (Pleguezuelos-Villa et al. 2019). The treated dorsal skin was excised, weighed and used to measure oedema formation. For histological assays, tissue samples were stored in formaldehyde (0.4%, V/V) and longitudinal sections (5 mm) of the skin, obtained using a rotary microtome, were mounted on slides and marked with haematoxylin and eosin according to standard protocols. Tissues were observed and analysed using an optical microscope (DMD 108 Digital Micro-Imaging Device, Leica, Wetzlar, Germany).

2.10 Statistical analysis of data

Statistical differences were determined by one-way ANOVA test and Tukey's test for multiple comparisons with a significance level of $p < 0.05$. All statistical analyses were performed using IBM SPSS statistics 22 for Windows (Valencia, Spain). Data are shown as mean ± standard deviation.

3. Results and discussion

3.1 Preparation and characterization of vesicles

In this study, aiming at promoting the effectiveness of mangiferin in the treatment of psoriasis or atopic dermatitis, new phospholipid vesicles were designed. To achieve

versatile and stable formulations, capable of incorporating high amount of mangiferin, a preformulation study was carried out. Lipoid S75 were use as phospholipid (100 mg/mL) and combined with tween 80 (5 mg/mL). The last acts as edge activator and improve the flexibility of the bilayer (Perez et al. 2016). Mangiferin were loaded at concentration of 2 mg/mL. Lipids, surfactant and payload were mixed and hydrate with water to obtain liposomes, water and glycerol (50:50 v/v) to obtain glycerosomes, water and ethanol (50:50 v/v) to obtain ethosomes, glycerol, ethanol and water (50:25:25 v/v) to obtain glycethosomes. Composition of hydrating medium as well mean diameter, polydispersity index and zeta potential of vesicles loading mangiferin are reported in Table 1. Glycethosomes was the smallest vesicles (~140 nm), most homogeneously dispersed (PI 0.32) and highly negatively charged (-42 mV). The mean diameter of other vesicles was 2-3 times higher. Additionally, the dispersion was very instable and after few days formed two phases. As a consequence, the further studies were focuses on glycethosomes. The same formulation was prepared using the same amount of phospholipid, tween and increasing concentrations of mangiferin (2, 4, 6 and 8 mg/mL), in order to find the highest amount of phytodrug which should be loaded. Empty glycethosomes were also prepared and used as reference. The mean physico-chemical characteristics of vesicles were measured (Table 2). Empty vesicles and those loading 2, 4 and 6 mg/mL showed the same mean diameter (~140 nm), polydispersity index and zeta potential without differences statistically significant among the group ($p > 0.05$). The highest concentrations of mangiferin seem to be critic and the mean diameter of these vesicles was double (~288 nm) compared with the other samples. Probably, using this concentration, the mangiferin which preferentially located in the vesicle bilayer, saturated it modifying the its assembling and curvature radius leading to the increase of particle size (Huang et al. 2017). However, according to other authors, vesicles sized between 100 and 1000 nm are suitable for transdermal administration (Hussain et al. 2017).

The entrapment efficiency (EE%) of mangiferin in glycethosomes slightly decrease as the amount of mangiferin loaded in the formulation increased (Table 2).

Table 2

Mangiferin concentration (MC), mean diameter (MD), polydispersity index (PI), zeta potential (ZP) and entrapment efficiency of 2-glycethosomes, 4-glycethosomes,6-glycethosomes,8-glycethosomes. Each value represents the mean ± standard deviation of at least three determinations.

Formulation	MC (mg/mL)	MD (nm)	PI	ZP (mV)	EE (%)
	0	141±2	0.32	-40±1	
2-Glycethosomes	2	140±2	0.31	-43±2	78±1
4-Glycethosomes	4	149±2	0.33	-40±1	70±1
6-Glycethosomes	6	151±3	0.29	-38±1	65±1
8-Glycethosomes	8	288±2	0.32	-39±2	62±1

Vesicle morphology was evaluated by using Cryo-TEM, which underline the formation of uni- and oligolamellar, spherical and regularly shaped vesicles. These results are in agreement with those obtained by using dynamic light scattering technique, as particle size was ~140 nm for 2-, 4- and 6-glycethosomes and bigger for 8-glycethosomes, (Fig. 1).

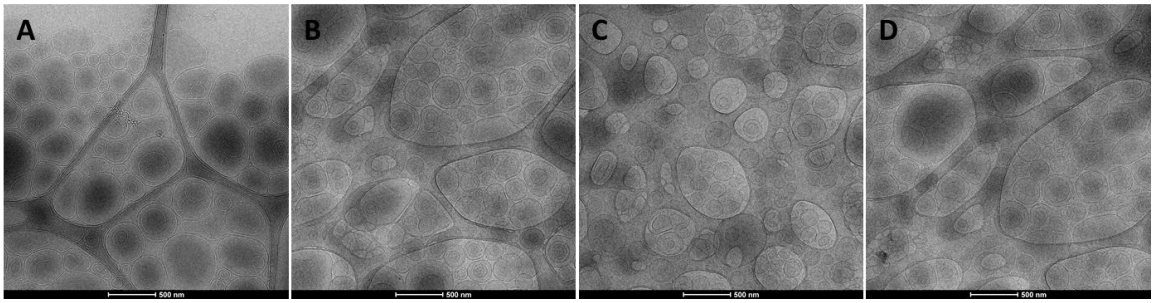

Fig. 1. Representative cryo-TEM images of 2-glycethosomes (A), 4-glycethosomes (B), 6-glycethosomes (C) and 8-glycethosomes (D).

The prepared vesicles were stored at 4°C for 3 mouths and their physico-chemical characteristics (size, PI and zeta potential) were measured at scheduled times. All vesicles desperations were highly stable as any significant variation ($p<0.05$) of the measured parameters were detected during the storage (Fig. 2).

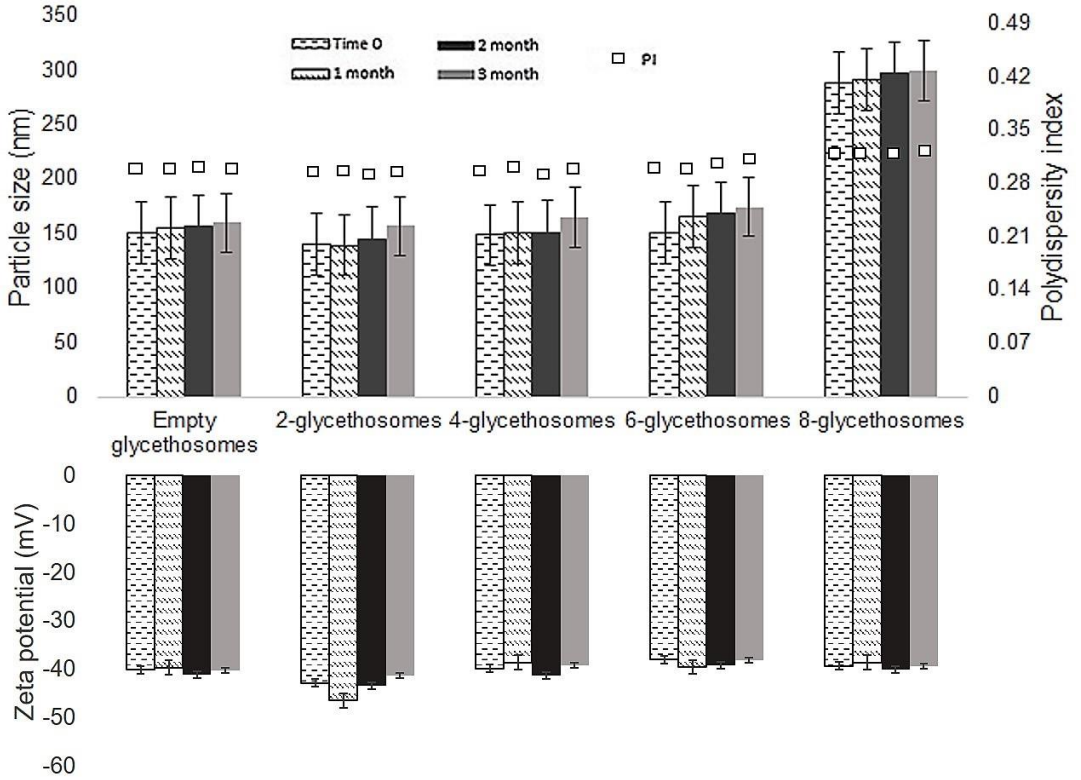

Fig. 2. Mean diameter (MD), polydispersity index (PI) and zeta potential (ZP) of mangiferin loaded into 2-glycethosomes, 4-glycethosomes, 6-glycethosomes and 8-glycethosomes stored for 3 months at 4°C. Data are reported as mean values ± standard deviations (error bars).

3.2 Rheological measurements

The physical state of dispersions and the possible interactions between the vesicles were evaluated by rheological analyses. Viscoelastic properties of the different glycethosomes were evaluated by measuring their viscosity (Fig. 3).

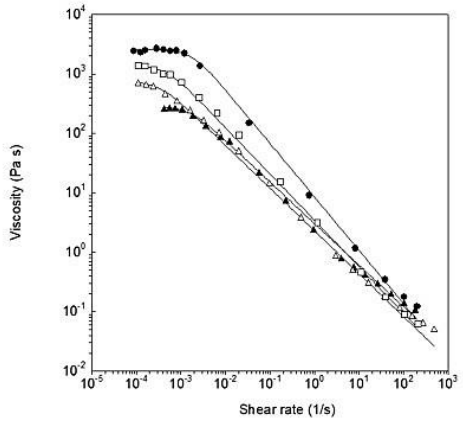

Fig. 3. Representative flow curves fitted to Carreau model for 2-glycethosomes (▲), 4-glycethosomes (Δ), 6-glycethosomes (□) and 8-glycethosomes (●).

As expected, 8-glycethosomes were the most viscous (2584±46 Pa s) as the viscosity increased as the mangiferin concentration increased: 2-glycethosomes (279±4 Pa s); 4-glycethosomes (730±12 Pa s) and 6-glycethosomes (1364±33 Pa s). Besides, all formulations had a similar pseudoplastic behavior (s ~ 0.42). The highest value of viscosity measured for 8-glycethosomes was clearly dependent to the increased mean diameter of vesicles which can encapsulated a large amount of aqueous medium reducing that free in intervesicle spaces. However, a viscosity increase was observed as a function of other mangiferin concentrations too (2, 4 and 6 mg/mL) while the mean diameter of these vesicles remained unchanged. This increase can be related to an improvement of interactions between vesicles, which decreased the kinetic energy.

3.3 In vitro skin penetration and permeation studies

The ability of the new vesicles to facilitate the skin delivery of mangiferin was evaluate by using franz diffusion cells (Manca et al. 2016). Additionally, mangiferin (8 mg/mL) was dispersed in a blend of water, ethanol, and glycerol and the obtained dispersion was used as reference to compare the vesicle performances (Fig. 4).

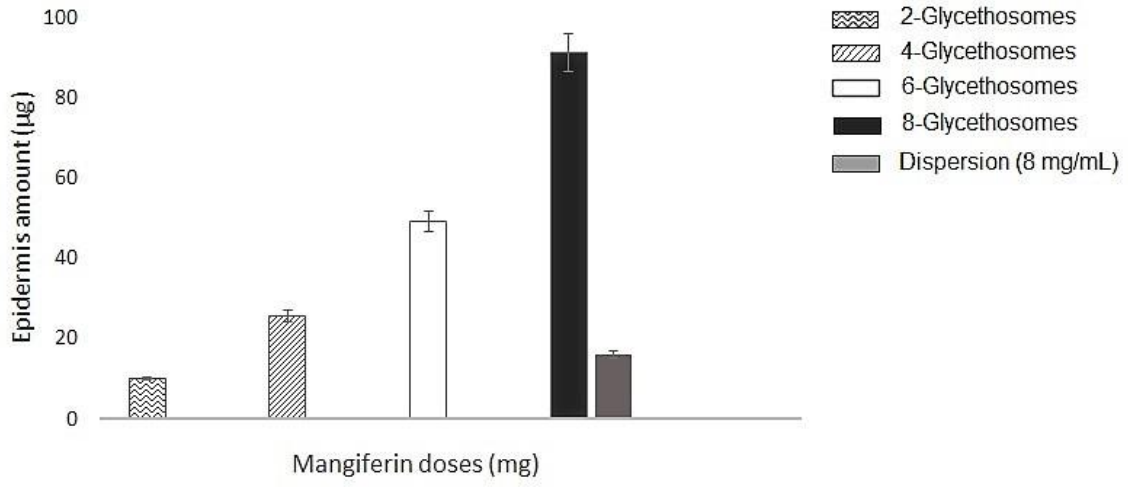

Fig.4. Mangiferin accumulated in epidermis (EP) after 24 h of experiment. Bars represent the mean ± standard deviation of at least six independent experimental determinations.

Using the mangiferin (8 mg/mL) in dispersion the deposition in the skin was ~15 μg like to that provided by the vesicles (~15 μg, $p>0.05$) loading the lowest concentration of mangiferin (2 mg/mL). Using the mangiferin loaded in vesicles the amount of phytodrug accumulated in the epidermis was closely related to the administered dose. Indeed, the amount deposited in the skin after the application of 8-glycethosomes which loaded 8 mg/mL of mangiferin was 9-fold higher than that accumulated after the application of mangiferin dispersion which contained the same amount of phytodrug. Results disclosed the optimal performance of glycethosomes in the skin delivery of mangiferin.

The amount of phytodrug which permeated in the receptor fluid was the lowest using the dispersion and increased as a function of the loaded mangiferin in the vesicles, as follows: mangiferin dispersion <2-glycethosomes (0.81%) <4-glycethosomes (0.86%) <6-glycethosomes (1.52%) <8-glycethosomes (1.70 %) ($p<0.05$). The lower permeation of mangiferin in dispersion may be related to its high molecular weight (~422.34 g/mol) and hydrophilicity (log P oct= -0.65), which make difficulty its permeation through the stratum corneum. Moreover, it was observed that the permeation of the drug through the skin was independent of the vesicle size as the best results were obtained with 8-glycethosomes, which were significantly larger than the other vesicles. Given that, the accumulated amount in the RC was ~1.70% or lower, thus it can be considered negligible.

3.4 In vitro cell viability and protection against oxidative stress

The biocompatibility of mangiferin in dispersion or loaded into glycethosomes was evaluated by using fibroblasts (3T3 cells, Fig. 5A).

The vesicle viability was slight lower using the lower dilution corresponding to 10 μg/mL of mangiferin irrespective to the used formulation. Using the other dilutions any mortality was detected and the viability of cells was ≥100%. Results confirmed a great bioavailability of mangiferin dispersion which was not affected by the loading in vesicles.

The ability of mangiferin in dispersion or loaded in glycethosomes to protect the cells against oxidative stress was evaluated (Fig. 5B).

The cells were stressed with hydrogen peroxide and simultaneously treated with formulations. The viability of stressed cells was very low (~40%). The addition of mangiferin in dispersion was able to slightly counteract the oxidative stress as the viability

increased up to (~70%). However, the best results were obtained when the mangiferin was loaded in glycethosomes as the viability reached ~100% irrespective of the used amount of phytodrug ($p < 0.01$ versus result provided by mangiferin dispersion).

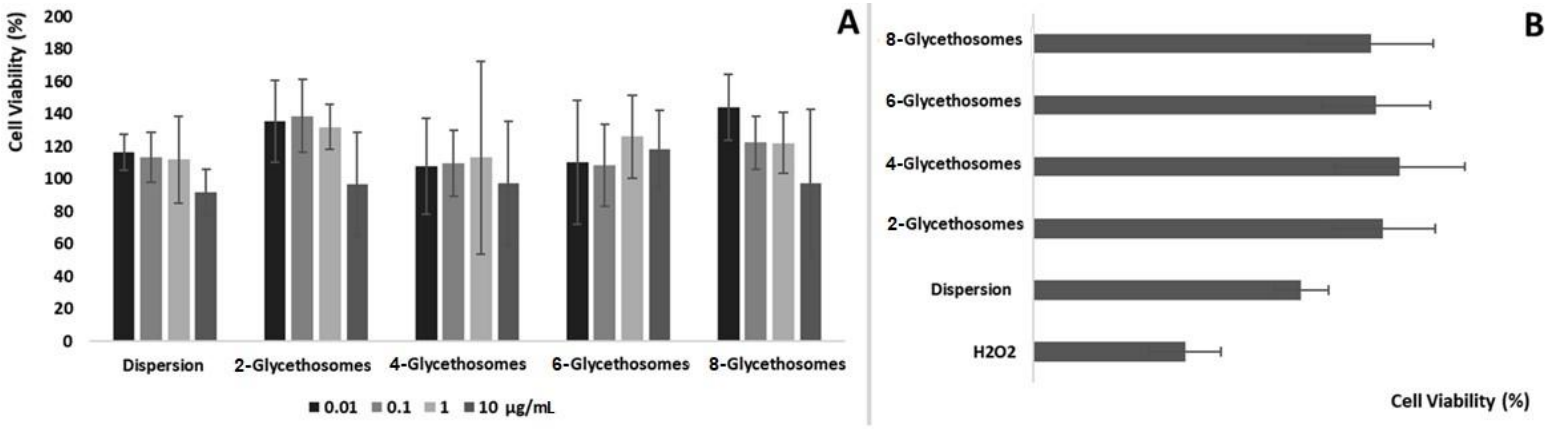

Fig. 5. A Viability of 3T3 cells incubated for 48 h with different concentrations of mangiferin in dispersion or loaded into glycethosomes. **B** Protective effect of mangiferin in dispersion (8 mg/mL) or loaded in glycethosomes against hydrogen peroxide-induced oxidative stress in 3T3 cells. Data are reported as mean values ± standard deviations (error bars) of cell viability expressed as the percentage of control (100% viability).

These results underlined the ability of the vesicles to promote the protection of cells against oxidative stress by reducing the damages caused by the oxygen reactive species. Considering that this process is involved in the pathogenesis of psoriasis, these new mangiferin loaded glycethosomes represent a promising tool for the treatment of this pathology (Lai et al. 2018).

3.5 Inflammatory TPA mice models

Psoriasis is an inflammatory skin disorder characterized by the hyperproliferation of basal epidermal cells. It has been postulated that potent anti-inflammatory and antioxidant agents can play an important role in restoring physiological conditions (Pivetta et al. 2018; Zengin et al. 2019).

In the present study, TPA was applied topically on mice skin to induce ulceration and inflammation effects. The therapeutic efficacy of mangiferin in dispersion or loaded in

glycethosomes was evaluated in vivo by measuring the inhibition of oedema and inflammatory cell activation, typical events associated with skin lesion. To evaluate the effect of the vesicles alone, empty vesicles were also tested.

TPA-induced oedema was significantly reduced ($p<0.05$) by treating the wounded skin with mangiferin loaded vesicles, (~51% inhibition), irrespective to the mangiferin concentration used ($p>0.05$), while the inhibition was only ~6 and 9% ($p>0.05$) when empty vesicles and mangiferin loaded vesicles were used (Table 3).

Table 3

Inhibition of oedema and MPO activity in mice exposed to TPA and treated with mangiferin in dispersion or loaded into glycethosomes. Mean values ± standard deviation is reported. * indicate values significantly different from glycethosomes, # indicate values significantly different from 8-glycethosomes ($p < 0.05$).

Formulations	Oedema inhibition (%)	MPO inhibition (%)
TPA	0	0
Mangiferin dispersion	9±0.1*	30±0.6*
Empty glycethosomes	6±0.1*	26±2.4*
4-glycethosomes	47±3.2	80±5.1
6-glycethosomes	51±2.9	81±4.4
8-glycethosomes	58±2.6	87±3.0#

MPO activity was inhibited as follows: mangiferin loaded vesicles (~83%) > mangiferin dispersion (~30%) > empty vesicles (~25%). These findings demonstrated that the delivery of mangiferin at the wound site using phospholipid vesicles, improves the effectiveness of phytodrug against skin inflammation and this effect should be facilitated by the penetration effect of ethanol and emollient and hydrating properties of glycerol. In addition, different studies suggested that the combination of anti-inflammatory and antioxidant compounds as mangiferin (Biswas et al. 2015; Bairy et al. 2002) with emollients should be used as second and third-line psoriasis therapies (Khosravi et al. 2017). However, all consensus conferences and guidelines supported the use of emollients as a first-line therapy for the treatment of atopic dermatitis (Ring et al. 2012; Eichenfield et al. 2014).

Macroscopic evaluation of the treated skin underlined the superior ability of glycethosomes to heal the wound in comparison with the dispersion used as reference, irrespective of the concentration tested (Fig.6), even if better results were obtained using 6- and 8-glycethosomes (loading 6 and 8 mg/mL of mangiferin).

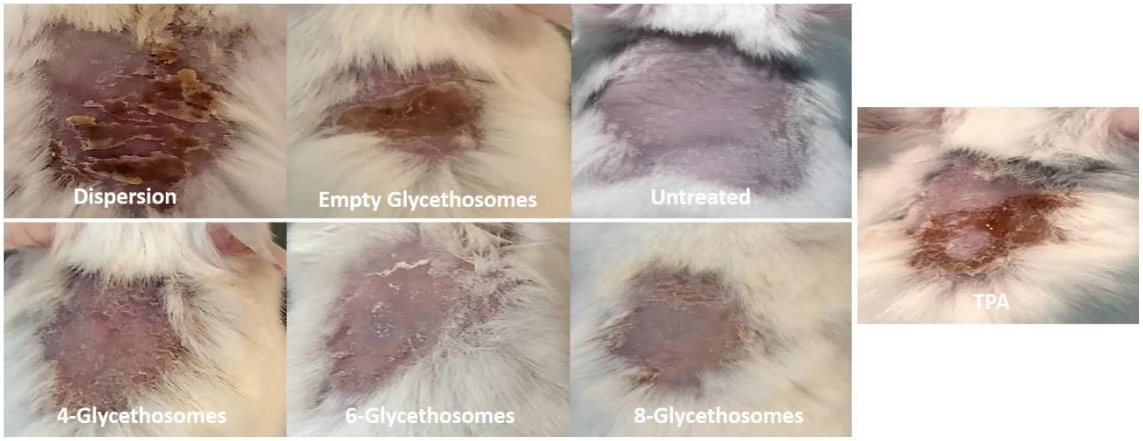

Fig. 6. Mice skin lesions caused by TPA application and treated with empty glycethosomes, mangiferin in dispersion or loaded into 4-glycethosomes, 6-glycethosomes and 8-glycethosomes, and untreated skin.

Histological analysis (Fig. 7) showed that topical application of mangiferin loaded vesicles, irrespective to the used mangiferin concentration, were able to reduce the pathological effect induced by TPA in comparison with mangiferin dispersion and empty glycethosomes. In agreement with the macroscopic observation, 4-glycethosomes showed a slight accumulation of inflammatory cells in the epidermis with parakeratosis evidences and a moderate inflammatory infiltration in dermis.

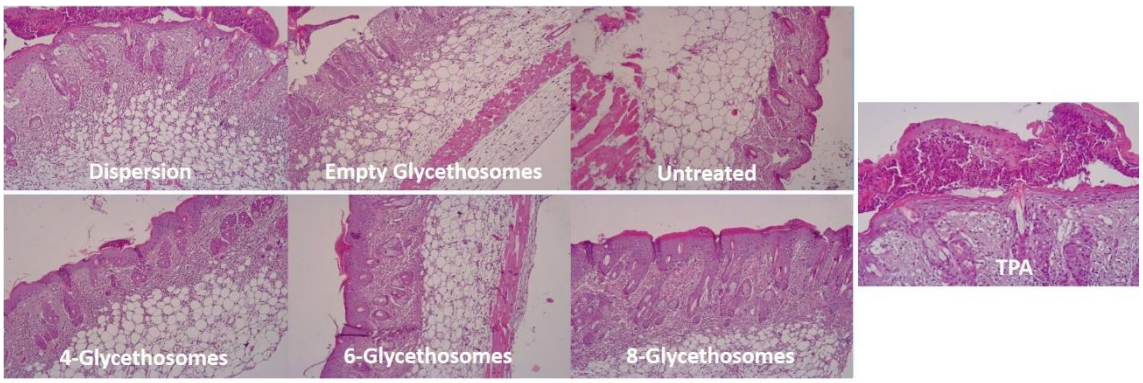

Fig. 7. Histological determination of the mice skin exposed to TPA, treated with empty glycethosomes and with mangiferin in dispersion or loaded into 4-glycethosomes, 6-glycethosomes and 8-glycethosomes, and untreated skin. Original magnification 10x.

However, as the mangiferin concentration increased (6- and 8-glycethosomes), the protection against damaging effects of TPA also increased. Otherwise, skin treated with TPA only, displayed inflammatory infiltrates of mononuclear cells, eosinophils and neutrophils, along with severe dermal and subcutaneous alteration. These alterations are slightly reduced by treating the skin with mangiferin dispersion.

4. Conclusions

The delivery of mangiferin in glycethosomes, along with the high viscosity of these vesicles, favoured the retention of the drug in the epidermis and provided a depot of mangiferin on the skin that could be released slowly. All vesicles tested were highly biocompatible and promoted the effectiveness of mangiferin against the oxidative stress induced in fibroblasts using hydrogen peroxide. In vivo results underlined one time more the superior ability of vesicles to promote the heal of the wound induced by TPA. Overall results seemed to indicate a remarkable therapeutic potential of mangiferin loaded glycethosomes for the treatment of psoriasis or other skin disorders.

Funding

This research did not receive any specific grant from funding agencies in the public, commercial, or not-for-profit sectors.

Declaration of Competing Interest

The authors declare that they have no known competing financial interests or personal relationships that could have appeared to influence the work reported in this paper.

References

Abrahams, Shameemah, William L. Haylett, Glynis Johnson, Jonathan A. Carr, Soraya Bardien, 2019. Antioxidant Effects of Curcumin in Models of Neurodegeneration, Aging, Oxidative and Nitrosative Stress: A Review. Neuroscience 406: 1–21.

Alves, Marta P, Ana L. Scarrone, Marcos Santos, Adriana R. Pohlmann, and Sílvia S. Guterres, 2007. Human Skin Penetration and Distribution of Nimesulide from Hydrophilic Gels Containing Nanocarriers. International Journal of Pharmaceutics 341 (1–2): 215–20.

Angelova-Fischer, Irena, Frank Rippke, Daniel Richter, Alexander Filbry, Craig Arrowitz, Teresa Weber, Tobias W. Fischer, Detlef Zillikens, 2018. Stand-Alone Emollient Treatment Reduces Flares After Discontinuation of Topical Steroid Treatment in Atopic Dermatitis: A Double-Blind, Randomized, Vehicle-Controlled, Left-Right Comparison Study. Acta Dermato-Venereologica 98 (5): 517–23.

Bairy, Indira, S. Reeja, null Siddharth, P. Suganghi Rao, Mahalinga Bhat, P. G. Shivananda, 2002. Evaluation of Antibacterial Activity of Mangifera Indica on Anaerobic Dental Microglora Based on in Vivo Studies. Indian Journal of Pathology & Microbiology 45 (3): 307–10.

Biswas, Taniya, Argha Sen, Rini Roy, Sushomasri Maji, Himangshu Sekhar Maji, 2015. Isolation of Mangiferin from Flowering Buds of Mangifera Indica L and Its Evaluation of in Vitro Antibacterial Activity 4 (3): 8.

Body-Malapel, M., M. Djouina, C. Waxin, A. Langlois, C. Gower-Rousseau, P. Zerbib, A.-M. Schmidt, P. Desreumaux, E. Boulanger, C. Vignal, 2018. The RAGE Signaling Pathway Is Involved in Intestinal Inflammation and Represents a Promising Therapeutic Target for Inflammatory Bowel Diseases. Mucosal Immunology, 25-35

Doppalapudi, Sindhu, Shaheen Mahira, Wahid Khan, 2017. Development and in Vitro Assessment of Psoralen and Resveratrol Co-Loaded Ultradeformable Liposomes for the Treatment of Vitiligo. Journal of Photochemistry and Photobiology. B, Biology 174: 44–57.

Du, Suya, Huirong Liu, Tiantian Lei, Xiaofang Xie, Hailian Wang, Xia He, Rongsheng Tong, Yi Wang, 2018. Mangiferin: An Effective Therapeutic Agent against Several Disorders (Review). Molecular Medicine Reports 18 (6): 4775–86.

Eichenfield, Lawrence F., Wynnis L. Tom, Timothy G. Berger, Alfons Krol, Amy S. Paller, Kathryn Schwarzenberger, James N. Bergman, et al. 2014. Guidelines of Care for the Management of Atopic Dermatitis: Section 2. Management and Treatment of Atopic Dermatitis with Topical Therapies. Journal of the American Academy of Dermatology 71 (1): 116–32.

Fang, Chien-Liang, Yiwei Wang, Kevin H.-Y. Tsai, and Hsin-I Chang, 2018. Liposome-Encapsulated Baicalein Suppressed Lipogenesis and Extracellular Matrix Formation in Hs68 Human Dermal Fibroblasts. Frontiers in Pharmacology 256: 45-50.

Furue, Masutaka, Hiroshi Uchi, Chikage Mitoma, Akiko Hashimoto-Hachiya, Takahito Chiba, Takamichi Ito, Takeshi Nakahara, Gaku Tsuji, 2017. Antioxidants for Healthy Skin: The Emerging Role of Aryl Hydrocarbon Receptors and Nuclear Factor-Erythroid 2-Related Factor-2. Nutrients 9 (3).

Gu, Peng-Cheng, Lan Wang, Mei-Na Han, Jun Peng, Jing-Chuan Shang, Yong-Quan Pan, Wen-Li Han, 2018. Comparative Pharmacokinetic Study of Mangiferin in Normal and Alloxan-Induced Diabetic Rats after Oral and Intravenous Administration by UPLC-MS/MS. Pharmacology 103 (1–2): 30–37.

Guo, Hong-Wei, Chen-Xia Yun, Guang-Han Hou, Jun Du, Xin Huang, Yi Lu, Evan T. Keller, Jian Zhang, Jia-Gang Deng, 2014. Mangiferin Attenuates Th1/Th2 Cytokine Imbalance in an Ovalbumin-Induced Asthmatic Mouse Model. PLoS ONE 9 (6).

Huang, Changjin, David Quinn, Yoel Sadovsky, Subra Suresh, K. Jimmy Hsia, 2017. Formation and Size Distribution of Self-Assembled Vesicles. Proceedings of the National Academy of Sciences 114 (11): 2910–15.

Hussain, Afzal, Sima Singh, Dinesh Sharma, Thomas J. Webster, Kausar Shafaat, Abdul Faruk, 2017. Elastic Liposomes as Novel Carriers: Recent Advances in Drug Delivery. International Journal of Nanomedicine 12: 5087–5108.

Imran, Muhammad, Muhammad Sajid Arshad, Masood Sadiq Butt, Joong-Ho Kwon, Muhammad Umair Arshad, Muhammad Tauseef Sultan, 2017. Mangiferin: A Natural Miracle Bioactive Compound against Lifestyle Related Disorders. Lipids in Health and Disease

Janeczek, Monica, Lauren Moy, Eden P. Lake, James Swan,2018. Review of the Efficacy and Safety of Topical Mahonia Aquifolium for the Treatment of Psoriasis and Atopic Dermatitis. The Journal of Clinical and Aesthetic Dermatology 11 (12): 42–47.

Khosravi, Hasan, Michael P. Siegel, Abby S. Van Voorhees, Joseph F. Merola., 2017. Treatment of Inverse/Intertriginous Psoriasis: Updated Guidelines from the Medical

Board of the National Psoriasis Foundation. Journal of Drugs in Dermatology: JDD 16 (8): 760–66.

Lai, Rui, Dehai Xian, Xia Xiong, Lingyu Yang, Jing Song, Jianqiao Zhong, 2018. Proanthocyanidins: Novel Treatment for Psoriasis That Reduces Oxidative Stress and Modulates Th17 and Treg Cells. Redox Report: Communications in Free Radical Research 23 (1): 130–35.

Manca, Maria Letizia, Pietro Matricardi, Claudia Cencetti, Josè Esteban Peris, Virginia Melis, Claudia Carbone, Elvira Escribano, Marco Zaru, Anna Maria Fadda, and Maria Manconi, 2016. Combination of Argan Oil and Phospholipids for the Development of an Effective Liposome-like Formulation Able to Improve Skin Hydration and Allantoin Dermal Delivery. International Journal of Pharmaceutics 505 (1–2): 204–11.

Manca, Maria Letizia, Silvia Mir-Palomo, Carla Caddeo, Amparo Nacher, Octavio Díez-Sales, Josè Esteban Peris, Josè Luis Pedraz, Anna Maria Fadda, and Maria Manconi, 2019. Sorbitol-Penetration Enhancer Containing Vesicles Loaded with Baicalin for the Protection and Regeneration of Skin Injured by Oxidative Stress and UV Radiation. International Journal of Pharmaceutics 555:175–83.

Manconi, Maria, Maria Letizia Manca, Carla Caddeo, Donatella Valenti, Claudia Cencetti, Octavio Diez-Sales, Amparo Nacher, et al. 2018. Nanodesign of New Self-Assembling Core-Shell Gellan-Transfersomes Loading Baicalin and in Vivo Evaluation of Repair Response in Skin. Nanomedicine: Nanotechnology, Biology, and Medicine 14 (2): 569–79.

Martinez, Renata M., Felipe A. Pinho-Ribeiro, Vinicius S. Steffen, Thais C. C. Silva, Carla V. Caviglione, Carolina Bottura, Maria J. V. Fonseca, et al. 2016. Topical Formulation Containing Naringenin: Efficacy against Ultraviolet B Irradiation-Induced Skin Inflammation and Oxidative Stress in Mice. PLoS ONE 11 (1).

Mir-Palomo, Silvia, Amparo Nácher, M. A. Ofelia Vila Busó, Carla Caddeo, Maria Letizia Manca, Maria Manconi, Octavio Díez-Sales, 2019. Baicalin and Berberine Ultradeformable Vesicles as Potential Adjuvant in Vitiligo Therapy. Colloids and Surfaces. B, Biointerfaces 175: 654–62.

Owczarek, Krzysztof, Mariusz Jaworski, 2016. Quality of Life and Severity of Skin Changes in the Dynamics of Psoriasis. Postepy Dermatologii I Alergologii 33 (2): 102–8.

Perez, Ana Paula, Maria Julia Altube, Priscila Schilrreff, Gustavo Apezteguia, Fabiana Santana Celes, Susana Zacchino, Camila Indiani de Oliveira, Eder Lilia Romero, and Maria Jose Morilla, 2016. Topical Amphotericin B in Ultradeformable Liposomes: Formulation, Skin Penetration Study, Antifungal and Antileishmanial Activity in Vitro. Colloids and Surfaces. B, Biointerfaces 139: 190–98.

Pimentel-Moral, S., M. C. Teixeira, A. R. Fernandes, D. Arráez-Román, A. Martínez-Férez, A. Segura-Carretero, E. B. Souto, 2018. Lipid Nanocarriers for the Loading of Polyphenols - A Comprehensive Review. Advances in Colloid and Interface Science 260: 85–94.

Pivetta, Thais P., Sandra Simões, Margarete M. Araújo, Tânia Carvalho, Caroline Arruda, and Priscyla D. Marcato, 2018. Development of Nanoparticles from Natural Lipids for Topical Delivery of Thymol: Investigation of Its Anti-Inflammatory Properties. Colloids and Surfaces. B, Biointerfaces 164: 281–90.

Pleguezuelos-Villa, María, Amparo Nácher, M. J. Hernández, M. A. Ofelia Vila Buso, Amparo Ruiz Sauri, Octavio Díez-Sales, 2019. Mangiferin Nanoemulsions in Treatment of Inflammatory Disorders and Skin Regeneration. International Journal of Pharmaceutics, 564:299-307.

Rauf, Abdur, Muhammad Imran, Imtiaz Ali Khan, Mujeeb- Ur-Rehman, Syed Amir Gilani, Zaffar Mehmood, Mohammad S. Mubarak, 2018. Anticancer Potential of Quercetin: A Comprehensive Review. Phytotherapy Research: PTR 32 (11): 2109–30.

Ring, J., A. Alomar, T. Bieber, M. Deleuran, A. Fink-Wagner, C. Gelmetti, U. Gieler, et al. 2012. Guidelines for Treatment of Atopic Eczema (Atopic Dermatitis) Part I. Journal of the European Academy of Dermatology and Venereology: JEADV 26 (8): 1045–60.

Rodríguez-Luna, Azahara, Elena Talero, María Del Carmen Terencio, María Luisa González-Rodríguez, Antonio M. Rabasco, Carolina de Los Reyes, Virginia Motilva, and Javier Ávila-Román, 2017. Topical Application of Glycolipids from Isochrysis Galbana Prevents Epidermal Hyperplasia in Mice. Marine Drugs 16 (1).

Saha, Sukanya, Pritam Sadhukhan, Krishnendu Sinha, Namrata Agarwal, and Parames C. Sil, 2016. Mangiferin Attenuates Oxidative Stress Induced Renal Cell Damage through Activation of PI3K Induced Akt and Nrf-2 Mediated Signaling Pathways. Biochemistry and Biophysics Reports 5: 313–27.

Szandruk, Marta, Anna Merwid-Ląd, Adam Szeląg, 2018. The Impact of Mangiferin from Belamcanda Chinensis on Experimental Colitis in Rats. Inflammopharmacology 26 (2): 571–81.

Tanaka, Miori, Yoshimi Kishimoto, Mizuho Sasaki, Akari Sato, Tomoyasu Kamiya, Kazuo Kondo, Kaoruko Iida, 2018. Terminalia Bellirica (Gaertn.) Roxb. Extract and Gallic Acid Attenuate LPS-Induced Inflammation and Oxidative Stress via MAPK/NF-KB and Akt/AMPK/Nrf2 Pathways. Oxidative Medicine and Cellular Longevity 2018: 9364364.

Zengin, Gokhan, Azzurra Stefanucci, Maria João Rodrigues, Adriano Mollica, Luisa Custodio, Muhammad Zakariyyah Aumeeruddy, Mohamad Fawzi Mahomoodally, 2019. Scrophularia Lucida L. as a Valuable Source of Bioactive Compounds for Pharmaceutical Applications: In Vitro Antioxidant, Anti-Inflammatory, Enzyme Inhibitory Properties, in Silico Studies, and HPLC Profiles. Journal of Pharmaceutical and Biomedical Analysis 162: 225–33.

Zou, Bingyu, Hailian Wang, Yilong Liu, Ping Qi, Tiantian Lei, Minghan Sun, Yi Wang. 2017. Mangiferin Induces Apoptosis in Human Ovarian Adenocarcinoma OVCAR3 Cells via the Regulation of Notch3. Oncology Reports 38 (3): 1431–41.

CHAPTER IV.

Mangiferin-naringin vesicles: Improvements in the treatment of chronic inflammatory and oxidative skin diseases

Pleguezuelos-Villa M, Octavio Diez-Sales, Maria Letizia Manca, Carla Caddeo, Maria Manconi, Amparo Ruiz Sauri, Amparo Nácher

Draft to be submitted

Abstract

In this study, new biocompatible nanovesicles are proposed as tools to evaluate the efficacy of the combination of mangiferin and naringin in the treatment of skin diseases connected with inflammatory and oxidative processes, such as psoriasis or atopic dermatitis. Mangiferin and naringin, at high concentrations, were loaded into transfersomes, glycethosomes, glycerosomes, glycethohyalurosomes and glycerohyalurosomes, which were obtained by varying the composition of the dispersing medium (water; glycerol-ethanol-water; glycerol-water; glycerol-ethanol-sodium hyaluronate aqueous solution; glycerol-sodium hyaluronate aqueous solution). The use of a high amount of sodium hyaluronate solution (40 and 50%), improved the vesicle stability and induced a decrease in vesicles' mean diameter. An extensive study was carried out to evaluate the physico-chemical features and properties of the vesicles. All the vesicles were highly biocompatible and showed a strong ability to protect fibroblasts against oxidative damages induced by hydrogen peroxide *in vitro*. Percutaneous studies on intact pig skin showed an improved ability of glycethohyalurosomes and glycerohyalurosomes to favour the deposition of both mangiferin and naringin in the whole skin. Moreover, *in vivo* tests on mice underlined the higher efficacy of co-loaded mangiferin and naringin in glycethohyalurosomes and glycerohyalurosomes in counteracting inflammation, myeloperoxydase activity, and especially oedema formation, induced by a phorbol ester (TPA) treatment.

Keywords: Mangiferin; naringin; phospholipid vesicles; sodium hyaluronate; rheology; oxidative stress; skin delivery.

1. Introduction

Psoriasis and atopic dermatitis are the most common chronic and recurrent inflammatory skin diseases, which affect 15–20% of children and 1–3% of adults worldwide (1). They are characterized by infiltration of inflammatory cells, increased vascularization of the skin, hyperproliferation and abnormal differentiation of epidermal keratinocytes (2,3). Multiple mechanisms are involved in these diseases: early factors include activation of innate immunity, inflammation, and oxidative stress (4).

Although good progress has been made in the knowledge of these chronic diseases, safe and effective treatments are still lacking. The challenge is therefore to explore alternative therapies that can avoid the problems often associated with the traditional treatments, thus capable of reducing the administered dose, the frequency of administration, and the side effects (atrophy, immunosuppression, organ toxicity and infection), with the consequent improvement of the quality of life of patients (5). In recent years, alternative therapies have been proposed, mainly based on the incorporation of natural products into innovative nanocarriers, especially liposomes, which can potentiate the anti-inflammatory effect of the payload and thus reduce the symptoms of the disease (6,7). Among the natural substances, polyphenols seem to be the most promising compounds for the treatment of diseases connected with oxidative and inflammatory processes. In light of this, in this work, mangiferin and naringin, flavonoids with anticarcinogenic, anti-inflammatory, and antioxidants properties (8–11), were combined to evaluate their efficacy in the treatment of skin diseases.

Our previous studies suggested that the incorporation of mangiferin or naringin into nanosystems could improve their therapeutic potential, as naringin transfersomes, mangiferin glycethosomes or mangiferin nanoemulsions were more effective than the corresponding dispersions in counteracting psoriasis or other skin disorders. Moreover, the critical importance of the composition of the dispersing medium used to obtain phospholipid vesicles to promote the efficacy of the payload was highlighted (12–14).

Taking into account these findings, in this work, different phospholipid vesicles, namely transfersomes, glycethosomes and glycerosomes, were prepared by varying the composition and proportions of the dispersing medium to determine the best formulations for mangiferin and naringin. In addition, considering the importance of using biocompatible materials for a better stabilization of the formulation and aiming at

promoting the performance of the delivery systems (15), sodium hyaluronate, a natural biopolymer, was included in the vesicles, thus producing glycethohyalurosomes and glycerohyalurosomes. All the vesicles were characterized by analyzing their average diameter, polydispersity index (PDI) and zeta potential; FTIR and rheological measurements were performed as well. *In vitro* study on the protective effect of the formulations against oxidative stress damages in mouse fibroblasts, along with a permeation assays to evaluate the accumulation and distribution of mangiferin and naringin into and through pig skin, were carried out.

Furthermore, the possible synergistic anti-inflammatory/antioxidant effects of mangiferin-naringin against TPA-induced skin lesion in mice was investigated.

2. Materials and methods

2.1 Materials

Lipoid® S75, soybean lecithin containing lysophosphatidylcholine (3% maximum), phosphatidylcholine (70%), phosphatidylethanolamine (10%), fatty acids (0.5% maximum), and triglycerides (3% maximum), was purchased from Lipoid Gmbh (Ludwigshafen, Germany). Sodium hyaluronate of low molecular weight (200-400 kDa) was purchased from DSM Nutritional Products AG Branch Pentapharm (Aesch, Switzerland). Naringin, glycerol, tween 80, MTT (3-[4,5-dimethylthiazol-2-yl]-2,5-diphenyl tetrazolium bromide), TPA (12-O-tetradecanoyl-phorbol-13-acetate) and all the other reagents of analytical grade were purchased from Sigma-Aldrich (Milan, Italy). Mangiferin was purchased from Carbosynth Limited (UK). Cell medium, foetal bovine serum, penicillin and streptomycin, fungizone, and all the other reagents for cell studies were purchased from Thermo-Fisher Scientific Inc. (Waltham, MA, US)

2.2 Analytical method

Mangiferin and naringin contents were determined by high-performance liquid chromatography (HPLC) using a Perkin Elmer® Series 200 equipped with a photodiode array UV detector and a C_{18} reverse-phase column (Teknokroma®Brisa “LC2” 5.0 µm, 150 × 4.6 mm). The isocratic mobile phase consisted of a mixture of hydrochloric acid (pH 4.0) and methanol (50:50, v/v), the flow rate was 0.8 mL/min, and the injection volume was 20 µL. The detection wavelength was set at 280 nm.

2.3 Vesicles preparation

Different types of vesicles were formulated in order to determine the best composition for the co-incorporation of mangiferin and naringin. Lipoid ® S75 (180 mg/mL), tween 80 (5 mg/mL), mangiferin (10 mg/mL) and naringin (10 mg/mL) were mixed and dispersed in water to obtain transfersomes, or water/glycerol (50:50) to obtain glycerosomes, or glycerol/ethanol/water (33.33:33.33:33.33 and 40:20:40) to obtain glycethosomes A and glycethosomes B, respectively. The dispersions were sonicated (5 s on and 2 s off, 30 cycles; 14 µm of probe amplitude) with a Soniprep 150 ultrasonic disintegrator (MSE Crowley, London, UK) to obtain small and homogeneous vesicles. Furthermore, to improve the stability and performance of the formulations, an aqueous solution of sodium hyaluronate (0.1% w/v) was added to the dispersing medium mixtures of glycerol/ethanol/sodium hyaluronate solution (33.33:33.33:33.33 and 40:20:40) were used to produce glycethohyalurosomes A and glycethohyalurosomes B; a mixture of glycerol/sodium hyaluronate solution (50:50) was used to produce glycerohyalurosomes. The dispersions were sonicated (5 s on and 2 s off, 30 cycles; 14 µm of probe amplitude). Vesicles' composition is given in Table 1.

Mangiferin-naringin aqueous dispersion and empty vesicles were also prepared and used as references.

2.4 Vesicles characterization

The average diameter, polydispersity index (PI) and zeta potential of the vesicles were determined by Dynamic and Electrophoretic Light Scattering using a Zetasizer nano-ZS (Malvern Instruments, Worcestershire, UK). These parameters were also measured over a storage period of 90 days at 4 °C to evaluate vesicles' stability.

The interactions between the vesicles and mangiferin-naringin were evaluated by Fourier transform infrared (FTIR) studies, at room temperature in a spectral region between 500 and 4000 cm^{-1}, by using ATR Agilent Cary 630 (Germany).

The vesicle formulations (1 mL) were purified from the non-incorporated mangiferin-naringin by dialysis (Spectra/Por membranes: 12–14 kDa MW cut-off, 3 nm pore size; Spectrum Laboratories Inc., DG Breda, The Netherlands) against 2 L of water for 2 h, with water refreshed after 1 h.

The antioxidant activity (AA) of mangiferin and naringin in aqueous dispersion or loaded into the vesicles was assessed by measuring their ability to scavenge DPPH (2,2'-diphenyl-1-picrylhydrazyl) radical. Samples (10 µL) were dissolved in 1990 µL of DPPH methanolic solution (4 mg/100 mL) and incubated for 30 min at room temperature, in the dark. Then, the absorbance (ABS) was measured at 517 nm against blank. All the experiments were performed in triplicate. AA was calculated according to the following formula:

$$AA = (ABS_{DPPH} – ABS_{sample}/ABS_{DPPH}) \times 100$$

AA was also measured before and after dialysis of the vesicle formulations and the entrapment efficiency (EE) of the vesicles was calculated as the percentage of the AA of dialyzed versus non-dialyzed samples (16).

Table1. Composition of vesicle formulations.

Formulation	S75 (mg/mL)	Naringin (mg/mL)	Mangiferin (mg/mL)	Tween80 (mg/mL)	Glycerol (%)	Ethanol (%)	Water (%)	Sodium hyaluronate solution (%)
Transfersomes	180	10	10	5	----	-----	100	-----
Glycethosomes A	180	10	10	5	33.33	33.33	33.33	-----
Glycethosomes B	180	10	10	5	40	20	40	-----
Glycethohyalurosomes A	180	10	10	5	33.33	33.33	----	33.33
Glycethohyalurosomes B	180	10	10	5	40	20	-----	40
Glycerosomes	180	10	10	5	50	-----	50	----
Glycerohyalurosomes	180	10	10	5	50	----	-----	50

2.5 Rheological measurements

A controlled stress rheometer (RheoStress 1, Thermo Haake, Germany) equipped with control and data logging software (RheoWin 4.0.1) and a Haake K10 thermostatic bath for temperature control, was used. After loading, samples were allowed to rest for at least 300 s for stress relaxation and temperature equilibrium. A cone-plate sensor (2°, 35 mm diameter) was used. Two types of rheological measurements were performed: flow curves and small amplitude oscillation sweeps tests. All measurements were performed in triplicate, at 25 °C.

Step flow curves were performed in controlled stress mode (30 s each step in logarithmic distribution). The viscosity results were fitted to the simplified Carreau model.

$$\eta = \frac{\eta_0}{\left(1+\left(\frac{\dot{\gamma}}{\dot{\gamma}_c}\right)^2\right)^s}$$

where η_0 is the zero-shear viscosity, γ_c is the critical shear rate, and s the shear thinning index.

Viscoelastic properties were determined by oscillatory measurements. Both elastic (G') and viscous (G") moduli were measured varying the frequency sweep from 0.01 to 10 Hz, at a constant stress (within the linear viscoelastic region, formerly determined from stress sweep tests at 1 Hz). The loss tangent (tanδ= G''/G') was calculated as the ratio between the viscous and the elastic moduli.

2.6 *In vitro* cytocompatibility and antioxidant effect of the vesicular formulations.

3T3 mouse fibroblasts (ATCC collection, Manassas, VA, US) were grown with 100% humidity and 5% CO_2 at 37 °C. Dulbecco's Modified Eagle Medium (DMEM) with 10% foetal bovine serum, 1% penicillin-streptomycin and fungizone, was used to culture the cells. Cell viability was measured by means of the MTT test (18). The cells ($7.5x10^3$ cells/well) were seeded into 96-well plates, cultured for 24 h, and exposed for 48 h to the samples diluted with medium to achieve the desired concentrations (10, 1, 0.1, 0.01 μg/mL). Thereafter, an MTT solution (0.5 mg/mL final concentration) was added to each well, removed after 3 h, and replaced with dimethyl sulfoxide. The absorbance was read at 570 nm with a microplate reader (Multiskan EX, Thermo Fisher Scientific Inc., Waltham, MA, US). The results are shown as a percentage of live cells in comparison with untreated control cells (100% viability).

To evaluate the protective ability of the vesicles against oxidative damages induced by hydrogen peroxide, the cells were seeded into 96-well plates, incubated for 24 h, and exposed simultaneously to hydrogen peroxide (1:50000 dilution) and mangiferin- naringin loaded vesicles (1 μg/mL). After 4 h, the cells were washed with PBS, and the MTT assay was performed to assess cell viability. Untreated cells (100% viability) were used as a

negative control, and cells exposed only to hydrogen peroxide were used as a positive control.

2.7 *In vitro* skin delivery studies

Skin delivery experiments were performed by using the dorsal skin of pigs (~1.5 kg) died of natural causes, provided by a local slaughterhouse. The skin was pre-equilibrated in saline prior to the experiments. Full-thickness skin specimens (n = 6) were placed between the donor and receptor compartments of Franz vertical cells (effective diffusion area of 0.785 cm^2). The receptor compartment was filled with a 1% tween 80 aqueous solution, thermostated at 37±1 °C, under stirring. The vesicle formulations were applied (200 µL) onto the skin surface.

At regular intervals up to 24 h, the receiving solution was withdrawn, replaced and analyzed by HPLC to quantify mangiferin and naringin. After 24 h, the skin surface was dried with filter paper and the stratum corneum was removed by stripping with adhesive tape (Tesa® AG, Hamburg, Germany) (17). Epidermis was separated from dermis with a surgical scalpel. The tape strips and the skin strata were cut, placed each in a glass vial with methanol and sonicated for 2 min. The tape strips and skin suspensions were filtered and tested for mangiferin and naringin content by HPLC.

2.8 *In vivo* assay

Female CD-1 mice (5–6 weeks old, 25–35 g) were provided by Envigo laboratories (Barcelona, Spain) and acclimatized for one week in the animal facility of the University of Valencia, prior to the experiments. The studies were performed in accordance with the European Union regulations for the handling and use of laboratory animals. The protocols were approved by the Institutional Animal Care and Use Committee of the University of Valencia (code 2018/VSC/PEA/0032 type 2).

A short-term topical TPA treatment was performed following a previously reported method (12). Briefly, one day after shaving, TPA dissolved in acetone (3 µg/20 µL) was applied on the dorsal skin of mice. After 3 h, 200 µL of each formulation was topically applied on the same area. This procedure was repeated for 3 consecutive days. Mice (n=5 per group) were sacrificed on day 4 by cervical dislocation.

Oedema formation and myeloperoxidase (MPO) activity were measured. The treated dorsal skin area of mice was excised and weighed to evaluate oedema formation. MPO

assay was carried out as previously detailed (13). Briefly, skin biopsies were homogenized and centrifuged, the supernatant was incubated with a mixture of sodium phosphate buffer (pH 5.4), phosphate buffer (pH 7.4), hydrogen peroxide and 3,30,5,50-tetramethylbenzidine dihydrochloride, and then MPO activity was measured spectrophotometrically at 450 nm. MPO activity was calculated from the linear portion of a standard curve.

For histological assessment, dorsal skin specimens of treated mice were fixed in 0.4% formaldehyde, embedded in paraffin, and sectioned at 5 mm. The sections were counterstained with hematoxylin and eosin. The tissues were observed under a light microscope (DMD 108 Digital Micro-Imaging Device, Leica, Wetzlar, Germany).

2.9 Statistical analysis of data

Statistical differences were determined by one-way ANOVA test and Tukey's test for multiple comparisons with a significance level of $p < 0.05$. All statistical analyses were performed using IBM SPSS statistics 22 for Windows (Valencia, Spain). Data are shown as means ± standard deviations.

3. Results and discussion

3.1 Vesicle characterization

Mangiferin and naringin were co-loaded into different vesicular systems: transfersomes, glycethosomes, glycethohyalurosomes, glycerosomes and glycerohyalurosomes. The physico-chemical characteristics of the vesicles are reported in Table 2. Glycethosomes A and glycethohyalurosomes A were the largest vesicles (~250 nm), and glycethohyalurosomes B were the smallest vesicles (~100 nm). The other vesicles ranged between 131 and 170 nm. The vesicles were highly homogeneous, as indicated by polydispersity index values <0.3, except for transfersomes and glycethosomes A (Table 2). By comparing glycethohyalurosomes A and B, it can be concluded that B ratios (40:20:40) favoured the formation of smaller and more homogeneous vesicles. All the vesicles were highly negatively charged, with values around -50 mV.

The stability of the formulations was evaluated by measuring their size, polydispersity index and zeta potential for 3 months (Figure 1). Transfersomes and glycerosomes were stable over the monitoring period in terms of size and polydispersity index ($p < 0.05$). Glycethosomes A and B and glycethohyalurosomes A underwent a significant increase in

size (up to ~500 nm) throughout the studied period. On the contrary, glycethohyalurosomes B and glycerohyalurosomes were highly stable on storage, as the studied parameters did not change. Probably, the combination of high amounts of glycerol and sodium hyaluronate solution promoted the stabilization of the formulations. It was previously reported that sodium hyaluronate could be embedded into the lipid bilayer and improve the stability of the vesicle system (19).The zeta potential of glycethohyalurosomes B and glycerohyalurosomes remained unchanged, while the values for the other vesicles became less negative (~−30 mV, $p < 0.05$).

Table2. Mangiferin and naringin co-loaded vesicles: mean diameter (MD), polydispersity index (PDI), zeta potential (ZP) and entrapment efficiency. Each value represents the mean ± standard deviation of at least three determinations.

Formulation	MD (nm±SD)	PDI	ZP (mV±SD)	EE (%±SD)
Transfersomes	140±6	0.34	-48±4	85±2
Glycethosomes A	264±7	0.31	-50±3	87±3
Glycethosomes B	170±8	0.28	-45±2	88±2
Glycethohyalurosomes A	243±9	0.29	-55±4	90±2
Glycethohyalurosomes B	94±8	0.15	-56±3	88±2
Glycerosomes	157±6	0.22	-50±4	86±3
Glycerohyalurosomes	131±6	0.21	-54±3	88±2

The behavior of empty vesicles was similar to that of mangiferin-naringin co-loaded vesicles, even though the stability on storage of empty glycethohyalurosomes B and empty glycerohyalurosomes was slightly reduced, pointing to a stabilizing effect of the two loaded flavonoids.

All the vesicles were able to incorporate the flavonoids in good yields, as shown by the entrapment efficiency values ≥ 85% (Table 2).

Fourier Transform Infrared (FTIR) studies were performed to better understand the interactions of the vesicles' components, the contribution of sodium hyaluronate to vesicle assembly. As shown in Figure 2, the FTIR spectrum of mangiferin showed characteristic absorption bands at 3373 cm^{-1} (hydroxyl group); 2933 cm^{-1} (C–H asymmetric stretching), 1255 cm^{-1} (–C–O–) and 1093 cm^{-1} (–C–O–C). Similarly, the spectrum of naringin revealed the presence of an intense band at 286 nm and another

band at 327 nm, which are characteristic of flavonoids, along with bands at 1080 cm^{-1} (-C–O-), 1641 cm^{-1} (-C=O-) and 1357 cm^{-1} (–C–O–C). The incorporation of both flavonoids into the vesicles caused a significant reduction of the intensity of the peaks, confirming the intercalation of these compounds in the bilayer of the formulations. By comparing the spectra of the raw flavonoids and the flavonoids in the vesicles, the majority of changes were observed in the region between 1800 to 500 cm^{-1}.

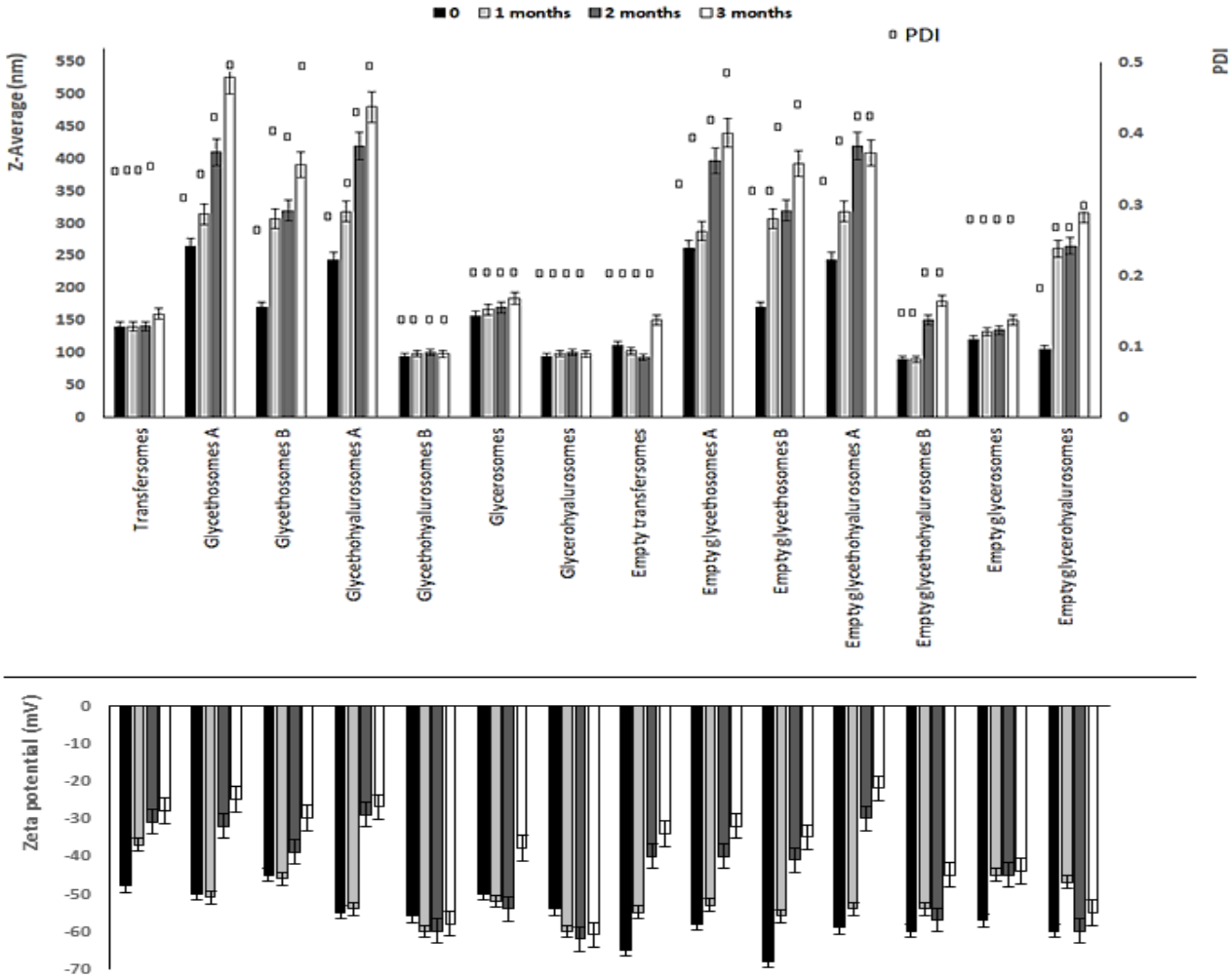

Figure 1. Mean diameter, polydispersity index (PDI) and zeta potential values of both empty and mangiferin-naringin co-loaded vesicles stored for 3 months at 4 °C. Data are reported as mean values ± standard deviations (error bars) (n=3).

Sodium hyaluronate displayed a peak at 1040 cm^{-1} (skeletal vibrations involving the C-O-C bridge), due to its saccharide structure (20). According to other authors, glycerol spectrum presents a peak at 1045 cm^{-1} associated to the stretching of the C–O linkage in C_1 and C_3 (21). The characteristic peak of glycerol at 1045 cm^{-1} was shifted to 1060 and 1063 cm^{-1} in glycethohyalurosomes B and glycerohyalurosomes, respectively, when a high percentage of sodium hyaluronate (≥40%) was used, confirming an interaction between the biopolymer and the primary alcohol of glycerol. Besides, it is noteworthy that, in the region of hydroxyl vibration (3500–3000 cm^{-1}), a slight shift of the peak of the mixtures to higher frequencies was detected when the percentage of sodium hyaluronate increased.

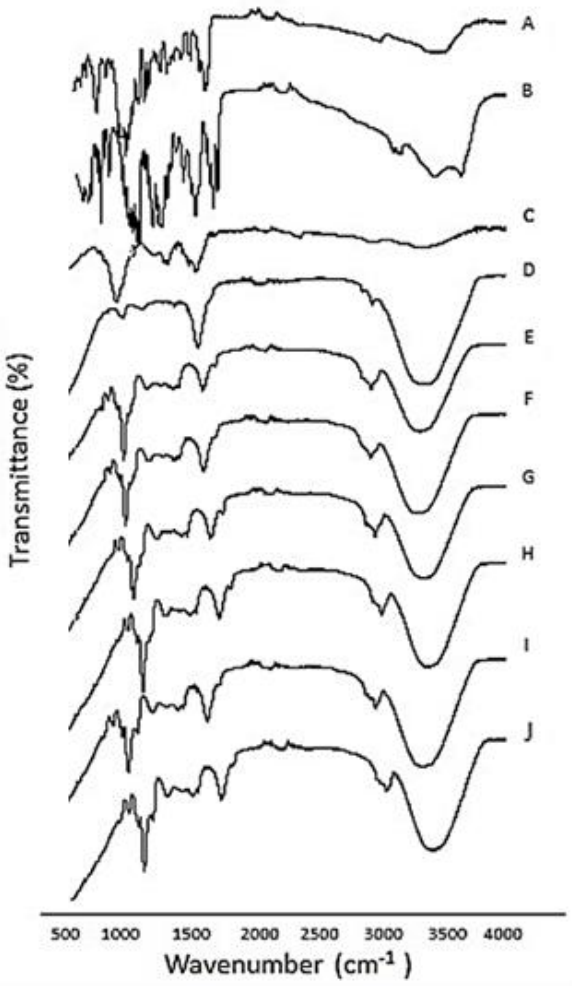

Figure 2. FT-IR spectra of A) naringin; B) mangiferin; C) sodium hyaluronate; D) transfersomes; E) glycethosomes A; F) glycethosomes B; G) glycethohyalurosomes A; H) glycethohyalurosomes B; I) glycerosomes; J) glycerohyalurosomes.

3.2 Rheological measurements

An extensive rheological analysis was carried out to investigate the possible supramolecular interactions between the different components of the vesicles and the influence of sodium hyaluronate on the rheological behavior of the vesicle systems. As can be seen in Figure 3A, glycerosomes were the most viscous formulation (60051±1063 Pa s): glycerol increased the viscosity by ~24 times in comparison with transfersomes (2469±54 Pa s). The addition of ethanol and the consequent reduction in the amount of glycerol, made the system less viscous. Indeed, the viscosity of glycethosomes A and B was (1602±52 and 487±6 Pa s, respectively). On the other hand, the presence of sodium hyaluronate (33.33%) increased the viscosity, which was 6537±200 Pa s for glycethohyalurosomes A. However, no further increase in viscosity was detected when the amount of sodium hyaluronate was increased (40% in glycethohyalurosomes B and 50% in glycerohyalurosomes), suggesting a possible interaction between glycerol and the polymer (as already detected by FTIR studies) that drastically modified the assembly of the vesicles producing a more fluid and stable system. Indeed, an increase in the amount of sodium hyaluronate aqueous solution can produce a conformational change in the chains of the polymer influenced by the ionic strength, so that the viscosity is significantly reduced. Besides, increasing the shear rates, the polymer chains deformed and aligned along the streamlines of flow, which resulted in a reduction of the viscosity (22). As shown by the flow curves in Figure 3A, glycethohyalurosomes B and glycerohyalurosomes were the least viscous formulations (229±8 and 68±1.5 Pa s, respectively).

In order to obtain information about the internal structure of the systems, oscillatory measurements at a constant stress, in the linear viscoelastic region (LVR), were also performed.

Dynamic moduli of glycethosomes A, glycethohyalurosomes A and transfersomes were characterized by a higher elastic modulus (G`) than the viscous modulus (G''), especially for glycethohyalurosomes A, which indicates a more structured and stronger (weak gel) system (data not shown). It is interesting to note that glycethohyalurosomes B showed a higher tan δ than glycethosomes B (0.21 and 0.05, respectively, at 1 Hz; Figure 3B), which is indicative of a less structured system, in agreement with the viscosity values. The effect of sodium hyaluronate in combination with high amounts of glycerol was more evident

between glycerohyalurosomes and glycerosomes, which may be due to the polyelectrolyte character of sodium hyaluronate in aqueous solution (23). Glycerohyalurosomes showed a loss tangent value (tan δ) greater than 1 (1.25 at 1 Hz; Figure 3B) and strongly dependent on the frequency, while tan δ was 0.04 (at 1 Hz; Figure 3B) for glycerosomes. Moreover, the viscous modulus (G") was greater than the elastic modulus (G'), which could indicate macromolecular interactions, but not the formation of a three-dimensional network. These results were in accordance with flow curves and the viscosity values, confirmed that a strong interaction between sodium hyaluronate and the solvents occurred.

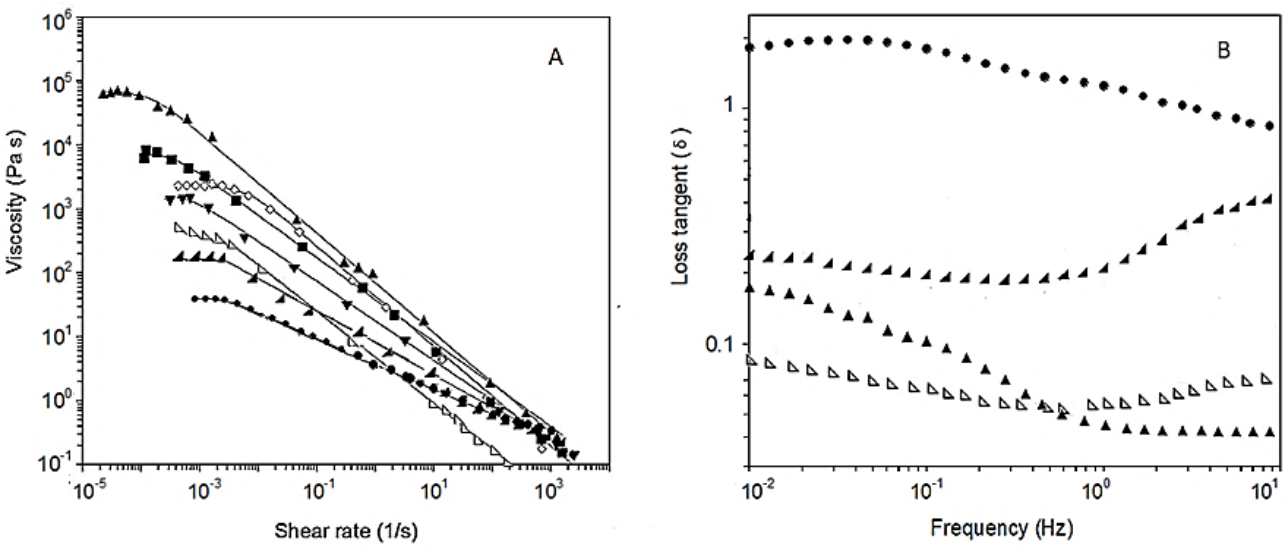

Figure 3. Rheological measurements. A) Flow curves fitted to Carreau model for glycerohyalurosomes (●), glycethohyalurosomes B (◢), glycethosomes B (◿), glycerosomes (▲), glycethosomes A (▼), transfersomes (◊), glycethohyalurosomes A (■). B) Loss tangent versus frequency for glycerohyalurosomes (●), glycethohyalurosomes B (◢), glycethosomes B (◿), glycerosomes (▲).

3.3 *In vitro* cytocompatibility of vesicular formulations and protective effect against oxidative damage in fibroblasts

The cytocompatibility of mangiferin and naringin co-loaded into vesicles was evaluated in fibroblasts (Figure 4A) by means of the MTT assay. The viability of the cells treated with transfersomes was the lowest (~ 90%) and concentration-dependent: it decreased as the concentration of mangiferi-naringin increased. The cell viability was higher (~ 104%,

p>0.05) when the other vesicular formulations were used, irrespective of their composition.

Moreover, to evaluate the efficacy of mangiferin and naringin co-loaded in the vesicles in counteracting the damaging effects of oxidative stress in fibroblasts, the cells were treated with hydrogen peroxide and simultaneously with the formulations (Figure 4B)

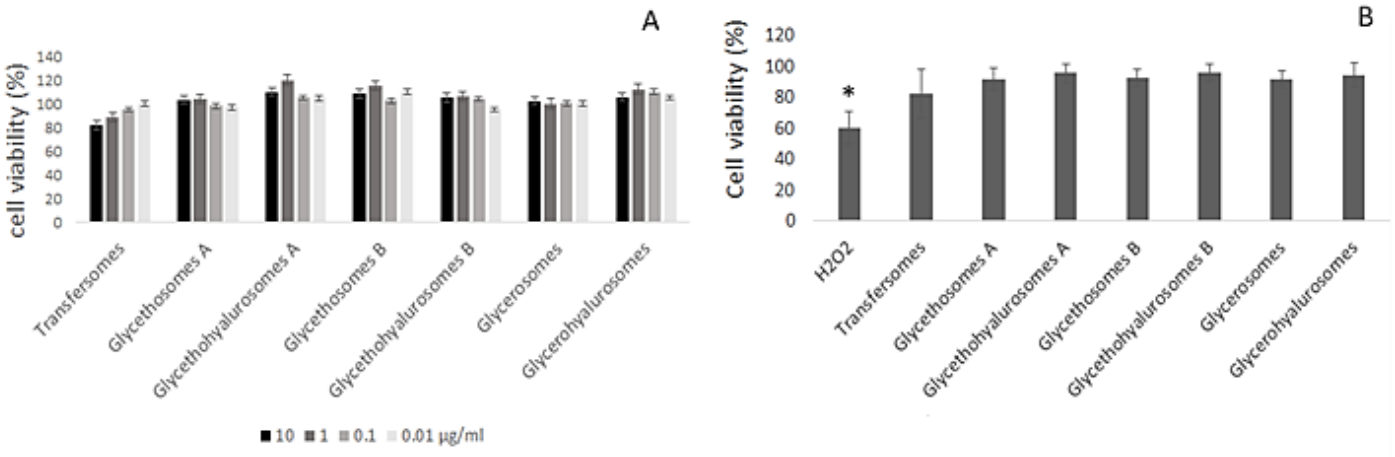

Figure 4. A) Viability of 3T3 cells incubated for 48 h with different concentrations of mangiferin-naringin co-loaded vesicles. B) Protective effect of mangiferin-naringin co-loaded vesicles against hydrogen peroxide induced oxidative stress in 3T3 cells. Data are reported as mean values ± standard deviations (error bars) of cell viability expressed as the percentage of control (100% viability). * symbol indicates statistically different values ($p < 0.05$) obtained by comparing compared cells treated with vesicles treated and cells treated with hydrogen peroxide.

The treatment with hydrogen peroxide caused a significant decrease in cell viability (~60%), while mangiferin and naringin co-loaded in the vesicles were able to counteract oxidative stress, as the viability increased (> 80%; $p<0.05$ *vs.* positive control). The best results were obtained when mangiferin and naringin were co-loaded in glycethosomes and glycerosomes, regardless of the presence of sodium hyaluronate, as the viability reached ~94% ($p>0.05$ *vs.* the other vesicles). These results underlined the ability of the vesicles to promote the protective/antioxidant activity of mangiferin-naringin against the damages caused by reactive oxygen species.

3.4 *In vitro* transdermal delivery

To evaluate the ability of the vesicles to promote the accumulation of mangiferin and naringin in the skin layers (i.e., stratum corneum, SC; epidermis, EP; dermis, DE) and their diffusion into the receptor compartment (RC) mimicking the subcutaneous tissues, *in vitro* studies were carried out by using pig skin and Franz diffusion cells (Figure 5). Due to the large size and instability of glycethosomes A and B and glycethohyalurosomes A and their statistical non-significance observed in cell cultures, the transdermal studies were not performed with these formulations.

When transfersomes were used, the amounts of mangiferin-naringin accumulated in EP and DE were ~1.5 and 2-fold higher than those accumulated after the application of mangiferin-naringin in aqueous dispersion. Better results were obtained by using glycerosomes, which showed a superior ability, in comparison with transfersomes, to promote the deposition of the flavonoids in SC (~5% for both mangiferin and naringin), EP (~2 % naringin and ~ 3% mangiferin, $p<0.05$) and DE (0.7% naringin and 1.2% mangiferin, $p<0.05$). The best results were obtained by using glycethohyalurosomes B and glycerohyalurosomes ($p<0.05$), suggesting the important role of the association of sodium hyaluronate, glycerol and ethanol in promoting the deposition of the flavonoids in the different skin layers, especially in epidermis and dermis. In the case of glycethohyalurosomes B, the accumulated mangiferin was ~5, 9 and 4% in SC, EP and DE, respectively; the accumulated naringin was ~9, 7 and 2% in SC, EP and DE, respectively. In the case of glycerohyalurosomes, the accumulated mangiferin was ~3, 7 and 2% and naringin was ~6, 5 and 1% in SC, EP and DE, respectively. Moreover, only the formulations containing sodium hyaluronate allowed the permeation in the receptor fluid of both mangiferin and naringin. Especially glycethohyalurosomes B showed a great permeation of both flavonoids (1.7 and 4-fold higher than glycerohyalurosomes), highlighting the ability of these systems to promote the diffusion through the skin (24,25).

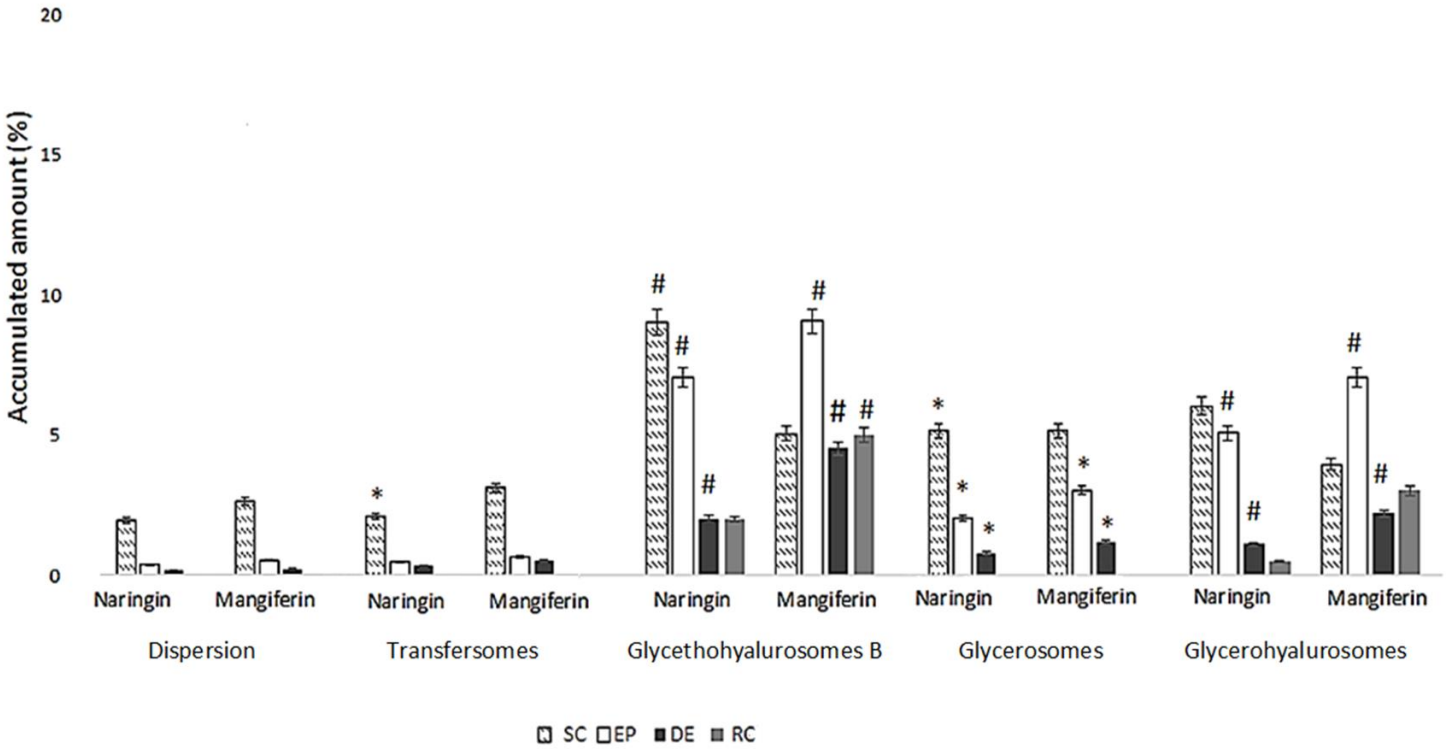

Figure 5. Amounts of mangiferin and naringin accumulated in stratum corneum (SC), epidermis (EP), dermis (DE) and receptor compartment (RC) after 24 h of treatment with dispersion, transfersomes, glycethohyalurosomes B, glycerosomes and glycerohyalurosomes. Mean values ± standard deviations are reported (n=6). *$p < 0.05$: values statistically different comparing glycerosomes and transfersomes; $^{\#}p < 0.05$: values statistically different comparing glycethohyalurosomes B and glycerohyalurosomes with the other formulations.

3.5 *In vivo* assays

TPA was topically applied on the shaved dorsal skin of mice aiming at inducing inflammation and ulceration. Given the results of the transdermal studies, only mangiferin-naringin co-loaded glycethohyalurosomes B and glycerohyalurosomes were tested. Mangiferin-naringin in aqueous dispersion or in transfersomes were used as controls. Upon visual inspection, the animals treated with TPA only, showed a loss of superficial skin layers and the formation of crusts. The treatment with empty vesicles or the aqueous dispersion reduced the extent of the damage induced by TPA, but crusts were still present. On the other hand, mangiferin-naringin co-loaded vesicles were capable of preventing the lesions caused by the daily application of TPA. The superior ability of glycethohyalurosomes B and glycerohyalurosomes to promote the healing of

the wound was evident (Figure 6A). Histological analysis (Figure 6B) showed that, despite the topical application of mangiferin-naringin dispersion, there was a loss of epidermis and a moderate accumulation of inflammatory cells in dermis. The application of transfersomesreduced the infiltration of the inflammation mediators of at dermal level.

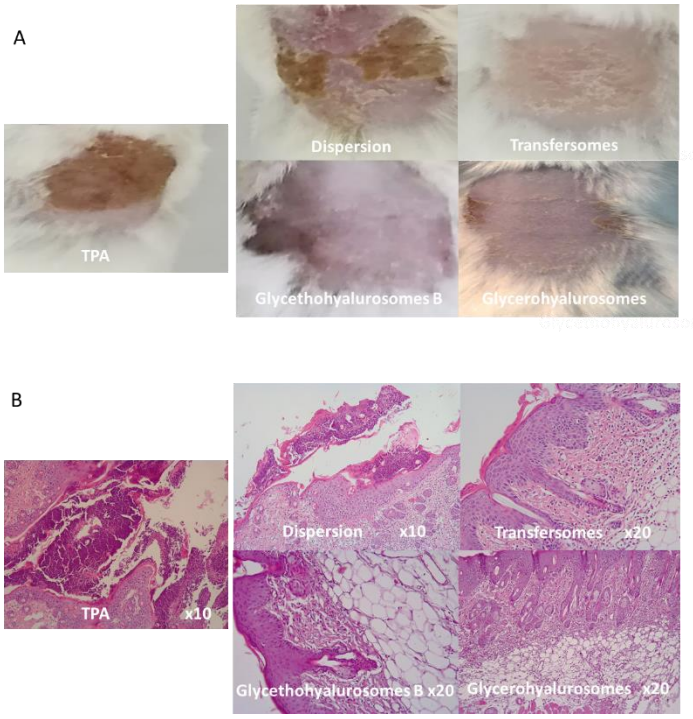

Figure 6. A) Macroscopic appearance and B) histological examination of skin lesions in mice treated with mangiferin-naringin co-loaded glycethohyalurosomes B and glycerohyalurosomes in comparison with transfersomes and aqueous dispersion.

As expected, the skin treated with glycethohyalurosomes B and glycerohyalurosomes showed a further reduction of the inflammation, and epidermis and dermis were especially preserved, confirming their superior ability to promote the healing of the wound in comparison with the other formulations. Moreover, two biomarkers involved in the inflammation process (oedema and MPO) were quantified to confirm the beneficial effect of the mangiferin-naringin co-loaded vesicles. Both glycethohyalurosomes B and glycerohyalurosomes induced a great inhibition (>80%, $p<0.05$ *vs.* TPA) of the two biomarkers MPO and oedema (Figure 7), probably because of the ability of sodium hyaluronate to favour the accumulation and permeation of mangiferin and naringin in the skin, and the moisturizing properties of glycerol, which together may promote the efficacy

of both flavonoids. Transfersomes produced a moderate oedema and MPO inhibition (~49 and 65%, respectively), suggesting a partial promotion of the therapeutic effect of naringin and mangiferin, which is probably due to the limited ability of transfersomes to enhance the accumulation of the flavonoids in the deep skin. The effect of the dispersion was very similar and significantly lower ($p<0.05$) than the effect produced by glycethohyalurosomes B and glycerohyalurosomes.

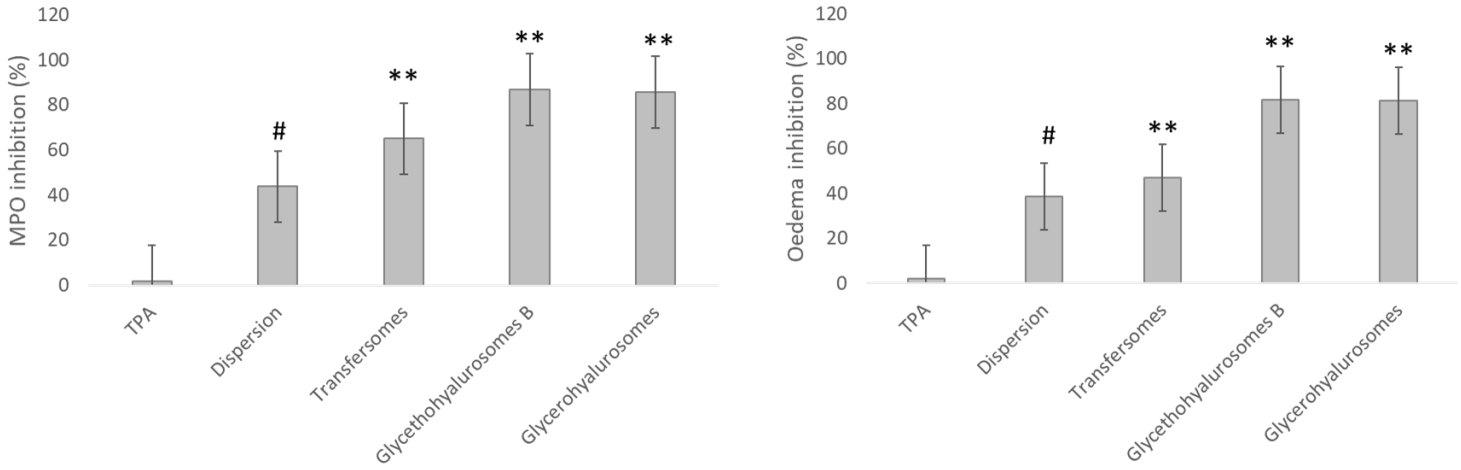

Figure 7. Myeloperoxidase (MPO) inhibition (%) and oedema inhibition (%) values, obtained after the application of TPA and the treatment with mangiferin-naringin co-loaded glycethohyalurosomes B and glycerohyalurosomes in comparison with transfersomes and aqueous dispersion. Mean values ± standard deviations are reported. **$p < 0.01$: values statistically different from TPA. #$p < 0.05$: values statistically different comparing glycethohyalurosomes B and glycerohyalurosomes vs dispersion.

4. Conclusions

This research reveals that the co-loading of mangiferin and naringin into vesicular systems can be a promising alternative for the treatment of skin diseases. The composition of the dispersing medium used to prepare the vesicles, significantly affected their physico-chemical features and the ability of mangiferin-naringin to diffuse through the skin, inhibit skin oedema and inflammation, and promote wound healing. The vesicles containing equal amounts (50:50) of glycerol and sodium hyaluronate solution or glycerol, ethanol and sodium hyaluronate (40:20:40) were found to be the most promising formulations.

These findings support the use of glycerohyalurosomes and glycethohyalurosomes for the treatment of skin diseases associated with inflammatory and oxidative processes.

References

1. Sampogna F, Fania L, Mazzanti C, Caggiati A, Pallotta S, Panebianco A, et al. The Broad-Spectrum Impact of Hidradenitis Suppurativa on Quality of Life: A Comparison with Psoriasis. Dermatology (Basel). 2019, 23;1–7.

2. Bocheńska K, Smolińska E, Moskot M, Jakóbkiewicz-Banecka J, Gabig-Cimińska M. Models in the Research Process of Psoriasis. Int J Mol Sci. 2017;18(12).

3. Chiricozzi A, Romanelli P, Volpe E, Borsellino G, Romanelli M. Scanning the Immunopathogenesis of Psoriasis. Int J Mol Sci.2018;19(1).

4. Huang T-H, Lin C-F, Alalaiwe A, Yang S-C, Fang J-Y. Apoptotic or Antiproliferative Activity of Natural Products against Keratinocytes for the Treatment of Psoriasis. Int J Mol Sci.2019 ;20(10).

5. Mikhaylov D, Hashim PW, Nektalova T, Goldenberg G. Systemic Psoriasis Therapies and Comorbid Disease in Patients with Psoriasis: A Review of Potential Risks and Benefits. J Clin Aesthet Dermatol. 2019;12(6):46–54.

6. Doppalapudi S, Jain A, Chopra DK, Khan W. Psoralen loaded liposomal nanocarriers for improved skin penetration and efficacy of topical PUVA in psoriasis. Eur J Pharm Sci. 2017; 96:515–29.

7. Hatahet T, Morille M, Hommoss A, Devoisselle JM, Müller RH, Bégu S. Liposomes, lipid nanocapsules and smartCrystals®: A comparative study for an effective quercetin delivery to the skin. Int J Pharm. 2018;542(1–2):176–85.

8. El-Desoky AH, Abdel-Rahman RF, Ahmed OK, El-Beltagi HS, Hattori M. Anti-inflammatory and antioxidant activities of naringin isolated from Carissa carandas L.: In vitro and in vivo evidence. Phytomedicine. 2018; 42:126–34.

9. Rocha LW, Bonet IJM, Tambeli CH, de-Faria FM, Parada CA. Local administration of mangiferin prevents experimental inflammatory mechanical hyperalgesia through CINC-1/epinephrine/PKA pathway and TNF-α inhibition. Eur J Pharmacol. 2018; 830:87–94.

10. Zhou C, Lai Y, Huang P, Xie L, Lin H, Zhou Z, et al. Naringin attenuates alcoholic liver injury by reducing lipid accumulation and oxidative stress. Life Sci. 2019; 216:305–12.

11. Peng S, Hou Y, Yao J, Fang J. Neuroprotection of mangiferin against oxidative damage via arousing Nrf2 signaling pathway in PC12 cells. Biofactors. 2019; *45*(3), 381-392.

12. Pleguezuelos-Villa M, Mir-Palomo S, Díez-Sales O, Buso MAOV, Sauri AR, Nácher A. A novel ultradeformable liposomes of Naringin for anti-inflammatory therapy. Colloids Surf B Biointerfaces. 2018; 162:265–70.

13. Pleguezuelos-Villa M, Nácher A, Hernández MJ, Ofelia Vila Buso MA, Ruiz Sauri A, Díez-Sales O. Mangiferin Nanoemulsions in treatment of Inflammatory Disorders and Skin Regeneration. Int J Pharm.2019;564,299-307

14. Pleguezuelos-Villa M, Diez-Sales O, Letizia Manca M, Manconi M, Ruiz Sauri A, Escribano-Ferrer E, et al. Mangiferin glycethosomes as a new potential adjuvant for the treatment of psoriasis. Int J Pharm. 2020;573,118844.

15. Song R, Murphy M, Li C, Ting K, Soo C, Zheng Z. Current development of biodegradable polymeric materials for biomedical applications. Drug Des Devel Ther. 2018; 12:3117–45.

16. Manconi M, Marongiu F, Manca ML, Caddeo C, Sarais G, Cencetti C, et al. Nanoincorporation of bioactive compounds from red grape pomaces: In vitro and ex vivo evaluation of antioxidant activity. International Journal of Pharmaceutics. 2017;523(1):159–66.

17. Vitonyte J, Manca ML, Caddeo C, Valenti D, Peris JE, Usach I, et al. Bifunctional viscous nanovesicles co-loaded with resveratrol and gallic acid for skin protection against microbial and oxidative injuries. Eur J Pharm Biopharm. 2017; 114:278–87.

18. Castangia I, Marongiu F, Manca ML, Pompei R, Angius F, Ardu A, et al. Combination of grape extract-silver nanoparticles and liposomes: A totally green approach. European Journal of Pharmaceutical Sciences. 2017; 97:62–9.

19. Han N-K, Shin DH, Kim JS, Weon KY, Jang C-Y, Kim J-S. Hyaluronan-conjugated liposomes encapsulating gemcitabine for breast cancer stem cells. Int J Nanomedicine. 2016; 11:1413–25.

20. Quiñones JP, Brüggemann O, Covas CP, Ossipov DA. Self-assembled hyaluronic acid nanoparticles for controlled release of agrochemicals and diosgenin. Carbohydr Polym. 2017; 173:157–69.

21. Basiak E, Lenart A, Debeaufort F. How Glycerol and Water Contents Affect the Structural and Functional Properties of Starch-Based Edible Films. Polymers (Basel). 2018;10(4).

22. Fallacara A, Baldini E, Manfredini S, Vertuani S. Hyaluronic Acid in the Third Millennium. Polymers (Basel). 2018;10(7).

23. Krause WE, Bellomo EG, Colby RH. Rheology of sodium hyaluronate under physiological conditions. Biomacromolecules. 2001;2(1):65–9.

24. Xie J, Ji Y, Xue W, Ma D, Hu Y. Hyaluronic acid-containing ethosomes as a potential carrier for transdermal drug delivery. Colloids Surf B Biointerfaces. 2018; 172:323–9.

25. Avadhani KS, Manikkath J, Tiwari M, Chandrasekhar M, Godavarthi A, Vidya SM, et al. Skin delivery of epigallocatechin-3-gallate (EGCG) and hyaluronic acid loaded nano-transfersomes for antioxidant and anti-aging effects in UV radiation induced skin damage. Drug Deliv. 2017;24(1):61–74.

DISCUSSION

Psoriasis and atopic dermatitis represent nowadays the most common chronic inflammatory skin diseases in the world (Schwingen, Kaplan, and Kurschus 2020) . The current treatment of these diseases involves the combination of topical, systemic and biological therapies that are generally able to counteract the inflammatory and oxidative phenomena and the symptoms connected with them. However, most of the drug used to control the advancement of both psoriasis and atopic dermatitis are characterized by numerous adverse effects, which reduce patient compliance, limit their long-term use, and reduce the therapeutic efficacy. In the light of this, there is a great need of innovative, effective and safe coadjuvant treatments, especially those based on the use of natural substances, which seem to be safer and characterized by reduced secondary effects. Among all, phytodrugs represent a valid alternative for the treatment of both diseases. However, the most natural bioactives are poorly absorbed especially when topically applied because of their low stability under particular conditions (light, pH and heat) and their physico-chemical properties (molecular weight, lipophilicity or hydrophilicity). To avoid these problems, in the last decades many efforts have been carried out to formulate innovative nanocarriers capable of protecting the incorporated bioactives and improving their accumulation in the specific site where they are needed. Among the nanocarriers, those based on the use of phospholipids or lipids such as liposomes and liposome-like vesicles or nanoemulsions have been considered the most promising especially for the topical administration of plant-derived bioactives or phytocomplexes. It is well known that the composition of both phospholipid vesicles and nanoemulsions may significantly influence the release mechanism of phytodrugs, altering the skin barrier properties or promoting their solubilities in the stratum corneum. Besides, to achieve an effective accumulation or permeation into or through the skin barriers, it is very important to consider the physicochemical characteristic of these natural bioactives. This project focuses on the use of natural bioactives as adjuvants in the treatment of both psoriasis and atopic dermatitis. Naringin and mangiferin were selected as plant-derived bioactives due to their pharmacological properties and either individually or/and in combination were incorporated in two of the most promising nanocarrier i.e. nanoemulsions and specific phospholipid vesicles. Naringin, a flavonone glycoside, was incorporated into ultradeformables liposomes. Mangiferin, a xanthone glycoside, was formulated both in nanoemulsion containing hyaluronate gels with and without transcutol-P and in ad hoc

formulated phospholipids vesicles (glycethosomes, hydrated with a blend of glycerol, water and ethanol). Based on the results obtained in the previous works, both bioactives have been co-loaded into innovative vesicular formulations. For each formulation tested, physico-chemical properties, stability, rheological behavior, transdermal delivery, in vitro biocompatibility, antioxidant activity and in vivo anti-inflammatory properties were evaluated.

Naringin ultradeformable liposomes

Naringin is a natural antioxidant isolated from citrus fruits, with potent pharmacological properties such as anti-inflammatory, anti-diabetic, anti-osteoporotic, among others. However, its poor aqueous solubility and bioavailability limits its use in clinical applications. Considering that the naringin solubility depends on the pH of the medium, and that its solubility in presence of polysorbate 80 aqueous medium is ~14 mg/mL, transfersomes were formulated by using polysorbate 80 as “edge activator”, which modify the bilayer lipids organization and increase vesicles elasticity. The ultradeformable liposomes were prepared by sonication technique keeping constant the amount of phospholipid and tween 80, while naringin was used at different concentrations: 3, 6 and 9 mg/mL to obtain liposomes I, liposomes II and liposomes III respectively. The extrusion method was selected to optimize both liposomes size and homogeneity of the system. Analyses on the morphology of the formulations underlined the formation of uni- and oligolamellar, spherical and regularly shaped vesicles. These results agreed with those obtained by using dynamic light scattering technique as particle size was ~ 100 nm in all ultradeformable liposomes and samples were highly monodisperse (PI<0.30). Further, transfersomes showed highly negative zeta potential values (-30 mV) and incorporated naringin in high amount (EE~90 %) irrespective of the concentration used. Physico-chemical properties remained unchanged during storage for 30 days at 4°C, thus confirming their good stability and the absence of fusion and aggregation phenomena. Indeed, in vitro skin permeation studies underlined the superior ability of all vesicles in enhancing the amount of naringin accumulated in epidermis (~10%). The amount of naringin accumulated in the skin treated with liposomes I (3 mg/mL) was similar to that founded after application of the dispersion (9 mg/mL), pointing that vesicles were more effective in improving the amount of the bioactive accumulated in the skin. Any significant

permeation of naringin was detected for both dispersion and vesicular systems confirming the low distribution of the bioactive at systemic level, mainly due to its high molecular weight and crystalline structure.

In vitro studies have been performed by using fibroblasts (3T3 mouse dermal fibroblasts), which have been chosen because of their important role in wound healing, especially in the treatment of inflammatory diseases such as psoriasis or atopic dermatitis (Bocheńska et al. 2017)**.** The cell viability was ~100% after 24 h of treatment without significant differences between the control group and the vesicular formulations, confirming the safety of this bioactive (Cao et al. 2015).

TPA-induced ulceration and inflammation in mice was used as in vivo model to evaluate the anti-inflammatory properties of naringin in dispersion or loaded into vesicles. The macroscopic observation of the injured skin and the determination of MPO and oedema, as the two main biomarkers of inflammation phenomena, confirmed a greater anti-inflammatory activity of transfersomes in comparison with betamethasone cream and naringin dispersion both used as references. Transfersomes, irrespective of the concentration of bioactive used, improved the deposition of naringin into the skin lesion, and its interaction with cells. Indeed, these ultradeformable liposomes promoted the internalization of naringin in epithelial cells, avoiding vascular congestion and oedema formation. The histological evaluation of skin treated with TPA and naringin in dispersion or loaded into vesicles, or with betamethasone cream confirmed the superior ability of vesicles in counteracting the inflammatory disease induced by TPA. Even the treatment with betamethasone cream showed severe dermal and subcutaneous alteration with many leukocytes infiltrating and vascular congestion at the end of the treatment, suggesting an only partial control of the inflammatory response. On the contrary, the histological evaluation of TPA-induced lesions treated with naringin transfersomes underlined a significant reduction of inflammatory infiltrates (mononuclear cells, eosinophils and neutrophils). Thus, naringin loaded ultradeformables liposomes seem to be a valid approach for the treatment of skin diseases connected with inflammatory and oxidative phenomena as they improve (i) the ability of naringin in counteracting the injuries produced by the free radicals in wound; (ii) the migration and proliferation of cells (i.e. fibroblasts), and (iii) restore the skin lesion induced by TPA. Previous studies have confirmed the beneficial effects in wound healing of naringin ointment formulation

(Kandhare et al. 2016) but the potential of naringin transfersomes in attenuating skin inflammation process induced by TPA, was presented for the first time in this paper.

Mangiferin loaded nanoemulsion and mangiferin glycethosomes

Mangiferin is a natural antioxidant principally isolated from Mangifera indica L., with strong anti-inflammatory properties. It is also effective in several autoimmune diseases such as rheumatoid arthritis, diabetes, tumorigenesis and others. However, as already showed for naringin, its low solubility (0.11mg/mL) and bioavailability (1.71%) (Du et al. 2018; Gu et al. 2018) significantly reduced its effectiveness, especially when applied in the skin. To overcome these restrictions and improve the efficacy of mangiferin after topical application, new lipid-based nanocarriers have been formulated: nanoemulsions containing hyaluronate gels and liposome-like vesicles so called glycethosomes.

Nanoemulsion in hyaluronate gel have been chosen as they may represent a good alternative for the treatment of both psoriasis and atopic dermatitis. Two different nanoemulsions were prepared (NE I, HA with high molecular weight and NE III, HA with low molecular weight), in order to evaluate the effect of the molecular weight of hyaluronic acid on the physico-chemicals properties and stability of the systems. Besides, Transcutol-P was added as well to the nanoemulsions aiming at promoting the permeation/retention of mangiferin through/into the skin, (NE II, HA with high molecular weight and Transcutol-P and NE IV, HA with low molecular weight and Transcutol-P).

Physico-chemical features of both mangiferin nanoemulsions containing hyaluronate and nanoemulsions without polymer were evaluated. The mean oil droplet size was determined by Photon Correlation Spectroscopy studies, which disclosed that any significant difference in droplet size was detected for nanoemulsion without polymer and nanoemulsions with low molecular weight hyaluronic acid as the mean diameter was similar (~320 nm). On the contrary, nanoemulsions combined with high molecular weight hyaluronic acid gel were characterized by a significant increase in droplet size, while zeta potential became less negative, probably because both size and surface charge of the oil core droplets depends on the length of polymer chains. The addition of transcutol-P did not affect significantly the properties of nanoemulsions. Stability studies underlined that physico-chemical properties (mean diameter, polydispersity index and zeta potential) of

nanoemulsions did not undergo significant variations (<10%) on storage (30 day at 4°C) confirming the great stability of nanoemulsions.

FTIR and rheological measurements confirmed the incorporation of mangiferin into nanoemulsions along with interactions between the polymer and mangiferin. As expected, the molecular weight of hyaluronic acid affected the viscoelastic properties of the different systems. Indeed, the use of high molecular weight hyaluronic acid led to an increase in viscosity probably due to the interaction between the different components that formed an internal structured network (typical weak gel) capable of controlling the release of the bioactive incorporated. As a confirmation, nanoemulsions showed a zero-order release kinetics, mainly connected with the ability of the polymer to retained water (obstructive mechanism) and control the release of the bioactive as a function of its molecular weight.

Moreover, mangiferin was incorporated into phospholipids vesicles as an attractive alternative to nanoemulsions. A pre-formulation study, performed to evaluate the best vesicular formulation in terms of physico-chemical properties and stability, underlined that among the different vesicular formulations tested, glycethosomes (glycerol-ethanol phospholipids vesicles) were the smallest and homogeneously dispersed. In the light of this, different glycethosomes formulations were prepared by increasing the amount of mangiferin incorporated: 2-glycethosomes (2mg/mL), 4-glycethosomes (4 mg/mL), 6-glycethosomes (6 mg/mL) and 8-glycethosomes (8 mg/mL). As the amount of mangiferin increased the mean diameter also increased becoming 2-fold bigger for 8-glycethosomes in comparison with the others (~288 nm for 8-glycethosomes and ~140 nm for 2-,4- and 6- glycethosomes, respectively). The same trend was detected also analyzing the viscosity of the samples, as it increased as the concentration of mangiferin also increased. This rheological behavior was clearly dependent to the increased mean diameter of 8-glycethosomes which can encapsulate a larger amount of aqueous medium reducing it in the intervesicle spaces, thus improving the viscosity of the system. Besides, using the higher concentration (8 mg/mL), mangiferin is mainly located in the bilayer thus modifying the assembling and reducing the curvature radius of the vesicle that became bigger. Vesicles were uni- and oligo-lamellar, spherical and regularly shaped and stable on storage. Their ability to incorporate mangiferin decreased as mangiferin amount increased.

To determine the ability of both nanoemulsions and glycethosomes to promote the delivery of mangiferin into and through the skin, in vitro skin penetration and permeation studies were carried out. Overall results underlined the ability of nanoemulsions with low molecular weight hyaluronic acid, to promote the permeation of mangiferin through the skin, which can be mainly connected to synergic effect of hyaluronic acid and Transcutol-P. Indeed, the best percutaneous absorption was obtained by using nanoemulsion containing HA low molecular weight, as it was 2.5 - 5 times higher in comparison with the permeation obtained by using nanoemulsions with high molecular weight hyaluronic acid. This is in agreement with Farwick et al. (2011), which demonstrated the molecular weight-depending ability of hyaluronic acid to promote mangiferin permeation.

Differently, glycethosomes promoted the accumulation of mangiferin in epidermis, being a local system capable of delivering the bioactive in the target site avoiding systemic distribution. The accumulation of mangiferin in the epidermis provided by the nanoemulsion containing 10 mg/mL of mangiferin and both transcutol-P and hyaluronic acid (~29 μg) was similar to that obtained by using mangiferin 4-glycethosomes (~26 μg), which contained a lower amount of mangiferin (4 mg/mL). The amount of mangiferin deposited in the epidermis by using 8-glycethosomes was ~ 91 μg while the maximum amount of mangiferin retained in the epidermis after treatment with the nanoemulsions was ~ 29 μg, even if the dose of mangiferin contained in 500 mg of nanoemulsion and applied on the skin (5 mg) was around 3 times higher than that applied with 8-glycethosomes (1.6 mg of mangiferin contained in 200 μl of vesicular dispersion). These findings demonstrated that phospholipids vesicles were more effective in improving the retention of the bioactive into the epidermis providing a depot, from which mangiferin was slowly released.

The ability of both nanoemulsions and glycethosomes to potentiate the wound healing ability of mangiferin was confirmed in vivo by means of TPA-induced wound in a mouse model. As the amount of mangiferin increased in glycethosomes, the reestablishment of physiological conditions on skin wound also increased. Mangiferin containing nanoemulsions were able to promote the wound healing as well, regardless of their composition. The measurement of the biomarkers of inflammation, such as oedema and MPO, underlined that using both nanocarriers the efficacy of mangiferin against skin

inflammation was improved and it was significantly higher in comparison with that provided by empty formulations and mangiferin dispersion ($p<0.05$). It must be underlined that nanoemulsions (containing 10 mg/mL of mangiferin) did not provided a significant different inhibition of MPO and oedema in comparison with 8-glycethosomes (containing 8 mg/mL of mangiferin), suggesting that the composition of vehicle as well as the type of nanocarriers chosen have a key role in the achievement of the desired effect. The best performances obtained by using 8-glycethosomes could be attributed to the superior ability of the phospholipid vesicles and the appropriate blend of glycerol and ethanol, in improving the therapeutic effect of mangiferin in skin diseases connected with inflammation and oxidative stress such as psoriasis or atopic dermatitis.

Glycethosomes showed a high biocompatibility and antioxidant activity in vitro by using the most representative cells of the skin, fibroblast. Indeed, the viability of cells treated with all vesicular formulations was ≥100% irrespective of the concentration used. Further, glycethosomes were also able to counteract the damages induced in fibroblast by using hydrogen peroxide, as after treatment with vesicles the viability was ~100% probably thanks to the ability of vesicle to interact with cells favouring the release of the bioactive inside them, improving its efficacy against the reactive species, which are involved as well in the skin diseases caused by inflammatory phenomena.

Mangiferin-naringin vesicles

Considering the previous results, which underlined that mangiferin glycethosomes (8 mg/mL) were as effective as mangiferin nanoemulsion (10 mg/mL) and the potential of naringin loaded transfersomes in the treatment of skin diseases connected with inflammation and oxidative stress, the next step of this project was focused on the development of new kinds of phospholipids vesicles in which mangiferin and naringin were co-loaded aiming at evaluating their possible synergistic effect against skin diseases. Besides, these vesicular systems were modified using biocompatible materials as sodium hyaluronate for a better stabilization of the vesicles and the promotion of the performance of the delivery system. Mangiferin and naringin were co-loaded into different types of vesicles: transfersomes, glycethosomes (in which different proportions of water, ethanol and glycerol were tested, 33:33:33, A or 40:20:40, B) and glycerosomes (water and glycerol, 50:50). Besides, based on previous studies that hypothesized a

positive effect of sodium hyaluronate on the stability of vesicles (Han et al. 2016; Maria Letizia Manca et al. 2019), glycethosomes and glycerosomes were modified by adding sodium hyaluronate. As expected, glycethohyalurosomes (composed of a blend of 40% glycerol, 20% ethanol and 40% solution sodium hyaluronate 0.1% w/v) and glycerohyalurosomes (with a slightly higher amount of sodium hyaluronate, 50% solution sodium hyaluronate 0.1% w/v) were the smallest (~100 nm), homogeneous vesicles (PDI~0.18) and they were highly stables on storage. Probably, the combination of high amounts of glycerol and sodium hyaluronate promoted the stabilization of the formulations. The behavior of empty vesicles was similar to that of mangiferin-naringin co-loaded vesicles, even though the stability on storage of empty glycethohyalurosomes B and empty glycerohyalurosomes was slightly reduced, pointing to a stabilizing effect of the two loaded flavonoids. It is important to highlight that all the vesicles were able to incorporate the flavonoids in good yields (EE ≥ 85%). FTIR and rheological analysis were performed to better understand the interactions of the vesicles' components and the contribution of sodium hyaluronate to vesicle assembly. Sodium hyaluronate lead to an increase in viscosity which was not as a function of the amount added in the vesicles. Indeed, the higher viscosity was detected for glycethohyalurosomes (33.33:33.33:33.33) containing the smaller amount of sodium hyaluronate. A further improvement of the viscosity could not be detected when the amount of sodium hyaluronate was increased (i.e. glycethohyalurosomes 40:20:40 and glycerohyalurosomes) as oscillatory measurements showed a less structured system (G´´>G´), that confirmed the presence of macromolecular interactions but not the formation of a three-dimensional network.

An increase in the amount of sodium hyaluronate aqueous solution can produce a conformational change in the chains of the polymer influenced by the ionic strength, so that the viscosity is significantly reduced. Besides, increasing the shear rates, the polymer chains deformed and aligned along the streamlines of flow, which resulted in a reduction of the viscosity (Krause, Bellomo, and Colby 2001; Fallacara et al. 2018b). It is noteworthily that in FTIR spectrum the characteristic peak of glycerol was shifted to ~1061 cm^{-1} and the hydroxyl vibration region was also shifted to higher frequencies when sodium hyaluronate was added in high amount (i.e. glycethohyalurosomes 40:20:40 and glycerohyalurosomes) suggesting an interaction between primary alcohol of glycerol and sodium hyaluronate, which drastically modified the assembling of the vesicles giving more

fluid and stable system according with rheological measurements. The amount of both mangiferin and naringin retained/accumulated in the different skin layers was affected by the dispersion medium used to prepare the vesicles. Glycethohyalurosomes 40:20:40 and glycerohyalurosomes seemed to be the most promising vesicles as both bioactives were mainly accumulated in the deeper skin layers, probably thanks to the moisturizing properties of glycerol, the penetration enhancer ability of ethanol and the improved stability given by sodium hyaluronate. Indeed, the combination of glycerol, ethanol and sodium hyaluronate may favour the skin hydration along with the modification of the ordered structure of the stratum corneum, which became more permeable (Witting et al. 2015).

Mangiferin-naringin co-loaded into vesicles were highly biocompatible and able to effectively protect fibroblast against oxidative injures induced by using hydrogen peroxide. The best results were obtained in both cases by using glycethosomes and glycerosomes, regardless of the presence of sodium hyaluronate, probably because these systems were able to interact with cells favouring the uptake of both bioactives that could exert their scavenging activity in the intracellular environmental avoiding cell damages and subsequent death.

The anti-inflammatory effect of mangiferin-naringin co-loaded vesicles was also evaluated in vivo by means of TPA-mouse model. The treatment with transfersomes produced a moderate oedema and MPO inhibition, suggesting an only partial promotion of the therapeutic effect of both mangiferin and naringin, which may be due to the limited ability of conventional transfersomes to reach the deeper skin strata. The macroscopic evaluation of the injured skin, the biomarkers measurement and the histological evaluation underlined a superior ability of both glycethohyalurosomes 40:20:40 and glycerohyalurosomes to counteract the damages induced by TPA as the skin was almost completely restored, the inhibition of MPO was the highest in comparison with all the other samples, and a significant reduction of inflammatory infiltrates (mononuclear cells, eosinophils and neutrophils) was underlined after histological observation/studies. Overall results confirmed that the promotion of the therapeutic activity of bioactives can be affected by the composition of vesicle, which can be considered a key factor for the success of a specific treatment. Indeed, the best performances obtained by using glycethohyalurosomes 40:20:40 and glycerohyalurosomes can be mainly due to the

combination of anti-inflammatory/antioxidant activity of both natural compounds, the moisturing properties of glycerol, the penetration enhancer capacity of ethanol and the tissue remodeling properties of the polymer, which synergically promote the accumulation of both bioactives in the deeper skin strata and stimulate the proliferation and migration of skin cells thus accelerating the wound healing process.

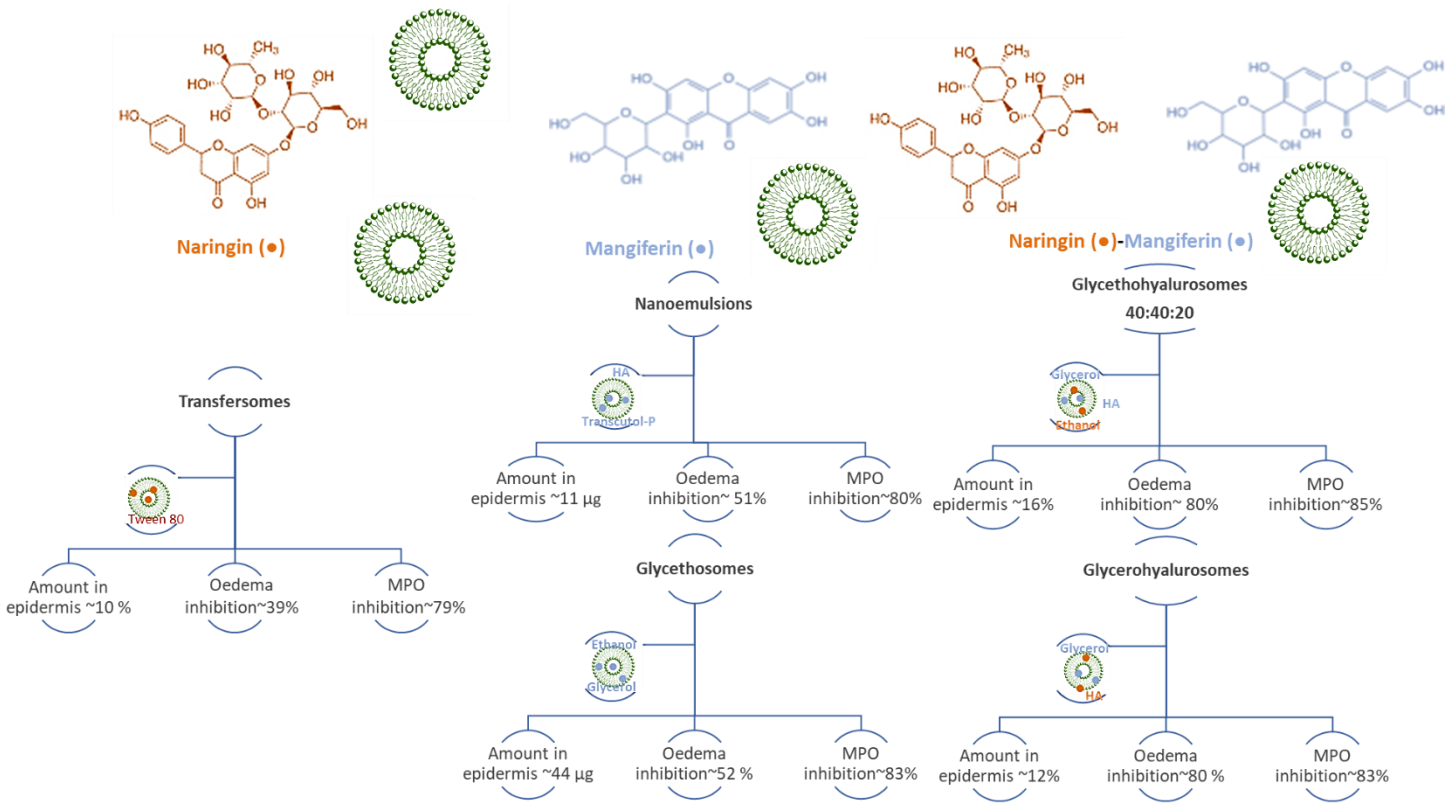

Summary of the different lipid-based nanocarries

CONCLUSIONS

The work provides important advances in the use of plant-derived antioxidant bioactives (naringin and mangiferin) and their incorporation into lipidic nanocarriers (i.e. nanoemulsions and phospholipid vesicles).

The following conclusions can be drawn from the results obtained:

- The loading of naringin into ultradeformable liposomes represents an innovative approach to prevent and treat skin lesion and restore skin integrity. Results demonstrated that naringin liposomes were highly biocompatible and more effective than betamethasone cream and naringin dispersion in promoting the healing of induced wound, as demonstrate in *in vivo* model (TPA test).
- Administration of mangiferin nanoemulsions on TPA-inflamed skin mice model provided an attenuation of oedema and leucocyte infiltration. Macroscopic appearance of mice skin lesions has a good correlation with the histological study. The topical application of these formulations shows an appropriate anti-inflammatory effect.
- Mangiferin glycethosomes were highly biocompatible and showed a strong ability to protect *in vitro* fibroblasts against damages induced by hydrogen peroxide. *In vivo* results underlined the superior ability of mangiferin loaded glycethosomes respect to the mangiferin dispersion to promote the healing of the wound induced by TPA, confirming their potential application for the treatment of psoriasis or other skin disorders.
- Glycethohyalurosomes 40:20:40 (glycerol: ethanol: sodium hyaluronate solution) and glycerohyalurosomes 50:50 (glycerol: sodium hyaluronate solution), in which mangiferin and naringin were co-loaded, were the most promising vesicles capable of restoring the wound and inhibiting the oedema induced by TPA.
- The use of these specific nanocarriers for the treatment of psoriasis and atopic dermatitis may reduce the problems associated with these diseases (pain, local heat and skin redness), thus improving the compliance of the patients.
- Further studies will be necessary to support these results by means of immunohistochemical analysis or proteins expression to elucidate the main mechanism involved in the anti-inflammatory effect of mangiferin and naringin.

BIBLIOGRAPHY

Ahmad, Niyaz, Rizwan Ahmad, Ali Al-Qudaihi, Salman Edrees Alaseel, Ibrahim Zuhair Fita, Mohammed Saifuddin Khalid, and Faheem Hyder Pottoo. 2019. 'Preparation of a Novel Curcumin Nanoemulsion by Ultrasonication and Its Comparative Effects in Wound Healing and the Treatment of Inflammation'. *RSC Advances*.

Alexander, Helen, Thomas Patton, Zarif K. Jabbar-Lopez, Andrea Manca, and Carsten Flohr. 2019. 'Novel Systemic Therapies in Atopic Dermatitis: What Do We Need to Fulfil the Promise of a Treatment Revolution?' *F1000Research* 8.

AlMatar, Manaf, Işıl Var, Begüm Kayar, Emel Eker, Ebru Kafkas, Mozhgan Zarifikhosroshahi, and Fatih Köksal. 2019. 'Evaluation of Polyphenolic Profile and Antibacterial Activity of Pomegranate Juice in Combination with Rifampin (R) against MDR-TB Clinical Isolates'. *Current Pharmaceutical Biotechnology*.

Amnuaikit, Thanaporn, Tunyaluk Limsuwan, Pasarat Khongkow, and Prapaporn Boonme. 2018. 'Vesicular Carriers Containing Phenylethyl Resorcinol for Topical Delivery System; Liposomes, Transfersomes and Invasomes'. *Asian Journal of Pharmaceutical Sciences*, Special Issue: Pharmaceutical Innovation, 13 (5): 472–84.

Andersen, Yuki M. F., Alexander Egeberg, Gunnar H. Gislason, Lone Skov, and Jacob P. Thyssen. 2017. 'Autoimmune Diseases in Adults with Atopic Dermatitis'. *Journal of the American Academy of Dermatology* 76 (2): 274-280.e1.

Ayala-Fontánez, Nilmarie, David C Soler, and Thomas S McCormick. 2016. 'Current Knowledge on Psoriasis and Autoimmune Diseases'. *Psoriasis (Auckland, N.Z.)*. 7–32.

Bhatia, Harsharan, Eduardo Candelario-Jalil, Antonio de Oliveira, Olumayokun Olajide, Gregorio Martínez-Sánchez, and Bernd Fiebich. 2008. 'Mangiferin Inhibits Cyclooxygenase-2 Expression and Prostaglandin E-2 Production in Activated Rat Microglial Cells'. *Archives of Biochemistry and Biophysics.* 477: 253–58.

Biswas, Taniya, Argha Sen, Rini Roy, Sushomasri Maji, and Himangshu Sekhar Maji. 2015. 'Isolation of Mangiferin from Flowering Buds of Mangifera Indica L and Its Evaluation of in Vitro Antibacterial Activity' 4 (3): 8.

Bocheńska, Katarzyna, Elwira Smolińska, Marta Moskot, Joanna Jakóbkiewicz-Banecka, and Magdalena Gabig-Cimińska. 2017. 'Models in the Research Process of Psoriasis'. *International Journal of Molecular Sciences* 18 (12).

Boehncke, Wolf-Henning. 2018. 'Systemic Inflammation and Cardiovascular Comorbidity in Psoriasis Patients: Causes and Consequences'. *Frontiers in Immunology* 9.

Brandt, Eric B., and Umasundari Sivaprasad. 2011. 'Th2 Cytokines and Atopic Dermatitis'. *Journal of Clinical & Cellular Immunology* 2 (3).

Bruin-Weller, M. de, D. Thaçi, C. H. Smith, K. Reich, M. J. Cork, A. Radin, Q. Zhang, et al. 2018. 'Dupilumab with Concomitant Topical Corticosteroid Treatment in Adults with Atopic Dermatitis with an Inadequate Response or Intolerance to Ciclosporin'. *The British Journal of Dermatology* 178 (5): 1083–1101.

Bukhari, Syed Nasir Abbas, Nur Liyana Roswandi, Muhammad Waqas, Haroon Habib, Fahad Hussain, Shahzeb Khan, Muhammad Sohail, Nor AmLizan RamLi, Hnin Ei

Thu, and Zahid Hussain. 2018. 'Hyaluronic Acid, a Promising Skin Rejuvenating Biomedicine: A Review of Recent Updates and Pre-Clinical and Clinical Investigations on Cosmetic and Nutricosmetic Effects'. *International Journal of Biological Macromolecules* 120 (Pt B): 1682–95.

Cao, Xvhai, Weilong Lin, Chengwei Liang, Dong Zhang, Fengjian Yang, Yan Zhang, Xuelin Zhang, Jianyong Feng, and Cong Chen. 2015. 'Naringin Rescued the TNF-α-Induced Inhibition of Osteogenesis of Bone Marrow-Derived Mesenchymal Stem Cells by Depressing the Activation of NF-KB Signaling Pathway'. *Immunologic Research* 62 (3): 357–67.

Castangia, Ines, Maria Letizia Manca, Ana Catalán-Latorre, Anna Maria Maccioni, Anna Maria Fadda, and Maria Manconi. 2016. 'Phycocyanin-Encapsulating Hyalurosomes as Carrier for Skin Delivery and Protection from Oxidative Stress Damage'. *Journal of Materials Science. Materials in Medicine* 27 (4): 75.

Chaulagain, Bivek, Ankit Jain, Ankita Tiwari, Amit Verma, and Sanjay K. Jain. 2018. 'Passive Delivery of Protein Drugs through Transdermal Route'. *Artificial Cells, Nanomedicine, and Biotechnology* 46 (sup1): 472–87.

Chen, Li Hui, Jian Feng Xue, Zhi Yong Zheng, Muhammad Shuhaidi, Hnin Ei Thu, and Zahid Hussain. 2018. 'Hyaluronic Acid, an Efficient Biomacromolecule for Treatment of Inflammatory Skin and Joint Diseases: A Review of Recent Developments and Critical Appraisal of Preclinical and Clinical Investigations'. *International Journal of Biological Macromolecules* 116: 572–84.

Chew, Yik-Ling. 2019. 'The Beneficial Properties of Virgin Coconut Oil in Management of Atopic Dermatitis'. *Pharmacognosy Reviews* 13 (25): 24.

Chilcott, R. P., J. Jenner, S. a. M. Hotchkiss, and P. Rice. 2001. 'In Vitro Skin Absorption and Decontamination of Sulphur Mustard: Comparison of Human and Pig-Ear Skin'. *Journal of Applied Toxicology* 21 (4): 279–83.

Chtourou, Yassine, Brahim Gargouri, Mohammed Kebieche, and Hamadi Fetoui. 2015. 'Naringin Abrogates Cisplatin-Induced Cognitive Deficits and Cholinergic Dysfunction Through the Down-Regulation of AChE Expression and INOS Signaling Pathways in Hippocampus of Aged Rats'. *Journal of Molecular Neuroscience: MN* 56 (2): 349–62.

Drucker, Aaron M., and Paula J. Harvey. 2019. 'Atopic Dermatitis and Cardiovascular Disease: What Are the Clinical Implications?' *Journal of Allergy and Clinical Immunology* 143 (5): 1736–38.

Du, Suya, Huirong Liu, Tiantian Lei, Xiaofang Xie, Hailian Wang, Xia He, Rongsheng Tong, and Yi Wang. 2018. 'Mangiferin: An Effective Therapeutic Agent against Several Disorders (Review)'. *Molecular Medicine Reports* 18 (6): 4775–86.

El-Desoky, Ahmed H., Rehab F. Abdel-Rahman, Osama K. Ahmed, Hossam S. El-Beltagi, and Masao Hattori. 2018. 'Anti-Inflammatory and Antioxidant Activities of Naringin Isolated from Carissa Carandas L.: In Vitro and in Vivo Evidence'.

Phytomedicine: International Journal of Phytotherapy and Phytopharmacology 42: 126–34.

Fallacara, Arianna, Erika Baldini, Stefano Manfredini, and Silvia Vertuani. 2018a. 'Hyaluronic Acid in the Third Millennium'. *Polymers* 10 (7).

Farwick, M., G. Gauglitz, T. Pavicic, T. Köhler, M. Wegmann, K. Schwach-Abdellaoui, B. Malle, V. Tarabin, G. Schmitz, and H. C. Korting. 2011. 'Fifty-KDa Hyaluronic Acid Upregulates Some Epidermal Genes without Changing TNF-α Expression in Reconstituted Epidermis'. *Skin Pharmacology and Physiology* 24 (4): 210–17.

Farzanfar, Delaram, Yekta Dowlati, Lars E. French, Michelle A. Lowes, and Afsaneh Alavi. 2018. 'Inflammation: A Contributor to Depressive Comorbidity in Inflammatory Skin Disease'. *Skin Pharmacology and Physiology* 31: 246–51.

Fragoulis, George E., Iain B. McInnes, and Stefan Siebert. 2019. 'JAK-Inhibitors. New Players in the Field of Immune-Mediated Diseases, beyond Rheumatoid Arthritis'. *Rheumatology* 58 (Supplement_1): i43–54.

Franken, Linda E., Egbert J. Boekema, and Marc C. A. Stuart. 2017. 'Transmission Electron Microscopy as a Tool for the Characterization of Soft Materials: Application and Interpretation'. *Advanced Science* 4 (5).

Gharib, Riham, Hélène Greige-Gerges, Sophie Fourmentin, Catherine Charcosset, and Lizette Auezova. 2015. 'Liposomes Incorporating Cyclodextrin–Drug Inclusion Complexes: Current State of Knowledge'. *Carbohydrate Polymers* 129 (September): 175–86.

Giavina-Bianchi, Mara, and Pedro Giavina-Bianchi. 2019. 'Systemic Treatment for Severe Atopic Dermatitis'. *Archivum Immunologiae Et Therapiae Experimentalis* 67 (2): 69–78.

Griffiths, Christopher E. M., Peter van de Kerkhof, and Magdalena Czarnecka-Operacz. 2017. 'Psoriasis and Atopic Dermatitis'. *Dermatology and Therapy* 7 (Suppl 1): 31–41.

Gu, Peng-Cheng, Lan Wang, Mei-Na Han, Jun Peng, Jing-Chuan Shang, Yong-Quan Pan, and Wen-Li Han. 2018. 'Comparative Pharmacokinetic Study of Mangiferin in Normal and Alloxan-Induced Diabetic Rats after Oral and Intravenous Administration by UPLC-MS/MS'. *Pharmacology* 103 (1–2): 30–37.

Gupta, Ankur, H. Burak Eral, T. Alan Hatton, and Patrick S. Doyle. 2016. 'Nanoemulsions: Formation, Properties and Applications'. *Soft Matter* 12 (11): 2826–41.

Gupta, Praveen Kumar, Nividha Bhandari, Hardik N. Shah, Vartika Khanchandani, R. Keerthana, Vidhyavathy Nagarajan, and Lingayya Hiremath. 2019. 'An Update on Nanoemulsions Using Nanosized Liquid in Liquid Colloidal Systems'. *Nanoemulsions - Properties, Fabrications and Applications*.

Gurpreet, K., and S. K. Singh. 2018. 'Review of Nanoemulsion Formulation and Characterization Techniques'. *Indian Journal of Pharmaceutical Sciences* 80 (5): 781–89.

Guttman-Yassky, Emma, Patrick M. Brunner, Avidan U. Neumann, Saakshi Khattri, Ana B. Pavel, Kunal Malik, Giselle K. Singer, et al. 2018. 'Efficacy and Safety of

Fezakinumab (an IL-22 Monoclonal Antibody) in Adults with Moderate-to-Severe Atopic Dermatitis Inadequately Controlled by Conventional Treatments: A Randomized, Double-Blind, Phase 2a Trial'. *Journal of the American Academy of Dermatology* 78 (5): 872-881.e6.

Hajialyani, Marziyeh, Devesh Tewari, Eduardo SOBARZO-SÁNCHEZ, Seyed Nabavi, Mohammad Hosein Farzaei, and Mohammad Abdollahi. 2018. 'Natural Product-Based Nanomedicines for Wound Healing Purposes: Therapeutic Targets and Drug Delivery Systems'. *International Journal of Nanomedicine.* Volume 13.

Han, Na-Kyung, Dae Hwan Shin, Jung Seok Kim, Kwon Yeon Weon, Chang-Young Jang, and Jin-Seok Kim. 2016. 'Hyaluronan-Conjugated Liposomes Encapsulating Gemcitabine for Breast Cancer Stem Cells'. *International Journal of Nanomedicine* 11: 1413–25.

Hasanpouri, Azam, Farzaneh Lotfipour, Saeed Ghanbarzadeh, and Hamed Hamishehkar. 2018. 'Improvement of Dermal Delivery of Tetracycline Using Vesicular Nanostructures'. *Research in Pharmaceutical Sciences* 13 (5): 385–93.

Hatahet, T., M. Morille, A. Hommoss, J. M. Devoisselle, R. H. Müller, and S. Bégu. 2018. 'Liposomes, Lipid Nanocapsules and SmartCrystals®: A Comparative Study for an Effective Quercetin Delivery to the Skin'. *International Journal of Pharmaceutics* 542 (1–2): 176–85.

Hathout, Rania M., Heba A. Gad, and Abdelkader A. Metwally. 2017. 'Gelatinized-Core Liposomes: Toward a More Robust Carrier for Hydrophilic Molecules'. *Journal of Biomedical Materials Research. Part A* 105 (11): 3086–92.

Hawkes, Jason E., Tom C. Chan, and James G. Krueger. 2017. 'Psoriasis Pathogenesis and the Development of Novel, Targeted Immune Therapies'. *The Journal of Allergy and Clinical Immunology* 140 (3): 645–53.

Hu, Stephen Chu-Sung, and Cheng-Che E. Lan. 2017. 'Psoriasis and Cardiovascular Comorbidities: Focusing on Severe Vascular Events, Cardiovascular Risk Factors and Implications for Treatment'. *International Journal of Molecular Sciences* 18 (10).

Hua, Susan. 2015. 'Lipid-Based Nano-Delivery Systems for Skin Delivery of Drugs and Bioactives'. *Frontiers in Pharmacology* 6.

Hussain, Afzal, Abdus Samad, S. K. Singh, M. N. Ahsan, M. W. Haque, A. Faruk, and F. J. Ahmed. 2016. 'Nanoemulsion Gel-Based Topical Delivery of an Antifungal Drug: In Vitro Activity and in Vivo Evaluation'. *Drug Delivery* 23 (2): 642–47.

Jacobi, Arnd, Anke Mayer, and Matthias Augustin. 2015. 'Keratolytics and Emollients and Their Role in the Therapy of Psoriasis: A Systematic Review'. *Dermatology and Therapy* 5 (1): 1–18.

Jacobus Berlitz, Simone, Damiê De Villa, Luiz Augusto Maschmann Inácio, Samuel Davies, Kelly Cristine Zatta, Silvia Stanisçuaski Guterres, and Irene Clemes Külkamp-Guerreiro. 2019. 'Azelaic Acid-Loaded Nanoemulsion with Hyaluronic Acid - a New

Strategy to Treat Hyperpigmentary Skin Disorders'. *Drug Development and Industrial Pharmacy* 45 (4): 642–50.

Jain, Akhlesh K., and Suresh Thareja. 2019. 'In Vitro and in Vivo Characterization of Pharmaceutical Nanocarriers Used for Drug Delivery'. *Artificial Cells, Nanomedicine, and Biotechnology* 47 (1): 524–39.

Janeczek, Monica, Lauren Moy, Eden P. Lake, and James Swan. 2018. 'Review of the Efficacy and Safety of Topical Mahonia Aquifolium for the Treatment of Psoriasis and Atopic Dermatitis'. *The Journal of Clinical and Aesthetic Dermatology* 11 (12): 42–47.

Jankowski, A., R. Dyja, and B. Sarecka-Hujar. 2017. 'Dermal and Transdermal Delivery of Active Substances from Semisolid Bases'. *Indian Journal of Pharmaceutical Sciences* 79 (4): 488–500.

Jasmina, Hadžiabdić, Orman Džana, Elezović Alisa, Vranić Edina, and Rahić Ognjenka. 2017. 'PREPARATION OF NANOEMULSIONS BY HIGH-ENERGY AND LOWENERGY EMULSIFICATION METHODS'. In *CMBEBIH 2017*, edited by Almir Badnjevic, 62:317–22. Singapore: Springer Singapore.

Jeon, S. M., S. H. Bok, M. K. Jang, M. K. Lee, K. T. Nam, Y. B. Park, S. J. Rhee, and M. S. Choi. 2001. 'Antioxidative Activity of Naringin and Lovastatin in High Cholesterol-Fed Rabbits'. *Life Sciences* 69 (24): 2855–66.

Johnson, Brian B., Abigail I. Franco, Lisa A. Beck, and James C. Prezzano. 2019. 'Treatment-Resistant Atopic Dermatitis: Challenges and Solutions'. *Clinical, Cosmetic and Investigational Dermatology* 12: 181–92.

Kandhare, Amit D., Javed Alam, Mithun V. K. Patil, Akanksha Sinha, and Subhash L. Bodhankar. 2016. 'Wound Healing Potential of Naringin Ointment Formulation via Regulating the Expression of Inflammatory, Apoptotic and Growth Mediators in Experimental Rats'. *Pharmaceutical Biology* 54 (3): 419–32.

Kawar, Dana, and Hamdy Abdelkader. 2019. 'Hyaluronic Acid Gel-Core Liposomes (Hyaluosomes) Enhance Skin Permeation of Ketoprofen'. *Pharmaceutical Development and Technology* 24 (8): 947–53.

Khan, Nauman R., Mohd S. Harun, Asif Nawaz, Nurulaini Harjoh, and Tin W. Wong. 2015. 'Nanocarriers and Their Actions to Improve Skin Permeability and Transdermal Drug Delivery'. *Current Pharmaceutical Design* 21 (20): 2848–66.

Khan, Nauman Rahim, and Tin Wui Wong. 2018. '5-Fluorouracil Ethosomes - Skin Deposition and Melanoma Permeation Synergism with Microwave'. *Artificial Cells, Nanomedicine, and Biotechnology* 46 (sup1): 568–77.

Kim, Hee J., and Mark G. Lebwohl. 2019. 'Biologics and Psoriasis: The Beat Goes On'. *Dermatologic Clinics* 37 (1): 29–36. https://doi.org/10.1016/j.det.2018.07.004.

Kim, Jin Hong, Myeong Ju Moon, Dong Yi Kim, Suk Hee Heo, and Yong Yeon Jeong. 2018. 'Hyaluronic Acid-Based Nanomaterials for Cancer Therapy'. *Polymers* 10 (10).

Kim, Mun Jeong, Mi Ae Im, Ji-Sook Lee, Ji Young Mun, Da Hye Kim, Ayoung Gu, and In Sik Kim. 2019. 'Effect of S100A8 and S100A9 on Expressions of Cytokine and Skin

Barrier Protein in Human Keratinocytes'. *Molecular Medicine Reports* 20 (3): 2476–83.

Kizilyel, Okan, Necmettin Akdeniz, Mahmut Sami Metin, and Ömer Faruk Elmas. 2019. 'Investigation of Oxidant and Antioxidant Levels in Patients with Psoriasis'. *Turkish journal of medical sciences* 49 (4): 1085–88.

Klonowska, Jolanta, Jolanta Gleń, Roman J. Nowicki, and Magdalena Trzeciak. 2018. 'New Cytokines in the Pathogenesis of Atopic Dermatitis—New Therapeutic Targets'. *International Journal of Molecular Sciences* 19 (10).

Krause, W. E., E. G. Bellomo, and R. H. Colby. 2001. 'Rheology of Sodium Hyaluronate under Physiological Conditions'. *Biomacromolecules* 2 (1): 65–69.

Kumar, Manish, Ram Singh Bishnoi, Ajay Kumar Shukla, and Chandra Prakash Jain. 2019. 'Techniques for Formulation of Nanoemulsion Drug Delivery System: A Review'. *Preventive Nutrition and Food Science* 24 (3): 225–34.

Lee, Eun-Hye, Soo-Jeong Lim, and Mi-Kyung Lee. 2019. 'Chitosan-Coated Liposomes to Stabilize and Enhance Transdermal Delivery of Indocyanine Green for Photodynamic Therapy of Melanoma'. *Carbohydrate Polymers* 224 (November): 115143.

Lee, Song Yi, Suyeong Nam, In Kee Hong, Hill Kim, Heejung Yang, and Hyun-Jong Cho. 2018. 'Antiproliferation of Keratinocytes and Alleviation of Psoriasis by the Ethanol Extract of Artemisia Capillaris'. *Phytotherapy Research: PTR* 32 (5): 923–32.

Liao, Wenzhen, Zhijun Liu, Tiantian Zhang, Suxia Sun, Jufeng Ye, Ziyin Li, Lianzhi Mao, and Jiaoyan Ren. 2018. 'Enhancement of Anti-Inflammatory Properties of Nobiletin in Macrophages by a Nano-Emulsion Preparation'. *Journal of Agricultural and Food Chemistry* 66 (1): 91–98.

Llorens-Gámez, Mar, and Ángel Serrano-Aroca. 2018. 'Low-Cost Advanced Hydrogels of Calcium Alginate/Carbon Nanofibers with Enhanced Water Diffusion and Compression Properties'. *Polymers* 10 (4): 405.

Mahajan, Vikram K. 2016. 'Psoriasis Treatment: Unconventional and Non-Standard Modalities in the Era of Biologics'. *World Journal of Dermatology* 5 (1): 17–51.

Malm, Alexander V., and Jason C. W. Corbett. 2019. 'Improved Dynamic Light Scattering Using an Adaptive and Statistically Driven Time Resolved Treatment of Correlation Data'. *Scientific Reports* 9 (1): 1–11.

Manca, M. L., I. Castangia, M. Zaru, A. Nácher, D. Valenti, X. Fernàndez-Busquets, A. M. Fadda, and M. Manconi. 2015. 'Development of Curcumin Loaded Sodium Hyaluronate Immobilized Vesicles (Hyalurosomes) and Their Potential on Skin Inflammation and Wound Restoring'. *Biomaterials* 71: 100–109.

Manca, Maria Letizia, Claudia Cencetti, Pietro Matricardi, Ines Castangia, Marco Zaru, Octavio Diez Sales, Amparo Nacher, et al. 2016. 'Glycerosomes: Use of Hydrogenated Soy Phosphatidylcholine Mixture and Its Effect on Vesicle Features and Diclofenac Skin Penetration'. *International Journal of Pharmaceutics* 511 (1): 198–204.

Manca, Maria Letizia, Donatella Lattuada, Donatella Valenti, Ornella Marelli, Costantino Corradini, Xavier Fernàndez-Busquets, Marco Zaru, Anna Maria Maccioni, Anna Maria Fadda, and Maria Manconi. 2019. 'Potential Therapeutic Effect of Curcumin Loaded Hyalurosomes against Inflammatory and Oxidative Processes Involved in the Pathogenesis of Rheumatoid Arthritis: The Use of Fibroblast-like Synovial Cells Cultured in Synovial Fluid'. *European Journal of Pharmaceutics and Biopharmaceutics* 136: 84–92.

Manconi, Maria, Carla Caddeo, Amparo Nacher, Octavio Diez-Sales, Josè Esteban Peris, Elvira Escribano Ferrer, Anna Maria Fadda, and Maria Letizia Manca. 2019. 'Eco-Scalable Baicalin Loaded Vesicles Developed by Combining Phospholipid with Ethanol, Glycerol, and Propylene Glycol to Enhance Skin Permeation and Protection'. *Colloids and Surfaces. B, Biointerfaces* 184: 110504.

Manconi, Maria, Maria Letizia Manca, Carla Caddeo, Donatella Valenti, Claudia Cencetti, Octavio Diez-Sales, Amparo Nacher, et al. 2018. 'Nanodesign of New Self-Assembling Core-Shell Gellan-Transfersomes Loading Baicalin and in Vivo Evaluation of Repair Response in Skin'. *Nanomedicine: Nanotechnology, Biology, and Medicine* 14 (2): 569–79.

Maniadakis, Nikos, Emese Toth, Michael Schiff, Xuan Wang, Maria Nassim, Boglarka Szegvari, Irina Mountian, and Jeffrey R. Curtis. 2018. 'A Targeted Literature Review Examining Biologic Therapy Compliance and Persistence in Chronic Inflammatory Diseases to Identify the Associated Unmet Needs, Driving Factors, and Consequences'. *Advances in Therapy* 35 (9): 1333–55.

Marto, Joana, Catarina Vitor, Ana Guerreiro, Cristiana Severino, Carla Eleutério, Andreia Ascenso, and Sandra Simões. 2016. 'Ethosomes for Enhanced Skin Delivery of Griseofulvin'. *Colloids and Surfaces. B, Biointerfaces* 146: 616–23.

Marzuki, Nur Haziqah Che, Roswanira Abdul Wahab, and Mariani Abdul Hamid. 2019. 'An Overview of Nanoemulsion: Concepts of Development and Cosmeceutical Applications'. *Biotechnology & Biotechnological Equipment* 33 (1): 779–97.

Mengoni, Tamara, Manuela Adrian, Susana Pereira, Beatriz Santos-Carballal, Mathias Kaiser, and Francisco M. Goycoolea. 2017. 'A Chitosan-Based Liposome Formulation Enhances the In Vitro Wound Healing Efficacy of Substance P Neuropeptide'. *Pharmaceutics* 9 (4).

Mihara, Ryosuke, Kenji Kabashima, Masutaka Furue, Miwa Nakano, and Thomas Ruzicka. 2019. 'Nemolizumab in Moderate to Severe Atopic Dermatitis: An Exploratory Analysis of Work Productivity and Activity Impairment in a Randomized Phase II Study'. *The Journal of Dermatology* 46 (8): 662–71.

Ming, He, Qiu Chuang, Wang Jiashi, Li Bin, Wang Guangbin, and Ji Xianglu. 2018. 'Naringin Targets Zeb1 to Suppress Osteosarcoma Cell Proliferation and Metastasis'. *Aging* 10 (12): 4141–51.

Mishra, Dinesh K., Ruchita Shandilya, and Pradyumna K. Mishra. 2018. 'Lipid Based Nanocarriers: A Translational Perspective'. *Nanomedicine: Nanotechnology, Biology, and Medicine* 14 (7): 2023–50.

Mohamed, M. A., J. Jaafar, A. F. Ismail, M. H. D. Othman, and M. A. Rahman. 2017. 'Chapter 1 - Fourier Transform Infrared (FTIR) Spectroscopy'. In *Membrane Characterization*, edited by Nidal Hilal, Ahmad Fauzi Ismail, Takeshi Matsuura, and Darren Oatley-Radcliffe, 3–29. Elsevier.

Musa, Siti Hajar, Mahiran Basri, Hamid Reza Fard Masoumi, Norashikin Shamsudin, and Norazlinaliza Salim. 2017. 'Enhancement of Physicochemical Properties of Nanocolloidal Carrier Loaded with Cyclosporine for Topical Treatment of Psoriasis: In Vitro Diffusion and in Vivo Hydrating Action'. *International Journal of Nanomedicine* 12: 2427–41.

Nardo, Veronica Di, Serena Gianfaldoni, Georgi Tchernev, Uwe Wollina, Victoria Barygina, Jacopo Lotti, Farah Daaboul, and Torello Lotti. 2018. 'Use of Curcumin in Psoriasis'. *Open Access Macedonian Journal of Medical Sciences* 6 (1): 218–20.

Natsheh, Hiba, Elisa Vettorato, and Elka Touitou. 2019. 'Ethosomes for Dermal Administration of Natural Active Molecules'. *Current Pharmaceutical Design* 25 (21): 2338–48.

Nisini, Roberto, Noemi Poerio, Sabrina Mariotti, Federica De Santis, and Maurizio Fraziano. 2018. 'The Multirole of Liposomes in Therapy and Prevention of Infectious Diseases'. *Frontiers in Immunology* 9.

Niyonsaba, François. 2016. 'Novel Insight Into the Role of Antimicrobial (Host Defense) Peptides/Proteins in Human Skin Diseases'. *Juntendo Medical Journal* 62 (2): 120–31.

Nkanga, Christian Isalomboto, Alain Murhimalika Bapolisi, Nnamdi Ikemefuna Okafor, and Rui Werner Maçedo Krause. 2019. 'General Perception of Liposomes: Formation, Manufacturing and Applications'. *Liposomes - Advances and Perspectives*.

Oliveira, Clara, and Tiago Torres. 2019. 'More than Skin Deep: The Systemic Nature of Atopic Dermatitis'. *European Journal of Dermatology: EJD* 29 (3): 250–58.

Parisi, Rosa, Deborah P. M. Symmons, Christopher E. M. Griffiths, Darren M. Ashcroft, and Identification and Management of Psoriasis and Associated ComorbidiTy (IMPACT) project team. 2013. 'Global Epidemiology of Psoriasis: A Systematic Review of Incidence and Prevalence'. *The Journal of Investigative Dermatology* 133 (2): 377–85.

Patil, Kalpesh R., Umesh B. Mahajan, Banappa S. Unger, Sameer N. Goyal, Sateesh Belemkar, Sanjay J. Surana, Shreesh Ojha, and Chandragouda R. Patil. 2019. 'Animal Models of Inflammation for Screening of Anti-Inflammatory Drugs: Implications for the Discovery and Development of Phytopharmaceuticals'. *International Journal of Molecular Sciences* 20 (18).

Pedrosa, Tatiana do Nascimento, Carolina Motter Catarino, Paula Comune Pennacchi, Sílvia Romano de Assis, Fabrícia Gimenes, Márcia Edilaine Lopes Consolaro, Silvia

Berlanga de Moraes Barros, and Silvya Stuchi Maria-Engler. 2017. 'A New Reconstructed Human Epidermis for in Vitro Skin Irritation Testing'. *Toxicology in Vitro: An International Journal Published in Association with BIBRA* 42: 31–37.

Peng, Shoujiao, Yanan Hou, Juan Yao, and Jianguo Fang. 2019. 'Neuroprotection of Mangiferin against Oxidative Damage via Arousing Nrf2 Signaling Pathway in PC12 Cells'. *BioFactors (Oxford, England)*.

Pinson, Roxanne, Bahman Sotoodian, and Loretta Fiorillo. 2016. 'Psoriasis in Children'. *Psoriasis (Auckland, N.Z.)* 6: 121–29.

Pireddu, Rosa, Carla Caddeo, Donatella Valenti, Francesca Marongiu, Alessandra Scano, Guido Ennas, Francesco Lai, Anna Maria Fadda, and Chiara Sinico. 2016. 'Diclofenac Acid Nanocrystals as an Effective Strategy to Reduce in Vivo Skin Inflammation by Improving Dermal Drug Bioavailability'. *Colloids and Surfaces. B, Biointerfaces* 143 (July): 64–70.

Powers, Dana, and Nasim Nosoudi. 2019. 'Liposomes; from Synthesis to Targeting Macrophages'. *Biomedical Research* 30 (2).

Pradhan, Madhulika, Amit Alexander, Manju Rawat Singh, Deependra Singh, Swarnlata Saraf, Shailendra Saraf, and Ajazuddin. 2018. 'Understanding the Prospective of Nano-Formulations towards the Treatment of Psoriasis'. *Biomedicine & Pharmacotherapy* 107: 447–63.

Prudente, Arthur S., Graziela Sponchiado, Daniel A. G. B. Mendes, Bruna S. Soley, Daniela A. Cabrini, and Michel F. Otuki. 2017. 'Pre-Clinical Efficacy Assessment of Malva Sylvestris on Chronic Skin Inflammation'. *Biomedicine & Pharmacotherapy = Biomedecine & Pharmacotherapie* 93: 852–60.

Puig, Lluís. 2017. 'Cardiometabolic Comorbidities in Psoriasis and Psoriatic Arthritis'. *International Journal of Molecular Sciences* 19 (1).

Rai, Shubhra, Vikas Pandey, and Gopal Rai. 2017. 'Transfersomes as Versatile and Flexible Nano-Vesicular Carriers in Skin Cancer Therapy: The State of the Art'. *Nano Reviews & Experiments* 8 (1).

Raval, Nidhi, Vishakha Tambe, Rahul Maheshwari, Pran Kishore Deb, and Rakesh Tekade. 2018. 'Scale-Up Studies in Pharmaceutical Products Development'. In, 669–700.

Rocha, Lilian Wünsch, Ivan José Magayewski Bonet, Claudia Herrera Tambeli, Felipe Meira de-Faria, and Carlos Amilcar Parada. 2018. 'Local Administration of Mangiferin Prevents Experimental Inflammatory Mechanical Hyperalgesia through CINC-1/Epinephrine/PKA Pathway and TNF-α Inhibition'. *European Journal of Pharmacology* 830 (July): 87–94.

Ruff, Samine, Alexander Egeberg, Yuki M. F. Andersen, Gunnar Gislason, Lone Skov, and Jacob P. Thyssen. 2017. 'Prevalence of Cancer in Adult Patients with Atopic Dermatitis: A Nationwide Study'. *Acta Dermato-Venereologica* 97 (9): 1127–29.

Sampogna, Francesca, Luca Fania, Cinzia Mazzanti, Alessio Caggiati, Sabatino Pallotta, Annarita Panebianco, Simona Mastroeni, Biagio Didona, Giusi Pintori, and Damiano Abeni. 2019. 'The Broad-Spectrum Impact of Hidradenitis Suppurativa

on Quality of Life: A Comparison with Psoriasis'. *Dermatology (Basel, Switzerland)*, 1–7.

Sánchez-López, Elena, Mariana Guerra, João Dias-Ferreira, Ana Lopez-Machado, Miren Ettcheto, Amanda Cano, Marta Espina, Antoni Camins, Maria Luisa Garcia, and Eliana B. Souto. 2019. 'Current Applications of Nanoemulsions in Cancer Therapeutics'. *Nanomaterials* 9 (6): 821.

Santangelo, Carmela, Rosariax Vari, Beatrice Scazzocchio, Patrizia De Sanctis, Claudio Giovannini, Massimo D'Archivio, and Roberta Masella. 2018. 'Anti-Inflammatory Activity of Extra Virgin Olive Oil Polyphenols: Which Role in the Prevention and Treatment of Immune-Mediated Inflammatory Diseases?' *Endocrine, Metabolic & Immune Disorders Drug Targets* 18 (1): 36–50.

Schwingen, Julius, Mustafa Kaplan, and Florian C. Kurschus. 2020. 'Review—Current Concepts in Inflammatory Skin Diseases Evolved by Transcriptome Analysis: In-Depth Analysis of Atopic Dermatitis and Psoriasis'. *International Journal of Molecular Sciences* 21 (3).

Shaker, Dalia S., Rania A. H. Ishak, Amira Ghoneim, and Muaeid A. Elhuoni. 2019. 'Nanoemulsion: A Review on Mechanisms for the Transdermal Delivery of Hydrophobic and Hydrophilic Drugs'. *Scientia Pharmaceutica* 87 (3): 17.

Shi, Nian-Qiu, and Qi Xianrong. 2018. 'Preparation of Drug Liposomes by Reverse-Phase Evaporation'. In, 1–10.

Shin, Kyounghee, Hayoung Choi, Sun Kwang Song, Ji Won Yu, Jin Yong Lee, Eun Ji Choi, Dong Hee Lee, Sun Hee Do, and Jin Woong Kim. 2018. 'Nanoemulsion Vehicles as Carriers for Follicular Delivery of Luteolin'. *ACS Biomaterials Science & Engineering* 4 (5): 1723–29.

Silverberg, Jonathan I. 2018. 'Associations between Atopic Dermatitis and Other Disorders'. *F1000Research* 7.

Son, Seong Uk, Jae-woo Lim, Taejoon Kang, Juyeon Jung, and Eun-Kyung Lim. 2017. 'Hyaluronan-Based Nanohydrogels as Effective Carriers for Transdermal Delivery of Lipophilic Agents: Towards Transdermal Drug Administration in Neurological Disorders'. *Nanomaterials* 7 (12).

Su, Runping, Li Yang, Yue Wang, Shanshan Yu, Yu Guo, Jiayu Deng, Qianqian Zhao, and Xiangqun Jin. 2017. 'Formulation, Development, and Optimization of a Novel Octyldodecanol-Based Nanoemulsion for Transdermal Delivery of Ceramide IIIB'. *International Journal of Nanomedicine* 12: 5203–21.

Sutradhar, Kumar, and Md Amin. 2013. 'Nanoemulsions: Increasing Possibilities in Drug Delivery'. *European Journal of Nanomedicine* 5: 97–110.

Suzuki, Yasuyuki, Tomio Ogasawara, Yuki Tanaka, Hiroyuki Takeda, Tatsuya Sawasaki, Masaki Mogi, Shuang Liu, and Kazutaka Maeyama. 2018. 'Functional G-Protein-Coupled Receptor (GPCR) Synthesis: The Pharmacological Analysis of Human Histamine H1 Receptor (HRH1) Synthesized by a Wheat Germ Cell-Free Protein

Synthesis System Combined with Asolectin Glycerosomes'. *Frontiers in Pharmacology* 9.

Thomas, Jayakar, and Kumar Parimalam. 2016. 'Treating Pediatric Plaque Psoriasis: Challenges and Solutions'. *Pediatric Health, Medicine and Therapeutics* 7: 25–38.

Thomas, Lydia, Foziyah Zakir, Mohd Aamir Mirza, Md Khalid Anwer, Farhan Jalees Ahmad, and Zeenat Iqbal. 2017. 'Development of Curcumin Loaded Chitosan Polymer Based Nanoemulsion Gel: In Vitro, Ex Vivo Evaluation and in Vivo Wound Healing Studies'. *International Journal of Biological Macromolecules* 101: 569–79.

Todo, Hiroaki. 2017. 'Transdermal Permeation of Drugs in Various Animal Species'. *Pharmaceutics* 9 (3).

Torsekar, R., and Manjyot M. Gautam. 2017. 'Topical Therapies in Psoriasis'. *Indian Dermatology Online Journal* 8 (4): 235–45.

Villablanca, Salvador, Cristián Fischer, S. Cecilia García-García, J. Manuel Mascaró-Galy, and Juan Ferrando. 2017. 'Primary Scarring Alopecia: Clinical-Pathological Review of 72 Cases and Review of the Literature'. *Skin Appendage Disorders* 3 (3): 132–43.

Vitonyte, Justina, Maria Letizia Manca, Carla Caddeo, Donatella Valenti, Josè Esteban Peris, Iris Usach, Amparo Nacher, et al. 2017. 'Bifunctional Viscous Nanovesicles Co-Loaded with Resveratrol and Gallic Acid for Skin Protection against Microbial and Oxidative Injuries'. *European Journal of Pharmaceutics and Biopharmaceutics: Official Journal of Arbeitsgemeinschaft Fur Pharmazeutische Verfahrenstechnik e.V* 114: 278–87.

Walicka, A., J. Falicki, and B. Iwanowska-Chomiak. 2019. 'Rheology of Drugs for Topical and Transdermal Delivery'. *International Journal of Applied Mechanics and Engineering* Vol. 24 (1).

Wang, Xiaohong, Qiang Ao, Xiaohong Tian, Jun Fan, Hao Tong, Weijian Hou, and Shuling Bai. 2017. 'Gelatin-Based Hydrogels for Organ 3D Bioprinting'. *Polymers* 9 (9): 401.

Wang, Yuanduo, Ziyang Guo, Yongfang Qian, Zhen Zhang, Lihua Lyu, Ying Wang, and Fang Ye. 2019. 'Study on the Electrospinning of Gelatin/Pullulan Composite Nanofibers'. *Polymers* 11 (9): 1424.

Werfel, Thomas, Jean-Pierre Allam, Tilo Biedermann, Kilian Eyerich, Stefanie Gilles, Emma Guttman-Yassky, Wolfram Hoetzenecker, et al. 2016. 'Cellular and Molecular Immunologic Mechanisms in Patients with Atopic Dermatitis'. *Journal of Allergy and Clinical Immunology* 138 (2): 336–49.

Witting, Madeleine, Alexander Boreham, Robert Brodwolf, Kateřina Vávrová, Ulrike Alexiev, Wolfgang Friess, and Sarah Hedtrich. 2015. 'Interactions of Hyaluronic Acid with the Skin and Implications for the Dermal Delivery of Biomacromolecules'. *Molecular Pharmaceutics* 12 (5): 1391–1401.

Wollenberg, Andreas, Michael D. Howell, Emma Guttman-Yassky, Jonathan I. Silverberg, Christopher Kell, Koustubh Ranade, Rachel Moate, and René van der Merwe.

2019. ‘Treatment of Atopic Dermatitis with Tralokinumab, an Anti-IL-13 MAb’. *The Journal of Allergy and Clinical Immunology* 143 (1): 135–41.

Xu, Hui, Yun-Wen Zheng, Qi Liu, Li-Ping Liu, Feng-Lin Luo, Hu-Chen Zhou, Hiroko Isoda, Nobuhiro Ohkohchi, and Yu-Mei Li. 2017. ‘Reactive Oxygen Species in Skin Repair, Regeneration, Aging, and Inflammation’. *Reactive Oxygen Species (ROS) in Living Cells*,72747.

Yang, Guang, Xiao Shang, Guozhen Cui, Lingling Zhao, Hengjun Zhao, and Nanya Wang. 2019. ‘Mangiferin Attenuated Diethynitrosamine-Induced Hepatocellular Carcinoma in Sprague-Dawley Rats via Alteration of Oxidative Stress and Apoptotic Pathway’. *Journal of Environmental Pathology, Toxicology and Oncology: Official Organ of the International Society for Environmental Toxicology and Cancer* 38 (1): 1–12.

Yang, Meng, Yongwei Gu, Xiaomeng Tang, Ting Wang, and Jiyong Liu. 2019. ‘Advancement of Lipid-Based Nanocarriers and Combination Application with Physical Penetration Technique’. *Current Drug Delivery* 16 (4): 312–24.

Yin, Lihua, Wenxiao Cheng, Zishun Qin, Hongdou Yu, Zhanhai Yu, Mei Zhong, Kemo Sun, and Wei Zhang. 2015. ‘Effects of Naringin on Proliferation and Osteogenic Differentiation of Human Periodontal Ligament Stem Cells In Vitro and In Vivo’. *Stem Cells International* 2015: 758706.

Yousef, Shereen A., Yousuf H. Mohammed, Sarika Namjoshi, Jeffrey E. Grice, Heather A. E. Benson, Wedad Sakran, and Michael S. Roberts. 2019. ‘Mechanistic Evaluation of Enhanced Curcumin Delivery through Human Skin In Vitro from Optimised Nanoemulsion Formulations Fabricated with Different Penetration Enhancers’. *Pharmaceutics* 11 (12).

Zeng, Wei-Jie, Zhi Tan, Xing-Fei Lai, Ya-Nan Xu, Chun-Lin Mai, Jun Zhang, Zhen-Jia Lin, Xian-Guo Liu, Shi-Li Sun, and Li-Jun Zhou. 2018. ‘Topical Delivery of L-Theanine Ameliorates TPA-Induced Acute Skin Inflammation via Downregulating Endothelial PECAM-1 and Neutrophil Infiltration and Activation’. *Chemico-Biological Interactions* 284: 69–79.

Zhang, Hongwei. 2017. ‘Thin-Film Hydration Followed by Extrusion Method for Liposome Preparation’. *Methods in Molecular Biology (Clifton, N.J.)* 1522: 17–22.

Zhang, Jingze, Wenyuan Gao, Zhen Liu, Zhidan Zhang, and Changxiao Liu. 2014. ‘Systematic Analysis of Main Constituents in Rat Biological Samples after Oral Administration of the Methanol Extract of Fructus Aurantii by HPLC-ESI-MS/MS’. *Iranian Journal of Pharmaceutical Research: IJPR* 13 (2): 493–503.

Zhang, Kai, Yongtai Zhang, Zhe Li, Nana Li, and Nianping Feng. 2017. ‘Essential Oil-Mediated Glycerosomes Increase Transdermal Paeoniflorin Delivery: Optimization, Characterization, and Evaluation in Vitro and in Vivo’. *International Journal of Nanomedicine* 12: 3521–32.

Zhang, Yong-Tai, Li-Na Shen, Ji-Hui Zhao, and Nian-Ping Feng. 2014. 'Evaluation of Psoralen Ethosomes for Topical Delivery in Rats by Using in Vivo Microdialysis'. *International Journal of Nanomedicine* 9: 669–78.

Zhang, Yongtai, Qing Xia, Yanyan Li, Zehui He, Zhe Li, Teng Guo, Zhonghua Wu, and Nianping Feng. 2019. 'CD44 Assists the Topical Anti-Psoriatic Efficacy of Curcumin-Loaded Hyaluronan-Modified Ethosomes: A New Strategy for Clustering Drug in Inflammatory Skin'. *Theranostics* 9 (1): 48–64.

Zhou, Chuying, Yuling Lai, Peng Huang, Lingpeng Xie, Haiyan Lin, Zhenting Zhou, Chan Mo, et al. 2019. 'Naringin Attenuates Alcoholic Liver Injury by Reducing Lipid Accumulation and Oxidative Stress'. *Life Sciences* 216: 305–12.

Zsikó, Stella, Erzsébet Csányi, Anita Kovács, Mária Budai-Szűcs, Attila Gácsi, and Szilvia Berkó. 2019. 'Methods to Evaluate Skin Penetration In Vitro'. *Scientia Pharmaceutica* 87 (3): 19.

ANNEXES I

Colloids and Surfaces B: Biointerfaces 162 (2018) 265–270

Contents lists available at ScienceDirect

Colloids and Surfaces B: Biointerfaces

journal homepage: www.elsevier.com/locate/colsurfb

A novel ultradeformable liposomes of Naringin for anti-inflammatory therapy

María Pleguezuelos-Villa[a,*], Silvia Mir-Palomo[a], Octavio Díez-Sales[a,b], M.A. Ofelia Vila Buso[c], Amparo Ruiz Sauri[d], Amparo Nácher[a,b]

[a] Department of Pharmacy, Pharmaceutical Technology and Parasitology, Faculty of Pharmacy, University of Valencia,Av. Vicent Andrés Estellés s/n, 46100, Burjassot, Valencia, Spain
[b] Instituto Interuniversitario de Investigación de Reconocimiento Molecular y Desarrollo Tecnológico (IDM), Universitat Politècnica de València, Universitat de València, Av. Vicent Andrés Estellés s/n, 46100, Burjassot, Valencia, Spain
[c] Department of Physical Chemistry, Faculty of Pharmacy, University of Valencia, Av. Vicent Andrés Estellés s/n, 46100, Burjassot, Valencia, Spain
[d] Department of Pathology, University of Valencia, Av. Blasco Ibañez 17, 46010 Valencia, Spain

ARTICLE INFO

Article history:
Received 28 September 2017
Received in revised form
25 November 2017
Accepted 30 November 2017
Available online 1 December 2017

Keywords:
Naringin
Ultradeformable liposomes
Anti-inflammatory
Transdermal penetration
Fibroblasts
In vivo studies

ABSTRACT

Ultradeformable liposomes were formulated using naringin (NA), a flavanone glycoside, at different concentrations (3, 6 and 9 mg/mL). Nanovesicles were small size (~100 nm), regardless of the NA concentration used, and monodisperse (PI < 0.30). All formulations showed a high entrapment efficiency (~88%) and a highly negative zeta potential (around −30 mV). The selected formulations were highly biocompatible as confirmed by *in vitro* studies using 3T3 fibroblasts. *In vitro* assay showed that the amounts (%) of NA accumulated in the epidermis (~10%) could explain the anti-inflammatory properties of ultradeformable liposomes. *In vivo* studies confirmed the higher effectiveness of ultradeformable liposomes respect to betamethasone cream and NA dispersion in reducing skin inflammation in mice. Overall, it can conclude that NA ultradeformable liposomes can be considered as a promising formulation for the treatment of skin inflammatory diseases.

1. Introduction

The incidence of skin inflammatory diseases (dermatitis, psoriasis, rash) has increased significantly in the last decades and bioflavonoids such as quercetin, curcumin and baicalin have been widely used for treatment of this injures [1–4]. Citrus fruits peels represent an important source of phenolic acids and flavonoids, mainly polymethoxyflavones (PMFs), flavanones and glycosylated flavanones [5,6]. Naringin (NA), a bioactive component of citrus species, is a glycosylated flavanone formed by naringenin (flavanone) and the disaccharide neohesperidose (Fig. 1). This compound shows a wide variety of pharmacological effects such as antioxidant, blood lipid–lowering and anticarcinogenic activity. Moreover, several studies have highlighted its potential to suppress the production of proinflammatory cytokines and attenuate the inflammatory response [7–12] and it has been proposed in combination with corticoids to treat skin diseases such as dermatitis [13].

On the other hand, most of conventional therapies failed because of their low capacity to deliver therapeutic drug concentrations to the target tissue. Different approaches have been attempted to overcome this problem by providing "selective" delivery of drugs to the affected area, using various pharmaceutical carriers. In the last years, among the different types of particulate carriers, liposomes have received a great attention [14] and have been used as delivery systems of different bioactive agents. The list of actives incorporated in nanoliposomes is huge, ranging from pharmaceutical to cosmetics and nutraceuticals substances (opiods, curcumin, resveratrol, quercetin, silibinin, glycyrrhizic acid, vitamin C, and others) [15–21]. In general, these systems are able to enhance the performance of the incorporated bioactive agents by improving their solubility and bioavailability, their *in vitro* and *in vivo* stability, as well as preventing their unwanted interactions with other molecules [22,23]. Another advantage of nanoliposomes is cell-specific targeting, which is a prerequisite to ensure the adequate drug concentrations required for optimum therapeutic effects in the target site while minimizing adverse effects on healthy cells

* Corresponding author.
E-mail address: maplevi@alumni.uv.es (M. Pleguezuelos-Villa).

https://doi.org/10.1016/j.colsurfb.2017.11.068
0927-7765/

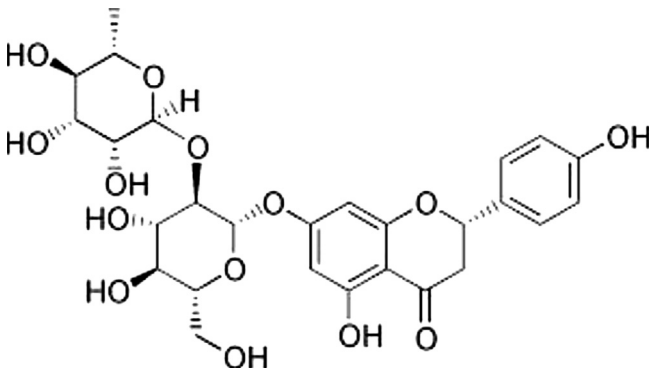

Fig. 1. Chemical structure of Naringin (NA).

and tissues. Among them, ultradeformable liposomes have been found to be promising for herbal extracts delivery [6,24]. Since, this type of phospholipid vehicles increases the accumulation on the skin as well as reduces adverse effects. Recent reports showed that ultradeformable nanosized liposomes may be postulated as a novel dermal delivery carrier due to their biocompatibility and high elasticity [25,26], which is attributed to of the combination of phospholipids and surfactant (such as sodium cholate, deoxycholate, Span, Tween and dipotasium glycyrrhizinate). The surfactant acts as an íedge activatorí that modify the organization of the lipid bilayers increasing its deformability [27].

The purpose of this study is to develop ultradeformable liposomes. To do this, the vesicles were formulated using different concentrations of naringin (NA) and characterized in terms of zeta potential, mean size, size distribution and vesicles encapsulation efficiency. *In vitro* transdermal penetration was also quantified. Cytotoxicity test was carried out as well to evaluate the biocompatibility of the formulations on 3T3 mouse dermal fibroblast cells. In addition, NA ultradeformable liposomes ability to attenuate skin inflammation induced by phorbol 1, 2-myristate 1, 3-acetate (TPA) in mice was studied.

2. Materials and methods

2.1. Materials

Monosodium phosphate was purchased from Panreac quimica S.A. (Barcelona, Spain). Lipoid® S75, a mixture of soybean lecithin containing lysophosphatidylcholine (3% maximum), phosphatidylcholine (70%), phosphatidylethanolamine (10%), fatty acids (0.5% maximum), triglycerides (3% maximum), and tocopherol (0.1–0.2%) were a gift from Lipoid GmbH (Ludwigshafen, Germany). Polysorbate 80 was purchased from Scharlab S.L. (Barcelona, Spain). Glycerin and ethanol were purchased from Guinama S.L.U. (Valencia, Spain), *N*-octanol (special grade for measurement of partition coefficients) was purchased from VWR chemicals S.A. S (France), Disodium phosphate were purchased from Scharlab S.L. (Barcelona, Spain). Betamethasone was from IFC Acofarma S.A. (Santander, Spain). Phorbol 1,2-myristate 1,3-acetate and naringin with a molecular formula ($C_{27}H_{32}O_{14}$) and weight (580.54 g/mol) were purchased from Sigma-Aldrich.

2.2. Analytical method

A high-performance liquid chromatograph (HPLC) PerkinElmer® Series 200 equipped with an auto-injector and a photodiode array UV detector was used for NA quantification in experimental samples [28]. The column used was a Teknokroma® Brisa "LC2" C18, 5.0 μm (150 cm × 4.6 mm). The mobile phase consisted of a mixture 50:50 (V/V) of methanol and ultrapure water adjusted at pH 4. The detection wavelength was 280 nm, the injection volume was 20 μL and the flow rate was 1.0 mL/min. Linearity, limit of quantification (LOQ), detection (LOD), precision and accuracy of the analytic method were carried out.

2.3. Physicochemical properties

2.3.1. Crystalline structure

NA structure was analyzed with the X-ray diffractometer KAPPA CCD. The system has a goniometer of four circles and a two-dimensional KAPPA CCD detector with beryllium window of 90 mm diameter maintained at −60 °C.

2.3.2. Solubility

The solubility of the flavonoid at 25 °C was determined in different vehicles: water, pH 7.4 buffered solution and polysorbate 80 (1%, w/w) in aqueous medium. Flavonoid was added to saturation in each system during 24 h under constant agitation (500 rpm). Finally, an aliquot of each sample was filtered (0.22 μm) and quantified.

2.3.3. Partition coefficient determination

Octanol-water partition coefficient (P_{oct}) value was obtained by equilibrating the NA aqueous solution with 1-octanol in a shaker bath at 25 °C overnight [29]. Distribution of NA between the aqueous and the organic phase was estimated by the differences between the NA concentration at the beginning and at the equilibrium step, according to the following equation (Eq. (1)):

$$P_{oct} = \frac{(Co - Ce)/Vo}{Co/Va} \quad (1)$$

where C_o, is the initial NA aqueous solution concentration, C_e, the solution concentration at equilibrium, V_o, volume of the organic phase (50 mL) and V_a, the volume of aqueous solution (50 mL).

2.4. Ultradeformable liposomes

A preformulation studies was carried out in order to select the best formulations able to load increasing amount of NA (from 1 to 24 mg/mL). According to stability data (average particle size <150 nm, polydispersity values <0.5 and zeta potential value <−25 mV), one formulation was selected with different amount of NA: liposomes I (3 mg/mL), liposomes II (6 mg/mL) and liposomes III (9 mg/mL). NA (3 or 6 or 9 mg/mL), polysorbate 80 (2.5 mg/mL) and Lipoid® S75 (120 mg/mL) were added in a glass vial. These mixtures were hydrated overnight at room temperature (25 °C) with a buffer phosphate solution (pH 7.4). The obtained dispersions were sonicated for 4 min using an ultrasonic disintegrator (CY-500, Optic Ivymen system, Barcelona, Spain). Then liposome suspensions were extruded through a 0.20 μm membrane with an Avanti® Mini-Extruder (Avanti Polar Lipids, Alabaster, Alabama) to obtain homogeneous dispersions. NA dispersion (9 mg/mL) in phosphate buffer solution containing polysorbate 80 (1%, w/w) and empty liposomes (without NA) were prepared as control.

2.5. Characterization of liposomes

2.5.1. Transmission electron microscopy

Ultradeformable liposomes morphology was examined through a negative staining technique using a JEM-1010 microscope (Jeol Europe, Croissy-sur-Seine, France), equipped with a digital camera MegaView III at an accelerating voltage of 80 Kv.

2.5.2. Determination of entrapment efficiency (EE%)

1 mL of each sample and dialyzed against buffer (100 mL) for 24 h, at room temperature using a membrane Spectra/Por,

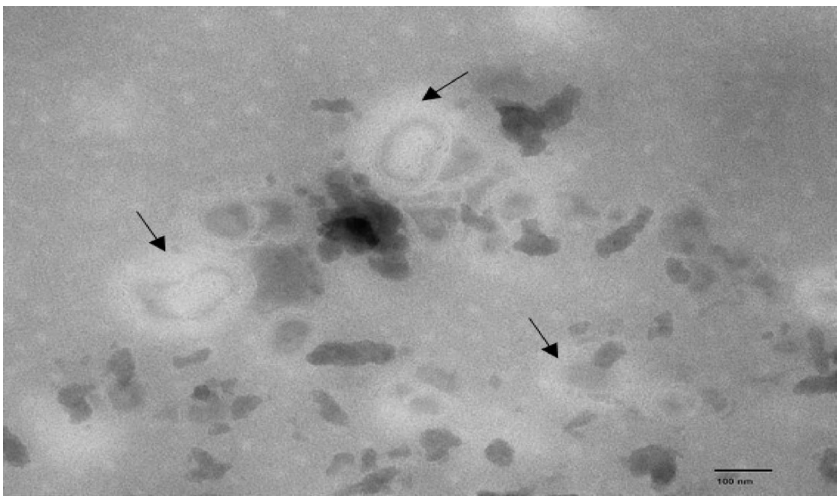

Fig. 2. TEM (Transmission electron microscopy) images of ultradeformable liposomes. The arrows indicate the lamellae of vesicles.

(12–14 kDa MW cut-off; Spectrum Laboratories Inc., DG Breda, The Netherlands). Dialyzed and non-dialyzed ultradeformable liposomes were disrupted with methanol (1:100). The samples were assayed by HPLC as described in Section 2.2.

EE (%) of liposomes I, II and III was calculated as follows (Eq. (2)):

$$EE\% = \left(\frac{\text{actual NA}}{\text{initial NA}}\right) \times 100 \quad (2)$$

where actual NA is the amount of the active in ultradeformable liposomes after dialysis, and initial NA is the amount before dialysis.

2.5.3. Determination of vesicle size, zeta potential and polydispersity index

Average diameter and polydispersity index (PI) of the samples were performed in triplicate by means of Photon Correlation Spectroscopy using a Zetasizer Nano-S® (Malvern Instruments, Worcester-shire, United Kingdom) at 25 °C. Moreover, zeta potential was estimated by electrophoretic light scattering in a thermostated cell in a Zetasizer Nano-S®. The ultradeformable liposomes stability was evaluated over 30 days at ~4 °C.

2.6. Cell viability studies

3T3 mouse fibroblasts (ATCC, Manassas, VA, USA) were cultured in Dulbecco's modified Eagle's medium (DMEM, Sigma Aldrich, Spain), supplemented with penicillin (100 U/mL), 10% (V/V) fetal bovine serum, and streptomycin (100 mg/mL) (Sigma Aldrich, Spain) in 5% CO_2 incubator at 37 °C to maintain cell growth.

3T3 cells (2×10^5 cells/well) were seeded in 96-well plates at passage 14–15. After one day of incubation, 3T3 cells were treated with NA dispersion (9 mg/mL) or empty or NA loaded liposomes I, II and III for 24 h. In each well 25 μL of formulation were added and filled with 225 μL of cultured medium.

Cell viability was evaluated by MTT [3 (4,5-dimethylthiazolyl-2)-2,5-diphenyltetrazolium bromide] colorimetric assay [30]. After 24 h experiment, 100 μL of MTT was added to each well, and then, after 3 h the formazan crystals formed were dissolved in DMSO (50 μL). The reaction was measured at 570 nm with a spectrophotometer. All experiments were repeated three-fold (n = 3).

2.7. In vitro *diffusion*

A diffusion study was performed using Franz diffusion cells (with an effective diffusion area of 0.784 cm^2) and new born pig skin from a local slaughterhouse. The receptor compartment (CR) was filled with buffer phosphate solution (pH 7.4), continuously stirred and thermostated at 32 °C. Epidermal membranes were obtained from heat separation through immersing in water (at 60 °C) for 75 s [31]. On the epidermis surface 800 μL of different formulations assayed were applied. At different time intervals up to 24 h, receptor solutions were withdrawn and assayed for drug content by HPLC, (Section 2.2). At the end of the experiment, 1 mL of phenol red solution (0.05%, w/w) was applied in the donor compartment for checking the integrity of the epidermis [32].

2.8. In vivo *assay*

Female CD-1 mice (5–6 weeks old, 25–35 g) were obtained from Harlan laboratories (Barcelona, Spain) and acclimatized for one week before use. All studies were performed in accordance with European Union regulations for the handling and use of laboratory animals and the protocols were approved by the Institutional Animal Care and Use Committee of the University of Valencia (code 2016/VSC/PEA/00112 type 2).

One day before the experiment the back skin of mice (n = 4 per group) was shaved. The first day, TPA dissolved in acetone (3 μg/20 μL) was applied to the shaved dorsal area to induce cutaneous inflammation and ulceration. Negative control mice only received acetone (20 μL). After 3 h, 200 μL of empty or NA loaded ultradeformable liposomes (I, II and III), NA dispersion or betamethasone cream (20 mg) were topically applied in the dorsal area. The procedure was repeated on the second and third day. The fourth day, mice were sacrificed by cervical dislocation.

Two biomarkers: oedema formation and myeloperoxidase (MPO) activity were used to evaluate the effect of the formulations [33]. First, dorsal skin area was excised, weighed to assess oedema formation and stored at −80 °C. Second, biopsies were dispersed in 750 μL of phosphate buffer (pH 5.4) and, with an Ultra-Turrax T25 homogenizer (IKA1 Werke GmbH & Co. KG, Staufen, Germany), were homogenized in an ice bath. The supernatant obtained after centrifugation was diluted with PBS 5.4 (1:10) in order to assay MPO activity. Briefly, in a 96-well plate, 10 μL of diluted sample, 20 μL of sodium phosphate buffer (pH 5.4), 200 μL of phosphate buffer (pH 7.4), 40 μL of 0.052% hydrogen peroxide and 20 μL of 18 mM 3,30,5,50-tetramethylbenzidine dihydrochloride were added to each well. At the end of experiment, 50 μL of SO_4H_2 2N was added to stop the reaction. The absorbance was measured at 450 nm. The MPO activity was calculated from the linear portion of a standard curve.

Table 1
Average size, polydispersity index (PI), zeta potential and NA (naringin) entrapment efficiency of liposome I (3 mg/mL), liposome II (6 mg/mL) and liposome III (9 mg/mL). All values are mean ± standard deviations (n = 3).

Formulations	Size (nm)		PI		Potential Z (mV)		EE (%)
	0 days	30 days	0 days	30 days	0 days	30 days	
Empty liposome	88.3 ± 1.7	100.1 ± 0.8	0.25	0.16	−32.5 ± 0.4	−31.9 ± 1.7	–
Liposome I	90.2 ± 1.6	90.9 ± 2.3	0.23	0.22	−33.9 ± 1.4	−30.1 ± 1.1	91.03 ± 0.04
Liposome II	86 ± 1.0	84.1 ± 2.5	0.25	0.20	−32.6 ± 1.1	−26.9 ± 0.8	88.70 ± 0.25
Liposome III	86.3 ± 1.1	84.6 ±0.9	0.22	0.22	−27.7 ± 1.1	−28.0 ± 1.5	92.72 ± 0.10

2.9. Histological examination

Mice skin was excised, fixed and stored in formaldehyde (0.4%, V/V). Longitudinal sections (5 mm) were marked with hematoxylin and eosin and observed using a light microscope (DMD 108 Digital Micro-Imaging Device, Leica, Wetzlar, Germany).

2.10. Statistical analysis of data

Statistical differences were determined by one-way ANOVA test and Tukey's test for multiple comparisons with a significance level of $p < 0.05$. All statistical analyses were performed using IBM SPSS statistics 22 for Windows (Valencia, Spain). Data are shown as mean ± standard deviation.

3. Results and discussions

3.1. Analytical method

The analytical method (HPLC) for NA quantification was firstly validated. Calibration curves covering the whole range of NA concentrations were prepared. Excellent plots correlating the peak areas and NA concentrations were obtained (r > 0.999), demonstrating good linearity. Precision was evaluated by calculating the relative error (RE, %) and accuracy by coefficient of variation (CV, %); both values were less than 9%. The limits of detection (LOD) and quantification (LOQ) were 0.11 μg/mL and 0.34 μg/mL, respectively. These data satisfy the standard validation.

3.2. Physicochemical properties

The flavanone glycoside (NA) was characterized with the RX technique. The spectrum shows that it is a flavonoid with crystalline structure. Molecules are spatially distributed in a regular and symmetrical form, so they require more energy for their separation. All this property may be responsible of their low solubility and bioavailability. Indeed, the solubility of NA in water and phosphate buffer at pH 7.4 is 2.69 ± 0.01 mg/mL and 1.94 ± 0.01 mg/mL, respectively. As it was expected, NA is more soluble (14.4 ± 0.4 mg/mL) in presence of polysorbate 80 (1%, w/w), probably because of the formation of micelles, which allows the solubilization of a greater amount of flavonoid. In addition, NA is a hydrophilic compound (log P_{oct} = −0.66 ± 0.03) with a molecular weight superior to 580 g/mol, which could lead to a low percutaneous absorption.

3.3. Characterization of ultradeformable liposomes

In Fig. 2 the formation of spherical nanometric vesicles can be observed. All ultradeformable liposomes (I, II and III) showed a monodisperse distribution (PI < 0.30) (Table 1). In all cases, the mean size was very similar (approximately 100 nm), and no statistical differences were observed from batch to batch. The zeta potential was highly negative (−30 mV), for the different NA concentrations. Liposomes were able to incorporate NA in high amount (entrapment efficiency approximately 90%), no significant differences were detected among the groups ($p > 0.05$), confirming that the flavonoid was effectively/efficiently incorporated into vesicle. Ultradeformable liposomes were stable during 30 days of storage, according to zeta potential and mean size values (Table 1). Such data ensure good stability of ultradeformable liposomes, due to the great electrostatic repulsion between the vesicles.

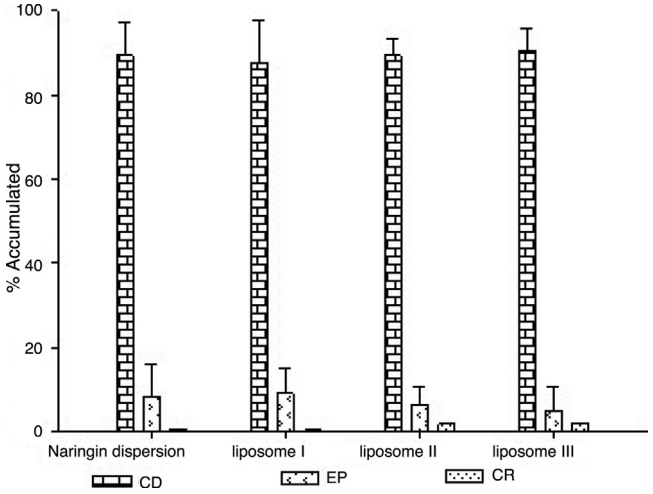

Fig. 3. Transdermal permeation of NA (naringin) dispersion and loading liposomes I (3 mg/mL), II (6 mg/mL), III (9 mg/mL). Amount accumulated in CR (receptor compartment), CD (donor compartment) and EP (epidermis) after 24 h at 32 °C. The results were expressed as the mean and standard deviation (error bars). No significate differences have been found among the groups (p > 0.05).

3.4. Cell viability studies

The biocompatibility of each formulation was evaluated *in vitro* on cells, which represents a good and reliable method to select formulations that will be used for further *in vivo* studies. 3T3 mouse dermal fibroblasts were incubated with different formulations: empty or NA ultradeformable liposomes (I, II and III). Cells viability after 24 h of incubation with the formulation is approximately 100% and similar to that of the control group ($p > 0.05$). These results are in accordance with Cao et al. [34], confirming the low toxicity of flavonoid and liposomes.

3.5. In vitro *diffusion*

Permeation study was performed for 24 h using ultradeformable liposomes (I, II and III). Fig. 3 shows the cumulative amounts (Q, %) of NA in the donor compartment (CD), epidermis (EP) and receptor compartment (CR) for all formulations tested at 24 h. The cumulative amount of NA (%) in the CR was negligible (less than 0.5%) regardless the formulation tested. The amounts (%) of NA accumulated in the EP (∼10%) could explain the anti-inflammatory properties of ultradeformable liposomes detected during the *in vivo* assay. Finally, the amount of NA present in the CD (>90%), confirmed the low flavonoid bioavailability. The NA low permeability

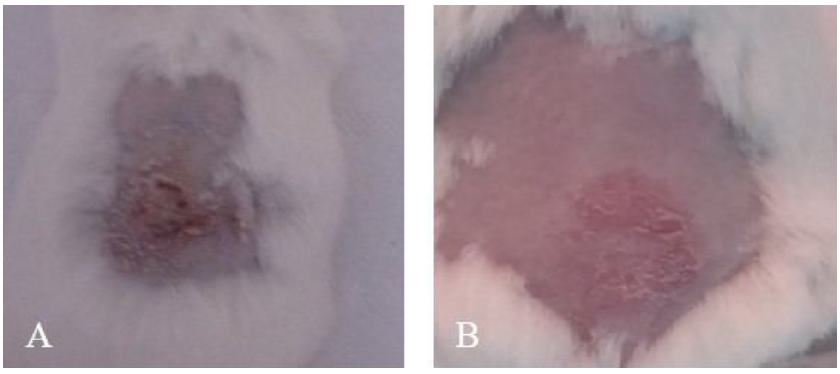

Fig. 4. Macroscopic appearance of mice skin lesions inducted with TPA (A) and treated with liposome III: 9 mg/mL (B).

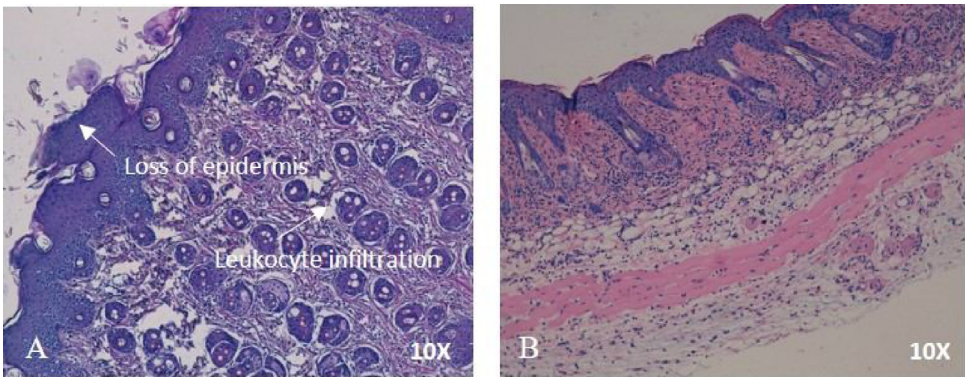

Fig. 5. Representative histological sections of mouse skin: treated with TPA-inflamed skin (A) and treated with liposome III: 9 mg/mL (B).

Table 2
Oedema inhibition and MPO (myeloperoxidase test) activity in skin mice inflamed with TPA (control +). Skin mice inflamed were treated to 200 μL of NA dispersion, empty liposomes or loading liposomes I (3 mg/mL), II (6 mg/mL), III (9 mg/mL) and betamethasone cream (20 mg). The results were expressed as the mean and standard deviation (error bars). * $p < 0.01$ liposomes (I, II and III) vs betamethasone cream and NA dispersion. ANOVA-Tukey. # $p < 0.01$ liposome III vs NA dispersion. ANOVA-Tukey.

Formulations	% Oedema inhibition	% MPO inhibition
Control +	0.5 ± 1.15	0.5 ± 1.01
Cream	13.06 ± 2.81	12.70 ± 1.81
NA dispersion	27.48 ± 3.37	65.82 ± 2.94
Empty liposome	23.67 ± 2.29	60.25 ± 3.05
Liposome I	36.01* ± 3.03	74.61 ± 4.03
Liposome II	37.29* ± 3.19	78.72 ± 4.59
Liposome III	43.18* ± 3.36	86.75# ± 4.93

could be mainly attributed to its difficulty to permeate through the stratum corneum, which serves as a lipophilic barrier against the penetration of hydrophilic molecules (NA has log P oct = −0.66). In addition, the high molecular weight (~580 g/mol) of NA could have limited its transdermal delivery by the high resistance of skin towards diffusion [35,36].

3.6. In vivo *assay*

TPA application in mice has been used for the evaluation of anti-inflammatory activity of drugs. This compound induces a variety of histological and biochemical changes in the skin [37]. In this work, TPA was daily applied on mice dorsal skin for 3 days, inducing skin ulceration, loss of epidermis integrity with scale and crust formation. Besides, it stimulates the oedema formation, due to an increase in vascular permeability. Table 2 summarizes the results obtained. The phorbol ester (TPA) caused a 3-fold increase in skin weight, compared to healthy mice. The administration of liposomes I, II and III was more active than NA dispersion and betamethasone cream in reducing skin oedema (~20%). Statistical differences were observed between samples ($p < 0.01$), probably because the ultradeformable liposomes promoted the internalization of NA in epithelial cells, avoiding vascular congestion and oedema formation. The MPO activity was quantified as a marker of the inflammatory process, since it is proportional to the neutrophil concentration in the inflamed tissue. The efficacy of NA loaded ultradeformable liposomes was assayed and compared with betamethasone cream, as commercial reference, and NA dispersion. The ultradeformable liposomes displayed a superior ability to reduce MPO activity in the injured tissue respect to the betamethasone cream (Table 2). No significant differences were observed ($p > 0.05$) between the three vesicular formulations containing different amounts of NA, which indicates that, in our experimental conditions, ultradeformable liposomes can promote the NA beneficial activity independent of the concentration used. Liposomes (III) have a greater activity respect to NA dispersion ($p < 0.01$), despite having the same concentration of flavonoid, as shown in Table 2. Thus, this phospholipidic system could be considered as promising tools for treatment of skin inflammation. The macroscopic observations are in agreement with the MPO and oedema values. The macroscopic images of mice clearly showed the positive effect of NA ultradeformable liposomes on injured skin (Fig. 4).

With regard to the histological study, morphological alterations of mice skin exposed to TPA were evaluated by hematoxylin and eosin staining, and compared with untreated skin (Fig. 5). The skin treated with acetone only (control −) showed a regular structure and normal appearance of both epidermis and dermis, as well as the tissues directly underneath (i.e., subcutaneous cellular tissue, skeletal muscle and adipose tissue), with only some mononuclear and polymorphonuclear cells in the muscular region. Otherwise,

mice skin treated with TPA displayed severe dermal and subcutaneous alteration, with a large number of leukocytes infiltrating, and showing pathological features of inflammatory damage, such as vascular congestion (control +). Similar results of injured skin were obtained using betamethasone cream, but the application of the NA ultradeformable liposomes reduced TPA-induced lesions, along with mild to moderate inflammatory infiltrates of mononuclear cells, eosinophils and neutrophils. Therefore, the results obtained *in vivo* seem to indicate a remarkable therapeutic potential of NA ultradeformable liposomes.

4. Conclusions

The loading of NA into ultradeformable liposomes represents an innovative approach to prevent and treat skin lesion and restore skin integrity. Results demonstrated that NA liposomes were highly biocompatible and more effective than betamethasone cream and NA dispersion as demonstrate *in vivo* model (TPA test). In conclusion NA ultradeformable liposomes can be considered as a promising formulation for the treatment of inflammatory diseases.

Acknowledgment

We wish to express our gratitude to Lipoid GmbH (Ludwigshafen, Germany) for providing the phospholipid used in this work for free.

References

[1] H. Chen, C. Lu, H. Liu, M. Wang, H. Zhao, Y. Yan, et al., Quercetin ameliorates imiquimod-induced psoriasis-like skin inflammation in mice via the NF-κB pathway, Int. Immunopharmacol. 48 (2017) 110–117.
[2] K.M. Parmar, P.R. Itankar, A. Joshi, S.K. Prasad, Anti-psoriatic potential of Solanum xanthocarpum stem in Imiquimod-induced psoriatic mice model, J. Etnopharmacol. 23 (198) (2017) 158–166.
[3] M.L. Manca, I. Castangia, M. Zaru, A. Nácher, D. Valenti, X. Fernàndez-Busquets, et al., Development of curcumin loaded sodium hyaluronate immobilized vesicles (hyalurosomes) and their potential on skin inflammation and wound restoring, Biomaterials 71 (2015) 100–109.
[4] C. Caddeo, A. Nacher, A. Vassallo, M.F. Armentano, R. Pons, X. Fernàndez-Busquets, et al., Effect of quercetin and resveratrol co-incorporated in liposomes against inflammatory/oxidative response associated with skin cancer, Int. J. Pharm. 513 (1) (2016) 153–163.
[5] L. Castro-Vazquez, M. Alañon, V. Rodriguez-Robledo, M.S. Pérez-Coello, Díaz-Maroto M.C. Hermosín-Gutierrez, Bioactive flavonoids, antioxidant behaviour, and cytoprotective effects of dried grapefruit peels (Citrus paradisi macf.), Oxid. Med. Cell. Longevity 2016 (2016) (2016) 8915729.
[6] M. Manconi, M.L. Manca, F. Marongiu, C. Caddeo, I. Castangia, G.L. Petretto, et al., Chemical characterization of Citrus limon var. pompia and incorporation in phospholipid vesicles for skin delivery, Int. J. Pharm. 506 (1) (2016) 449–457.
[7] R. Chen, Q.L. Qi, M.T. Wang, Q.Y. Li, Therapeutic potential of naringin: an overview, Pharm. Biol. 54 (12) (2016) 3203–3210.
[8] A. Ramakrishnan, N. Vijayakumar, M. Renuka, Naringin regulates glutamate-nitric oxide cGMP pathway in ammonium chloride induced neurotoxicity, Biomed. Pharmacother. 84 (2016) 1717–1726.
[9] S.F. Ahmad, S.M. Attia, S.A. Bakheet, K.M. Zoheir, M.A. Ansari, H.M. Korashy, et al., Naringin attenuates the development of carrageenan-induced acute lung inflammation through inhibition of NF-κb, STAT3 and pro-inflammatory mediators and enhancement of IκBα and anti-inflammatory cytokines, Inflammation 38 (2) (2015) 846–857.
[10] K. Gopinath, G. Sudhandiran, Naringin modulates oxidative stress and inflammation in 3-nitropropionic acid-induced neurodegeneration through the activation of nuclear factor-erythroid 2-related factor-2 signalling pathway, Neuroscience 227 (2012) 134–143.
[11] Y.L. Luo, C.C. Zhang, P.B. Li, Y.C. Nie, H. Wu, J.G. Shen, et al., Naringin attenuates enhanced cough, airway hyperresponsiveness and airway inflammation in a guinea pig model of chronic bronchitis induced by cigarette smoke, Int. Immunopharmacol. 13 (3) (2012) 301–307.
[12] X. Guihua, L. Shuyin, G. Jinliang, S. Wang, Naringin protects ovalbumin-induced airway inflammation in a mouse model of asthma, Inflammation 39 (2) (2016) 891–899.
[13] K. Itoh, M. Masuda, S. Naruto, K. Murata, H. Matsuda, Antiallergic activity of unripe Citrus hassaku fruits extract and its flavanone glycosides on chemical substance-induced dermatitis in mice, J. Nat. Med. 63 (4) (2009) 443–450.
[14] Tamer A. ElBayoumi, Vladimir P. Torchilin, Cap. 1 Current Trends in Liposomes Research in Liposomes Methods and Protocols, vol 1, Volkmar Weissig, 2010, pp. 1–27.
[15] S. Vahabi, A. Eatemadi, Nanoliposomes encapsulated anesthetics for local anesthesia application, Biomed. Phaemacother. 86 (2017) 1–7.
[16] N. Kianvash, A. Bahador, M. Pourhajibagher, H. Ghafari, V. Nikoui, S.M. Rezayat, et al., Evaluation of propylene glicol nanoliposomes containing curcumin on burn wound model in rat:biocompatibility, wound healing, and anti-bacterial effects, Drug Deliv. Transl.l Res. (2017).
[17] J. Rokka, A. Snellman, M. Kaasalainen, J. Salonen, C. Zona, B. La Ferla, et al., (18) F-labeling syntheses and preclinical evaluation of functionalized nanoliposomes for Alzheimer's disease, Eur. J. Pharm. Sci. 10 (88) (2016) 257–266.
[18] P. Ganesan, H.M. Ko, I.S. Kim, D.K. Choi, Recent trends in the development of nanophytobioactive compounds and delivery systems for their posible role in reducing oxidative stress in Parkinson's disease models, Int. J. Nanomed. 10 (2015) 6757–6772.
[19] M.M. Ochi, G. Amoabediny, S.M. Rezayat, A. Akbarzadeh, B. Ebrahimi, In vitro co-delivery of novel pegylated nanoliposomal herbal drugs of silibinin and glycyrrhizic acid (nano-phytosome) to hepatocellular carcinoma cells, Cell 18 (2) (2016) 135–148.
[20] H.J. Park, N. Liu, Factors effects on the loading efficiency of Vitamin C loaded chitosan-coated nanoliposomes, Colloids Surf. B: Biointerfaces 76 (1) (2010) 16–19.
[21] S. Yang, C. Liu, W. Liu, H. Yu, H. Zheng, W. Zhou, et al., Preparation and characterization of nanoliposomes entrapping medium-chain fatty acids and vitamin C by lyophilization, Int. J. Mol. Sci. 14 (10) (2013) 19763–19773.
[22] M.R. Mozafari, Cap. 2 Nanoliposomes: Preparation and Analysis in Liposomes Methods and Protocols, vol 1, Volkmar Weissig, 2010, pp. 29–50.
[23] P.G. Kakadia, B.R. Conway, Lipid nanoparticles for dermal drug delivery, Curr. Pharm. Des. 21 (20) (2015) 2823–2829.
[24] S. Mir-Palomo, A. Nácher, O. Díez-Sales, M.A. Ofelia Vila Busó, C. Caddeo, M.L. Manca, et al., Inhibition of skin inflammation by baicalin ultradeformable vesicles, Int. J. Pharm. 511 (1) (2016) 23–29.
[25] J. Vitonyte, M.L. Manca, C. Caddeo, D. Valenti, J.E. Peris, I. Usach, et al., Bifunctional viscous nanovesicles co-loaded with resveratrol and gallic acid for skin protection against microbial and oxidative injuries, Eur. J. Pharm. Biopharm. 114 (2017) 278–287.
[26] N. Kianvash, A. Bahador, M. Pourhajibagher, H. Ghafari, V. Nikoui, S.M. Rezayat, et al., Evaluation of propylene glycol nanoliposomes containing curcumin on burn wound model in rat: biocompatibility, wound healing, and anti-bacterial effects, Drug Deliv. Trans. Res. (2017) 1–10.
[27] J. Chen, W.L. Lu, W. Gu, S.S. Lu, Z.P. Chen, B.C. Cai, Skin permeation behavior of elastic liposomes: role of formulation ingredients, Expert Opin. Drug Deliv. 10 (6) (2013) 845–856.
[28] L.M. Cordenonsi, N.G. Bromberger, R.P. Raffin, E.E. Scherman, Simultaneous separation and sensitive detection of naringin and naringenin in nanoparticles by chromatographic method indicating stability and photodegradation kinetics, Biomed. Chromatogr. 30 (2) (2016) 155–162.
[29] G. Morikawa, C. Suzuka, A. Shoji, Y. Shibusawa, A. Yanagida, High-throughput determination of octanol/water partition coefficients using a shake-flask method and novel two-phase solvent system, J. Pharm. Biomed. Anal. 117 (2016) 338–344.
[30] W.M. Harris, P. Zhang, M. Plastini, T. Ortiz, N. Kappy, J. Benites, et al., Evaluation of function and recovery of adipose-derived stem cells after exposure to paclitaxel, Cytotherapy 19 (2) (2017) 211–221.
[31] R.P. Chilcott, J. Jenner, S.A.M. Hotchkiss, P. Rice, In vitro skin absorption and decontamination of sulphur mustard: comparison of human and pig-ear skin, J. Appl. Toxicol. 21 (4) (2001) 279–283.
[32] V. Merino, T. Micó-Albiñana, A. Nácher, O. Díez-Sales, M. Herráez, M. Merino-Sanjuán, Enhancement of nortriptyline penetration through human epidermis: influence of chemical enhancers and iontophoresis, J. Pharm. Pharmacol. 60 (4) (2008) 415–420.
[33] H. Sato, Y. Nakayama, C. Yamashita, H. Uno, Anti-inflammatory effects of tacalcitol (1, 24(R) (OH) 2D3, TV-02) in the skin of TPA-treated hairless mice, J. Dermatol. 31 (3) (2004) 200–217.
[34] X. Cao, W. Lin, C. Liang, D. Zhang, F. Yang, Y. Zhang, et al., Naringin rescued the TNF-α-induced inhibition of osteogenesis of bone marrow-derived mesenchymal stem cells by depressing the activation of NF-κB signaling pathway, Immunol. Res. 62 (3) (2015) 357–367.
[35] T. Han, D.B. Das, Permeability enhancement for transdermal delivery of large molecule using low-frequency sonophoresis combined with microneedles, J. Pharm. Sci. 102 (10) (2013) 3614–3622.
[36] Y. Gao, J. Ni, X. Yin, X. Shen, Study on transdermal absorption of piperine in Erxiekang plaster, J. Chin. Mater. Méd. 35 (24) (2010) 3294–3296.
[37] C. Caddeo, O.D. Sales, D. Valenti, A.R. Saurí, A.M. Fadda, M. Manconi, Inhibition of skin inflammation in mice by diclofenac in vesicular carriers: liposomes, ethosomes and PEVs, Int. J. Pharm. 443 (1) (2013) 128–136.

International Journal of Pharmaceutics 564 (2019) 299–307

Contents lists available at ScienceDirect

International Journal of Pharmaceutics

journal homepage: www.elsevier.com/locate/ijpharm

Mangiferin nanoemulsions in treatment of inflammatory disorders and skin regeneration

María Pleguezuelos-Villa[a], Amparo Nácher[a,b,*], M.J. Hernández[c], M.A. Ofelia Vila Buso[d], Amparo Ruiz Sauri[e], Octavio Díez-Sales[a,b]

[a] Department of Pharmacy, Pharmaceutical Technology and Parasitology, Faculty of Pharmacy, University of Valencia, Av. Vicent Andrés Estellés s/n, 46100 Burjassot, Valencia, Spain
[b] Instituto Interuniversitario de Investigación de Reconocimiento Molecular y Desarrollo Tecnológico (IDM), Universitat Politècnica de València, Universitat de València, Av. Vicent Andrés Estellés s/n, 46100 Burjassot, Valencia, Spain
[c] Department of Earth Physics and Thermodynamics, Faculty of Physics, University of Valencia, Av. Vicent Andrés Estellés s/n, 46100 Burjassot, Valencia, Spain
[d] Department of Physical Chemistry, Faculty of Pharmacy, University of Valencia, Av. Vicent Andrés Estellés s/n, 46100 Burjassot, Valencia, Spain
[e] Department of Pathology, University of Valencia, Av. Blasco Ibañez 17, 46010 Valencia, Spain

ARTICLE INFO

Keywords:
Nanoemulsions
Mangiferin
Transcutol-P
Hyaluronic acid
Skin regeneration

ABSTRACT

In this paper mangiferin nanoemulsions were developed using hyaluronic acid of different molecular weight, in absence or presence of Transcutol-P. An extensive study was carried out on the physico-chemical properties of nanoemulsions. Nanosizer and transmission electron microscopy showed oil droplets average size 296 nm with monodisperses distribution (PI ≤ 0.30). The zeta potential was highly negative (−30 mV). FTIR analysis confirms the existence of physical interactions among compounds. Rheological measurements allowed to conclude that all formulations present a pseudoplastic behavior (s ~ 0.4) in presence of the biopolymer. Moreover, mangiferin release depends on the molecular weight of the polymer. Permeability assays on pig epidermis showed that nanoemulsions with low molecular weight hyaluronic acid improve the permeation, being this effect more pronounced in nanoemulsions with Transcutol-P. Administration of mangiferin nanoemulsions on TPA-inflamed skin mice model provided an attenuation of oedema and leucocyte infiltration. Macroscopic appearance of mice skin lesions has a good correlation with the histological study. The topical application of these formulations shows an appropriate anti-inflammatory effect.

1. Introduction

The interest in natural pharmacologically active compounds has widely increased in the recent years (Riccardo et al., 2017; Agrawal et al., 2017; Shal et al., 2018). Experimental studies reported that herbs and/or their constituents have anti-inflammatory, anti-proliferative, anti-angiogenic, anti-cancerous properties, among others, together with anti-oxidative stress role and tissue repair action (Rady et al., 2018; Fujii et al., 2017; Khazdair et al., 2018). These activities may explain the apparent benefits of the topical multi-herbal formulations on skin disease treatments. Moreover, no serious adverse events have been associated with their use (Deng et al., 2017, Deng et al., 2014; Liu et al., 2016; Sheng et al., 2018; Zhao et al., 2017). Natural products as baicalin or naringin could represent a potential adjuvant treatment (Mir-Palomo et al., 2016; Pleguezuelos-Villa et al., 2018) as conventional therapies in topical disorders.

In this sense, other natural products as mangiferin (Imran et al., 2017; Zhao et al., 2017; Ochocka et al., 2017) used in several autoimmune inflammatory diseases, such as rheumatoid arthritis, dermatitis and psoriasis have been analyzed (Jeong et al., 2014; Garrido-Suárez et al., 2014). Mangiferin is a natural xanthone glycoside, isolated from various plants such as Gentianaceae, Zingiberaceae and Mangiferaceae (Morais et al., 2012). Due to its low hydrosolubility (0.111 mg/mL) (Acosta et al., 2016; Van der Merwe et al., 2012), the mangiferin has a poor bioavailability, which restricts its clinical application. Therefore, new formulation strategies should be developed to improve this topical efficacy.

Special attention has lately been focused on different nanosystems, such as nanoemulsions, solid lipid nanoparticles and nanovesicles, as potential vehicles for active agent delivery. These nanosystems enhance

* Corresponding author at: Department of Pharmacy, Pharmaceutical Technology and Parasitology, Faculty of Pharmacy, University of Valencia, Av. Vicent Andrés Estellés s/n, 46100 Burjassot, Valencia, Spain.
E-mail address: amparo.nacher@uv.es (A. Nácher).

https://doi.org/10.1016/j.ijpharm.2019.04.056
Received 12 November 2018; Received in revised form 15 April 2019; Accepted 18 April 2019
Available online 20 April 2019
0378-5173/

skin permeation, pharmacological activity and stability of different active substances (Roberts et al., 2017; Dong et al., 2017).

Nanoemulsions are metastable colloidal systems consisting on droplets of one liquid dispersed within another immiscible liquid (Rosen and Kunjappu 2012). They represent versatile carriers for local delivery of hydrophilic, lipophilic and amphiphilic molecules. In fact, these systems have arisen as a novel carrier system for improving the bioavailability of poorly absorbed herbs actives/extracts (Yoo et al., 2010; Wais et al., 2017).

Several studies have concluded that incorporation of surfactants, as phospholipids or polysorbate, enhances nanoemulsions stability, and improves drug release and skin permeation (El-Leithy et al., 2018; Sedaghat Doost et al., 2018; Zhang et al., 2014). These surfactants are biocompatible with the skin and have non-toxic properties (Manconi et al., 2011). In addition, the incorporation of cosurfactants, such as Transcutol-P, which may improve the retention/permeation of compounds into and through the skin has been also investigated.

Hyaluronic acid (HA) is a biopolymer that promotes the stabilization of the formulation and plays a role for the controlled release drug delivery (Gao et al., 2014; Rodríguez-Belenguer et al., 2015). It exhibits biomedical implications in tissue regeneration (Badawi et al., 2013), specific tumor-targeting affinity for CD 44 cancer cells (Kim and Park 2017) and anti-inflammatory diseases (Chen et al., 2018; Xiao et al., 2017). To extend the residence time of a topical formulation and improve mangiferin bioavailability, hyaluronate muco-adhesive nanoemulsions could be formulated.

The aim of this paper was to develop mangiferin nanoemulsion hyaluronate gels for inflammatory disorders in absence or presence of transcutol-P. Nanoemulsions were elaborated and characterized by analyzing their droplet size, polydispersity index (PDI), zeta potential and performing electronic microscopy, FTIR and rheological measurements. Ex vivo permeation assays and release studies were also carried out. The efficacy of the formulations was evaluated by means of an in vivo mice model of acute inflammation.

2. Material and methods

2.1. Materials

Lipoid® S75 a mixture of soybean lecithin containing lysophosphatidylcholine (3% maximum), phosphatidylcholine (70%), phosphatidylethanolamine (10%), fatty acids (0.5% maximum), triglycerides (3% maximum), and tocopherol (0.1–0.2%) were a gift from Lipoid GmbH (Ludwigshafen, Germany). Polysorbate 80 and tocopherol were purchased from Scharlab S.L. (Barcelona, Spain). HA of different molecular weights: low (40.000–50.000 Da), high (1.000.000–1.200.000 Da) were purchased from Carbosynth Limited (UK) and biophil Iberia S.L. (Barcelona, Spain), respectively. Mangiferin was purchased to Carbosynth Limited (UK). Glycerin were purchased from Guinama S.L.U. (Valencia, Spain), N-octanol (special grade for measurement of partition coefficients) was purchased from VWR chemicals S.A. (France). Diethylene glycol monoethyl ether (Transcutol-P) was obtained from Alfa Aesar (Kandel, Germany). Almond oil and dexamethasone (DXM) were from Acofarma S.A. (Barcelona, Spain). Phorbol 1, 2-myristate 1, 3-acetate was purchased from Sigma-Aldrich.

2.2. Content and physico-chemical mangiferin properties

Mangiferin content was analyzed by a high-performance liquid chromatography (HPLC) Perkin Elmer® Series 200 equipped with a photodiode array UV detector. Samples were injected in a C18 reverse-phase column (Teknokroma®Brisa “LC2” 5.0 µm, 150 mm × 4.6 mm). The isocratic mobile phase was a mixture of hydrochloric acid (pH 4.0) and methanol (60:40, v/v) and the flow rate 1.2 mL/min (Bartoszewski et al., 2014). The detection wavelength was set at 254 nm. Standard calibration curves covering the whole mangiferin range concentrations in experimental samples were obtained. The limit of detection (LOD) and quantification (LOQ) were estimated using the calibration curve procedure. Three calibration curves were prepared (0.7 mg/mL-0.005 mg/mL) to determine the sensitivity of the method.

The limit of quantification may be expressed as follows:

$$LOD = \frac{3.3 * SD}{S} \quad (1)$$

The detection limit may be expressed as follows:

$$LOQ = \frac{10 * SD}{S} \quad (2)$$

The LOD and LOQ were determined based on the standard deviation (SD) of the y-intercept and the slope of the linear calibration curve (S).

Solubility determinations of mangiferin, mangiferin-phospholipid (1:10) and mangiferin-phospholipids-polysorbate 80 (1:10:5) were carried out by adding an excess of the different mixtures in water (2 mL). Samples were maintained under constant stirring for 24 h at 25 °C, then an aliquot of each dispersion was filtered through 0.22 µm membranes and injected into HPLC system to measure the mangiferin content.

In addition, an octanol-water partition coefficient values were obtained by equilibrating mangiferin, mangiferin-phospholipid or mangiferin-phospholipid-polysorbate 80 in aqueous solution with 1-octanol for 24 h at 25 °C in a shaker bath (Morikawa et al., 2016). Distribution of mangiferin between the aqueous and the organic phase was determined by HPLC method. Each sample was carried out in triplicate (n = 3).

2.3. Mangiferin nanoemulsion gel formulation

A preformulation design was carried out in order to select the final nanoemulsion gel composition. Different amounts of HA (between 0.25% and 1%), polysorbate 80 (1 and 5%), almond oil (5 and 10%) and phospholipid (5 and 10%) were formulated. According to the stability data (average particle size < 500 nm, polydispersity index < 0.5 and zeta potential value < -30 mV), the best nanoemulsion gel composition was selected. Moreover, HA of different molecular weight (low and high) in presence or absence of Transcutol-P were also evaluated.

In this study, mangiferin (1%) and glycerin (3%) were added to distilled water in a glass tube in absence or presence of HA (1%) to obtain aqueous phases. Lipoid ® S75 (5%), polysorbate 80 (1%), tocopherol (0.1%) and almond oil (10%) were also mixed inside a glass tube with or without Transcutol-P (4%) to obtain the oil phases. Both receptacles were placed in a thermostat bath at 55 ± 0.5 °C. Then, aqueous phase was poured over to oil phase and subsequently homogenized with an Ultraturrax (DI25-basic, IKA-Germany) at 10.000 rpm for 5 min. After this, nanoemulsions were sonicated (3 cycles of 10 min) with an ultrasonic disintegrator (CY-500, Optic Ivymen system, Barcelona, Spain) equipped with a continuous Flow Vessel. This vessel was surrounded by a cooling jacket with a suitable cooling liquid. This method allows the preparation of a stable nanoemulsion O/W with variable consistence according to HA the molecular weight of used.

Several formulations to evaluate the in vivo efficacy of mangiferin in a mice model were tested: NE 0 (control without HA), NE I (HA, high molecular weight), NE II (HA, high molecular weight with Transcutol-P), NE III (HA, low molecular weight) and NE IV (HA, low molecular weight with Transcutol-P). In order to know the vehicle influence, empty nanoemulsions (empty NE I, empty NE II, empty NE III and empty NE IV) were also prepared.

2.4. Characterization of formulations

Shape and surface morphology of nanoemulsions were examined using a JEM-1010 microscope (Jeol Europe, Croissy-sur-Seine, France),

Table 1
Average size, polydispersity index (PI) and zeta potential of nanoemulsions during 30 days of storage at 4 °C (Mean Value ± SD; n = 4).

Sample	Size (nm) 0 days 30 days	PI 0 days 30 days	Potential Z (mV) 0 days 30 days
NE 0 without polymer	319.4 ± 5.7 289.4 ± 5.7	0.26 0.24	−40.4 ± 1.3–39.1 ± 1.3
HA High molecular weight			
NE I	393.0 ± 4.1 372.3 ± 6.3	0.30 0.30	−37.2 ± 1.6–35.4 ± 1.3
NE II	397.9 ± 6.1 320.5 ± 2.7	0.25 0.25	−32.7 ± 0.4–33.5 ± 0.3
HA Low molecular weight			
NE III	221.5 ± 7.0 194.5 ± 3.4	0.19 0.21	−38.2 ± 0.1–38.2 ± 0.2
NE IV	323.2 ± 8.0 281.5 ± 7.2	0.23 0.20	−40.2 ± 2.0–38.3 ± 0.4

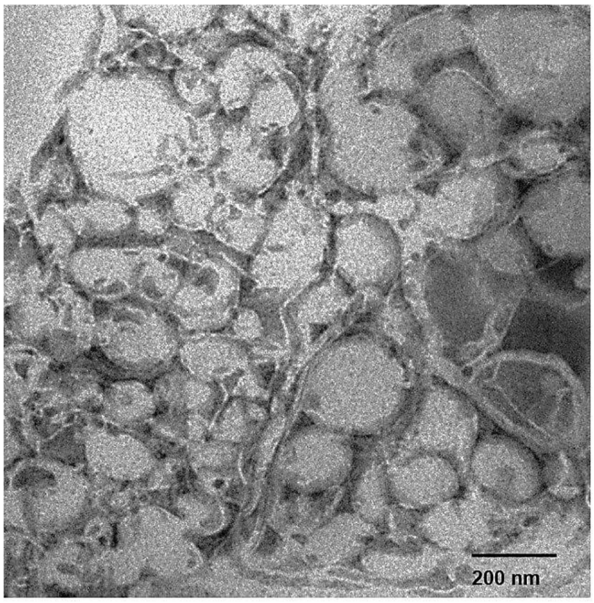

Fig. 1. TEM graphs of nanoemulsions.

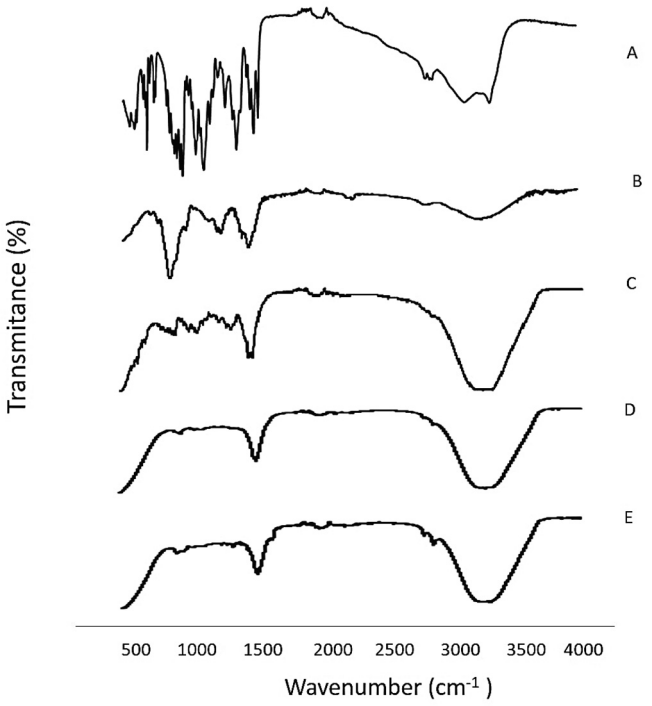

Fig. 2. FT-IR spectra of A) Mangiferin B) Mangiferin and hyaluronic acid (HA) C) Mangiferin and lipoid S®75 D) Mangiferin, lipoid S®75 and polysorbate 80 E) Nanoemulsion loaded with Mangiferin.

equipped with a digital camera MegaView III. A drop of the samples was spread on the coated copper grids and stained with phosphotungstic acid (2%, w/w) before observation. The TEM graphs were taken at an accelerating voltage of 80 KV.

Measurement of average diameter and polydispersity index (PI) of nanoemulsions were carried out by Photon Correlation Spectroscopy at 25 °C. The zeta potential was estimated by electrophoretic light scattering in a thermostatic cell. All determinations were performed using a Zetasizer Nano-S ® (Malvern Instruments, Worcester-shire, United Kingdom).

Nanoemulsions stabilities were assessed by monitoring the droplets average size of the internal phase and zeta potential over 30 days at 4 °C.

In order to evaluate nanoemulsion-flavonoid interactions Fourier transform infrared studies (FTIR) were taken using ATR Agilent Cary 630 (Germany) at room temperature in a spectral region between 500 and 4000 cm^{-1}.

2.5. Rheological measurements

A controlled stress rheometer (RheoStress 1, Thermo Haake, Germany) equipped with control and data logging software (RheoWin 4.0.1) and a Haake K10 thermostatic bath for temperature control was used. After loading, samples were allowed to rest for at least 300 s for stress relaxation and temperature equilibrium. Cone-plate sensor (2°, 35 mm and 60 mm diameters) were used. Two types of rheological measurements were performed: flow curves and small amplitude oscillation sweeps tests. All measurements were performed in triplicate, at 25 °C.

Step flow curves were performed in controlled stress mode (30 s each step in logarithmic distribution), so shear stress range was chosen in order to obtain viscosities corresponding to very low shear rates until approx. 100 s^{-1}. The viscosities results can be fitted to the simplified Carreau model.

$$\eta = \frac{\eta_0}{\left(1 + \left(\frac{\dot{\gamma}}{\dot{\gamma}_c}\right)^2\right)^s} \quad (3)$$

where η_0 is the zero-shear viscosity, $\dot{\gamma}_c$ is critical shear rate, and s the shear thinning index. Oscillatory measurements at a constant stress in the linear viscoelastic region (LVR) were performed, varying the frequency from 0.01 to 10 Hz (9 points per decade). In order to establish LVR, stress sweeps at a frequency of 1 Hz were performed for all systems.

2.6. Flavonoid release studies

The release of mangiferin from nanoemulsions was determined with Franz diffusion cells. An artificial membrane (0.45 μm cellulose acetate membrane, Teknocroma, Barcelona, Spain) was placed between the

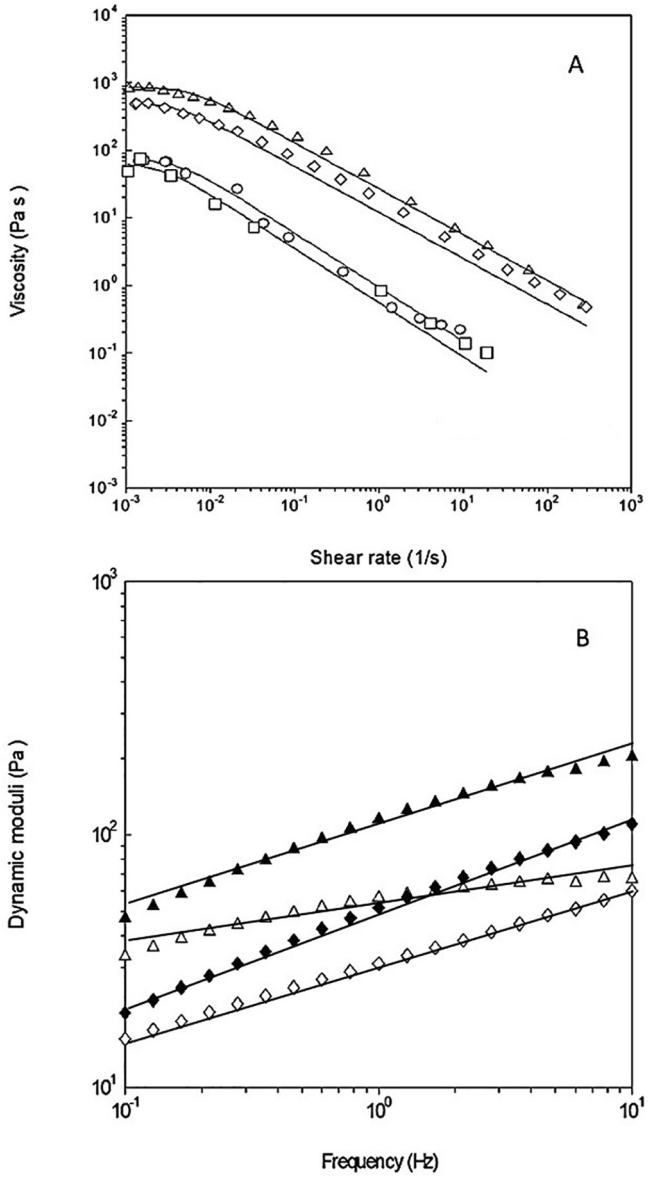

Fig. 3. Rheological measurements. A) Flow curves fitted to Carreau model for nanoemulsions: NE I (△), NE II (◊), NE III (○) and NE IV (□) B) Viscoelasticmoduli as a function of oscillation frequency for nanoemulsions: NE I (△), NE II (◊). Closed symbols: elastic modulus, G′; open symbols: viscous modulus, G″.

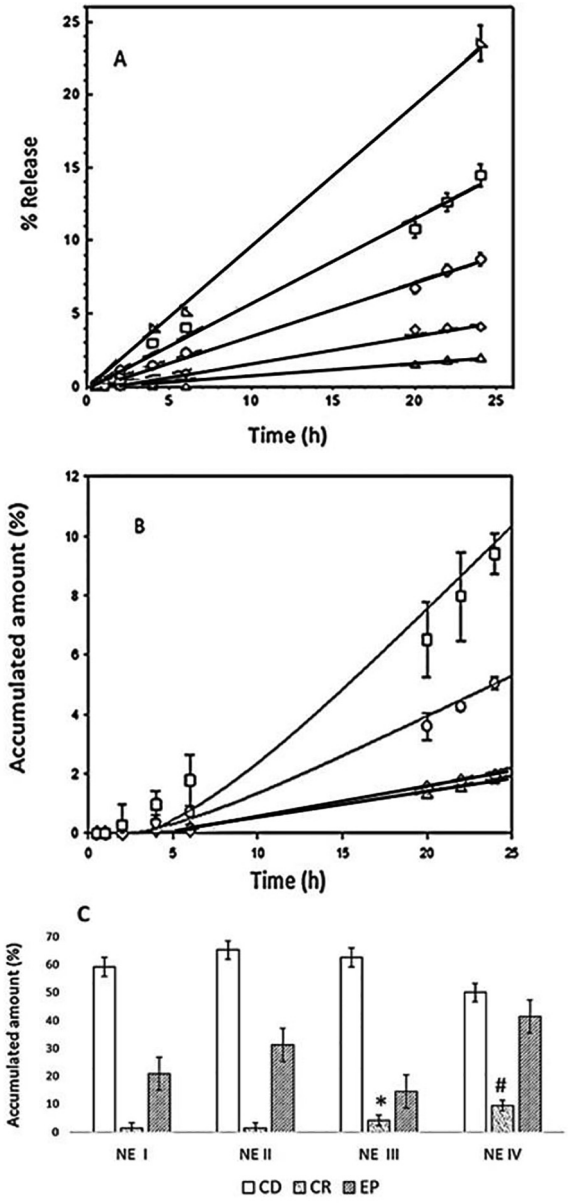

Fig. 4. A) Graphical representation of percentage of mangiferin released in function of time for the differents nanoemulsions: NE 0 (◺) NE I (△), NE II (◊), NE III (○) and NE IV (□). B) Profiles of cumulative amount of mangiferin accumulated in receptor compartment after 24 h treatment with nanoemulsions (NE I-NE IV). C) Cumulative amount of mangiferin accumulated in receptor compartment (CR), epidermis (EP) and donor compartment (CD) after 24 h of treatment with nanoemulsions (NE I-NE IV). Bars represent the mean ± standard deviation of at least four independent experimental determinations. $^{*}p < 0.05$ values statistically different compared permeation of NE III vs NE I. $^{\#}p < 0.05$ values statistically different compared permeation of NE II vs NE IV.

donor and receptor compartments of the Franz cells (effective diffusion area of 0.784 cm^2). The Franz cells were immersed in a bath system at 37.0 ± 0.5 °C and kept under agitation. The receptor compartment (6 mL) was filled with an aqueous solution of polysorbate 80 (1%) to maintain sink conditions. A weighted amount of each nanoemulsion (500 mg) was loaded onto the surface of the membrane. At regular intervals, up to 24 h, the receptor solution was removed (200 µL), replaced with the same volume of a fresh aqueous solution and analysed by HPLC to determine the content of mangiferin.

In order to describe the flavonoid release mechanism, the mean percentages of cumulative amounts of mangiferin were fitted according to Power law model (Table 2).

2.7. In vitro permeation assays

The experiments were performed using Franz diffusion cells according to the procedure described previously in epigraph 2.6. In this case, cellulose-acetate membrane was replaced by new born pig epidermal skin from a local slaughterhouse. The epidermis was mounted between the donor and receptor compartments of the Franz cells with the stratum corneum side facing upward the donor compartment. Epidermal membranes were obtained from heat separation through immersing in water (at 60 °C) for 75 s (Chilcott et al., 2001).

The cumulative amounts of mangiferin (Q) permeated through the epidermis were fitted to the equation derived of the Fick's Second Law to the diffusion process (Eq. (4)):

Table 2
Results of release mangiferin fitting different models at 24 h (Mean Value ± SD; n = 4).

Nanoemulsions Models	Without polymer	HA High molecular weight		HA Low molecular weight	
	NE 0	NE I	NE II	NE III	NE IV
Power law $M_t = K \cdot t$					
K (h^{-1})	0.69 ± 0.12	0.010 ± 0.006	0.08 ± 0.04	0.36 ± 0.07	0.57 ± 0.16
n	1.09 ± 0.05	1.58 ± 0.13	1.26 ± 0.18	0.99 ± 0.06	1.01 ± 0.07
R >	0.997	0.998	0.992	0.997	0.990

M_t is the fraction of flavonoid release at each time t; K is a constant reflecting structural and geometric characteristic of the device; n is the release exponent characterizing the diffusion mechanism.

Table 3
Results of in vitro permeation studies on nanoemulsions (Mean Value ± SD; n = 4).

Nanoemulsions	Q_{24} (μg, cm^2)	P	D *10^2 (cm/h)	Lag time (h)	Flux (μg/cm^2/h)	R_{24} (μg/cm^2)	R_{24}/Q_{24}
HA High molecular weight							
NE I	1.81 ± 0.01	4.79 ± 1.10	2.1 ± 0.4	8 ± 1	0.10 ± 0.01	2.03 ± 0.08	1.12
NE II	1.93 ± 0.01	7.33 ± 2.14	1.9 ± 0.3	9 ± 2	0.13 ± 0.01	2.02 ± 0.04	1.04
HA Low molecular weight							
NE III	5.04 ± 0.01	9.09 ± 2.65	2.9 ± 0.7	6 ± 1	0.26 ± 0.02	10.52 ± 0.02	2.08
NE IV	9.41 ± 0.01	23.19 ± 10.60	2.4 ± 0.8	7 ± 2	0.55 ± 0.09	28.94 ± 0.07	3.07

Q_{24} is the amount of mangiferin through the skin and reaches the receptor solution; P is the partition coefficient of mangiferin between the skin and the donor solution; D is the diffusion coefficient of mangiferin in the skin; R_{24} is the concentration of mangiferin retained in epidermis.

$$Q_{(t)} = A \cdot P \cdot L \cdot C \left[D \cdot \frac{t}{L^2} - \frac{1}{6} - \frac{2}{x^2} \cdot \sum_{n=1}^{\infty} \cdot \mathrm{Exp}\left(\frac{-D \cdot n^2 \cdot x^2 \cdot t}{L^2} \right) \right] \quad (4)$$

where Q (t) is the amount of mangiferin through the skin and reaches the receptor solution at a given time t; A is the diffusion surface area (0.784 cm^2); P is the partition coefficient of mangiferin between the skin and the donor solution; L is the diffusion pathway; D is the diffusion coefficient of mangiferin in the skin; and C is the concentration of mangiferin in the donor vehicle. By fitting the equation (4), lag time (t_L = 1/6D, h), permeability coefficient (K_p = P·D, cm/h) and flux ($J = k_p \cdot C$, μg/cm^2/h) were calculated.

At the end of the permeation experiments, the epidermis integrity was verified. Briefly, 1 mL of phenol red solution (0.5 mg/mL) was applied onto the skin surface in the donor compartment. When the phenol red amount in receptor compartment was < 1%, the epidermis was considered intact. The concentration of mangiferin retained in the epidermis (R_{24}) was also quantified. The epidermis sheet was removed from the Franz diffusion cell and extracted with 10 mL of methanol. Subsequently, it was maintained for 24 h at 2–8 °C. The suspension was homogenized with an Ultratturrax and sonicated for 30 min. Finally, the supernatant was filtered through a 0.45 μm filter and analysed by HPLC. To evaluate the affinity of mangiferin for the epidermal layers and the influence of the formulation R_{24}/Q_{24} ratios were calculated.

2.8. Acute inflammation assays

For the inflammation study, female CD-1 mice (5–6 weeks old, 25–35 g) were supplied by Harlan laboratories (Barcelona, Spain). Mice were acclimated for one week before use. All studies were performed in accordance with European Union regulations for the handling and use of laboratory animals. The protocols were approved by the Institutional Animal Care and Use Committee of the University of Valencia (code 2016/VSC/PEA/00112 type 2). Briefly, dorsal skin of mice (n = 4 per group) was shaved and 24 h later the topical formulations were applied. The first day, TPA dissolved in acetone (3 μg/20 μL) was topically administered to the shaved dorsal area (1 cm^2) to induce cutaneous inflammation and ulceration. After 3 h, 200 μL of five formulations selected were topically applied in the same areas. This procedure was repeated for two consecutive days. Mice were sacrificed on day fourth by cervical dislocation and biopsies from the treated dorsal skin were excised and weighed to evaluated oedema and histological study, previously stored at −80 °C.

For histological assays, tissue samples were stored in formaldehyde (0.4%, V/V). Longitudinal sections (5 mm) on a rotary microtome were mounted on slides and marked with hematoxylin and eosin according to standard protocols. The tissues were analyzed and observed using a light microscope (DMD 108 Digital Micro-Imaging Device, Leica, Wetzlar, Germany).

Myeloperoxidase (MPO) activity was determined using a minor modification of the method of Grisham et al. (1990). The tissue was thawed and homogenized in 750 μL of phosphate buffer (pH 5.4) with an Ultra-Turrax T25 homogenizer (IKA1 Werke GmbH & Co. KG, Staufen, Germany). The homogenate was centrifuged at 10.000 g for 15 min at 4 °C. The supernatant obtained was diluted with PBS 5.4 (1:10). A sample of supernatant (10 μL) was added to a 96-well plate and incubated at 37 °C for 5 min with a mixture of 20 μL of sodium phosphate buffer (pH 5.4), 200 μL of phosphate buffer (pH 7.4), 40 μL of 0.052% hydrogen peroxide and 20 μL of 18 mM 3,30,5,50-tetramethylbenzidine dihydrochloride. The reaction is finalized by 50 μL of SO_4H_2 2 N. The absorbance was determined at 450 nm. The MPO activity was calculated from the linear portion of a standard curve. The oedema was expressed as the percentage of inhibition versus the positive control (TPA) value and MPO was expressed as percentage of activity.

2.9. Statistical analysis

Statistical differences were determined by one-way ANOVA test and Tukey's test for multiple comparisons with a significance level of $p < 0.05$. All statistical analyses were performed using IBM SPSS statistics 22 for Windows (Valencia, Spain). Data are shown as mean ± standard deviation.

3. Results and discussion

In the present study, the effect of biopolymer (HA) on the properties

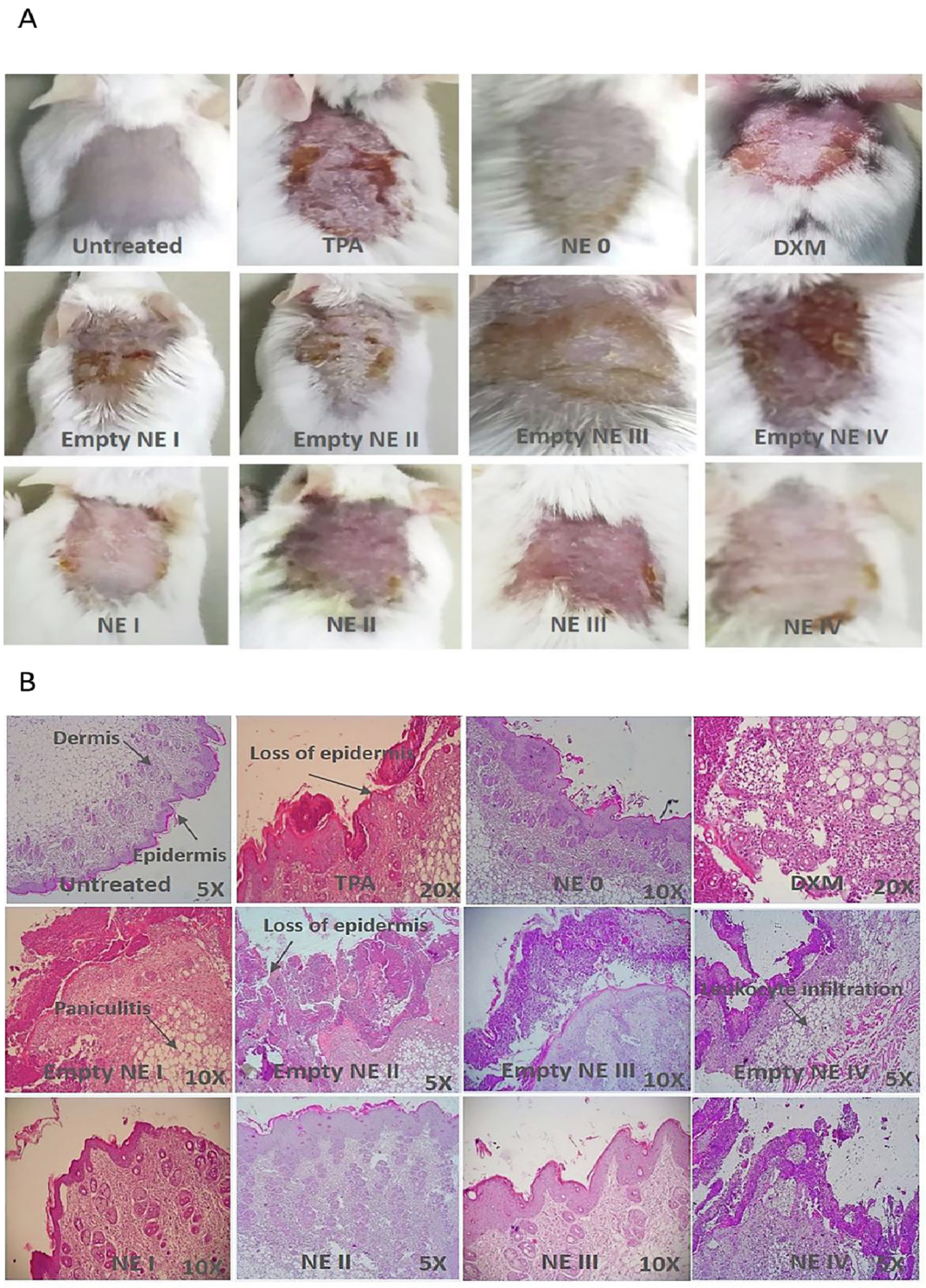

Fig. 5. A) Macroscopic appearance of skin lesions of mice treated with dexametasone (DXM), nanoemulsions (NE 0, NE I, NE II, NE III and NE IV) in comparison with untreated skin and empty nanoemulsions. B) Histological appearance of mice skin treated with dexametasone (DXM), nanoemulsions (NE 0, NE I, NE II, NE III and NE IV) in comparison with untreated skin and empty nanoemulsions.

of nanoemulsions was evaluated, in order to optimize the formulation for the transdermal mangiferin administration.

3.1. Content and physico-chemical mangiferin properties

Excellent plots correlating the peak areas and mangiferin concentrations were obtained. Calibration graphs presented a correlation coefficient value $r > 0.999$, demonstrating good linearity. The limits of detection and quantification were 0.21 μg/mL and 0.54 μg/mL, respectively.

Mangiferin solubility values from different mixtures were determined. The mangiferin-phospholipid-polysorbate 80 solubility (0.71 ± 0.03 mg/mL) was higher than mangiferin and mangiferin-phospholipid solubilities: 0.10 ± 0.01 mg/mL and 0.25 ± 0.02 mg/mL, respectively.

Octanol-water partition coefficient value was obtained in different

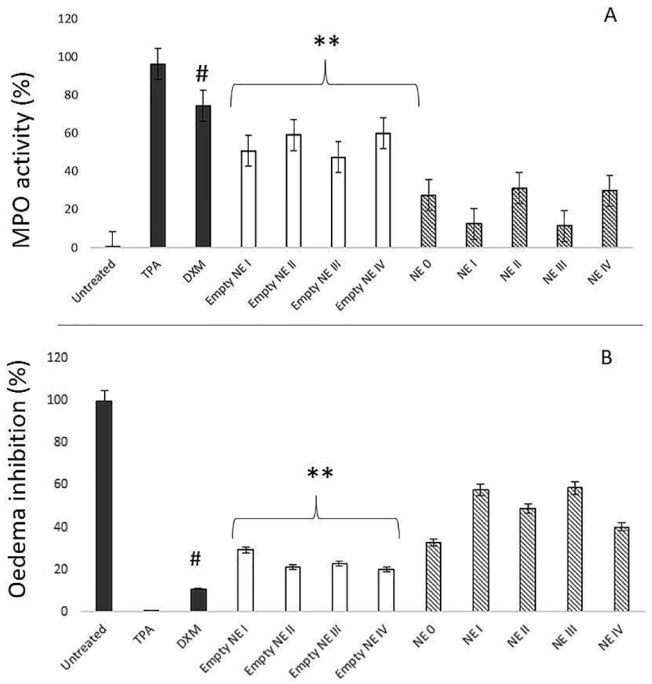

Fig. 6. A) Myeloperoxidase activity (%) (MPO) and B) oedema inhibition (%) values, obtained after TPA treatment and application of nanoemulsions (NE 0 – NE IV), dexametasone (DXM) and empty nanoemulsions (n = 4). Mean values ± standard deviation were reported. $^{**}p < 0.01$ values statistically different from those of skin treated with empty nanoemulsions. $^{\#}p < 0.05$ values statistically different compared DXM with mangiferin nanoemulsions.

mixtures. Mangiferin-phospholipid-polysorbate 80 partition coefficient (5.23 ± 0.17) was also higher than mangiferin and mangiferin-phospholipid partition coefficients: 0.12 ± 0.01 and 2.10 ± 0.12, respectively.

3.2. Characterization of formulations

Nanoemulsions present oil droplets size range from 194.5 to 397.9 nm (Table 1). These results are in accordance with Callender Shannon et al. (2017). All nanoemulsions showed monodisperses distribution (PI ≤ 0.30) and spherical shape (Fig. 1). The zeta potential was always highly negative (< −30 mV). The physical stability of nanoemulsions (NE 0 to NE IV) was monitored over 30 days of storage at 4 °C. As can be seen in Table 1 nanoemulsions were stable. The average size and zeta potential of the oil core depend on HA molecular weight. Short-chain HA nanoemulsions have smaller particle sizes and zeta potentials more negative, being similar to the nanoemulsion without polymer.

FTIR analyses provided information about the interactions of the different components of nanoemulsions (Ferreira et al., 2013). Fourier transform infrared (FTIR) studies are indicated in Fig. 2. In these spectra, profiles the mangiferin (A), mangiferin and HA (B), mangiferin and lipoid ®S 75 (C), mangiferin with lipoid S ®75 and polysorbate 80 (D) and nanoemulsion loaded with mangiferin (E) were shown. The FT-IR spectrum of mangiferin showed absorption bands at 3373 cm^{-1} (hydroxyl group) and 2933 cm^{-1} (C–H asymmetric stretching). Bands at 1255 cm^{-1} (–C–O–) and 1093 cm^{-1} (–C–O–C). An aromatic conjugated carbonyl group can be observed at 1651 cm^{-1} together with signals of aromatic nucleus. By comparison of the spectra, the major changes observed occurred in the region from 1800 to 500 cm^{-1}. Some IR bands of mangiferin had disappeared completely or had their intensities altered. In nanoemulsion, bands at 1651, 1622 cm^{-1} were observed, confirming the presence of mangiferin. In addition, at 3373 cm^{-1} the band intensifies verifying the integration of the hydroxyl groups of mangiferin in the system. Mangiferin interactions with HA of different molecular weight showed satisfactory physicochemical properties related with the formulation stability.

3.3. Rheological measurements

The low viscosity of the NE 0 nanoemulsion (data not shown) is not the most suitable for topical administration. For this reason, new formulations were developed in presence of HA different molecular weight (high and low). A rheological test was performed in order to understand the nanoemulsions gel properties. The experimental data fits to the simplified Carreau model showed that nanoemulsions with HA high molecular weight had a higher viscosity (NE I, 863.5 ± 16.8 Pa s and NE II, 508.5 ± 11.2 Pa s) than the HA low molecular weight nanoemulsions (NE III, 68.8 ± 2.9 Pa s and NE IV, 64.8 ± 8.9 Pa s). Flow curves obtained for nanoemulsions NE I, NE II, NE III and NE IV are presented in Fig. 3A. Also, all nanoemulsions had a pseudoplastic behavior (s ~ 0.40). The presence of Transcutol-P did not modify the pseudoplastic behavior.

To investigate the nanoemulsions gel structure, oscillatory measurements at a constant stress, in the linear viscoelastic region (LVR), were performed. Nanoemulsions with HA low molecular weight (NE III and NE IV) were out of the LVR, for this reason it was not possible to measure dynamic curves. Fig. 3B shows results obtained on dynamic tests. As can be seen, NE I and NE II, in the presence and absence of Transcutol-P, exhibited an elastic behavior (G > G) and low frequency dependence, which promoted the formation of controlled release systems (Díez-Sales et al., 2005). This behavior was confirmed with loss tangent (tan δ, 1 Hz) values, 0.59 and 0.49 for NE I and NE II, respectively.

3.4. Flavonoid release studies

The amount of mangiferin released at 24 h was greater than 20% in nanoemulsions without polymer (NE 0). The mangiferin release can be significantly modified depending on the molecular weight of the biopolymer (Agubata et al., 2014; Morsi et al., 2017). In fact, the presence of HA reduces the percentage released (Fig. 4A), being more evident in high molecular weight nanoemulsions (NE I, NE II). Nanoemulsions with Transcutol-P (NE II and NE IV) showed a slight ability to enhance mangiferin release in comparison with the other nanoemulsions.

Mangiferin release data were analyzed according to power law equation (epigraphs 2.6). The fitting results are summarized in Table 2. In accordance with the power model, the release mechanism is zero order (n ~ 1) (Siepmann and Peppas, 2001). These results could be attributed to polymer obstructive mechanism, which depends on the molecular weight of the polymer.

In accordance with the following equation, (Barry, 1983).

$$Kp = \frac{Ko}{1 + 2\varnothing/3} \quad (5)$$

where K_0 and Kp are the diffusion constants of the mangiferin in water in absence and presence of polymer, respectively. ∅ is the proportion of water immobilized by the polymer.

The water retention values (∅) have been determined (Eq. (5)): $\varnothing_{NE\ I} = 17.3$ and $\varnothing_{NE\ III} = 2.5$. In fact, the greater amount of water retained by the polymer, the less amount of mangiferin released.

3.5. In vitro permeation assays

The results of in vitro permeation studies are showed in Table 3. As can be observed, the molecular weight of HA affects a percutaneous absorption. For the lag time, no significant differences were shown between formulations ($p > 0.05$). Nanoemulsions with HA of high molecular weight presented a lower penetration at 24 h (Q_{24}). In the case NE I (1.81 ± 0.01 μg/cm^2) and NE II (1.93 ± 0.01 μg/cm^2) the

presence of Transcutol-P does not significantly enhance ($p > 0.05$) the skin permeation. The highest penetration occurs in low molecular weight HA nanoemulsions. NE III increase 2.5-fold the mangiferin amount in the receptor compartment ($Q_{24} = 5.04 \pm 0.01\ \mu g/cm^2$), and the incorporation of Transcutol-P (NE IV) increase 5-fold the amount permeated ($Q_{24} = 9.41 \pm 0.01\ \mu g/cm^2$). As expected, the last nanoemulsion has the highest flux value ($J = 0.55 \pm 0.09\ \mu g/cm^2/h$). These results were confirmed by R_{24} / Q_{24} ratio.

Fig. 4B showed the profiles of cumulative amount of mangiferin and Fig. 4C the cumulative amount of mangiferin (%) in donor compartment (CD), epidermis (EP) and receptor compartment (CR). As can be seen in this figure, nanoemulsions with Transcutol-P showed the highest accumulation in the epidermis (NE II, 35% and NE IV, 45%). Probably, the oil core could penetrate into the epidermis, due to a synergistic mechanism between surfactants and the intercellular lipids of pig skin (Manconi et al., 2011; Blume et al., 1993).

3.6. Acute inflammation assays

Topical application of TPA was used in skin to induce oxidative stress, oedema and infiltration of inflammatory cells and inflammation. By repeating TPA application scaly, peeling and crusted mice skin with desquamation was observed (Fig. 5A).

All animals treated with mangiferin formulations presented a significant amelioration of the skin. The ability of mangiferin nanoemulsion to wound healing in comparison with empty nanoemulsions was evidenced (Fig. 5A). Histological study showed that mice skin treated with TPA displayed severe dermal and subcutaneous alteration, with a large number of leukocytes infiltrating, and showing pathological features of inflammatory damage, such as vascular congestion. Untreated skin with TPA showed a regular structure and normal appearance of epidermis. As can be observed in Fig. 5B, nanoemulsions with mangiferin reduced TPA-induced lesions. Nanoemulsions loaded with mangiferin (NE I, NE II, NE III, NE IV) induced both strong inhibition of oedema and reduction of MPO activity. Statistic differences ($p < 0.01$) have been found with respect to empty nanoemulsions and TPA treatment results (Fig. 6A). Nanoemulsions with mangiferin showed a significant decrease in oedema inhibition: ~20-fold higher than empty nanoemulsions (Fig. 6B). MPO levels dramatically increased with repeated TPA and DXM exposure, it was ~80-fold higher than those found in untreated skin. Therefore, the results obtained in vivo seem to indicate a remarkable therapeutic potential of mangiferin nanoemulsions.

4. Conclusion

This investigation reveals that the design and development of nanoemulsions could be a promising device to restore inflammatory skin disorders. The topical application of these formulations shows an appropriate anti-inflammatory effect.

Funding

This research did not receive any specific grant from funding agencies in the public, commercial, or not-for-profit sectors.

Disclosure of conflicts of interest

None.

References

Jhoany, Acosta, Sevilla, Iliana, Salomón, Suslebys, Nuevas, Lauro, Romero, Aylema, Amaro, Daniel, 2016. Determination of mangiferin solubility in solvents used in the biopharmaceutical industry. J. Pharmacy Pharmacognosy Res. 4 (2), 49–53.

Shivankar, Agrawal, Acharya, Debabrata, Adholeya, Alok, Barrow, Colin J., Deshmukh, Sunil K., 2017. Nonribosomal peptides from marine microbes and their antimicrobial and anticancer potential. Front. Pharmacol. 8, 828.

Agubata, Chukwuma O., Nzekwe, Ifeanyi T., Obitte, Nicholas C., Ugwu, Calister E., Onunkwo, Godswill C., 2014. Effect of oil, surfactant and co-surfactant concentrations on the phase behavior, physicochemical properties and drug release from self-emulsifying drug delivery systems. J. Drug Discov. Development 1, 1–7.

Badawi, Alia A., El-Laithy, Hanan M., Nesseem, Demiana I., El-Husseney, Shereen S., 2013. Pharmaceutical and medical aspects of hyaluronic acid-ketorolac combination therapy in osteoarthritis treatment: radiographic imaging and bone mineral density. J. Drug Target. 21 (6), 551–563.

Rafal, Bartoszewski, Hering, Anna, Marszałł, Marcin, Hajduk, Justyna Stefanowicz, Bartoszewska, Sylwia, Kapoor, Niren, Kochan, Kinga, Ochocka, Renata, 2014. Mangiferin has an additive effect on the apoptotic properties of hesperidin in cyclopia sp. tea extracts. PloS One 9 (3).

Alfred, Blume, Jansen, Michael, Ghyczy, Miklos, Gareiss, J., 1993. Interaction of phospholipid liposomes with lipid model mixtures for stratum corneum lipid. Int. J. Pharmaceutics 99 (2), 219–228.

Barry, Brian W., 1983. Dermatological Formulations: Percutaneous Absorption. Marcel Dekker, New York.

Callender Shannon, P., Mathews, Jessica A., Kobernyk, Katherine, Wettig, Shawn D., 2017. Microemulsion utility in pharmaceuticals: implications for multi-drug delivery. Int. J. Pharm. 526 (1–2), 425–442.

Hui, Chen Li, Xue, Jian Feng, Zheng, Zhi Yong, Shuhaidi, Muhammad, Thu, Hnin Ei, Hussain, Zahid, 2018. Hyaluronic acid, an efficient biomacromolecule for treatment of inflammatory skin and joint diseases: a review of recent developments and critical appraisal of preclinical and clinical investigations. Int. J. Biol. Macromol. 116, 572–584.

Chilcott, R.P., Jenner, J., Hotchkiss, S.A., Rice, P., 2001. In vitro skin absorption and decontamination of sulphur mustard: comparison of human and pig-ear skin. J. Appl. Toxicol. 21 (4), 279–283.

Shiqiang, Deng, Cheng, Jianwen, Zhao, Jinmin, Yao, Felix, Jiake, Xu, 2017. Natural compounds for the treatment of psoriatic arthritis: a proposal based on multi-targeted osteoclastic regulation and on a preclinical study. Res. Protocols 6 (7), e132.

Shiqiang, Deng, May, Brian H., Zhang, Anthony L., Chuanjian, Lu, Xue, Charlie C.L., 2014. Topical herbal formulae in the management of psoriasis: systematic review with meta-analysis of clinical studies and investigation of the pharmacological actions of the main herbs. Phytotherapy Res. 28 (4), 480–497.

Díez-Sales, O., Garrigues, T.M., Herráez, J.V., Belda, R., Martín-Villodre, A., Herráez, M., 2005. In vitro percutaneous penetration of acyclovir from solvent systems and carbopol 971-P hydrogels: influence of propylene glycol. J. Pharm. Sci. 94 (5), 1039–1047.

Zhaoqiang, Dong, Guo, Jing, Xing, Xiaowei, Zhang, Xuguang, Yimeng, Du, Qinghua, Lu, 2017. RGD modified and PEGylated lipid nanoparticles loaded with puerarin: formulation, characterization and protective effects on acute myocardial ischemia model. Biomed. Pharmacother. 89, 297–304.

El-Leithy, Eman S., Makky, Amna M., Khattab, Abeer M., Hussein, Doaa G., 2018. Optimization of nutraceutical coenzyme Q10 nanoemulsion with improved skin permeability and anti-wrinkle efficiency. Drug Dev. Ind. Pharm. 44 (2), 316–328.

Ferreira, Fabricia da Rocha, Valentim, Iara Barros, Ramones, Edgar Luís Catarí, Trevisan, Maria Teresa Salles, Olea-Azar, Claudio, Perez-Cruz, Fernanda, de Abreu, Fabiane Caxico, Goulart, Marília Oliveira Fonseca, 2013. Antioxidant activity of the mangiferin inclusion complex with β-cyclodextri. Food Sci. Technol. 51 (1), 129–134.

Airi, Fujii, Okuyama, Tetsuya, Wakame, Koji, Okumura, Tadayoshi, Ikeya, Yukinobu, Nishizawa, Mikio, 2017. Identification of anti-inflammatory constituents in Phellodendri cortex and Coptidis rhizoma by monitoring the suppression of nitric oxide production. J. Nat. Med. 71 (4), 745–756.

Yuanyuan, Gao, Cheng, Xiaojie, Wang, Zhiguo, Wang, Juan, Gao, Tingting, Li, Peng, Kong, Ming, Chen, Xiguang, 2014. Transdermal delivery of 10,11-methylenedioxycamptothecin by hyaluronic acid based nanoemulsion for inhibition of keloid fibroblast. Carbohydr. Polym. 112, 376–386.

Garrido-Suárez, Bárbara B., Garrido, Gabino, Castro-Labrada, Marian, Merino, Nelson, Valdés, Odalys, Rodeiro, Idania, Hernández, Ivonnes, Godoy-Figueiredo, Jozi, Ferreira, Sergio H., Delgado-Hernández, René, 2014. Anti-hypernociceptive effect of mangiferin in persistent and neuropathic pain models in rats. Pharmacol. Biochem. Behav. 124, 311–319.

Grisham, M.B., Benoit, J.N., Granger, D.N., 1990. Assessment of leukocyte involvement during ischemia and reperfusion of intestine. Methods Enzymol. 186, 729–742.

Muhammad, Imran, Arshad, Muhammad Sajid, Butt, Masood Sadiq, Kwon, Joong-Ho, Arshad, Muhammad Umair, Sultan, Muhammad Tauseef, 2017. Mangiferin: a natural miracle bioactive compound against lifestyle related disorders. Lipids Health Dis. 16 (1), 84.

Jeong, Jin-Ju, Jang, Se-Eun, Hyam, Supriya R., Han, Myung Joo, Kim, Dong-Hyun, 2014. Mangiferin ameliorates colitis by inhibiting IRAK1 phosphorylation in NF-KB and MAPK pathways. Eur. J. Pharmacol. 652–661.

Khazdair, Mohammad Reza, Ghorani, Vahideh, Alavinezhad, Azam, Boskabady, Mohammad Hossein, 2018. Pharmacological effects of zataria Multiflora Boiss L. and its constituents focus on their anti-inflammatory, antioxidant, and immunomodulatory effects. Fundam. Clin. Pharmacol. 32 (1), 26–50.

Kim, Joo-Eun, Park, Young-Joon, 2017. Improved antitumor efficacy of hyaluronic acid-complexed paclitaxel nanoemulsions in treating non-small cell lung cancer. Biomolecules and Therapeutics 25 (4), 411–416.

Kang, Liu, Wu, Lianguo, Shi, Xiaolin, Wu, Fengqing, 2016. Protective effect of naringin against ankylosing spondylitis via ossification, inflammation and oxidative stress in mice. Exp. Therapeutic Medicine 12 (2), 1153–1158.

Maria, Manconi, Caddeo, Carla, Sinico, Chiara, Valenti, Donatella, Mostallino, Maria Cristina, Biggio, Giovanni, Fadda, Anna Maria, 2011a. Ex vivo skin delivery of

diclofenac by transcutol containing liposomes and suggested mechanism of vesicle-skin interaction. Eur. J. Pharm. Biopharm. 78 (1), 27–35.
Maria, Manconi, Sinico, Chiara, Caddeo, Carla, Vila, Amparo Ofelia, Valenti, Donatella, Fadda, Anna Maria, 2011b. Penetration enhancer containing vesicles as carriers for dermal delivery of tretinoin. Int. J. Pharm. 412 (1–2), 37–46.
Riccardo, Martini, Esposito, Francesca, Corona, Angela, Ferrarese, Roberto, Ceresola, Elisa Rita, Visconti, Laura, Tintori, Cristina, 2017. Natural product kuwanon-L inhibits HIV-1 replication through multiple target binding. Chembiochem: Eur. J. Chem. Biol. 18 (4), 374–377.
Debora van der, Merwe J., Joubert, Elizabeth, Manley, Marena, de Beer, Dalene, Malherbe, Christiaan J., Gelderblom, Wentzel C.A., 2012. Mangiferin glucuronidation: important hepatic modulation of antioxidant activity. Food Chem. Toxicol. 50 (3–4), 808–815.
Silvia, Mir-Palomo, Nácher, Amparo, Octavio Díez-Sales, M.A., Busó, Ofelia Vila, Caddeo, Carla, Manca, Maria Letizia, Manconi, Maria, Fadda, Anna Maria, Saurí, Amparo Ruiz, 2016. Inhibition of skin inflammation by baicalin ultradeformable vesicles. Int. J. Pharm. 511 (1), 23–29.
Cavalcante, MoraisTalita, Lopes, Synara Cavalcante, Carvalho, Karine Maria Martins Bezerra, Arruda, Bruno Rodrigues, Correia, Francisco Thiago, de Souza, Maria, Trevisan, Teresa Salles, Rao, Vietla Satyanarayana, Santos, Flávia Almeida, 2012. Mangiferin, a natural xanthone, accelerates gastrointestinal transit in mice involving cholinergic mechanism. World J. Gastroenterol. 18 (25), 3207–3214.
Go, Morikawa, Suzuka, Chihiro, Shoji, Atsushi, Shibusawa, Yoichi, Yanagida, Akio, 2016. High-throughput determination of octanol/water partition coefficients using a shake-flask method and novel two-phase solvent system. J. Pharm. Biomed. Anal. 338–344.
Nadia, Morsi, Ibrahim, Magdy, Refai, Hanan, El Sorogy, Heba, 2017. Nanoemulsion-based electrolyte triggered in situ gel for ocular delivery of acetazolamide. Eur. J. Pharm. Sci. 302–314.
Ochocka, Renata, Hering, Anna, Stefanowicz-Hajduk, Justyna, Cal, Krzysztof, Barańska, Helena, 2017. The effect of mangiferin on skin: penetration, permeation and inhibition of ECM enzymes. PLoS ONE 12, (7).
Pleguezuelos-Villa, María, Mir-Palomo, Silvia, Octavio Díez-Sales, M.A., Buso, Ofelia Vila, Sauri, Amparo Ruiz, Nácher, Amparo, 2018. A novel ultradeformable liposomes of naringin for anti-inflammatory therapy. Colloids and Surfaces. B, Biointerfaces 265–270.
Rady Islam, Melissa B. Bloch, Roxane-Cherille N. Chamcheu, Sergette Banang Mbeumi, Md Rafi Anwar, Hadir Mohamed, Abiola S. Babatunde, 2018. Anticancer properties of graviola (Annona Muricata): a comprehensive mechanistic review. Oxidative Medicine and Cellular Longevity 2018, 1826170.
Roberts, M.S., Mohammed, Y., Pastore, M.N., Namjoshi, S., Yousef, S., Alinaghi, A., Haridass, I.N., 2017. Topical and cutaneous delivery using nanosystems. J. Control. Release 247, 86–105.
Rodríguez-Belenguer, P., Nácher, A., Hernández, M.J., Díez-Sales, O., 2015. Characterization of novel hyaluronic acid matrix systems for vaginal administration of metronidazole. J. Appl. Polym. Sci. 132 (3).
Rosen, Milton J., Kunjappu, Joy T., 2012. Surfactants and Interfacial Phenomena, 4th ed. Wiley.
Sedaghat Doost, Ali, Koen Dewettinck, Frank Devlieghere, Paul Van der Meeren, 2018. Influence of non-ionic emulsifier type on the stability of cinnamaldehyde nanoemulsions: a comparison of polysorbate 80 and hydrophobically modified inulin. Food Chemistry, 237–244.
Bushra, Shal, Ding, Wei, Ali, Hussain, Kim, Yeong S., Khan, Salman, 2018. Anti-neuroinflammatory potential of natural products in attenuation of Alzheimer's disease. Front. Pharmacol. 9, 548.
Xuan, Sheng, Wang, Jiayue, Guo, Jingjing, Yurong, Xu, Jiang, Huaide, Zheng, Chaoran, Xu, Zixi, 2018. Effects of baicalin on diabetic cardiac autonomic neuropathy mediated by the P2Y12 receptor in rat stellate ganglia. Cell. Physiol. Biochem. 46 (3), 986–998.
Siepmann, J., Peppas, N.A., 2001. Modeling of drug release from delivery systems based on hydroxypropyl methylcellulose (HPMC). Adv. Drug Deliv. Rev. 48 (2–3), 139–157.
Mohammad, Wais, Aqil, Mohammad, Goswami, Priyanka, Agnihotri, Jaya, Nadeem, Sayyed, 2017. Nanoemulsion-based transdermal drug delivery system for the treatment of tuberculosis. Recent Pat. Anti-Infect. Drug Discovery 12 (2), 107–119.
Bo, Xiao, Zhigang, Xu, Viennois, Emilie, Zhang, Yuchen, Zhang, Zhan, Zhang, Mingzhen, Han, Moon Kwon, Kang, Yuejun, Merlin, Didier, 2017. Orally targeted delivery of tripeptide KPV via hyaluronic acid-functionalized nanoparticles efficiently alleviates ulcerative colitis. Mol. Ther. 25 (7), 1628–1640.
Hee, Yoo Jeoung, Shanmugam, Srinivasan, Thapa, Pritam, Lee, Eung-Seok, Balakrishnan, Prabagar, Baskaran, Rengarajan, Yoon, Sang-Kwon, 2010. Novel self-nanoemulsifying drug delivery system for enhanced solubility and dissolution of lutein. Pharmacal Res. 33 (3), 417–426.
Yue, Zhang, Shang, Zhenhua, Gao, Chunhui, Man, Du., Shixia, Xu., Song, Haiwen, Liu, Tingting, 2014. Nanoemulsion for solubilization, stabilization, and in vitro release of pterostilbene for oral delivery. AAPS PharmSciTech 15 (4), 1000–1008.
Le, Zhao, Cen, Fang, Tian, Feng, Li, Min-Jie, Zhang, Qi, Shen, Hong-Yi, Shen, Xiang-Chun, Zhou, Ming-Mei, Du, Jun, 2017. Combination treatment with quercetin and resveratrol attenuates high fat diet-induced obesity and associated inflammation in rats via the AMPKα1/SIRT1 signaling pathway. Exp. Therapeutic Med. 14 (6), 5942–5948.
Yunpeng, Zhao, Wang, Wenhan, Wu, Xihai, Ma, Xiaoqian, Qu, Ruize, Chen, Xiaomin, Liu, Chenghao, 2017. Mangiferin antagonizes TNF-α-mediated inflammatory reaction and protects against dermatitis in a mice model. Int. Immunopharmacol. 174–179.

International Journal of Pharmaceutics 573 (2020) 118844

Contents lists available at ScienceDirect

International Journal of Pharmaceutics

journal homepage: www.elsevier.com/locate/ijpharm

Mangiferin glycethosomes as a new potential adjuvant for the treatment of psoriasis

M. Pleguezuelos-Villa[a,*], Octavio Diez-Sales[a,b], Maria Letizia Manca[c], Maria Manconi[c], Amparo Ruiz Sauri[d], Elvira Escribano-Ferrer[e], Amparo Nácher[a,b]

[a] Department of Pharmacy, Pharmaceutical Technology and Parasitology, Faculty of Pharmacy, University of Valencia, Av. Vicent Andrés Estellés s/n, 46100 Burjassot, Valencia, Spain
[b] Instituto Interuniversitario de Investigación de Reconocimiento Molecular y Desarrollo Tecnológico (IDM), Universitat Politècnica de València, Universitat de València, Av. Vicent Andrés Estellés s/n, 46100 Burjassot, Valencia, Spain
[c] Dept. of Scienze della Vita e dell'Ambiente, University of Cagliari, via Ospedale 72, 09124 Cagliari, Italy
[d] Department of Pathology, University of Valencia, Av. Blasco Ibañez 17, 46010 Valencia, Spain
[e] Biopharmaceutics and Pharmacokinetics Unit, Institute for Nanoscience and Nanotechnology, University of Barcelona, Barcelona, Spain

ARTICLE INFO

Keywords:
Mangiferin
Phospholipid vesicles
Glycethosomes
Antioxidant
Skin permeation
Psoriasis

ABSTRACT

Mangiferin, a natural compound isolated from Mangifera indica L, was incorporated in glycerosomes, ethosomes and alternatively in glycerol-ethanol phospholipid vesicles (glycethosomes). Actually, only glycethosomes were able to stably incorporate the mangiferin that was loaded at increasing concentrations (2, 4, 6, 8 mg/mL). The morphology, size distribution, rheological properties, surface charge and entrapment efficiency of prepared vesicles were deeply measured. All vesicles were mainly spherical, oligolamellar, small in size (~145 nm) and negatively charged (~−40 mV), as confirmed by cryo-TEM observation and dynamic laser light scattering measurements. The higher concentration of mangiferin (8 mg/mL) allowed an increase of vesicle mean diameter up to ~288 nm. The entrapment efficiency was inversely proportional to the amount of loaded mangiferin.

In vitro studies performed by using human abdominal skin, underlined that, the dose-dependent ability of vesicles to promote mangiferin retention in epidermis. In addition, glycethosomes were highly biocompatible and showed a strong ability to protect in vitro the fibroblasts against damages induced by hydrogen peroxide. In vivo results underlined the superior ability of mangiferin loaded glycethosomes respect to the mangiferin dispersion to promote the heal of the wound induced by TPA, confirming their potential application for the treatment of psoriasis or other skin disorders.

1. Introduction

Inflammatory skin diseases are cause of important adverse events and disability for a large number of patients, thus negatively affecting their quality of life. The incidence of these skin diseases, which include atopic dermatitis and psoriasis acute, recurrent or chronic, is increasing in recent years, especially in developed countries (Owczarek and Jaworski, 2016).

Currently, the treatment of both atopic dermatitis and psoriasis includes the use of different drugs such as corticoids, calcineurin inhibitors, antihistamines, for topical application and immunosuppressants and biological drugs for systemic treatments (Rodríguez-Luna et al., 2017). However, many patients, especially those with generalized psoriasis, are not adequately treated and long-term therapies are often combined with various side effects of different degrees.

The role of oxidative stress in these diseases has been previously demonstrated in preclinical and clinical studies (Body-Malapel et al., 2018; Tanaka et al., 2018) and the use of antioxidants may represent an ideal strategy to reduce and control the damages caused by psoriasis and atopic dermatitis.

During the last decades, the use of phytodrugs for the treatment of different skin disorders has haroused a great scientific interest (Martinez et al., 2016; Furue et al., 2017; Janeczek et al., 2018). Among the different natural antioxidant molecules, curcumin and quercetin have generated great attention since their large number of important biological and beneficial activities (Abrahams et al., 2019; Rauf et al., 2018).

Considering the promising properties of these, new alternative natural antioxidant molecules such as baicalin, berberin and mangiferin

* Corresponding author.
E-mail address: maplevi@alumni.uv.es (M. Pleguezuelos-Villa).

https://doi.org/10.1016/j.ijpharm.2019.118844
Received 1 July 2019; Accepted 1 November 2019
Available online 18 November 2019
0378-5173/

have been isolated and their beneficial properties evaluated (Mir-Palomo et al., 2019; Manca et al., 2019). Mangiferin or 1,3,6,7-tetrahydroxyxanthone-C2-β-D-glucoside (C-glucosyl xanthone) is an antioxidant molecule isolated from Mangifera indica L, a member of the anacardiaceae family. It possesses strong free radical-scavenging (Saha et al., 2016) and anti-inflammatory activities (Szandruk et al., 2018) and it is effective in a variety of diseases, including tumorigenesis (Zou et al., 2017), hypersensitivity (Guo et al., 2014) and tissue repair (Imran et al., 2017). Like other natural antioxidants, it is in vivo biological effectiveness is limited by low bioavailability (1.71%) (Gu et al., 2018; Du et al., 2018) especially when applied on the skin. To overcome these limitations, the loading of natural antioxidants into nanocarriers has been proposed aiming at increasing their bioavailability and reducing possible side effects (Pimentel-Moral et al., 2018). Many studies have demonstrated an improvement of the effectiveness of these molecules when topically applied. In particular, liposomes or modified phospholipid vesicles disclosed optimal performances in the skin delivery providing an accumulation up to the lower tissues (Manconi et al., 2018; Fang et al., 2018; Doppalapudi et al., 2017). The analysis of research studies demonstrated that each molecule requires a specific ad hoc tailored phospholipid vesicle formulation to maximizes the efficacy.

Taking into account these results, in this work, specific phospholipid vesicles were tailored to stably deliver mangiferin in the skin. After a pre-formulation study, a special kind of phospholipid vesicles loading mangiferin were prepared hydrating phospholipid with a mixture of water, glycerol and ethanol and so called glycethosomes. Mangiferin was loaded at increasing concentrations (2, 4, 6, 8 mg/mL). The choice of glycerol was mainly related to its moisturizing and cosolvent properties (Angelova-Fischer et al., 2018), which are requested for the treatment of atopic dermatitis, as reported by the therapeutic guidelines (Ring et al., 2012; Eichenfield et al., 2014). While the addition of ethanol was linked to their penetration ability.

Glycethosomes loaded with mangiferin were fully characterized measuring size, size distribution, surface charge, stability on storage and rheological properties. Their ability to promote the accumulation and distribution of mangiferin into and through the skin was evaluated using human abdominal skin. In addition, their potential therapeutic application for the treatment of psoriasis was evaluated in vivo using a 12-O-tetradecanoylphorbol-13-acetate (TPA)-treated mice model.

2. Material and methods

2.1. Materials

Lipoid® S75 a mixture of soybean lecithin containing lysophosphatidylcholine (3% maximum), phosphatidylcholine (70%), phosphatidylethanolamine (10%), fatty acids (0.5% maximum), triglycerides (3% maximum) was purchased from Lipoid GmbH (Ludwigshafen, Germany). Tween 80 were purchased from Scharlab S.L. (Barcelona, Spain). Mangiferin was purchased to Carbosynth Limited (UK). Glycerol was purchased from Guinama S.L.U. (Valencia, Spain), Ethanol was purchased from VWR chemicals S.A. (France). Phorbol 1, 2-myristate 1, 3-acetate was purchased from Sigma-Aldrich (Madrid, Spain). Cell medium, foetal bovine serum, penicillin and streptomycin and all the other reagents for cells studies, were purchased from Thermo Fisher Scientific Inc. (Waltham, MA, US).

2.2. Analytical method

Mangiferin content was determined by high-performance liquid chromatography (HPLC) using a Perkin Elmer® Series 200 equipped with a photodiode array UV detector and a C18 reverse-phase column (Teknokroma®Brisa "LC2" 5.0 μm, 150 mm × 4.6 mm). The isocratic mobile phase consisted of a mixture of hydrochloric acid (pH 4.0) and methanol (60:40, v/v), the flow rate was 1.2 mL/min. The detection wavelength was set at 254 nm.

Table 1
Composition of hydrating medium, mean diameter (MD), polydispersity index (PI) and zeta potential (ZP) of liposomes, glycerosomes, ethosomes and glycethosomes loading mangiferin (2 mg/mL). Each value represents the mean ± standard deviation of at least three determinations.

Formulation	Hydrating medium	MD (nm)	PI	ZP (mV)
Liposomes	Water	452 ± 3	0.40	−37 ± 2
Glycerosomes	Glycerol:water	391 ± 2	0.50	−31 ± 1
Ethosomes	Ethanol: water	643 ± 3	0.40	−39 ± 1
Glycethosomes	Glycerol:ethanol:water	140 ± 1	0.32	−42 ± 1

2.3. Preparation of vesicles

A preformulation study was performed to evaluate the best composition able to incorporate and retain high amount of mangiferin and promote its efficacy for the topical treatment of psoriasis and atopic dermatitis. Various amounts of different phospholipids were tested, tween 80 was added as excipient aiming at ameliorating the physicochemical properties of vesicles, Table 1. Among all formulation tested, those obtained using S75 as phospholipid and a mixture of glycerol, ethanol and water (50:25:25) seemed to be the ideal vesicle as it was the smaller and homogeneous system. The glycerol: ethanol: water blend was used to hydrate S75 (100 mg/mL) and tween 80 (5 mg/mL). The mixture was slightly heated (40 °C) in a water bath and then different amounts of mangiferin (2, 4, 6 and 8 mg/mL) were added to evaluate the higher quantity of mangiferin which could be stably incorporated and retained in these systems. The dispersions were sonicated for 4 min with a CY-500 ultrasonic disintegrator (Optic Ivymen system, Barcelona, Spain) and then extruded through a 0.20 μm membrane (Whatman, GE Healthcare, Fairfield, Connecticut, US) by using Avanti® Mini Extruder (Avanti Polar Lipids, Alabaster, Alabama). Mangiferin dispersion (8 mg/mL) and empty glycethosomes were also prepared as control. The composition of vesicles is given in Table 2.

2.4. Characterization of vesicles

Vesicle formation and morphology were checked by cryogenic Transmission Electron Microscopy (cryo-TEM). A thin aqueous film was formed by placing a sample drop on a glow-discharged holey carbon grid and then blotting the grid against filter paper. The film was vitrified by plunging the grid in ethane maintained at its melting point with liquid nitrogen, using a Vitrobot (FEI Company, Eindhoven, The Netherlands). The vitreous films were transferred to a Tecnai F20 TEM (FEI Company) and the samples were observed in a low-dose mode. Images were acquired at 200 kV at a temperature between −170–175 °C, using low-dose imaging conditions not exceeding 20 e-/Å2, with a CCD Eagle camera (FEI Company).

The average diameter and polydispersity index (PI) of glycethosomes were measured by Photon Correlation Spectroscopy (PCS) using a Zetasizer nano-ZS® (Malvern Instruments, Worcestershire, UK). Zeta

Table 2
Mangiferin concentration (MC), mean diameter (MD), polydispersity index (PI), zeta potential (ZP) and entrapment efficiency of 2-glycethosomes, 4-glycethosomes, 6-glycethosomes, 8-glycethosomes. Each value represents the mean ± standard deviation of at least three determinations.

Formulation	MC (mg/mL)	MD (nm)	PI	ZP (mV)	EE (%)
	0	141 ± 2	0.32	−40 ± 1	
2-Glycethosomes	2	140 ± 2	0.31	−43 ± 2	78 ± 1
4-Glycethosomes	4	149 ± 2	0.33	−40 ± 1	70 ± 1
6-Glycethosomes	6	151 ± 3	0.29	−38 ± 1	65 ± 1
8-Glycethosomes	8	288 ± 2	0.32	−39 ± 2	62 ± 1

potential was estimated using the Zetasizer nano-ZS by means of the M3-PALS (Mixed Mode Measurement-Phase Analysis Light Scattering) technique, which measures the particle electrophoretic mobility.

The stability on storage was evaluated for 90 days at 4 °C, by measuring the particle size, PI and Zeta potential of glycethosomes every 30 days, which provided useful information about changes in size distribution and surface charge.

The entrapment efficiency (EE) of the glycethosomes was determined as the percentage of the amount of mangiferin recovered after dialysis versus the amount initially used. Each sample (1 mL) was loaded into Spectra/Por®tubing (12–14 kDa MW cut-off; Spectrum Laboratories Inc., DG Breda, The Netherlands) and dialyzed against 1L of water at room temperature for 8 h. The mangiferin content was measured by HPLC after disruption of non-dialysed and dialysed vesicles with Triton X-100 (10%).

2.5. Rheological measurements of mangiferin loaded vesicles

Rheological measurements were carried out at 25 ± 1 °C, using a controlled stress rheometer (RheoStress 1, Thermo Haake, Germany) equipped with a Haake *K*10 thermostatic bath control and data logging software (RheoWin 4.0.1). Samples were allowed to rest for at least 300 s for temperature equilibrium and stress relaxation. Cone-plate sensor (2°, 35 mm diameter) were used for the analyses.

Step flow curves were obtained in a controlled stress mode (30 s each step in logarithmic distribution). The shear stress range was chosen to evaluate viscosities corresponding to very low shear rates (up to ~100 s^{-1}). All measurements were performed in triplicate, at 25 °C. The viscosities results can be calculated by using the simplified Carreau model.

$$\eta = \frac{\eta_0}{\left(1 + \left(\frac{\dot{\gamma}}{\dot{\gamma}_c}\right)^2\right)^s} \quad (1)$$

where η_0 is the zero-shear viscosity, $\dot{\gamma}_c$ is the critical shear rate, and s the shear thinning index.

2.6. Evaluation of in vitro skin delivery of mangiferin loaded vesicles

Experiments were performed using human abdominal skin obtained from donors aged 40–50 years who undergone cosmetic surgical procedures. The skin was given by Hospital Clinic Universitario (Valencia, Spain) after informed consent obtained from patients. The skin was prepared within the first 3 h after excision, removing all subcutaneous fatty tissue, and was stored at −80 °C until use (Alves et al., 2007). The full-thickness human epidermis was placed between the donor and receptor compartments of Franz diffusion vertical cells (effective diffusion area of 0.784 cm^2). The receptor compartment (6 mL) was filled with an aqueous solution containing 1% of tween 80, thermostated at 37 ± 1 °C, and continuously stirred. The different formulations (200 μL) were applied onto the surface of epidermis. At regular time intervals, the receiving solution was withdrawn, replaced with the same volume of pre-thermostated fresh aqueous solution up to 24 h and analysed by HPLC for mangiferin content. At the end of the permeation experiments, to verify the integrity of the epidermis, 1 mL of phenol red solution (0.5 mg/mL) was applied on the skin surface, which was considered intact when the amount of phenol red in the receptor compartment was lower than 1%.

After 24 h the skin surface was removed and gently washed and dried with filter paper, then it was putted in glass vials and methanol (5 mL) was added to allow the extraction of mangiferin accumulated in the epidermis. The extraction procedure was performed for 24 h under constant stirring (350 rpm) at room temperature (25 ± 1 °C), then the extractive solution was analysed by HPLC for mangiferin content.

2.7. Evaluation of in vitro biocompatibility of mangiferin loaded vesicles

3T3 mouse fibroblasts (ATCC, Manassas, VA, USA) were grown as monolayers in 75-cm^2 flasks, incubated at 37 °C in 5% CO_2 and 100% humidity. Dulbecco's modified Eagle's medium (DMEM), supplemented with 10% (V/V) fetal bovine serum, penicillin/streptomicin (100 U/mL), and 0.1% fungizone was used as culture medium. For biocompatibility experiments, 3T3 cells were seeded in 96-well plates at density of 1×10^4 cell/well. After 24 h of incubation, 3T3 cells were exposed for 48 h to mangiferin in dispersion (8 mg/mL) or loaded in vesicles (2,4,6,8 mg/mL) at different dilutions (1:1000, 1:10000; 1:100000 and 1:1000000). Cell viability was evaluated by means of MTT [3 (4,5-dimethylthiazolyl-2)-2,5-diphenyltetrazolium bromide] colorimetric assay. MTT (100 μL, 0.5 mg/mL final concentration) was added to each well, and then, after 3 h the formazan crystals formed were dissolved in DMSO (100 μL). The reaction was spectrophotometrically measured at 570 nm using a microplate reader (Multiskan EX, Thermo Fisher Scientific, Inc., Waltham, MA, US). The experiments were repeated at least three times. The results are presented as a percentage of untreated cells (100% viability).

2.8. Protection of cells against oxidative stress by using mangiferin loaded vesicles

3T3 cells were seeded into 96-well plates and exposed to hydrogen peroxide (1:40000 dilution) and simultaneously treated with mangiferin in dispersion or loaded in vesicles (8 mg/mL and 2, 4, 6 and 8 mg/mL for dispersion and vesicles, respectively). After 4 h, the cells were washed with PBS and cell viability was evaluated by MTT assay. Untreated cells were used as negative control, while cells treated with hydrogen peroxide only were used as positive control. Final results are reported as the percentage of untreated cells (100% viability).

2.9. Study of effectiveness of mangiferin loaded vesicles in inflammatory mice models

Mice were supplied by Envigo laboratories (Barcelona, Spain), and were acclimated for one week before their use. All studies were performed in accordance with the European Union regulations for the handling and use of laboratory animals. The protocols were approved by the Institutional Animal Care and Use Committee of the University of Valencia (code 2018/VSC/PEA/0032 type 2).

Inflammation and ulceration were induced by applying topically TPA, dissolved in acetone (3 μg/20 μL), to the shaved dorsal area (1 cm^2) of female CD-1 mice (5–6 weeks old, 25–35 g). All glycethosomes (200 μL) were topically applied in the same dorsal site 3 h after TPA application. The protocol/experimental plan was repeated for 3 days. Mice (n = 5, per group) were sacrificed on day fourth by cervical dislocation. Visual inspection of the skin after the treatment, along with myeloperoxidase activity (MPO) and oedema formation were measured. Inhibition of MPO activity was evaluated as previously reported (Pleguezuelos-Villa et al. 2019). The treated dorsal skin was excised, weighed and used to measure oedema formation. For histological assays, tissue samples were stored in formaldehyde (0.4%, V/V) and longitudinal sections (5 mm) of the skin, obtained using a rotary microtome, were mounted on slides and marked with haematoxylin and eosin according to standard protocols. Tissues were observed and analysed using an optical microscope (DMD 108 Digital Micro-Imaging Device, Leica, Wetzlar, Germany).

2.10. Statistical analysis of data

Statistical differences were determined by one-way ANOVA test and Tukey's test for multiple comparisons with a significance level of $p < 0.05$. All statistical analyses were performed using IBM SPSS statistics 22 for Windows (Valencia, Spain). Data are shown as

mean ± standard deviation.

3. Results and discussion

3.1. Preparation and characterization of vesicles

In this study, aiming at promoting the effectiveness of mangiferin in the treatment of psoriasis or atopic dermatitis, new phospholipid vesicles were designed. To achieve versatile and stable formulations, capable of incorporating high amount of mangiferin, a preformulation study was carried out. Lipoid S75 were use as phospholipid (100 mg/mL) and combined with tween 80 (5 mg/mL). The last acts as edge activator and improve the flexibility of the bilayer (Perez et al., 2016). Mangiferin were loaded at concentration of 2 mg/mL. Lipids, surfactant and payload were mixed and hydrate with water to obtain liposomes, water and glycerol (50:50 v/v) to obtain glycerosomes, water and ethanol (50:50 v/v) to obtain ethosomes, glycerol, ethanol and water (50:25:25 v/v) to obtain glycethosomes. Composition of hydrating medium as well mean diameter, polydispersity index and zeta potential of vesicles loading mangiferin are reported in Table 1. Glycethosomes was the smallest vesicles (~140 nm), most homogeneously dispersed (PI 0.32) and highly negatively charged (−42 mV). The mean diameter of other vesicles was 2–3 times higher. Additionally, the dispersion was very instable and after few days formed two phases. As a consequence, the further studies were focuses on glycethosomes. The same formulation was prepared using the same amount of phospholipid, tween and increasing concentrations of mangiferin (2, 4, 6 and 8 mg/mL), in order to find the highest amount of phytodrug which should be loaded. Empty glycethosomes were also prepared and used as reference. The mean physico-chemical characteristics of vesicles were measured (Table 2). Empty vesicles and those loading 2, 4 and 6 mg/mL showed the same mean diameter (~140 nm), polydispersity index and zeta potential without differences statistically significant among the group ($p > 0.05$). The highest concentrations of mangiferin seem to be critic and the mean diameter of these vesicles was double (~288 nm) compared with the other samples. Probably, using this concentration, the mangiferin which preferentially located in the vesicle bilayer, saturated it modifying the its assembling and curvature radius leading to the increase of particle size (Huang et al. 2017). However, according to other authors, vesicles sized between 100 and 1000 nm are suitable for transdermal administration (Hussain et al. 2017).

The entrapment efficiency (EE%) of mangiferin in glycethosomes slightly decrease as the amount of mangiferin loaded in the formulation increased (Table 2).

Vesicle morphology was evaluated by using Cryo-TEM, which underline the formation of uni- and oligolamellar, spherical and regularly shaped vesicles. These results are in agreement with those obtained by using dynamic light scattering technique, as particle size was ~ 140 nm for 2-, 4- and 6-glycethosomes and bigger for 8-glycethosomes, (Fig. 1).

The prepared vesicles were stored at 4 °C for 3 mounts and their physico-chemical characteristics (size, PI and zeta potential) were measured at scheduled times. All vesicle desperations were highly stable as any significant variation ($p < 0.05$) of the measured parameters were detected during the storage (Fig. 2).

3.2. Rheological measurements

The physical state of dispersions and the possible interactions between the vesicles were evaluated by rheological analyses. Viscoelastic properties of the different glycethosomes were evaluated by measuring their viscosity (Fig. 3).

As expected, 8-glycethosomes were the most viscous (2584 ± 46 Pa s) as the viscosity increased as the mangiferin concentration increased: 2-glycethosomes (279 ± 4 Pa s); 4-glycethosomes (730 ± 12 Pa s) and 6-glycethosomes (1364 ± 33 Pa s). Besides, all formulations had a similar pseudoplastic behavior (s ~0.42). The highest value of viscosity measured for 8-glycethosomes was clearly dependent to the increased mean diameter of vesicles which can encapsulated a large amount of aqueous medium reducing that free in intervesicle spaces. However, a viscosity increase was observed as a function of other mangiferin concentrations too (2, 4 and 6 mg/mL) while the mean diameter of these vesicles remained unchanged. This increase can be related to an improvement of interactions between vesicles, which decreased the kinetic energy.

3.3. In vitro skin penetration and permeation studies

The ability of the new vesicles to facilitate the skin delivery of mangiferin was evaluate by using franz diffusion cells (Manca et al., 2016). Additionally, mangiferin (8 mg/mL) was dispersed in a blend of water, ethanol, and glycerol and the obtained dispersion was used as reference to compare the vesicle performances (Fig. 4).

Using the mangiferin (8 mg/mL) in dispersion the deposition in the skin was ~15 μg like to that provided by the vesicles (~15 μg, $p > 0.05$) loading the lowest concentration of mangiferin (2 mg/mL). Using the mangiferin loaded in vesicles the amount of phytodrug accumulated in the epidermis was closely related to the administered dose. Indeed, the amount deposited in the skin after the application of 8-glycethosomes which loaded 8 mg/mL of mangiferin was 9-fold higher than that accumulated after the application of mangiferin dispersion which contained the same amount of phytodrug. Results disclosed the optimal performance of glycethosomes in the skin delivery of mangiferin.

The amount of phytodrug which permeated in the receptor fluid was the lowest using the dispersion and increased as a function of the loaded mangiferin in the vesicles, as follows: mangiferin dispersion < 2-glycethosomes (0.81%) < 4-glycethosomes (0.86%) < 6-glycethosomes (1.52%) < 8-glycethosomes (1.70%) ($p < 0.05$). The lower permeation of mangiferin in dispersion may be related to its high molecular weight (~422.34 g/mol) and hydrophilicity (log P oct = −0.65), which make difficulty its permeation through the stratum corneum. Moreover, it was observed that the permeation of the drug through the skin was independent of the vesicle size as the best results were obtained with 8-glycethosomes, which were significantly larger than the

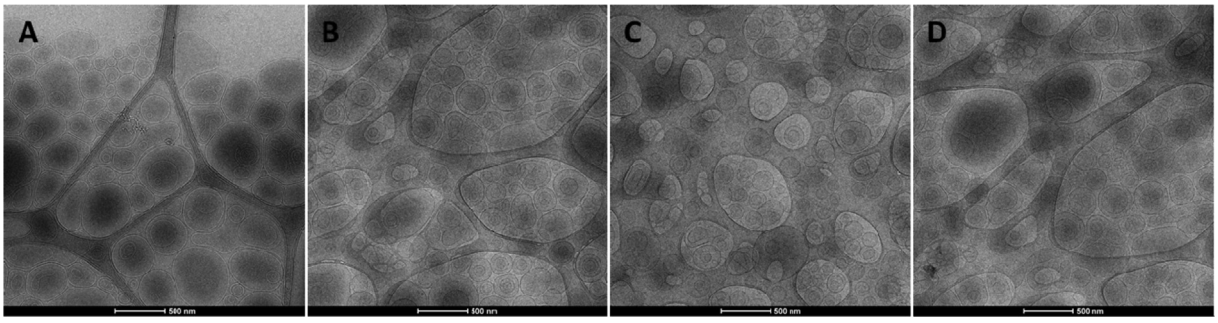

Fig. 1. Representative cryo-TEM images of 2-glycethosomes (A), 4-glycethosomes (B), 6-glycethosomes (C) and 8-glycethosomes (D).

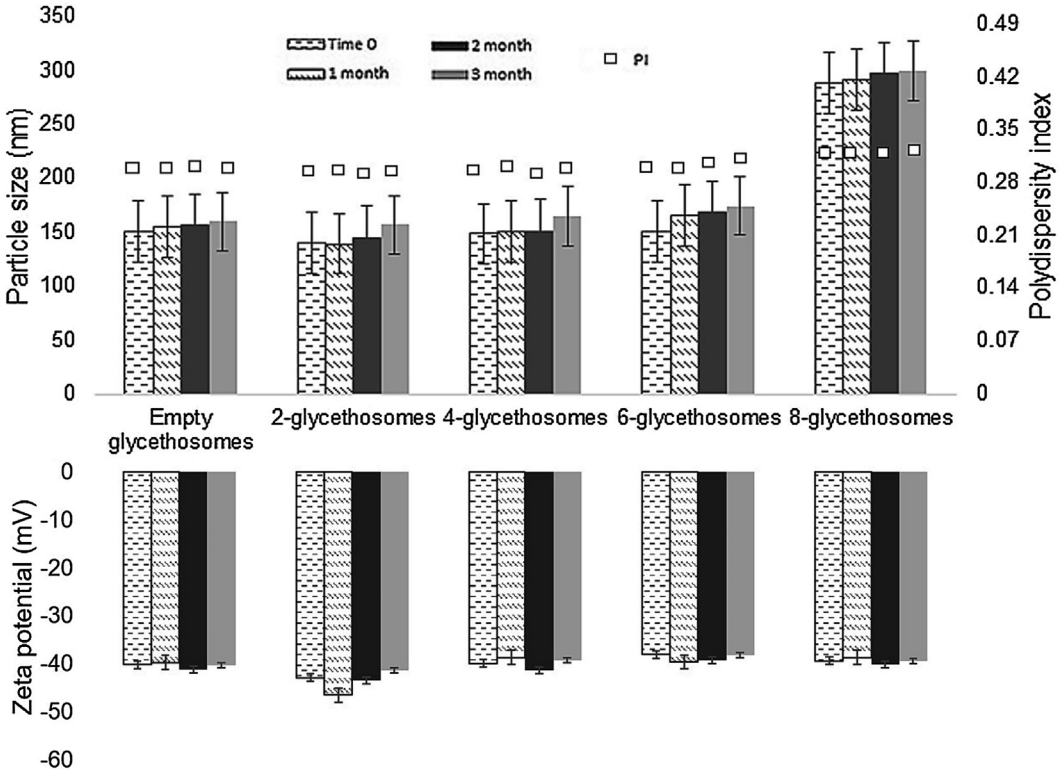

Fig. 2. Mean diameter (MD), polydispersity index (PI) and zeta potential (ZP) of mangiferin loaded into 2-glycethosomes, 4-glycethosomes, 6-glycethosomes and 8-glycethosomes stored for 3 months at 4 °C. Data are reported as mean values ± standard deviations (error bars).

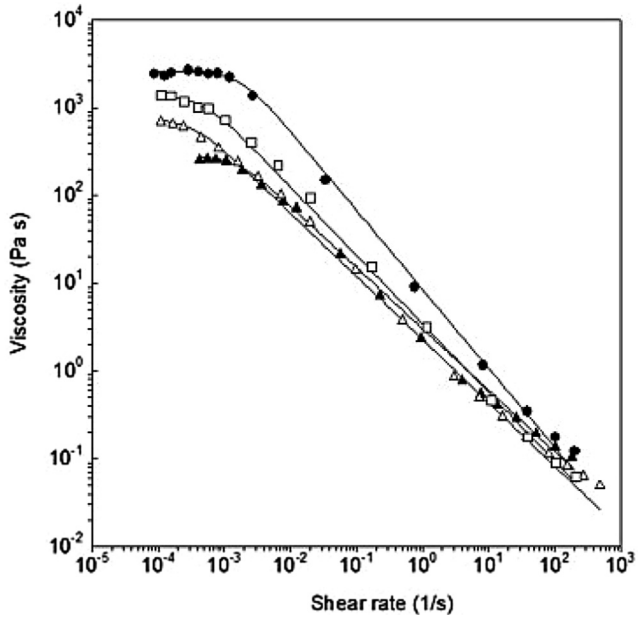

Fig. 3. Representative flow curves fitted to Carreau model for 2-glycethosomes (▲), 4-glycethosomes (Δ), 6-glycethosomes (□) and 8-glycethosomes (●).

other vesicles. Given that, the accumulated amount in the RC was ~1.70% or lower, thus it can be considered negligible.

3.4. In vitro cell viability and protection against oxidative stress

The biocompatibility of mangiferin in dispersion or loaded into glycethosomes was evaluated by using fibroblasts (3T3 cells, Fig. 5A). The vesicle viability was slight lower using the lower dilution corresponding to 10 μg/ml of mangiferin irrespective to the used formulation. Using the other dilutions any mortality was detected and the viability of cells was ≥100%. Results confirmed a great bioavailability of mangiferin dispersion which was not affected by the loading in vesicles.

The ability of mangiferin in dispersion or loaded in glycethosomes to protect the cells against oxidative stress was evaluated (Fig. 5B).

The cells were stressed with hydrogen peroxide and simultaneously treated with formulations. The viability of stressed cells was very low (~40%). The addition of mangiferin in dispersion was able to slightly counteract the oxidative stress as the viability increased up to (~70%). However, the best results were obtained when the mangiferin was loaded in glycethosomes as the viability reached ~100% irrespective of the used amount of phytodrug ($p < 0.01$ versus result provided by mangiferin dispersion). These results underlined the ability of the vesicles to promote the protection of cells against oxidative stress by reducing the damages caused by the oxygen reactive species. Considering that this process is involved in the pathogenesis of psoriasis, these new mangiferin loaded glycethosomes represent a promising tool for the treatment of this pathology (Lai et al., 2018).

3.5. Inflammatory TPA mice models

Psoriasis is an inflammatory skin disorder characterized by the hyperproliferation of basal epidermal cells. It has been postulated that potent anti-inflammatory and antioxidant agents can play an important role in restoring physiological conditions (Pivetta et al., 2018; Zengin et al., 2019).

In the present study, TPA was applied topically on mice skin to induce ulceration and inflammation effects. The therapeutic efficacy of mangiferin in dispersion or loaded in glycethosomes was evaluated in vivo by measuring the inhibition of oedema and inflammatory cell activation, typical events associated with skin lesion. To evaluate the effect of the vesicles alone, empty vesicles were also tested.

TPA-induced oedema was significantly reduced ($p < 0.05$) by

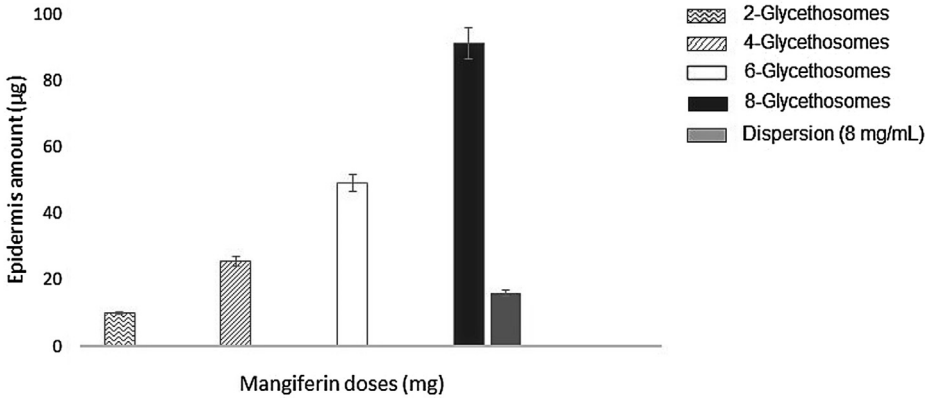

Fig. 4. Mangiferin accumulated in epidermis (EP) after 24 h of experiment. Bars represent the mean ± standard deviation of at least six independent experimental determinations.

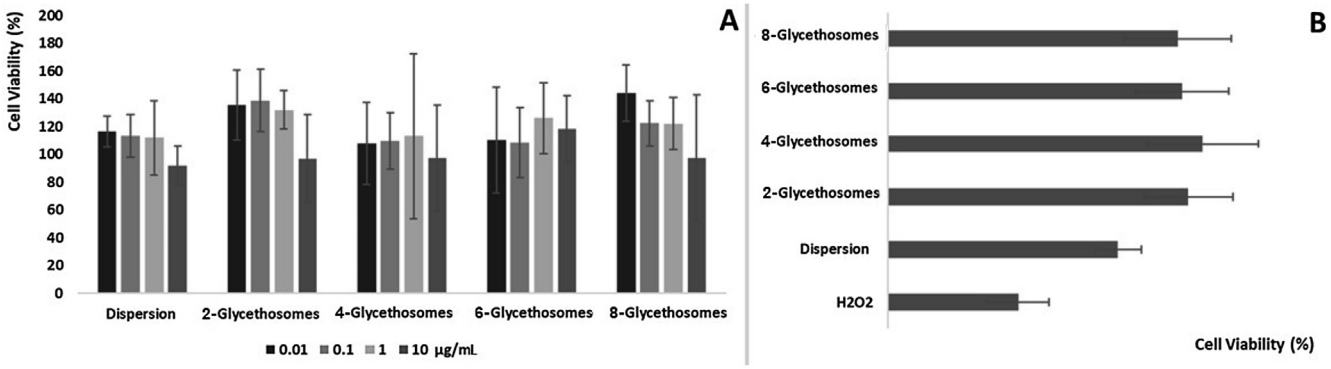

Fig. 5. A Viability of 3T3 cells incubated for 48 h with different concentrations of mangiferin in dispersion or loaded into glycethosomes. **B** Protective effect of mangiferin in dispersion (8 mg/mL) or loaded in glycethosomes against hydrogen peroxide-induced oxidative stress in 3T3 cells. Data are reported as mean values ± standard deviations (error bars) of cell viability expressed as the percentage of control (100% viability).

Table 3
Inhibition of oedema and MPO activity in mice exposed to TPA and treated with mangiferin in dispersion or loaded into glycethosomes. Mean values ± standard deviation is reported. * indicate values significantly different from glycethosomes, # indicate values significantly different from 8-glycethosomes ($p < 0.05$).

Formulations	Oedema inhibition (%)	MPO inhibition (%)
TPA	0	0
Mangiferin dispersion	9 ± 0.1*	30 ± 0.6*
Empty glycethosomes	6 ± 0.1*	26 ± 2.4*
4-glycethosomes	47 ± 3.2	80 ± 5.1
6-glycethosomes	51 ± 2.9	81 ± 4.4
8-glycethosomes	58 ± 2.6	87 ± 3.0#

treating the wounded skin with mangiferin loaded vesicles, (~51% inhibition), irrespective to the mangiferin concentration used ($p > 0.05$), while the inhibition was only ~6 and 9% ($p > 0.05$) when empty vesicles and mangiferin loaded vesicles were used (Table 3).

MPO activity was inhibited as follows: mangiferin loaded vesicles (~83%) > mangiferin dispersion (~30%) > empty vesicles (~25%). These findings demonstrated that the delivery of mangiferin at the wound site using phospholipid vesicles, improves the effectiveness of phytodrug against skin inflammation and this effect should be facilitated by the penetration effect of ethanol and emollient and hydrating properties of glycerol. In addition, different studies suggested that the combination of anti-inflammatory and antioxidant compounds as mangiferin (Biswas et al., 2015; Bairy et al., 2002) with emollients should be used as second and third-line psoriasis therapies (Khosravi et al., 2017). However, all consensus conferences and guidelines supported the use of emollients as a first-line therapy for the treatment of atopic dermatitis (Ring et al., 2012; Eichenfield et al., 2014).

Macroscopic evaluation of the treated skin underlined the superior ability of glycethosomes to heal the wound in comparison with the dispersion used as reference, irrespective of the concentration tested (Fig. 6), even if better results were obtained using 6- and 8-glycethosomes (loading 6 and 8 mg/mL of mangiferin). Histological analysis (Fig. 7) showed that topical application of mangiferin loaded vesicles, irrespective to the used mangiferin concentration, were able to reduce the pathological effect induced by TPA in comparison with mangiferin dispersion and empty glycethosomes. In agreement with the macroscopic observation, 4-glycethosomes showed a slight accumulation of inflammatory cells in the epidermis with parakeratosis evidences and a moderate inflammatory infiltration in dermis.

However, as the mangiferin concentration increased (6- and 8-glycethosomes), the protection against damaging effects of TPA also increased. Otherwise, skin treated with TPA only, displayed inflammatory infiltrates of mononuclear cells, eosinophils and neutrophils, along with severe dermal and subcutaneous alteration. These alterations are slightly reduced by treating the skin with mangiferin dispersion.

4. Conclusions

The delivery of mangiferin in glycethosomes, along with the high viscosity of these vesicles, favoured the retention of the drug in the epidermis and provided a depot of mangiferin on the skin that could be released slowly. All vesicles tested were highly biocompatible and promoted the effectiveness of mangiferin against the oxidative stress induced in fibroblasts using hydrogen peroxide. In vivo results

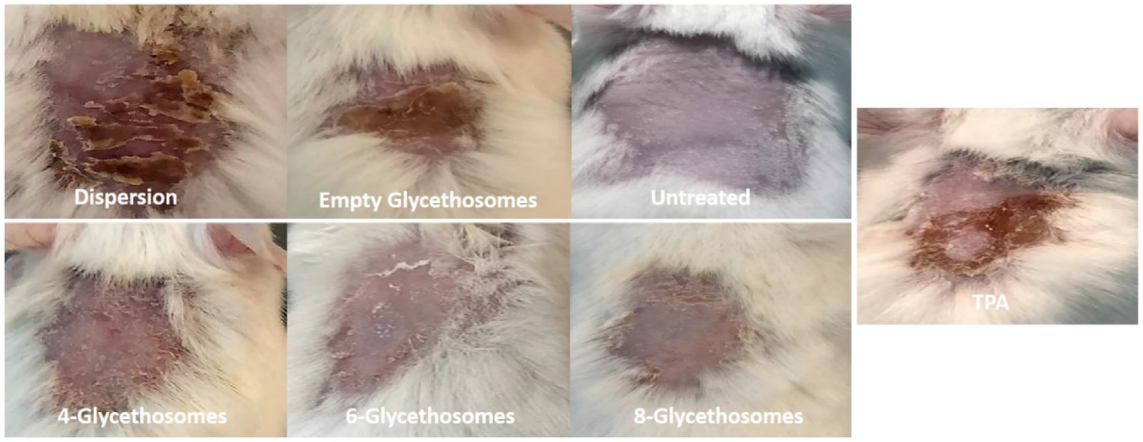

Fig. 6. Mice skin lesions caused by TPA application and treated with empty glycethosomes, mangiferin in dispersion or loaded into 4-glycethosomes, 6-glycethosomes and 8-glycethosomes, and untreated skin.

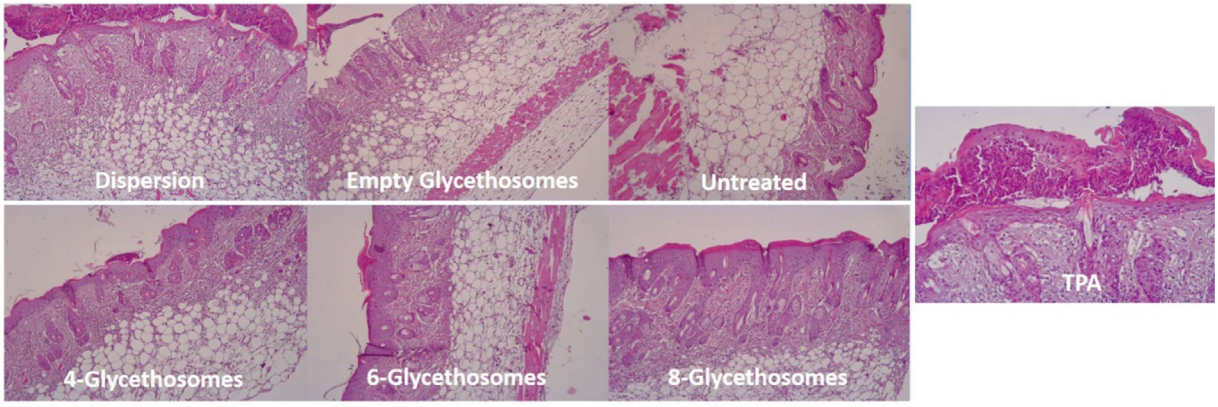

Fig. 7. Histological determination of the mice skin exposed to TPA, treated with empty glycethosomes and with mangiferin in dispersion or loaded into 4-glycethosomes, 6-glycethosomes and 8-glycethosomes, and untreated skin. Original magnification 10x.

underlined one time more the superior ability of vesicles to promote the heal of the wound induced by TPA. Overall results seemed to indicate a remarkable therapeutic potential of mangiferin loaded glycethosomes for the treatment of psoriasis or other skin disorders.

Funding

This research did not receive any specific grant from funding agencies in the public, commercial, or not-for-profit sectors.

Declaration of Competing Interest

The authors declare that they have no known competing financial interests or personal relationships that could have appeared to influence the work reported in this paper.

References

Abrahams, Shameemah, Haylett, William L., Johnson, Glynis, Carr, Jonathan A., Bardien, Soraya, 2019. Antioxidant effects of curcumin in models of neurodegeneration, aging, oxidative and nitrosative stress: A review. Neuroscience 406, 1–21.

Alves, Marta P, Scarrone, Ana L., Santos, Marcos, Pohlmann, Adriana R., Guterres, Sílvia S., 2007. Human skin penetration and distribution of nimesulide from hydrophilic gels containing nanocarriers. Int. J. Pharm. 341 (1–2), 215–220.

Angelova-Fischer, Irena, Rippke, Frank, Richter, Daniel, Filbry, Alexander, Arrowitz, Craig, Weber, Teresa, Fischer, Tobias W., Zillikens, Detlef, 2018. Stand-alone emollient treatment reduces flares after discontinuation of topical steroid treatment in atopic dermatitis: A double-blind, randomized, vehicle-controlled, left-right comparison study. Acta Dermato-Venereologica 98 (5), 517–523.

Bairy, Indira, Reeja, S., null Siddharth, Suganghi Rao, P., Bhat, Mahalinga, Shivananda, P.G., 2002. Evaluation of antibacterial activity of mangifera indica on anaerobic dental microglora based on in vivo studies. Indian J. Pathol. Microbiol. 45 (3), 307–310.

Biswas, Taniya, Sen, Argha, Roy, Rini, Maji, Sushomasri, Maji, Himangshu Sekhar, 2015. Isolation of mangiferin from flowering buds of *Mangifera Indica* L and its evaluation of in vitro antibacterial activity. J. Pharm. Anal. 4 (3), 8.

Body-Malapel, M., Djouina, M., Waxin, C., Langlois, A., Gower-Rousseau, C., Zerbib, P., Schmidt, A.-M., Desreumaux, P., Boulanger, E., Vignal, C., 2018. The RAGE signaling pathway is involved in intestinal inflammation and represents a promising therapeutic target for inflammatory bowel diseases. Mucosal Immunol. 25–35.

Doppalapudi, Sindhu, Mahira, Shaheen, Khan, Wahid, 2017. Development and in vitro assessment of psoralen and resveratrol co-loaded ultradeformable liposomes for the treatment of vitiligo. J. Photochem. Photobiol. B,Biol. 174, 44–57.

Du, Suya, Liu, Huirong, Lei, Tiantian, Xie, Xiaofang, Wang, Hailian, He, Xia, Tong, Rongsheng, Wang, Yi, 2018. Mangiferin: An effective therapeutic agent against several disorders (Review). Mol. Med. Rep. 18 (6), 4775–4786.

Eichenfield, Lawrence F., Tom, Wynnis L., Berger, Timothy G., Krol, Alfons, Paller, Amy S., Schwarzenberger, Kathryn, Bergman, James N., et al., 2014. Guidelines of care for the management of atopic dermatitis: Section 2. Management and treatment of atopic dermatitis with topical therapies. J. Am. Acad. Dermatol. 71 (1), 116–132.

Fang, Chien-Liang, Wang, Yiwei, Tsai, Kevin H.-Y., Chang, Hsin-I, 2018. Liposome-encapsulated baicalein suppressed lipogenesis and extracellular matrix formation in Hs68 human dermal fibroblasts. Front. Pharmacol. 256, 45–50.

Furue, Masutaka, Uchi, Hiroshi, Mitoma, Chikage, Hashimoto-Hachiya, Akiko, Chiba, Takahito, Ito, Takamichi, Nakahara, Takeshi, Tsuji, Gaku, 2017. Antioxidants for healthy skin: the emerging role of aryl hydrocarbon receptors and nuclear factor-erythroid 2-related factor-2. Nutrients 9 (3).

Gu, Peng-Cheng, Wang, Lan, Han, Mei-Na, Peng, Jun, Shang, Jing-Chuan, Pan, Yong-Quan, Han, Wen-Li, 2018. Comparative pharmacokinetic study of mangiferin in normal and alloxan-induced diabetic rats after oral and intravenous administration by UPLC-MS/MS. Pharmacology 103 (1–2), 30–37.

Guo, Hong-Wei, Yun, Chen-Xia, Hou, Guang-Han, Jun, Du., Huang, Xin, Yi, Lu., Keller, Evan T., Zhang, Jian, Deng, Jia-Gang, 2014. Mangiferin attenuates Th1/Th2 cytokine imbalance in an ovalbumin-induced asthmatic mouse model. PLoS ONE 9 (6).

Huang, Changjin, Quinn, David, Sadovsky, Yoel, Subra Suresh, K., Hsia, Jimmy, 2017. Formation and size distribution of self-assembled vesicles. Proc. Natl. Acad. Sci. 114 (11), 2910–2915.

Hussain, Afzal, Singh, Sima, Sharma, Dinesh, Webster, Thomas J., Shafaat, Kausar, Faruk, Abdul, 2017. Elastic liposomes as novel carriers: recent advances in drug delivery. Int. J. Nanomed. 12, 5087–5108.
Imran, Muhammad, Arshad, Muhammad Sajid, Butt, Masood Sadiq, Kwon, Joong-Ho, Arshad, Muhammad Umair, Sultan, Muhammad Tauseef, 2017. Mangiferin: A natural miracle bioactive compound against lifestyle related disorders. Lipids Health Dis.
Janeczek, Monica, Moy, Lauren, Lake, Eden P., Swan, James, 2018. Review of the efficacy and safety of topical mahonia aquifolium for the treatment of psoriasis and atopic dermatitis. J. Clin. Aesthetic Dermatol. 11 (12), 42–47.
Khosravi, Hasan, Siegel, Michael P., Van Voorhees, Abby S., Merola, Joseph F., 2017. Treatment of inverse/intertriginous psoriasis: updated guidelines from the medical board of the national psoriasis foundation. J. Drugs Dermatol.: JDD 16 (8), 760–766.
Lai, Rui, Xian, Dehai, Xiong, Xia, Yang, Lingyu, Song, Jing, Zhong, Jianqiao, 2018. Proanthocyanidins: novel treatment for psoriasis that reduces oxidative stress and modulates Th17 and Treg cells. Redox Rep.: Commun. Free Rad. Res. 23 (1), 130–135.
Manca, Maria Letizia, Matricardi, Pietro, Cencetti, Claudia, Peris, Josè Esteban, Melis, Virginia, Carbone, Claudia, Escribano, Elvira, Zaru, Marco, Fadda, Anna Maria, Manconi, Maria, 2016. Combination of argan oil and phospholipids for the development of an effective liposome-like formulation able to improve skin hydration and allantoin dermal delivery. Int. J. Pharm. 505 (1–2), 204–211.
Manca, Maria Letizia, Mir-Palomo, Silvia, Caddeo, Carla, Nacher, Amparo, Díez-Sales, Octavio, Peris, Josè Esteban, Pedraz, Josè Luis, Fadda, Anna Maria, Manconi, Maria, 2019. Sorbitol-penetration enhancer containing vesicles loaded with baicalin for the protection and regeneration of skin injured by oxidative stress and UV radiation. Int. J. Pharm. 555, 175–183.
Manconi, Maria, Manca, Maria Letizia, Caddeo, Carla, Valenti, Donatella, Cencetti, Claudia, Diez-Sales, Octavio, Nacher, Amparo, et al., 2018. Nanodesign of new self-assembling core-shell gellan-transfersomes loading baicalin and in vivo evaluation of repair response in skin. Nanomed.: Nanotechnol., Biol., Med. 14 (2), 569–579.
Martinez, Renata M., Pinho-Ribeiro, Felipe A., Steffen, Vinicius S., Silva, Thais C.C., Caviglione, Carla V., Bottura, Carolina, Fonseca, Maria J.V., et al., 2016. Topical formulation containing naringenin: efficacy against ultraviolet B irradiation-induced skin inflammation and oxidative stress in mice. PLoS ONE 11 (1).
Mir-Palomo, Silvia, Amparo Nácher, M.A., Busó, Ofelia Vila, Caddeo, Carla, Manca, Maria Letizia, Manconi, Maria, Díez-Sales, Octavio, 2019. Baicalin and berberine ultradeformable vesicles as potential adjuvant in vitiligo therapy. Colloids Surf. B, Biointerfaces 175, 654–662.
Owczarek, Krzysztof, Jaworski, Mariusz, 2016. Quality of life and severity of skin changes in the dynamics of psoriasis. Postepy Dermatologii I Alergologii 33 (2), 102–108.
Perez, Ana Paula, Altube, Maria Julia, Schilrreff, Priscila, Apezteguia, Gustavo, Celes, Fabiana Santana, Zacchino, Susana, Indiani, Camila, de Oliveira, Eder, Romero, Lilia, Morilla, Maria Jose, 2016. Topical amphotericin B in ultradeformable liposomes: formulation, skin penetration study, antifungal and antileishmanial activity in vitro. Colloids Surf. B, Biointerfaces 139, 190–198.
Pimentel-Moral, S., Teixeira, M.C., Fernandes, A.R., Arráez-Román, D., Martínez-Férez, A., Segura-Carretero, A., Souto, E.B., 2018. Lipid nanocarriers for the loading of polyphenols – A comprehensive review. Adv. Colloid Interface Sci. 260, 85–94.
Pivetta, Thais P., Simões, Sandra, Araújo, Margarete M., Carvalho, Tânia, Arruda, Caroline, Marcato, Priscyla D., 2018. Development of nanoparticles from natural lipids for topical delivery of thymol: investigation of its anti-inflammatory properties. Colloids Surf. B, Biointerfaces 164, 281–290.
Pleguezuelos-Villa, María, Amparo Nácher, M.J., Hernández, M.A., Buso, Ofelia Vila, Sauri, Amparo Ruiz, Díez-Sales, Octavio, 2019. Mangiferin nanoemulsions in treatment of inflammatory disorders and skin regeneration. Int. J. Pharm. 564, 299–307.
Rauf, Abdur, Imran, Muhammad, Khan, Imtiaz Ali, Ur-Rehman, Mujeeb-, Gilani, Syed Amir, Mehmood, Zaffar, Mubarak, Mohammad S., 2018. Anticancer potential of quercetin: A comprehensive review. Phytotherapy Res.: PTR 32 (11), 2109–2130.
Ring, J., Alomar, A., Bieber, T., Deleuran, M., Fink-Wagner, A., Gelmetti, C., Gieler, U., et al., 2012. Guidelines for treatment of atopic eczema (atopic dermatitis) Part I. J. Eur. Acad. Dermatol. Venereol.: JEADV 26 (8), 1045–1060.
Rodríguez-Luna, Azahara, Talero, Elena, Del Carmen, María, Terencio, María Luisa, González-Rodríguez, Antonio M., de Los Rabasco, Carolina, Motilva, Reyes Virginia, Ávila-Román, Javier, 2017. Topical application of glycolipids from isochrysis galbana prevents epidermal hyperplasia in mice. Marine Drugs 16 (1).
Saha, Sukanya, Sadhukhan, Pritam, Sinha, Krishnendu, Agarwal, Namrata, Sil, Parames C., 2016. Mangiferin attenuates oxidative stress induced renal cell damage through activation of PI3K induced Akt and Nrf-2 mediated signaling pathways. Biochem. Biophys. Rep. 5, 313–327.
Szandruk, Marta, Merwid-Ląd, Anna, Szeląg, Adam, 2018. The impact of mangiferin from belamcanda chinensis on experimental colitis in rats. Inflammopharmacology 26 (2), 571–581.
Tanaka, Miori, Kishimoto, Yoshimi, Sasaki, Mizuho, Sato, Akari, Kamiya, Tomoyasu, Kondo, Kazuo, Iida, Kaoruko, 2018. Terminalia Bellirica (Gaertn.) Roxb. extract and gallic acid attenuate LPS-induced inflammation and oxidative stress via MAPK/NF-KB and Akt/AMPK/Nrf2 pathways. Oxid. Med. Cell. Longevity 2018, 9364364.
Zengin, Gokhan, Stefanucci, Azzurra, Rodrigues, Maria João, Mollica, Adriano, Custodio, Luisa, Aumeeruddy, Muhammad Zakariyyah, Mahomoodally, Mohamad Fawzi, 2019. *Scrophularia Lucida* L. as a valuable source of bioactive compounds for pharmaceutical applications: in vitro antioxidant, anti-inflammatory, enzyme inhibitory properties, in silico studies, and HPLC profiles. J. Pharm. Biomed. Anal. 162, 225–233.
Zou, Bingyu, Wang, Hailian, Liu, Yilong, Qi, Ping, Lei, Tiantian, Sun, Minghan, Wang, Yi, 2017. Mangiferin induces apoptosis in human ovarian adenocarcinoma OVCAR3 cells via the regulation of Notch3. Oncol. Rep. 38 (3), 1431–1441.

ANNEXES II

GENERALITAT VALENCIANA
CONSELLERIA D'AGRICULTURA, MEDI AMBIENT, CANVI CLIMÀTIC I DESENVOLUPAMENT RURAL

Data 17 FEB 2017

REGISTRE D'EIXIDA
EIXIDA núm 8883

GENERALITAT VALENCIANA
CONSELLERIA DE AGRICULTURA, MEDIO AMBIENTE, CAMBIO CLIMÁTICO Y DESARROLLO RURAL

MARIA PLEGUEZUELOS VILLA
C/ REAL, 7-3º
06200 ALMENDRALEJO

Vista la propuesta del jefe de servicio de Producción y Sanidad Animal para la acreditación como personal de la función **C** de **MARIA PLEGUEZUELOS VILLA**, con DNI **76115811W**, de acuerdo con lo dispuesto en el Real Decreto 53/2013, expediente nº **2608** así como la documentación aportada al expediente.

Considerando la Disposición Transitoria Cuarta del Real Decreto 53/2013 de 1 de febrero por el que se establecen las normas aplicables para la protección de los animales utilizados en experimentación y otros fines científicos, incluyendo la docencia, para el mantenimiento de las diferentes categorías establecidas conforme al Real Decreto 1201/2005 de 10 de octubre.

Teniendo en cuenta el punto 2 de la Disposición Transitoria Primera de la Orden ECC/566/2015, de 20 de marzo por la que se establecen los requisitos de capacitación que debe cumplir el personal que maneje animales.

Dado que la Dirección General de Agricultura y Ganadería de la Comunidad de Madrid, ha reconocido el curso de **Experimentación Animal**, función **C** con Referencia **10/069861.9/16** de fecha 08/04/2016 y vista la documentación aportada por el titular, donde consta que ha superado el curso de experimentación animal, función C, impartido por **Animalaria, Formación y Gestión S.L.** Referencia **10/069861.9/16** y el período de trabajo en la Sección Producción Animal SCSIE, habiendo acreditado su capacitación el Servei Central de Suport a la Investigació Experimental (SCSIE).

RESUELVO: Conceder el reconocimiento como personal de la función **C**, para todas las especies del Anexo II de la Orden ECC/566/2015, de 20 de marzo, a **MARIA PLEGUEZUELOS VILLA**, DNI **76115811W** a los efectos de la normativa vigente en protección de los animales de experimentación y otros fines científicos.

La presente resolución no pone fin a la vía administrativa y contra ella puede interponerse, en el plazo de un mes a contar desde el día siguiente al de su recepción, recurso de alzada ante el secretario autonómico de Agricultura y Desarrollo Rural de conformidad con lo dispuesto en los artículos 121 y 122 de la Ley 39/2015, de 1 de octubre, del Procedimiento Administrativo Común de las Administraciones Públicas.

Valencia, a fecha de la firma electrónica
El director general de Agricultura, Ganadería y Pesca

GENERALITAT VALENCIANA

Firmado por LLANES RIBAS ROGELIO - 73502655Z
Fecha: 17/02/2017 08:52:32 CET

GENERALITAT VALENCIANA
CONSELLERIA DE AGRICULTURA, MEDIO AMBIENTE, CAMBIO CLIMÁTICO Y DESARROLLO RURAL
DIRECCIÓN GENERAL DE AGRICULTURA, GANADERÍA Y PESCA

Unión Europea

AUTORIZACION PROCEDIMIENTO 2016/VSC/PEA/00112

Vista la solicitud realizada en fecha **01/06/16** con nº reg. entrada **21725** por D/Dª. **Pilar Campins Falcó**, Vicerrectora de Investigación y Política Científica, centro usuario **ES460780001001**, para realizar el procedimiento:

"Evaluación de la eficacia antiinflamatoria de flavonoides vehiculizados en nanotransportadores para el tratamiento de enfermedades inflamatorias cutáneas"

Teniendo en cuenta la documentación aportada, según se indica en el artículo 33, punto 5 y 6, y puesto que dicho procedimiento se halla sujeto a autorización en virtud de lo dispuesto en el artículo 31 del Real Decreto 53/2013, de 1 de febrero,

Vista la propuesta del jefe del servicio de Ganadería y Sanidad y Bienestar Animal.

AUTORIZO:

la realización de dicho procedimiento al que se le asigna el código: **2016/VSC/PEA/00112** tipo **2,** de acuerdo con las características descritas en la propia documentación para el número de animales, especie y periodo de tiempo solicitado. Todo ello sin menoscabo de las autorizaciones pertinentes, por otras Administraciones y entidades, y llevándose a cabo en las siguientes condiciones:

Usuario: **Universitat de Valencia**

Responsable del proyecto: **Amparo Nácher Alonso**

Establecimiento: **Sección de Producción Animal SCIE-Campus Burjassot**

Necesidad de evaluación restrospectiva:

Condiciones específicas:

Observaciones:

Valencia a, 27 de junio de 2016

El director general de Agricultura, Ganadería y Pesca

Rogelio Llanes Ribas

GENERALITAT VALENCIANA
CONSELLERIA DE AGRICULTURA, MEDIO AMBIENTE, CAMBIO CLIMÁTICO Y DESARROLLO RURAL
DIRECCIÓN GENERAL DE AGRICULTURA, GANADERÍA Y PESCA

Unión Europea

AUTORIZACION PROCEDIMIENTO 2018/VSC/PEA/0032

Vista la solicitud realizada en fecha **12/02/18** con nº reg. entrada **3892** por D/Dª. **Pilar Campins Falcó**, Vicerrectora de Investigación y Política Científica, centro usuario **ES460780001001**, para realizar el procedimiento:

"Nuevas formas de administración tópica de polifenoles: evaluación de su eficacia antiinflamatoria. "

Teniendo en cuenta la documentación aportada, según se indica en el artículo 33, punto 5 y 6, y puesto que dicho procedimiento se halla sujeto a autorización en virtud de lo dispuesto en el artículo 31 del Real Decreto 53/2013, de 1 de febrero,

Vista la propuesta del jefe del servicio de Producción y Sanidad Animal.

AUTORIZO:

la realización de dicho procedimiento al que se le asigna el código: **2018/VSC/PEA/0032** tipo **2,** de acuerdo con las características descritas en la propia documentación para el número de animales, especie y periodo de tiempo solicitado. Todo ello sin menoscabo de las autorizaciones pertinentes, por otras Administraciones y entidades, y llevándose a cabo en las siguientes condiciones:

Usuario: **Universitat de Valencia**

Responsable del proyecto: **Amparo Nácher Alonso**

Establecimiento: **Sección de Producción Animal SCIE-Campus Burjassot**

Necesidad de evaluación restrospectiva:

Condiciones específicas:

Observaciones:

Valencia a, fecha de la firma electrónica

El director general de Agricultura, Ganadería y Pesca

GENERALITAT VALENCIANA
Signat per Rogelio Llanes Ribas el 16/02/2018 10:31:35
Càrrec: Dirección General